# Bio-based resins, polymers and composites based on waste vegetable oil valorisation

**by**

**Felipe Cicaroni Fernandes**

A thesis submitted in partial fulfilment of the requirements for the degree of

Doctor of Philosophy in Engineering

University of Warwick, Warwick Manufacturing Group

January 2019

# Table of Contents

# List of Figures

## List of Tables

## Acknowledgements

I want to thank Prof Kerry Kirwan and Dr Stuart Coles for the intellectual, academic and moral support throughout my Ph.D. Many thanks for welcoming myself and my ideas in the Sustainable Materials and Manufacturing Group, and for providing me with confidence and motivation to develop my thesis.

This Ph.D. thesis is especially dedicated to my family in Brazil, who demonstrated monumental strength throughout all these years despite the distance. The decision of spending all these years separated wasn't easy for any of us, but your encouragement and resilience were what kept me going. Mum and Dad: all the dedication put into this thesis is a simple way to thank your support and educational values shared with me since I was a child.

Similarly, I would like to thank Paula for all the support and help whilst also pursuing a doctoral degree herself. Your comprehension, positiveness and love in every single decision were fundamental.

Many thanks to all colleagues that passed through the Sustainable Materials and Manufacturing group during these years. Each one of you left a mark on my life and had contributed with something that shaped the person that I am today. Many thanks for the friendship and interactions.

A special thanks to all those from the PG Community Engagement Team (Mentors and Staff) involved in the Mentorship Scheme. I have learnt a lot during my involvement with the programme, and I sincerely appreciate all the opportunities you have given me.

I would like to thank all WMG academic and technical support staff that directly or indirectly have enabled my work and helped me in this journey.

Also, many thanks to Dave, Nick, Mark and Greg for being my judo mentors, teaching me self-discipline and love for life throughout inspiring muses. Many thanks to all the players in the University of Warwick Judo and BJJ Club for your friendship and mutual respect.

Thanks to Brazilian National Council for Scientific and Technological Development (CNPq, 203118/2014-6) for the financial support.

## Declaration

This thesis is submitted to the University of Warwick in support of my application for the degree of Doctor of Philosophy. It has been composed by myself and has not been submitted in any previous application for any degree to any other university or higher education institution or as any part of any other submission to the University of Warwick. Parts of this thesis have been published and submitted to journals during the PhD period by the author as detailed in the list of publications at the end of this section. DIC tests were carried out with the support of Dr Peter Wilson.

## Published Work from This Thesis

**From Chapter 4:**

F. C. Fernandes, D. Lehane, K. Kirwan and S. R. Coles, *Eur. Polym. J.*, 2017, **89**, 449–460.

**From Chapter 5:**

F. C. Fernandes, K. Kirwan, P. R. Wilson and S. R. Coles, *Green Mater.*, 2018, **6**, 38–46.

**From Chapter 7:**

F. C. Fernandes, K. Kirwan, P. Wilson, C. Froemder and S. R. Coles, *Proc. SAMPE Eur. 2018*.

**International Presentations:**

F.C. Fernandes, K. Kirwan, M. Sotenko and S. R. Coles. 23th Annual Meeting of the Bio-Environmental Polymer Society (BEPS), Karlsruhe, Germany, 2015 (Poster)

F. C. Fernandes, K. Kirwan, P. R. Wilson and S. R. Coles, American Chemical Society Green Chemistry & Engineering Conference, Portland, USA, 2016 (Poster)

F. C. Fernandes, K. Kirwan, P. R. Wilson and S. R. Coles, 3rd International Symposium on Green Chemistry, La Rochelle, France, 2017 (Oral)

F. C. Fernandes, K. Kirwan, P. R. Wilson and S. R. Coles, 46th World Chemistry Conference - IUPAC 2017, São Paulo, Brazil, 2017 (Poster)

F. C. Fernandes, K. Kirwan, P. R. Wilson and S. R. Coles. 24th Annual Meeting of the Bio-Environmental Polymer Society (BEPS), Albany, USA, 2017 (Oral)

F. C. Fernandes, K. Kirwan, P. R. Wilson and S. R. Coles. 3rd Frontiers in Green Materials, London, UK, 2017 (Poster)

F. C. Fernandes, K. Kirwan, P. R. Wilson and S. R. Coles. World Polymer Conference Macro 2018, Cairns, Australia, 2018 (Oral).

## Abstract

Historically, energy-intensive materials such as glass fibres and carbon fibres have been applied to reinforce thermoplastic and thermoset matrices from a petrochemical origin. However, recent ecological concerns and latent climate change problems have encouraged the development of environmentally-friendly alternatives for composite industry, creating a new class of materials that bring added technical performance and are produced more sustainably. In this scenario, vegetable fibres have been rediscovered as promising reinforcing agents and bio-based polymers have been developed to attend the demand for greener matrices. In the last decade, vegetable oils have emerged as a key platform to produce bio-based epoxy resins used as matrices for composite laminates, reducing the environmental footprint of composites production. Nevertheless, features such as the intrinsically limited mechanical performance, price and ethical discussions have restricted the applicability of these materials. In this regard, this thesis investigates the utilisation of waste vegetable oil (WVO) as a potential platform to create bio-based epoxy resins and consequently composites in a more sustainable fashion. Investigations have identified the best purification and chemical modification methodologies to enable the polymerisation of these triglycerides. They have also confirmed the possibility of applying such materials as reactive diluents for diglycidyl ether of Bisphenol A (DGEBA), or for the creation of networks exclusively made with waste-based epoxies. Nonetheless, one should ensure that anhydrides are used in excess as hardener to mitigate drops in performance and create networks with $T_g$ above room temperature. Studies also demonstrate the use of resins from WVO for the creation of a library of composite materials reinforced with glass, carbon fibres (virgin and recycled) and flax fibres. To address the challenge of compatibilizing vegetable fibres and the hydrophobic matrix, chemical treatments are explored to enhance the fibre/matrix interaction, with mercerisation leading to the best performance. Materials produced with glass demonstrate to be competitive alternatives for application that require stiffness and impact performance over strength, where the use of WVO-based epoxy also reduced the density of these materials. Finally, laminates reinforced with virgin and recycled carbon fibres reveal that the addition of resins from WVO to commercial formulations can reduce effects associated with barely-visible impact damage (BVID) as investigated in a compression after impact test. Overall, this thesis demonstrates the first developments of a new class of bio-based composites reliant on the exploration of the waste valorisation concept. Despite not being able to completely substitute DGEBA in technical applications, opportunities are explored according to the best features each system, so that WVO can be used as a co-resin in epoxy formulations for tuning (and improving) a number of engineering properties. Finally, these investigations encourage the maturation of WVO as a more environmentally-friendly chemical platform for a more sustainable polymer and composite industries.

## List of Abbreviations

| | |
|---|---|
| 2-MI | 2-Methylimidazole |
| ATR FTIR | Attenuated Total Reflectance - Fourier Transformation Infrared Spectroscopy |
| BVID | Barely Visible Impact Damage |
| CAI | Compression After Impact |
| DGEBA | Diglycidyl Ether of Bisphenol A |
| DMA | Dynamic Mechanic Analysis |
| DSC | Dynamic Scanning Calorimetry |
| E' | Storage Modulus |
| ELO | Epoxidized Linseed Oil |
| ENVO | Epoxidized Neat Vegetable Oil |
| EPVO | Epoxidized Purified Vegetable Oil |
| ESO | Epoxidized Sunflower Oil |
| EVO | Epoxidized Vegetable Oil |
| EWVO | Epoxidized Waste Vegetable Oil |
| FF | Flax Fibres |
| GF | Glass Fibres |
| GSM | Grams Per Square Meter |
| $^{1}$H NMR | Proton Nuclear Magnetic Resonance |
| HDPE | High-Density Polyethylene |
| HPLC | High Performance Liquid Chromatography |
| LCA | Life Cycle Assessment |
| MHHPA | Methylhexahydrophthalic Anhydride |
| NFF | NaOH-Treated Flax Fibres |
| PA | Phthalic Anhydride |
| PP | Polypropylene |
| PTFE | Polytetrafluoroethylene |
| PVC | Polyvinyl Chloride |
| SEM | Scanning Electron Microscope |
| SFF | Stearic Acid-Treated Flax Fibres |
| TEA | Tetraethylammonium |
| $T_g$ | Glass Transition Temperature |
| TGA | Thermogravimetric Analysis |
| $T_{Max}$ | Max Temperature of Degradation |
| $T_{Onset}$ | Onset Temperature of Degradation |
| VO | Vegetable Oil |
| WVO | Waste Vegetable Oil |
| $\nu_e$ | Crosslinking Density |

# Chapter 1

# Introduction and Motivations

## 1.1 Research Background

Composites are defined as multiphase and heterogeneous materials comprised of at least one continuous phase, also referred to as a matrix, and a dispersed and discontinuous phase.[1] Consequently, composites are constituted of the combination of two or more materials that are physically and chemically distinguished and separated by an interface.[2] More specifically, polymeric composites are a distinct class of materials presenting polymeric chains or polymeric networks as continuous phase embedding dispersed compounds that can actively change the mechanical properties. Another main consideration at this point is that reinforced composites must present physical or mechanical properties that are superior (or even unique) in comparison with those observed in the original materials that comprise this multi-phase system. For example, materials known as fillers (*e.g.* inorganic particles such as carbonates) can be added as the dispersed phase in polymeric matrices without positively impacting any engineering properties apart from costs by reducing the polymer volume fraction in the final product. In this particular case, these systems can be denominated as filled polymers.[3] Conversely, dispersed phases that improve properties of the polymeric matrix are known as reinforcements, and materials from different organic and inorganic origins have been investigated for this role.

Technologically speaking, polymeric composites have been explored along the decades in engineering applications as viable replacements for traditional materials such as steel and ceramics due to the combination of high mechanical properties, low density and cost.[4] In this regard, materials such as glass and carbon fibres have been extensively used to reinforce thermoplastic and thermoset matrices, providing these materials with unique properties when compared to traditional counterparts. Consequently, polymer composites have found applications in a number of sectors, transforming areas such as the transport, aerospace and construction industries. Recent advances in manufacturing technologies are unlocking novel applications for these lightweight materials, which will play a vital role towards a low-carbon economy in the future.[5–7]

On the other hand, recent environmental scenario and the latent hazards caused by climate change have also risen awareness about the expressive amounts of energy consumed to produce such materials, consequently increasing the carbon footprint of the manufacturing and partially nullifying the benefits observed in the use phase of composite parts.[8] Traditionally, literature has tackled this issue from the reinforcement perspective since the manufacturing processes associated with both glass and carbon fibres are highly energy-intensive.[9,10] A common approach in this regards is the utilisation of vegetable fibres as reinforcing agents, which were rediscovered in engineering applications due to characteristics such as lower density, low embodied energy, carbon neutrality, price and renewability.[11,12]

This has given rise to a new platform of materials, known as biocomposites, that integrate environmentally benign with technological and engineering performance. The growing interest in these materials can be visualised by the number of publications on the "biocomposites" topic according to a search in the Web of Science® database.

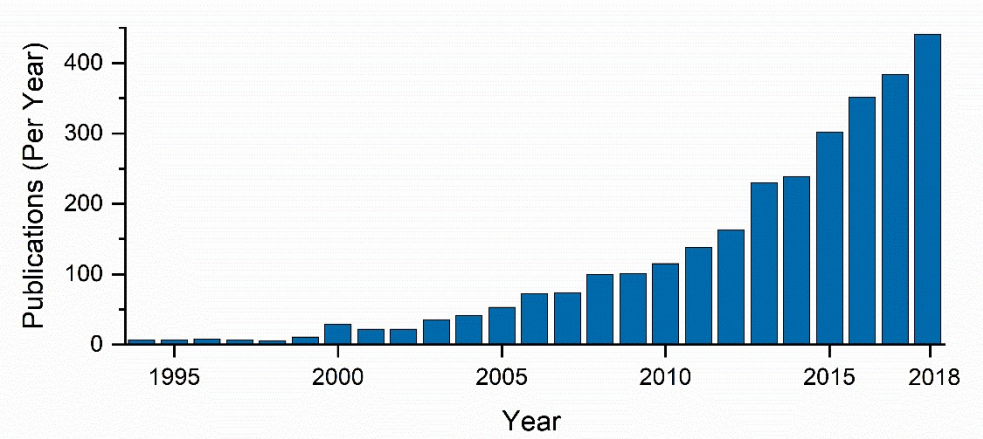


Figure 1.1: Evolution of the number of publications in the topic of biocomposites

Although the literature has demonstrated the incorporation of these vegetable fibres in a number of polymeric matrices (even at high volumetric fractions), the majority of composites reported still explore the utilisation of thermoplastic and thermoset matrices derived from petroleum. In turn, this characteristic compromises the sustainability of the value chain since petroleum-derived matrices will negatively contribute to carbon emissions, therefore limiting the environmental benefits of the resulting composites, and be susceptible volatility in the oil price.[13] In this regard, literature has concentrated in the last decades into giving a further step towards sustainability in the polymer and composites sector, and has started investigating the production of materials in which the matrix is also derived from renewable resources.[14] This practice has been explored both in the area of thermoplastics and thermosets composites, and have demonstrated to be a valid approach to produce materials with competitive mechanical performance, very low environmental impact and reduced toxicity associate with the resin handling.[15–19] The combination of both components (fibre and matrix) from renewable sources give rise to another class of materials known as green composites.[20] Furthermore, this concept can be expanded to incorporate biodegradability aspects, leading to green composites with a benign life cycle, being sustainably produced, used and disposed.[21,22]

Among the different strategies proposed in recent years, many researchers within this community have decided to explore vegetable oils as the preferred chemical platform to produce renewable polymers and composites.[23] Triglycerides, the main components found in the vegetable oils, are versatile molecules since they are diverse in terms of chemical

functionalities, presenting groups such as carbonyl, ester and double bonds, Figure 1.2. These reactive groups can be manipulated towards the insertion of polymerisable groups through different routes, enabling the production of polymeric materials from plants.[24] In this diverse chemical skillset, one of the most traditional approaches has been the insertion of oxirane groups in the unsaturation sites through epoxidation reactions, producing epoxidized vegetable oils (EVOs). Since these bio-based epoxy resins can be cured with amine and anhydrides to produce thermoset polymers, literature has demonstrated the successful application of these systems to manufacture composites with different vegetable fibres systems.[16,25–28] Additionally, further exploration of the reactivity of the epoxy group through the insertion of other polymerisable groups (*e.g.* acrylic or maleic groups) with distinct reactivity can expand even more the versatility of these products.[29,30] Potentially, these molecules can be explored to partially substitute diglycidyl ether of Bisphenol A (DGEBA) in epoxy formulations, molecule which presents a number of associated with its toxicity and currently accounts for a global market of 3 million tons (as in 2017).[31]

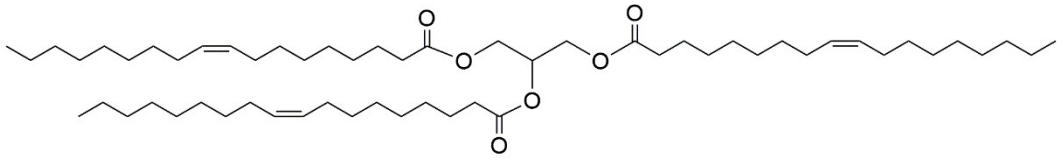

Figure 1.2: Schematic representation of a triglyceride, the main chemical platform of this study.

Despite the successful demonstration of the use of epoxy resins derived from vegetable oils in engineering applications, these systems present inherent challenges that hinder their full implementation in industrial scale. For instance, EVOs present reduced performance when compared to other epoxy systems such as those based on DGEBA, holding back its implementation and making these resins not fully economic competitive.[20,32] Furthermore, the exploitation of edible vegetable oils in engineering applications rises discussions about the ethical use of land, the exclusion of VOs from the food chain and how it can negatively affect the price of commodity food.[33–35] Therefore, there is a driving force in literature and industry towards the identification of sustainable sources of triglyceride to produce competitive and affordable epoxy resins with minimum environmental and social impact.

In this study, we propose the investigation of waste vegetable oil (WVO) as an alternative platform to produce epoxy resins in a more sustainable manner. This research represents an opportunity yet unexplored to valorise a challenging and significant waste stream by implementing it in polymer and composite science. To put in perspective, it is

estimated that the EU generates over 700,000 tonnes of WVO yearly; and this number is increased over 5 times considering the Chinese production of WVO, accounting for approximately 4.5 million tonnes per year.[36] This highlights not only the scale of the issue that needs to be addressed but also the abundance of this renewable feedstock to produce resins from recycled sources. In fact, the large-scale utilisation of this WVO post-use is currently limited to the production of biodiesel, representing space for further technological expansion based on this platform. Furthermore, the establishment technological valorisation of this material is aligned with the concepts of sustainability since it can bring environmental, economic and social benefits (further discussed in Chapter 2) and circular economy, maintaining the value of these triglycerides at a maximum for a longer period of time.

Despite the valorisation of WVO appearing as a novel and promising platform to build up polymers from renewable resources, there are major challenges associated with the nature of this material that should be addressed first to confirm the validity of this alternative for polymer and composite industry. For example, reactions that take place during the frying process are responsible for drastically altering chemical and physical properties of the virgin oil, and should be taking into consideration when exploring this material in engineering applications.[37] Consequently, the frying stage generates a substrate that is heterogeneous in composition and presents impurities that can potentially affect the formation of the thermoset polymer, thus the composite.

## 1.2 Research Gaps and Questions

The viability of WVO as feedstock for the synthesis of resins and manufacture of composites depends on the reliability of this material as a clean and consistent chemical platform. Since the application of WVO in the production of polymers and composites is a novel approach, no literature has explored how the purification influences further steps. In this regard, studies focused on the production of biodiesel from this feedstock offers different methodologies based on the use of adsorption agents and liquid extraction to eliminate by-products formed during the frying stage and produce a clean source of triglycerides.[38–40] In the biodiesel area, the presence of residual water can pose as a problem since it can interfere in the following modification steps.[41] However, this feature is not particularly problematic for the production of epoxy resins since most of the chemical modifications can take place in the aqueous medium, giving more flexibility in the approaches explored in this study. Therefore, the methodologies herein investigated will be adapted from the biodiesel area and be used to create guidelines for further developments with this waste feedstock.

Similarly, there is a gap in the literature in understanding how WVO can be chemically manipulated towards its transformation into EVO and consequently polymers from

renewable resources. Giving the importance of the epoxidation step in the properties of the resulting thermoset polymer (and composite), it is mandatory to comprehend the effectiveness of different chemical modification methodologies in inserting oxirane rings in the unsaturated sites. This can be assessed in terms of conversion and selectivity while avoiding the premature ring-opening of oxirane rings, which can lead to reduced crosslinking. These key points will be linked to comprehend how thermoset polymers can be obtained using waste-based resins in terms of the effect of parameters such as the curing regime and curing agent, which to the be best of our knowledge remains unexplored in literature.

The production of formulations capable of effectively producing polymers from WVO will enable further investigations about the manufacture of composites in later stages of this study. This application will allow the first demonstration of materials for engineering applications using a class of resins originated from waste sources. As a result, this study aims at producing a library of novel composite materials (reinforced with different agents) based on waste valorisation, providing the community with a comprehensive view of how the frying process affects the quality of different materials and exploring the best properties of each system. In addition, the maximisation of mechanical performance is considered as the overall goal throughout this study. More importantly, this collection of investigations invite researchers to rediscover materials and rethink about the role of waste valorisation in enabling a more sustainable polymer and composite industry. Therefore, the main research question considered for this thesis is the following:

*Can highly reactive epoxy resins be produced from waste vegetable oil and be used to manufacture polymer composite more sustainably with minimum compromises in mechanical performance?*

## 1.3 Thesis Objectives

In order to address the research questions discussed in section 1.2, the doctoral studies were divided in the following set of objectives:

I. *Review of the state-of-the-art for the transformation of vegetable oils into reactive resins, with a focus on epoxy resins;*
II. *Review of the state-of-the-art in the manufacture of green composites;*
III. *Develop a robust methodology for the obtainment of pure and reactive epoxy resins from WVO;*
IV. *Explore the use of WVO-derived resins for the production of thermoset polymers and optimised formulation parameters based the resin reactivity;*

V. *Build a library of composites using different reinforcing fibres, identifying the best opportunities in terms of mechanical properties.*

## 1.4 Thesis Outline

The present section (Chapter 1) introduces a brief overview of the motivations behind the investigations explored throughout the doctoral studies and an outline of each one of the following chapters in this thesis. Chapter 2 concentrates in reviewing the relevant literature regarding the production, characterisation, processing and chemical modification of vegetable oils. This review focuses on methodologies that can transform the double bonds through the insertion of polymerisable groups and how different classes of polymers can be obtained from triglycerides. Moreover, Chapter 2 discusses the viability of waste vegetable oils (WVO) as a technological platform from the physical and chemical perspective, as well as the transformations that occur in consequence of the use phase. Chapter 3 consists of a second literature view focusing the production of biocomposites from vegetable oil-based resins. This chapter covers different strategies to process and obtain these materials, as well as information about the production, characterisation and chemical modification of vegetable fibres for application as a reinforcing agent in composites.

Chapter 4 presents the first experimental chapter of the PhD thesis. This section covers the chemical characterisation of the WVO, focusing on the differences between this compound and an analogous platform from virgin vegetable oil. Later, the chapter presents the investigation of different purification and chemical modification methods of WVO via epoxidation to enable the production of bio-based epoxy resins. This section also contains the studies of the production and characterisation of partially bio-based resins combining the materials obtained from WVO (and analogous) with commercial epoxy resin (DGEBA). Finally, Chapter 4 presents the production of composites with these resins as a proof of concept.

Studies concentrated on the production of thermosets entirely derived from the bio-based resins are presented in Chapter 5. As the formulations are redesigned at this stage (no DGEBA utilised), this experimental chapter covers the investigation and optimisation of the physical and chemical properties of formulations consisting of epoxidised WVO and different anhydrides. Studies investigate parameters such as hardener ratio, catalyst and origin of the bio-based resin. Chapter 5 also presents a study about the classification of each parameter regarding their statistical significance towards increasing the glass transition temperature of the resulting thermosets. Therefore, this chapter presents guidelines for further investigations on the production of bio-based thermosets from WVO.

The third experimental chapter (Chapter 6) focuses on the production of biocomposites consisted in the reinforcement of the bio-based thermoset matrix with flax and glass fibres. Materials investigated in this chapter are considered as the main products of doctoral studies and are produced according to the optimised results in Chapter 5. A study of the performance of these composites from the thermal and mechanical point of view is presented in this Chapter 6. Furthermore, this chapter covers investigations about how to maximise the property of these biocomposites through the chemical modification of the vegetable fibres.

The last experimental section, Chapter 7, introduces recycled and virgin carbon fibres to reinforce the waste-based matrix as an alternative reinforcing agent to boost the performance of the laminates. At this stage, the work once again relies on the exploration of blends between commercial epoxy and bio-based epoxy to maximise the mechanical properties of such materials given the high-end application. A hypothesis that the addition of EVO-derived resin can enhance impact related properties such as impact strength and reduce barely-visible impact damage (BVID) is tested according to results collected in previous chapters. These investigations are complemented by static mechanical tests and exploration of physical properties in these different formulations. The overall goal of this chapter is to deliver tangible solutions for composite industry aligned with the needs of the manufacturers. Finally, Chapter 8 summarises the overall conclusions of each experimental chapter of the thesis and how they are linked with the motivations presented in the earlier chapters. In addition, this chapter presents perspectives of future works based on the main findings of the thesis. Figure 1.3 schematically presents the overall thesis plan.

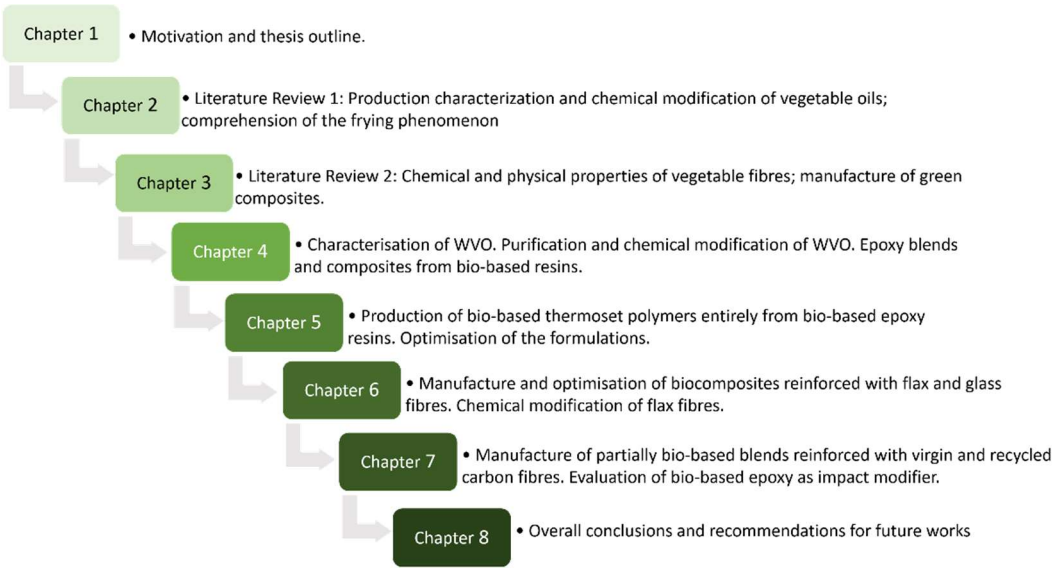


Figure 1.3: Thesis outline and overview of the content in each chapter.

## 1.5 References


1 W. R. Hibbard Jr, in *Fiber Composite Materials*, 1965, pp. 1–5.

2 W. D. Callister Jr, *Materials Science and Engineering: An Introduction*, John Wiley & Sons Inc, York, PA, 7th edn., 2007.

3 R. Petrucci and L. Torre, in *Modification of Polymer Properties*, Elsevier Inc., 2016, pp. 23–46.

4 J. F. Monk, *Thermosetting plastics: Moulkding Materials and Processes*, Addison Wesley Longman Limited, Essex, 2nd edn., 1997.

5 M. Belhaj, M. Deleglise, S. Comas-Cardona, H. Demouveau, C. Binetruy, C. Duval and P. Figueiredo, *Compos. Part B Eng.*, 2013, **50**, 107–111.

6 C. He, Q. Meng and H. Wang, in *Proceedings of 2015 2nd International Conference on Industrial Economics System and Industrial Security Engineering*, eds. M. Li, Q. Zhang, J. Zhang and Y. Li, Springer, Singapore, 2016, pp. 51–56.

7 E. Witten, T. Kraus and M. Kühnel, *Composites Market Report 2016*, 2016.

8 F. Meng, E. A. Olivetti, Y. Zhao, J. C. Chang, S. J. Pickering and J. McKechnie, *ACS Sustain. Chem. Eng.*, 2018, **6**, 9854–9865.

9 D. Hull and T. W. Clyne, *An Introduction to Composite Materials*, Cambridge Univerisity Press, Cambridge, United Kingdom, Second., 1996.

10 L. Shen and M. K. Patel, *J. Polym. Environ.*, 2008, **16**, 154–167.

11 A. K. Bledzki and J. Gassan, *Prog. Polym. Sci.*, 1999, **24**, 221–274.

12 B. M. Wood, S. R. Coles, S. Maggs, J. Meredith and K. Kirwan, *Compos. Sci. Technol.*, 2011, **71**, 1804–1810.

13 T. Corbiere-Nicollier, B. Gfeller Laban, L. Lundquist, Y. Leterrier, J.-A. Manson and O. Jolliet, *Resour. Conserv. Recycl.*, 2001, **33**, 267–287.

14 E. Zini and M. Scandola, *Polym. Compos.*, 2011, **32**, 1905–1915.

15 A. Gomes, T. Matsuo, K. Goda and J. Ohgi, *Compos. Part A Appl. Sci. Manuf.*, 2007, **38**, 1811–1820.

16 Z. Liu, S. Z. Erhan, D. E. Akin and F. E. Barton, *J. Agric. Food Chem.*, 2006, **54**, 2134–2137.

17 N. V. Patil, M. M. Rahman and A. N. Netravali, *Polym. Compos.*, 2017, 23–25.

18 Y. S. Song, J. R. Youn and T. G. Gutowski, *Compos. Part A Appl. Sci. Manuf.*, 2009, **40**, 1257–1265.

19 S. G. Tan and W. S. Chow, *Polym. Plast. Technol. Eng.*, 2010, **49**, 1581–1590.

20 F. P. La Mantia and M. Morreale, *Compos. Part A Appl. Sci. Manuf.*, 2011, **42**, 579–588.

21 S. Ochi, *Mech. Mater.*, 2008, **40**, 446–452.

22 P. Russo, C. Carfagna, F. Cimino, D. Acierno and P. Persico, *Adv. Polym. Technol.*, 2012, **32**, 474–485.

23 L. Montero de Espinosa and M. a. R. Meier, *Eur. Polym. J.*, 2011, **47**, 837–852.

24 M. a. R. Meier, J. O. Metzger and U. S. Schubert, *Chem. Soc. Rev.*, 2007, **36**, 1788.

25 N. Boquillon, *J. Appl. Polym. Sci.*, 2006, **101**, 4037–4043.

26 W. Liu, T. Chen, T. Xie and R. Qiu, *Compos. Part A Appl. Sci. Manuf.*, 2016, **82**, 1–7.

27 R. P. Wool, in *Bio-Based Polymers and Composites*, eds. R. P. Wool and X. S. Sun, Elsevier Inc., 2005, pp. 114–148.

28 D. P. Pfister and R. C. Larock, *J. Appl. Polym. Sci.*, 2013, **127**, 1921–1928.

29 S. N. Khot, J. J. Lascala, E. Can, S. S. Morye, G. I. Williams, G. R. Palmese, S. H. Kusefoglu and R. P. Wool, *J. Appl. Polym. Sci.*, 2001, **82**, 703–723.

30 G. Lligadas, J. C. Ronda, M. Galià and V. Cádiz, *Mater. Today*, 2013, **16**, 337–343.

31 C. Scarponi, F. Sarasini, J. Tirillò, L. Lampani, T. Valente and P. Gaudenzi, *Compos. Part B Eng.*, 2016, **91**, 162–168.

32 J.-M. Raquez, M. Deléglise, M.-F. C and P. Krawczak, *Prog. Polym. Sci.*, 2010, **35**, 487–509.

33 D. Pimentel, A. Marklein, M. A. Toth, M. N. Karpoff, G. S. Paul, R. McCormack, J. Kyriazis and T. Krueger, *Hum. Ecol.*, 2009, **37**, 1–12.

34 H. P. S. Makkar and K. Becker, *Eur. J. Lipid Sci. Technol.*, 2009, **111**, 773–787.

35 M. K. Lam, K. T. Tan, K. T. Lee and A. R. Mohamed, *Renew. Sustain. Energy Rev.*, 2009, **13**, 1456–1464.

36 M. M. Gui, K. T. Lee and S. Bhatia, *Energy*, 2008, **33**, 1646–1653.

37 E. Choe and D. B. Min, *J. Food Sci.*, 2005, **70**, 142–159.

38 Z. J. Predojević, *Fuel*, 2008, **87**, 3522–3528.

39 É. de Castro Vasques, C. R. Granhen Tavares, C. Itsuo Yamamoto, M. Rogério Mafra and L. Igarashi-Mafra, *Environ. Technol.*, 2013, **34**, 2361–2369.

40 V. K. W. S. Araujo, S. Hamacher and L. F. Scavarda, *Bioresour. Technol.*, 2010, **101**, 4415–22.

41 U. Schuchardt, R. Sercheli and R. Matheus, *J. Brazilian Chem. Soc.*, 1998, **9**, 199–210.

# Chapter 2

# Literature Review:

The Production of Added-Value Chemicals from Virgin and Waste Vegetable Oils

## 2.1 Vegetable Oils

Vegetable oils are natural products predominantly constituted by triglycerides (94-96 % of the total weight) and derived from sources such as seeds, cereal grains, nuts and fruits.[1] Triglycerides are comprised of a glycerol backbone linked to three fatty acid chains as substituents. Figure 2.1 illustrates the general molecular structure of a triglyceride based on a triolein, which presents three oleic acid chains attached to the backbone, emphasising the main chemical features present in this kind of molecules. This illustrates the chemical diversity that modulates the reactivity and therefore the applicability of these class of molecules.[2]

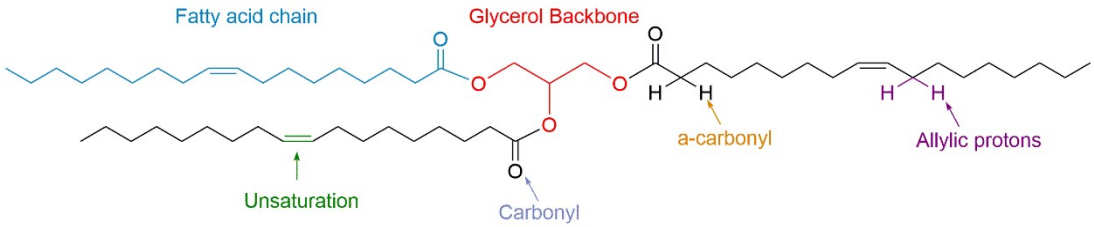


Figure 2.1: Representation of a model triglyceride (triolein) and the main chemical units present in its structure.

Triglycerides found in vegetable oils are considered as “mixed triglycerides” since fatty acids are statistically distributed amongst the glycerol units. This means that more than one kind of fatty acid can be found per triglyceride unit, adding to the chemical diversity of these molecules.[3] Fatty acid profiles vary significantly between plants with respect to the length of the carbon chain, the degree of unsaturation, the presence of substituents and stereochemistry of the double bonds. Therefore, oils expressed by different plants change regarding their physical-chemical properties. For example, not all these oils are found as liquids in ambient temperature, and their edibility varies drastically.[1] Table 2.1 presents the fatty acid profile of the most significant vegetable oils, exemplifying the notable distinct composition between different species. Although more than 1000 fatty acid have been identified in nature, only a small fraction of them are found in the most common vegetable oils.[4] Apart from triglycerides, secondary compounds such as are phospholipids, sterols, tocols and fat-soluble vitamins are also commonly found in vegetable oils in reduced quantities. Despite the reduced significance in terms of technological application, these compounds play an essential role in the nutritional aspects of vegetable oils.[4]

Table 2.1: Fatty acid profile of the most common oils in terms of percentage.[4]

| Name | Vegetable Oil | | | | | | | | |
|---|---|---|---|---|---|---|---|---|---|
| | **Canola** | **Corn** | **Cottonseed** | **Linseed** | **Olive** | **Palm** | **Rapeseed** | **Soybean** | **High Oleic** |
| Myristic | 0.1 | 0.1 | 0.7 | 0 | 0 | 1 | 0.1 | 0.1 | 0 |
| Myristoleic | 0 | 0 | 0 | 0 | 0 | 0 | 0 | 0 | 0 |
| Palmitic | 4.1 | 10.9 | 21.6 | 5.5 | 13.7 | 44.4 | 3 | 11 | 6.4 |
| Palmitoleic | 0.3 | 0.2 | 0.6 | 0 | 1.2 | 0.2 | 0.2 | 0.1 | 0.1 |
| Margaric | 0.1 | 0.1 | 0.1 | 0 | 0 | 0.1 | 0 | 0 | 0 |
| Margaroleic | 0 | 0 | 0.1 | 0 | 0 | 0 | 0 | 0 | 0 |
| Stearic | 1.8 | 2 | 2.6 | 3.5 | 2.5 | 4.1 | 1 | 4 | 3.1 |
| Oleic | 60.9 | 25.4 | 18.6 | 19.1 | 71.1 | 39.3 | 13.2 | 23.4 | 82.6 |
| Linoleic | 21 | 59.6 | 54.4 | 15.3 | 10 | 10 | 13.2 | 53.2 | 2.3 |
| Linolenic | 8.8 | 1.2 | 0.7 | 56.6 | 0.6 | 0.4 | 9 | 7.8 | 3.7 |
| Arachidic | 0.7 | 0.4 | 0.3 | 0 | 0.9 | 0.3 | 0.5 | 0.3 | 0.2 |
| Gadoleic | 1 | 0 | 0 | 0 | 0 | 0 | 9 | 0 | 0.4 |
| Eicosadienoic | 0 | 0 | 0 | 0 | 0 | 0 | 0.7 | 0 | 0 |
| Behenic | 0.3 | 0.1 | 0.2 | 0 | 0 | 0.1 | 0.5 | 0.1 | 0.3 |
| Erucic | 0.7 | 0 | 0 | 0 | 0 | 0 | 49.2 | 0 | 0.1 |
| Lignoceric | 0.2 | 0 | 0 | 0 | 0 | 0 | 1.2 | 0 | 0 |

Concerning nomenclature, fatty acids are commonly known by trivial names derived from their origins; however, they can also be named and systematically classified accordingly to their structures in the CX:Y form. In this terminology, the X represents the chain length, and the Y is the number of double bonds present along the carbon chain as shown in Table 2.2. This nomenclature can also include more information regarding the structure of the fatty acids[5]

Table 2.2: Different nomenclatures found for the most common fatty acids

| **Fatty Acid** | **Chain length** | **Double Bonds** | **Systematic Name** | **Lipid Name** |
|---|---|---|---|---|
| Lauric | 12 | 0 | dodecanoic acid | C12:0 |
| Myristic | 14 | 0 | tetradecanoic acid | C14:0 |
| Palmitic | 16 | 0 | hexadecanoic acid | C16:0 |
| Palmitoleic | 16 | 1 | 9-hexadecenoic acid | C16:1 |
| Stearic | 18 | 0 | octadecanoic acid | C18:0 |
| Oleic | 18 | 1 | 9-octadecenoic acid | C18:1 |
| Ricinoleic | 18 | 1 | 12-hydroxy-9-octadecenoic acid | C18:1 |
| Vaccenic | 18 | 1 | 11-octadecenoic acid | C18:1 |
| Linoleic | 18 | 2 | 9,12-octadecadienoic acid | C18:2 |
| α-Linolenic | 18 | 3 | 9,12,15-octadecatrienoic acid | C18:3 |
| γ-Linolenic | 18 | 3 | 6,9,12-octadecatrienoic acid | C18:3 |
| Arachidic | 20 | 0 | n-eicosanoic acid | C20:0 |
| Behenic | 22 | 0 | n-docosanoic acid | C22:0 |

Vegetable oils are obtained from the plants either mechanically or by chemical extraction with organic solvents (also known as a wet process). Before the oil extraction the plant is washed and unwanted materials are separated by shaker screens or aspirators.[3] The mechanical process consists in applying shear created by a screw or hydraulic press to impose the oil liberation, which makes this a low-cost and environmentally safe technique in comparison to the wet process. However, this process is slow and present limited efficiency of extraction. Additionally, the heat generated by the shearing process can negatively affect the organoleptic qualities as it induces the oil degradation. On the other hand, the wet process is based on the diffusion of organic solvents (most commonly hexane) into the interior of the seeds. This phenomenon leads to the solubilisation of the oils and extracts them from the plant material, where this process can be done in batches or continuously. Even though the extraction has superior efficiency than the mechanical counterpart, this process is expensive and has a higher environmental impact due to the utilisation of significant amounts of volatile solvents.[3]

Generally, commodity oils are not optimised to end-use straight after their extraction from the parent plants, therefore requiring additional processing steps. Blending is the simplest technique used industrially, and consists of mixing different oils to achieve the desired properties. This approach is used to improve nutritional and physical properties, as well as to reduce costs. On the other hand, fractionation separates the oil into two or more fractions that differ in fatty acid composition to produce added value oils. The separation process can be assisted by solvents or the precipitation of less soluble triglycerides from the crude oil. Both liquid and solid fractions can be commercially interesting, but there are cases where just one of them is commercially attractive. For example, palm oil is fractioned in a scale of 3000 tonnes/day, separating olein to be used for frying while stearin, less valuable, is blended with other oils for the production of spreads. Finally, partial hydrogenation is used to adjust the physical properties of the oil, converting it from a liquid into a semi-solid fat increasing it spreadability and oxidative stability but at the cost of reducing its nutritional value.[6]

## 2.2 Technological Exploration of Vegetable Oils

Civilisations have been exploring vegetable oils for over 7000 years for both nutritional value and versatility.[7] Vegetable oils are attractive resources due to their low cost, relative stability in price, renewability and considerable availability all over the globe.[8] Some, vegetable oils have been explored without prior chemical manipulation since they are capable of forming solid films when exposed to air due to a complex combination of auto-oxidative competing reactions. These are known as “drying oils”, and the presence of predominantly high unsaturated fatty acid chains (with two or more double bonds per fatty acid chain) is the

crucial to enables these physical-chemical transformations triggered $O_2$ and light. A classic of a drying oil is the linseed oi (illustrated in Figure 2.2), which is predominantly formed by trilinolenin.

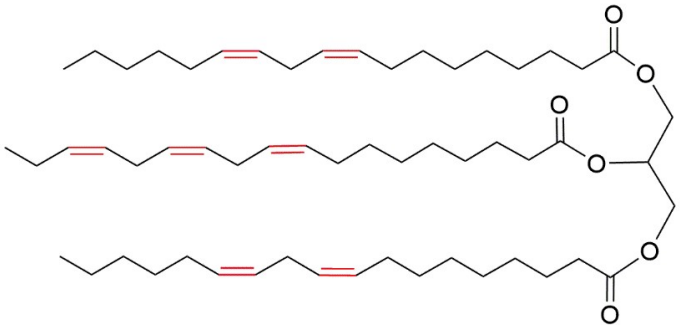

Figure 2.2: Representation of a triglyceride present in linseed oil, combining linolenic and linoleic units, highlighting its high degree of unsaturation.

Drying oils were historically used in paints formulations, coatings, as flooring materials and resins before petrochemical derivated became extensively and inexpensively available in the market. One iconic examples was the production of Linoleum, a floor covering material based on linseed oil developed in the UK in 1860`s by the Linoleum Manufacturing Company Ltd.[9] Also, tung oil, material extracted from the *Vernicia fordii* that is highly abundant in α-eleostearic acid, was traditionally used for paints and varnish for furniture and ships.[10]

Today, vegetable oils are considered the most important renewable raw material for industry, playing a major role in the 21$^{st}$ century green economy.[6,9] They represent an ideal alternative for the petroleum-based manufacturing model due to the combination of abundance, properties and cost. Data from 2012 shows that the global production of vegetable oils surpassed 150 million tonnes per year, where palm oil led the production followed by rapeseed and sunflower. The primary vegetable producers are Malaysia and Philippines, which together hold over 30% of the global production.[11] More recent data (2017/2018) demonstrated that these production levels already reached the 185 million tonnes per year.[12]

Although most of the vegetable oils is committed to food production (over 80%), advances in biodiesel area and other bio-based technologies caused a significant increase in its industrial us.[13] In this scenario, epoxidized vegetable oils (EVO) are gaining space as a bio-based bi-functional additive for the polyvinyl chloride (PVC) industry, substituting the highly toxic phthalates plasticisers whilst acting as acid scavengers.[14] Additional examples of the end-use application of vegetable oils in manufacturing can be found in the area of composites through the production of polymerisable resins. Figure 2.3 shows some applications that have already reached commercial maturity. Envirez® resin, an epoxy resin produced by Ashland

(USA) which contains 20-25% of bio-based materials, is currently used for the production of body parts found in some John Deere tractors and Campion Marine boats. Also, bio-based composite musical instrument cases produced by Jakob Winter GmbH (Germany) combine bio-based resins and reinforcing agents such as kenaf, flax and hemp for a higher renewable content. Nevertheless, these applications are only enabled after a chemical modification step, which relies on the exploration of chemical groups in the triglyceride molecular structure.


Figure 2.3: From the right upper corner clockwise: structural part of a Jhony Deere tractor made from partially bio-based resin, boat produced from the same resin and musical instrument cases produced by Jakob Winter GmbH (Germany).

## 2.3 Chemical Manipulation of Vegetable Oils

In most of the cases, the functional groups present in the triglyceride are not reactive enough to enable the direct polymerisation. In this respect, substantial efforts have been devoted to seeking methodologies to chemically modify these groups to tailor the properties of the oils to permit their polymerisation or transformation of these oils into useful chemicals. A field known as oleochemistry has emerged from these efforts and concerns the characterisation and chemical manipulation of vegetable oils and analogues (derivatives, animal fats, *etc.*). The following sections present several methodologies explored in the field oleochemistry in order to exemplify the kind of products that can be synthesised directly from vegetable oils.

### 2.3.1 Exploring the Double Bond Reactivity through Epoxidation

The modification of double bonds to introduce epoxy rings is one of the most traditional transformations in oleochemistry and can be achieved by a series of reactions known as epoxidation. The new functionality (oxirane ring) is highly reactive due to the polarity caused by the heteroatom and the formation of a three-member strained ring. This condition can be visualised through the C-O-C bond angle in the epoxy ring, which deviates from those typically found in analogous non-ringed C-O-C such as ester bonds, Figure 2.4.[15,16] These features highly increases the electrophilicity of the ring, which in turn can afford a versatile range of chemical modifications through a nucleophilic substitution.[15,17] As a consequence of this ring strain, ring-opening reactions of epoxies are typically exothermic, typically associated with an enthalpy of 25-45 kcal $mol^{-1}$ depending on the substituents.[18]

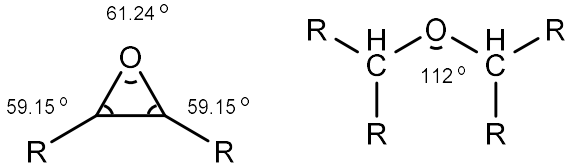


Figure 2.4: Difference of angles in cyclic versus acyclic ester bond.

The chemical transformation of vegetable oils into EVO is an industrially relevant process, with an annual production estimated at 200.000 tonnes. Currently, epoxidized linseed oil (ELO) and epoxidized soybean oil (ESO) are the two most representative bio-based epoxies that have reached industrial production due to a combination of properties and feedstock availability.[4] Interestingly, some vegetable oils naturally contains epoxy groups, such as those extracted from *Vernonia galamensis* and *Acacia albida*. These species are exceptionally rich (up to 40 wt%) in vegetable oils with a content of 80% of vernolic acid and its isomer coronaric acid, respectively (Figure 2.5A and B).[19,20] Despite the possibility of a direct application of these oils as a reactive diluent, the cultivation of these species is restricted to endogenous area. Consequently, it has been preferred to manipulate commodity oils rather than build a platform based on naturally epoxidized oils.[4]

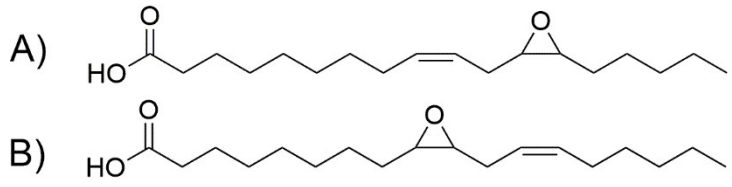


Figure 2.5: Schematic representations of the A) vernolic acid and B) coronaric acid structures.

The number of oxirane groups inserted in the triglyceride dependents on a combination of factors such as the methodology chosen and the number of double bonds available for reaction. Furthermore, scale and purity expected are practical aspects that influence the choice for the most suitable synthetic route. The following sections describe several methodologies explored in the oleochemistry to produce EVO.

**i) Epoxidation Using Peroxides**

The epoxidation based on peracids such as peracetic and performic acids (known as Prilezhaev reaction) is the most traditional methodology in industry, being developed since the 1940s.[21] Low price, relative stability at ordinary temperature and easy availability of chemicals utilised are the principal factors that popularised this epoxidation technique.[22,23] In this reaction, peracid are formed *in situ* using a strong oxidising agent, $H_2O_2$. This molecule acts as the oxygen donor that reacts with the corresponding acid (oxygen carrier) in the presence of a strong mineral acid as catalyst.[24] The addition of $H_2O_2$ should be carried out gradually to avoid the excessive formation of $O_2$ as a consequence of the degradation of the peroxide.[25] As presented in Figure 2.6, the acid and peracid species are present in equilibrium, which is shifted towards the formation of the reactive species as it donates the oxygen atom to the alkene.[4,26] The transition state presents a concerted rearrangement, in which the oxygen addition and the proton shifting occurs at the same time, resulting in conservation of the stereoselectivity.[27]

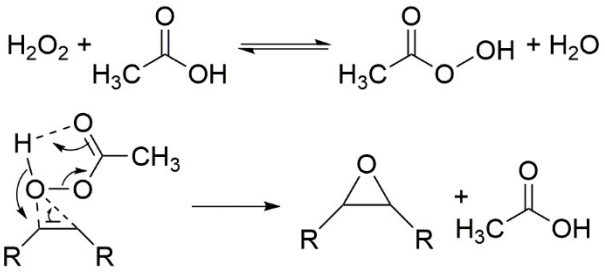


Figure 2.6*:* Formation of the reactive species in the epoxidation using peracid.

Several studies have investigated the influence of different oxygen carriers in parameters such as yield and selectivity. Although La Scala and Wool pointed out performic acid leads to higher substitution rates when compared to peracetic acid, Dinda *et al.* have demonstrated that the former methodology also leads to products with higher iodine value.[28,29] This observation indicated the reduced consumption of the double bonds and the increased the formation of undesired products, therefore acetic acid is preferred for due to better selectivity. According to Petrovic *et al.*, the formation of by-products is associated with lateral reactions involving the opening of the newly formed oxirane ring by nucleophilic species found in this reactive medium, as schematically shown in Figure 2.7.[30]

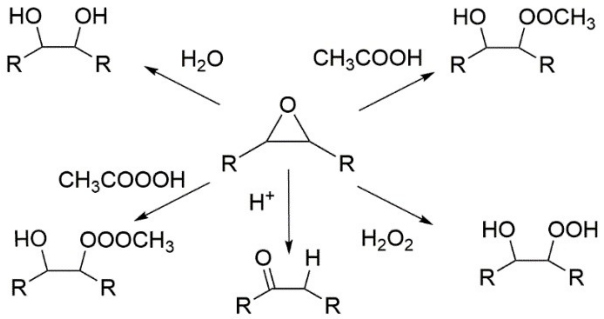


Figure 2.7: Potential side-reactions during the epoxidation using peracetic acid.

Abdullah and Salimon studied the influence of parameters such as the molar ratio of the vegetable oil, oxygen carrier (acetic acid) and oxygen donor (hydrogen peroxide) in the selectivity and conversion.[31] After exploring different scenarios, the authors concluded that the molar ratio of 1:5:2 optimised the epoxidation in terms of avoiding the formation of by-products. Additionally, the effect of acid catalyst was investigated in the epoxidation of cottonseed oil using the $H_2NO_3$, $H_2PO_4$, HCl and $H_2SO_4$, where the latter led to shorter reaction times. Cai *et al.* compared the epoxidation of corn, sunflower and soybean oils in the presence of peracetic acid and $H_2SO_4$, observing that the higher the unsaturation degree of the oil, the higher was the conversion rate and the lowest activation energy.[32] The same study also found that although higher temperatures (75 °C) could lead to higher consumption of the unsaturation sites, the same conditions resulted in more side-reactions such as the ring-opening of the newly formed oxirane ring, compromising selectivity. Therefore, the authors suggested temperatures around 45 °C as a way to balance these effects. Similar findings were reported by Goud and collaborators in the epoxidation of non-edible oils such as Karanja and jatropha oil.[33,34] Since both species are not edible and do not compete with the food chain if used for the manufacturing, they have been attracting attention to technological applications.

The use of acidic ion-exchange resins (AIER) as catalyst is suggested to minimize drawbacks associated with the use of strong acid catalysts, as well as to facilitate the reaction

between species with low reactivity.[35] With the addition of AIER to the reaction, three distinct phases are simultaneously present in the system: (i) the aqueous phase, (ii) organic phase, not miscible with the previous and iii) the AIER catalyst.[35,36] In this regard, the hydrogen peroxide and the oxygen carrier react in the aqueous phase to form the peracid species inside the resin. The peracid is transferred to the organic phase and reacts with the unsaturated sites present in vegetable oil, forming oxirane rings and acetic acid as a by-product, which returns to the aqueous phase.

In this respect, Mungroo *et al.* investigated the peracid-based epoxidation of canola oil (60% oleic acid and 20% linoleic acid) catalysed by AIER (Amberlite IR 120H).[37] The authors found that acetic acid was a more efficient oxygen carrier than formic acid in the presence of AIER, producing EVOs with higher epoxy content. Further improvements have optimised parameters such temperature, molar ratio and AIER loading. Also, the authors highlighted the reusability of the AIER catalyst, with negligible drops in the catalytic activity after five uses. Consequently, the exploration of AIER can be considered a clean and environmentally friendly strategy aligned with the pillars of green chemistry.[38] Similar strategies and results were observed during the epoxidation of Karanja oil, demonstrating that AIER could be reused four times without significant losses.[36]

The kinetics AIER-mediated epoxidation were investigated by Sinadinovic-Fiser *et al.*, who reacted soybean oil with peracetic acid and used a model that took into account the occurrence of side-reactions by ring-opening.[39] The authors observed that AIER was responsible for the adsorption of only acetic and peracetic acids on the active sulfonic sites, in which the rate of the reaction is determined by the irreversible reaction at the surface. The optimisation of the reactional parameters was also investigated, where a conversion of 91% was achieved using a molar ratio of 1:0.5:1.1 (double bond to acetic acid to hydrogen peroxide) and 5 wt% AIER. Similarly to what observed by Mungroo *et al.*, this study demonstrated that temperature and time favour more substituted products, but at the cost of the by-products formation. In terms of alternative strategies, Gurbanov and Mamedov investigated the epoxidation of flax oil using a different kind of ion-exchange resin (chlorinated cation exchanger), which successfully produced EVOs and proved to be highly sensitive to reaction parameter such as temperature and stirring rate.[40]

Despite the broad applicability of reactions based on peracetic and performic, they generally lead to limited selectivities due to the formation of by-products.[41] Additionally, intermediates species can corrode and to reactors in the long term. Therefore, the use of *m*-chloroperbenzoic acid (mCPBA) has been preferred for laboratory scale because it leads to more satisfactory results regarding selectivity, yield and avoids the manipulation of acid species. In solution, mCPBA molecules assume a special conformation due to the presence of intramolecular hydrogen bonds. This arrangement increases the degree of polarisation,

resulting in a highly electrophilic oxygen site.[42] The epoxidation with mCPBA follows a concerted mechanism known as "butterfly mechanism" due to the format of the transitional state, Figure 2.8.[43] Consequently, the epoxidation using mCPBA leads to retention of stereoconfiguration.

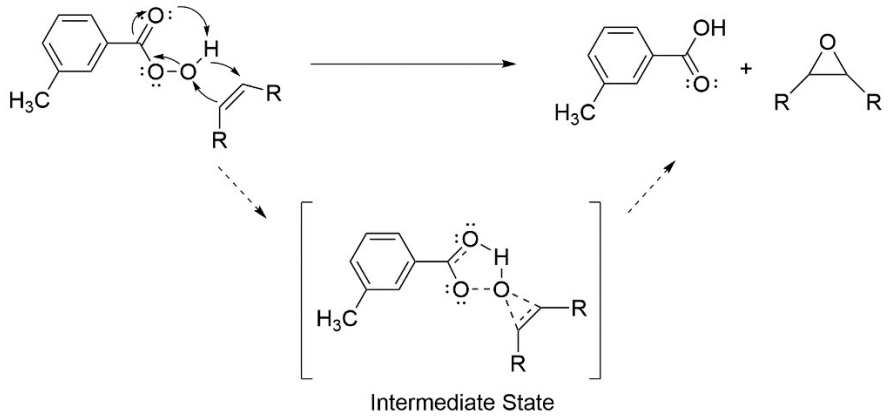


Figure 2.8: "Butterfly mechanism" of epoxidation of a generic alkene with m-chloroperoxybenzoic acid.

**ii) Chemo-Enzymatic Epoxidation**

The epoxidation of alkenes assisted by enzymes dates from the early 90's, and it has been recently rediscovered in oleochemistry due to its ability to suppress the formation of by-products and excellent conversion rates (above 90 %).[22,44,45] The most commonly reported enzyme for this application is the immobilised lipase from *Candida antactica*. The transformation promoted by this enzyme takes places in a two-step process that initially converts the fatty acid into a percaboxylic acid, which is subsequently self-epoxidised, Figure 2.9.[22] The enzyme catalyses only the first step: the step responsible for the insertion of the oxygen atom takes place in solution and is independent of the enzymatic action.[45]

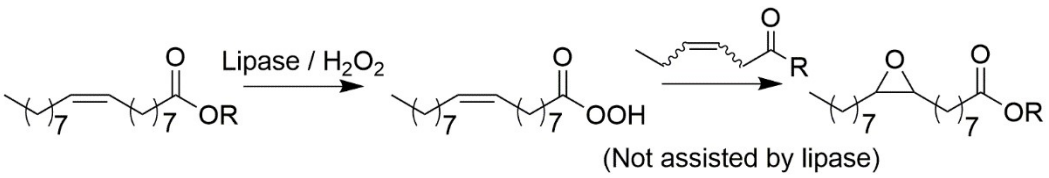


Figure 2.9: Schematic representation of the epoxidation promoted enzymatically by the immobilised lipase from *Candida antartica.*

In one of the earliest works exploring this strategy, Warwel and Klaas reported that the percarboxylic acids were the only intermediate species found during the reaction, and no side reactions were detected.[46] The authors also reported that the lipase was perfectly stable

under the reactional conditions and could be reutilised fifteen times keeping yields above 60 % on a multi-gramme scale. Further studies investigated the direct epoxidation of rapeseed, linseed and soybean oil with conversions always above the 80 % and excellent control of side-reactions.[47]

Several works investigated the optimisation of variables in chemo-enzymatic epoxidation. For example, Orellana-Coca *et al.* studied the epoxidation of oleic and linoleic acids and observed that a molar excess of $H_2O_2$ could lead to faster reaction rate.[48] Nevertheless, the accumulation of unreacted peroxide represents was potential problem, reduction of the enzymatic activity and limiting the reusability. Also, Vclek and Petrovic optimised the catalyst concentration, solvent concentration and the deliberate addition of free fatty acids to the reaction in order to successfully reduce the hydrolysis of the epoxidised triglycerides.[49]

Recently, Sun *et al.* examined the effect of temperature in the conversion of the oil from the *Sapindus mukorossi* (popular species from China),reporting that the substitution is favoured with temperatures up to 50 ºC.[50] After this threshold, temperature negatively affects the reaction by reducing the conversion rate, which was attributed to changes in enzymatic conformation, loss in the catalytic activity and $H_2O_2$ decomposition. Hilker *et al.* investigated the kinetics of enzymatic epoxidation of linseed oil in an enzyme-recycle reactor, separating the aqueous phase (with $H_2O_2$) from the enzyme phase to prevent its deactivation.[45] Kinetic constants and reaction rates were determined using a semi-batch model, and the values proved to be coherent with the predicted. More recently, Liu and collaborators have demonstrated the epoxidation of soybean oil in the presence of butyric acid as a strategy to avoid premature hydrolysis.[51,52] Studies successfully produced ESO in milder conditions in comparison to previous works, bringing chemo-enzymatic epoxidation closer to industrial application.

### iii) Metal-catalysed Epoxidation

More recently, catalytic processes promoted by molecules presenting high-valence metallic centres such as molybdenum, titanium, tungsten and rhenium have been developed with the purpose of promoting highly selective alternative routes for the epoxidation of vegetable oils.[53] Among the most commonly used systems, the ones based on methyltrioxorhenium (MTO) have been widely investigated in the literature. This class of catalysts was firstly used for the epoxidation of olefins by Herrmann *et al.* in the early 90's.[54] Sharpless *et al.* further improved its function by introducing of amines in the structure and reducing side reactions.[55–57] This strategy led to remarkably high yields and controlled selectivity due to a regiospecific mechanism, as schematised in Figure 2.10.[58,59]

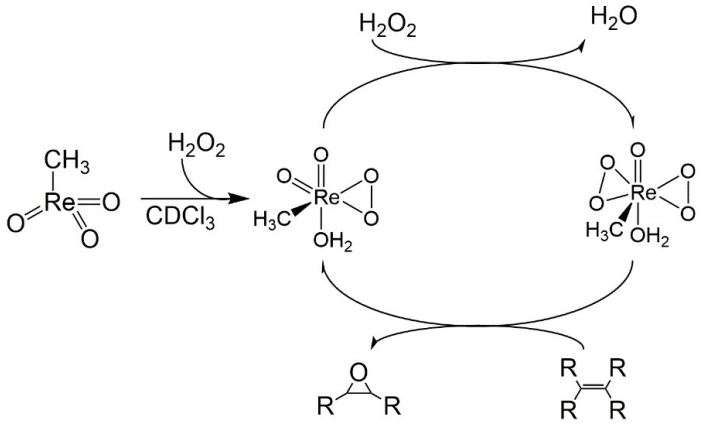


Figure 2.10: Scheme of the catalytic cycle for the epoxidation promoted by methyltrioxorhenium (MTO).

The utilisation of MTO-based systems to epoxidise vegetable oils has been demonstrated by Gerbase *et al.* in investigations of biphasic systems with MTO $CH_2Cl_2/H_2O_2$.[60] This setup was explored to produce ESO with high selectivity and reaction times lower than 2 h. As presented by Cai *et al.*, the manipulation parameters such as temperature, time and equivalents of oxidant contributed to excellent values of conversion and selectivity (> 95%).[61] Furthermore, Daniel *et al.* reported the utilisation of MTO to modify the *Jatropha curcas* oil with quantitative yields.[62] In this same work, epoxidised products were posteriorly functionalized with acetic- or hexanoic anhydrides to increase their reactivity, presenting interesting properties as bio-lubricant. Compared to traditional methodologies, MTO requires lower $H_2O_2$concentrations and reduced reaction times without the need of any assistant Lewis base. [53]

The use of metallic-based systems to modify the oil unsaturations is not restricted to MTO. For example, Campanella *et al.* synthesised ESO using $SiO_2$ impregnated with $TiO_2$ as catalyst, leading to levels of conversion above 90% without evidence of by-products.[63] Also, tungsten-catalysed systems based on Venturello-like reactions were also described in several studies with excellent conversions (> 90%).[64–66] Benaniba *et al.* investigated the kinetics of the epoxidation of sunflower oil catalysed by peroxotungstic acid.[67] Although that conversion using the tungsten-based catalyst was lower in comparison to traditional systems, the catalysed systems using lipophilic analogues such as $WO_5O{=}P(nlauryl_2)(NMe_2)_2$, $C_{12}H_{25}$-$PO_3(WO_5)_2(NBu_4)_2$ ammonium salt and $WO_5O{=}P(Nlauryl_2)_2(NMe_2)$ efficiently increased the conversion rates. An increase of up to 90% was observed at the same time that the formation of diols as by-products was significantly reduced.

**iv) Further Modification of Epoxy Groups**

The increased reactivity observed in epoxidized triglycerides enables further manipulation of these functionalities, and the insertion of new groups via the oxirane ring expands the potential of these oil-derived materials. The most common post-functionalisation strategy is the ring-opening promoted by nucleophilic substitutions, inserting new polymerisable groups in the fatty acid backbone. Usually, alcohol derivatives and dihydroxylation in one pot are formed in this process by acidification, but various additional nucleophiles can be used to generate a diverse range of products. Therefore, this approach permits tailoring the physical-chemical properties of the final resin and enable the utilisation of polymerisation techniques commonly applied to petrochemical-based polymers.[68]

In this regard, Wool and collaborators have extensively explored the acrylation of ESO promoted by acrylic acid, which occurs through the substitution mechanism illustrated in Figure 2.11.[28] In these works, vegetable oils from olive, cotton, canola, soybean, corn and *Carthamus tinctorius* were initially epoxidised via peracid-based methodology and sequentially reacted with the nucleophiles to produce acrylated oils, also refered as AESO resins. These studies established a direct correlation between the oil origin, its reactivity and functionalization rates.[69]

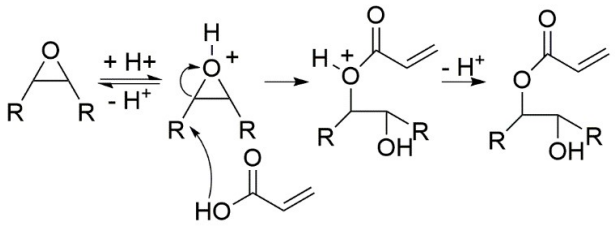


Figure 2.11: Ring-opening reaction with acrylic acid to functionalization with groups acrylates.

Furthermore, the authors described a novel soybean oil functionalization through a two-steps mechanism. The first stage involved the insertion of hydroxyl groups via ring-opening of the modified soybean oil, which was subsequently reacted with maleic anhydride to insert maleates groups (Figure 2.12A). This strategy produced another class of resins referred in literature as maleinated AESO, or MAESO.[70] Similarly, monoglycerides substituted with maleate groups were obtained by the glycerolysis of triglycerides, separating the fatty acid units from glycerol backbone and subsequently reacted with maleic anhydride (Figure 2.12B).[71] One of the main drawbacks of this strategy is the utilization of low-viscosity co-monomers such as styrene, hindering the environmental benefits of the system. Nevertheless, Zhang *et al.* have recently proposed alternative strategies based on the

exploration of vanillin derivatives (Figure 2.12C) to produce fully bio-based networks with $T_g$ above 78 °C.[72]

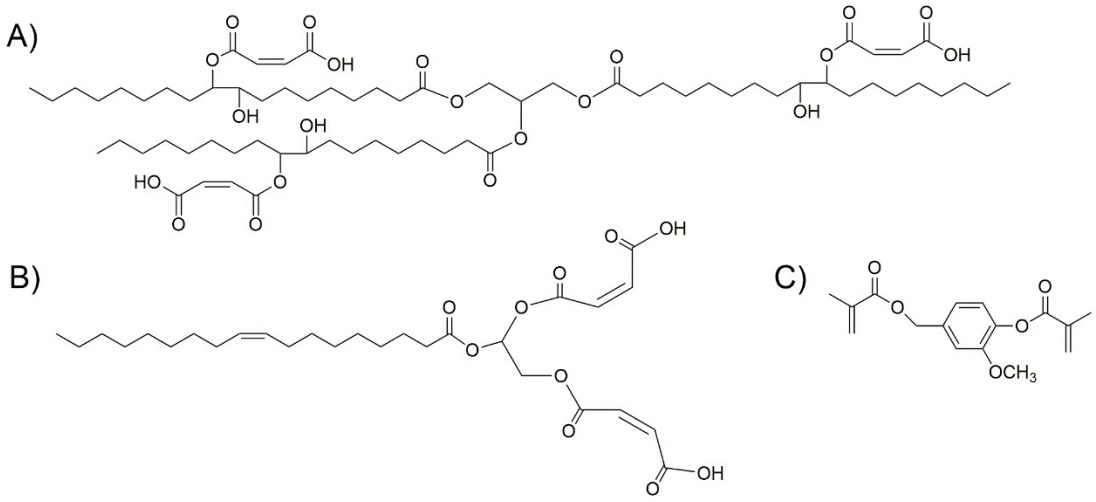


Figure 2.12: Structures of the products of A) hydroxylated soybean oil, B) maleinized soybean oil monoglycerides and C) vanillin derivative used to replace styrene.

The production of similar doubly functionalized vegetable oils was investigated by Skrifvars *et al.*.[73] To synthesise these materials, the ring-opening reaction was conducted with methacrylate acid, leading to an intermediate presenting both methacrylate and hydroxyl groups. The second functionality was introduced by reacting the hydroxyl groups with either acetic or methacrylic anhydrides, producing resins with suitable properties for the production of composites by resin transfer moulding (Figure 2.13).

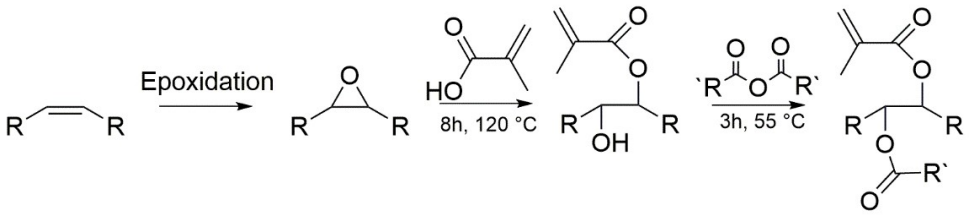


Figure 2.13: Scheme for the production of functionalized vegetable oil with acetates (R = $CH_3$) and methacrylate (R = $C_2H_5$) groups

In addition, the ring-opening of EVO is a valid approach to produce bio-based polyols for the synthesis of polyurethanes. These polymers can be prepared using a diverse range copolymerisation agents, such as isocyanates, toluenediisocyanate and methylene-4,4'-diphenyldiisocyanate (MDI), creating the urethane linkage [-NH-COO-]. An early report in this area by Petrovic *et al.* demonstrated the production of polyols from ESO, which was used to produce polyurethane foams.[74] In this work, authors have optimised conditions such as the

catalyst load, crosslinker load, blowing agent, surfactant and water content. Petrovic and collaborators further investigated the effects of the oil origin[75] and the isocyanate[76] in the resulting properties, as well as different routes to produce the key polyol.[77] Alternatively, authors have extensively explored the use of castor oil as feedstock to produce bio-based polyurethanes as it is both non-edible and rich in ricinoleic acid, fatty acid that naturally presents hydroxyl groups necessary for the creation of the urethane bonds.[78–81] Therefore, castor oil requires less synthetic steps to produce added-value materials.

### 2.3.2 Olefin Metathesis

Metathesis of olefins is a versatile synthetic tool to manipulate the double bond functionality in a myriad of areas. The use of this strategy with unsaturated fatty acids dates from the 70`s in works reported by Boelhouwer *et al.*[82] Recent developments of functional group tolerant-catalysts by Grubbs *et al.* popularised this methodology by making it more versatile, making it an attractive approach to produce monomers from triglycerides.[83] In this mechanism, olefins are converted into new products by the cleavage of C-C double bond that are subsequently reformed through the reaction of the olefin with a transition metal carbene complex.[84] These species form an unstable 4-member ring intermediate that can either be disjointed to form the original materials or produce a new olefin that gradually accumulate in this equilibrium step, Figure 2.14.

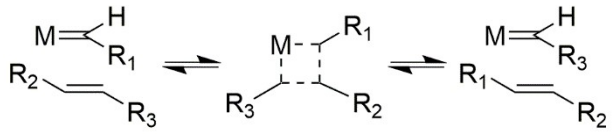


Figure 2.14: Scheme of mechanism for metathesis reaction involving metal carbene complex as intermediate.

Although the self-metathesis of unsaturated fatty acids produces multifunctional compounds, such as 9-octadecene-1,18-dioate obtained from methyl oleate, chemical diversity is limited by the nature of the starting material. In this respect, the development of cross-metathesis, the reaction in the presence of a secondary alkene, permitted the production of more complex esters. This approach significantly expanded the control over the properties of vegetable oil-derived monomers for different applications in oleochemistry. An example of cross-metathesis is found in Figure 2.15, where methyl oleate is reacted with 3-hexene to produce methyl 9-dodecenoate and 3-dodecene.

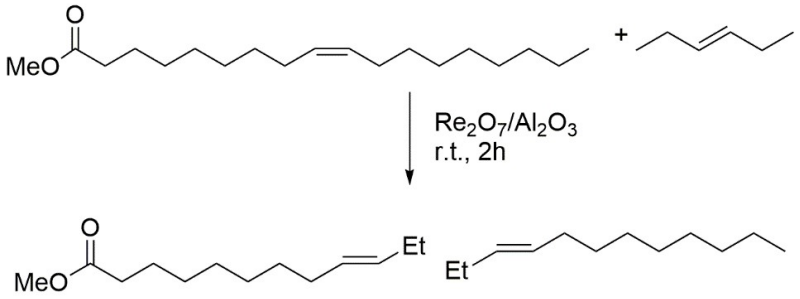


Figure 2.15: Example of cross-metathesis of methyl oleate with 3-hexene.

Cross-metathesis is an effective methodology to produce fatty acid methyl esters (FAME) with smaller carbon chain from naturally long-chain fatty acids to cope with the increasing demand for bio-derived $C_{12}$-$C_{14}$ acid esters for detergent applications.[22] Alternatively, the length of the carbon chain can be increased through cross-metathesis with long-chain alkenes. For example, the reaction of methyl erucate (C22:1) with 1-octadecene produces a 30 carbons-long precursor for 1-triacontanol, an important plant growth stimulator obtained in just two steps.[84] Despite the possibility of competition between self-metathesis and cross-metathesis, the use of excessive molar quantities of the secondary alkene suppress the side-reaction and increase yields of the desired product.

One of the most explored cross-metatheses in oleochemistry is the use of ethene as secondary alkene (also known as ethenolysis). The cross-metathesis of palm oil and ethene catalysed by $WCl_6/Me_4Sn$ was studied Ahmad *et al*., producing mixture of 1-decene, 1,4-decadiene, 1-heptene and the desired product methyl 9-decenoate.[85] The latter product has increased industrial relevance since it is used for the synthesis of bio-based surfactants and polymers. Moreover, the direct cross-metathesis of triolein with ethene in the presence of Grubbs's first-generation catalysts was investigated for the production of triacylglycerol, an interesting intermediate for the preparation of high $T_g$ polyurethanes.[86] The first report of cross-metathesis using methyl acrylates to produce long-chain diesters was presented by Meier *et al.* for the transformation of FAME into long-chain α,ω-diesters, Figure 2.16.[87] This approach proved to be efficient for the production of monomers for polycondensation reactions and precursors for detergents. The following optimisation of reactional parameters increased conversion and selectivity by introducing protective groups in oleyl derivatives, reducing the required amount of catalyst and self-metathesis.[88]

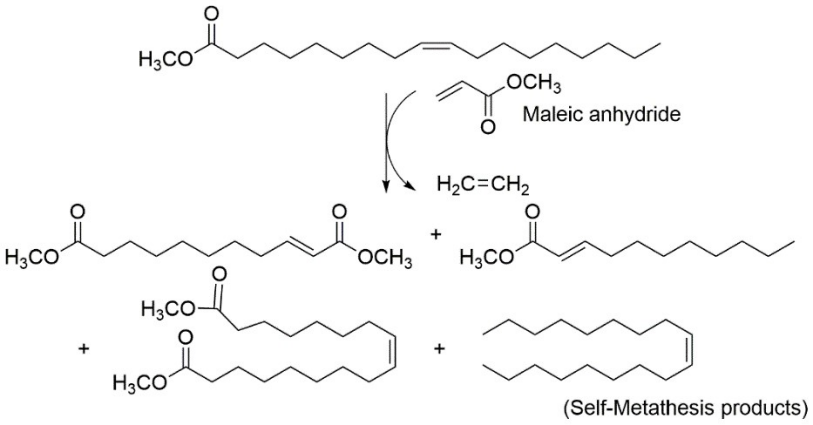


Figure 2.16: Cross-metathesis presented by Meier using methyl acrylates.

## 2.4 Curing Reactions

The conversion of the epoxy resin into a thermoset polymer is achieved through a step known as curing, which is responsible for the transformation of low-molecular-weight monomers into a three-dimensional macromolecular network.[15] This transformation is promoted by the use of crosslinking agents, also known as hardeners or curing agents that can be classified as catalytic or co-reactive. Catalytic curing agents are responsible to initiate the homopolymerisation of the epoxy resin, whereas co-reactive agent acts as comonomers getting incorporated into the polymeric network.[15] The influence of the curing agent is just as critical to the final properties of thermoset polymers as the resin component since they become part of the network structure, hence special attention should be paid to structure and stoichiometry.

Curing agents for epoxy resins are designed to explore the reactivity of the oxirane ring either via nucleophilic reactions in the carbon or electrophilic reactions in the electron-rich oxygen site. Features of the chemical structures of EVOs such as sterical hindrance and electron donating alkyl chain make the curing reactions based on nucleophiles slower in comparison to terminal epoxies (glycidyl) such as those found in the diglycidyl ether of bisphenol A (DGEBA). However, the same characteristics enhance the reaction rate for electrophilic curing agents so in many aspects the EVOs resemble the reactivity of commercial cycloaliphatic epoxies rather than DGEBA.

### 2.4.1 Nitrogen-Containing Agents

Aliphatic amines such as ethyleneamines were among the first curing agents used back in the 1950s.[15] The early utilisation of these compounds lies in their simplicity and predicted reactivity with epoxy rings due to its high reactiveness associated with the terminal polyfunctional groups.[89] The mechanism proposed for the cure between these components is presented in Figure 2.17. Structural aspects of ethyleneamines such as the small carbon chain

that connects the active sites make them capable of producing tightly cross-linked structures that will produce materials with remarkable mechanical properties and solvent resistance. In addition, the generally low molecular weight of these compounds translates into low viscosity, which is highly desirable to facilitate the resin processing. However, this same characteristic means that these compounds are volatile and present problems associated with their handling. Also, some aliphatic agents present relatively poor compatibility with some epoxy resins, which can provoke migration to the surface and result in materials with tacky surfaces.

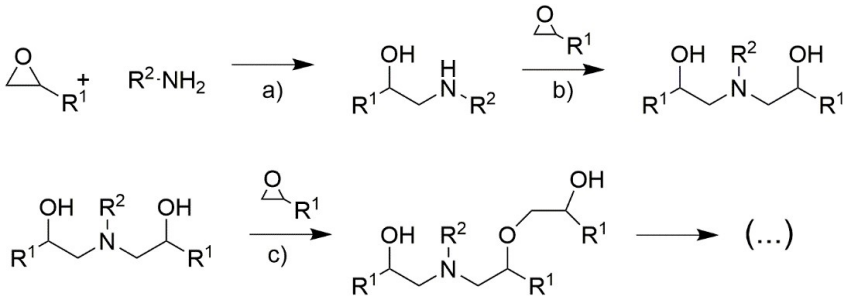


Figure 2.17: Mechanism of curing of epoxy groups with aliphatic amines.

Aliphatic polyamine as curing agents have risen as an alternative to overcome the problems associated with the volatility and toxicological effects of ethyleneamines. These materials are originated from the condensation of carboxylic acids and aliphatic amines, and curing agents with distinct properties are obtained from the variations in the ratio of these components. Low-molecular-weight polyamines have low viscosity and high reactivity and are generally used along with liquid epoxy resins in solid coatings, sealants and adhesives. On the other hand, high-molecular-weight polyamines and aromatic polyamines are used in corrosion-resistant coatings with solid epoxy resins. The rigid backbone from the diacid is responsible for providing chemical resistance and water-repelling properties but also alters the colour due to the presence of unsaturations.[15]

In comparison to aliphatic amines, polyamines cure more slowly and the aspect of the final material is generally is greasy due to exudation, which can be overcome by the use of tertiary amine accelerators. In the absence of hydrogen donors, the epoxy group and tertiary amine form a zwitterionic adduct that promote the anionic polymerisation of the epoxy group (Figure 2.18). With hydrogen donors (*e.g.* hydroxyl groups) the reaction is carried out through a mechanism that involves a two-step initiation. Imidazoles can be also used as catalysts at high to moderate temperatures, forming adducts with reactive alkoxide groups. The presence of compounds containing hydroxyl groups such as phenol, alcohol, water and some acids accelerate the curing reaction mediated by amines by the formation of a trimolecular complex that assists the amine group to perform the nucleophilic attack.[90]

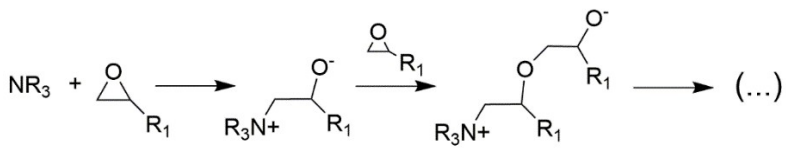


Figure 2.18: Formation of a zwitterionic adduct between tertiary amine and epoxy ring.

Cycloaliphatic amines were also investigated to produce materials with increased molecular stiffness in comparison to aliphatic amine agents, Figure 2.19. Nevertheless, their cure rate is slower than aliphatic analogous, limiting its commercial significance. They are liquid at room temperature, characteristic that is desirable from a processing standpoint, but also volatile, presenting safety hazards. In this class, *para*-aminocyclohexylmethane (PACM) has been preferred due to its lower steric hindrance that translates in higher reactivity and more efficient use at room temperature.[15]

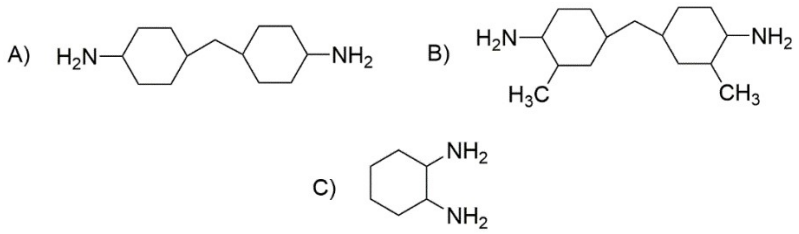


Figure 2.19: Representative aclycloaliphatic amine hardeners. a) 3,3`-dimethylmethylene-di(cyclohexylamine), b) *para*–aminocyclohexylmethane (PACM) and c) 1,2-diaminocyclohexane (1,2-DACH).

Aromatic polyamines, Figure 2.20, are less basic in comparison to cycloaliphatic and aliphatic polyamines as part of the electron-density is compromised with resonance structures. Consequently, these molecules react more slowly with the epoxy resin and require elevated curing temperatures. However, these characteristics can be exploited to increase the formulation pot life. As most of the aromatic amines and polyamines are solid, heating is required to facilitate the mixing with the epoxy resin. Meta-phenylenediamine (MPD) agent presents the shortest aromatic moiety possible, and therefore the curing of epoxy resins with this agent leads to materials with the tightest cross-linking density possible and excellent solvent resistance. Additionally, 4,4'-diaminodiphenylmethane (DDM) agents present a low polar structure that can be incorporated into epoxy resins during the curing to produce materials combining electric insulation and good mechanical properties.[15] Nevertheless, the potential carcinogenic effects associated with DDM forced the replacement of this compound by other less harmful.

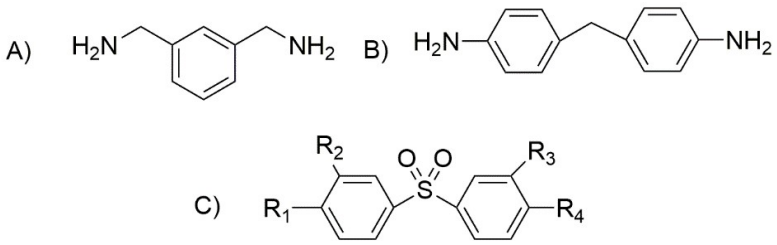


Figure 2.20: Representative aromatic amine hardeners: a) meta-phenylenediamine (MPD), b) 4'-diaminodiphenylmethane (DDM) and c) 4,4`-diamino-diphenylsulphone (DDS).

Regarding the application of amine-based agents to cure EVO, this reaction is less efficient due to lower reactivity of epoxy groups positioned internally in the fatty acid chains as they are less susceptible to nucleophilic attacks. Additionally, ester groups can react with primary amines (aminolysis) to form alcohols and amides adding by-products to the final formulation. Consequently, a limited number of works have explored this particular systems to produce bio-based networks. Studies carried by Wang *et al.* explored the cure of EVO with polyamines, investigating the curing mechanism of different EVO/polyamide systems through NMR and FTIR.[89] Authors have found that the ring-opening reaction of adjacent epoxy rings takes place just in one of the groups due to steric hindrance. In addition primary amines, although more reactive, led to aminolysis reactions that was avoided by using secondary amines. Similar findings were reported by Miao *et al.* for systems cured with PACM.[91] The study found that aromatic polyamines would lead to no cure with ESO, whereas triethylenetetramine-based systems presented rubbery characteristics and PACM was capable of increasing the $T_g$ of the cured system.

Furthermore, Manthey *et al.*[92] observed the occurrence of the autocatalytic process during the curing of epoxidized hemp oil with triethylenetetramine (TETA) and isophorone diamine (IPD). Systems using a mixture of the triethylenetetramine /IPD were investigated and proved to produce maximum conversion, where increments of IPD increased the curing rate. The dependence of the mechanism type with the curing temperature was also identified by del Rio *et al.*.[93] In the study, authors observed an autocatalytic curing mechanisms at a lower temperature but non-autocatalytic processes at higher temperatures, which led to aminolysis and consequently produced thermoset polymer with unsatisfactory mechanic performance.

### 2.4.2 Anhydrides

The mechanism of curing induced by anhydrides is considered a complex competition between several reactions. It is acknowledged that the first step is the formation of the carboxyl group from the combination of anhydride and a hydroxyl groups, which reacts with the epoxy ring forming a hydroxyl diester. This species can further react with another anhydride group to form a new carboxyl group, propagating the network creation. In the presence of tertiary amines or imidazole, the mechanism is accelerated by the formation of a carboxylate ion. This species acts as a nucleophile and lead to a ring-opening reaction of the epoxy ring, generating an alkoxide that ring-opens an anhydride to form another carboxylate and to give sequence to the chain of events that create the polymer.[15] Figure 2.21 represents the suggested mechanism of curing without the presence of catalysts. Also, compounds such as Lewis acids (e.g. $BF_3$ – latent amine complexes) and tetra-alkylammonium salts are known for activating the epoxy centre and catalyse the transformation although the mechanism behind these transformations is yet not understood entirely.[89]

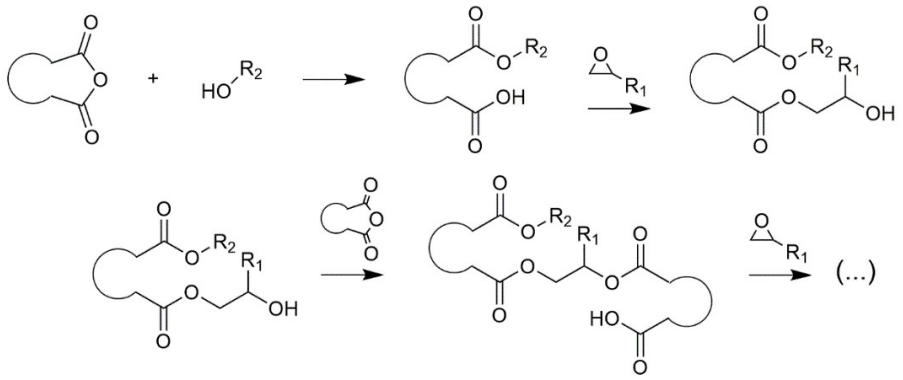


Figure 2.21: Mechanism of curing of epoxy groups with dicarboxylic cyclic anhydrides.

Dicarboxylic cycloaliphatic anhydrides represent the most important class of anhydride agents, and their use has been favoured for being liquid at room temperature and the properties conceded to the final materials, Figure 2.22. Despite the molecular stiffness and low price, phthalic anhydride (PA) is solid at room temperature and is difficult to handling due to its tendency to sublimate.[94] Consequently, cyclic anhydrides with lower melting temperature such as MHHPA, MTHPA and MNA have been preferred to produce networks with EVO.[95]

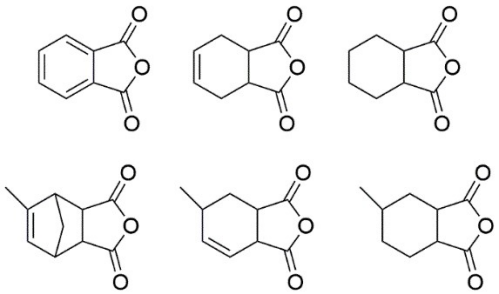

Figure 2.22: Structure of the most common dicarboxylic curing agents. From the top-left corner clockwise: phthalic anhydride (PA), tetrahydrophthalic anhydride (THPA), hexahydrophthalic anhydride (HHPA), nadic methyl anhydride (NMA), MTHPA methyltetrahydrophthalic anhydride (MTHPA) and methylhexahydrophthalic anhydride (MHHPA).

Anhydride agents have been preferred as curing agent for EVO over amines due to their enhanced reactivity with internal epoxy groups.[90] As previously mentioned, amine agents display sluggish reaction rates as consequence of the incompatibility between the nucleophile and the electron-rich centre found in the EVO. On the other hand, the reaction with anhydrides has an electrophile nature that is favoured by the presence of the triglyceride-based species. The mechanical and thermal properties of ESO cured with a range of anhydrides were investigated by Gerbase *et al.*[96] Succinic anhydride (SUC), hexahydrophthalic anhydride (CH), PA, MA and dodecenylsuccinic anhydride (DDS) were investigated in this study and thermoset polymers produced in the presence of initiators triethylamine (TEA), N,N0-dimethylaniline (ARO) and 1,4-diazobi-cyclo[2,2,2]octane (DABCO). Both properties proved to be sensitive to variations in the curing agent, concentration of initiator and anhydride/epoxy molar ratio. Materials with $T_g$ ranging from −16 to 65°C were prepared, where systems cured with PA, MA or CH presented higher $T_g$ due to the inherent rigidity of the chemical backbone.

Rosch *et al.* reported similar results for ESO systems cured with dicarboxylic anhydrides in the presence of tertiary amines, imidazoles, or aluminium acetylacetonate.[97] The authors revealed a strong dependence between the rigidity of the anhydride and properties such as cross-link density and $T_g$ ; HHPA and SUC resulted in rubbery solids whereas rigid anhydrides such as rigid MA and PA produced stiff materials with $T_g$ up to 73 ºC. In terms of using vegetable oils from residual sources, Clark *et al.* have investigated the valorisation of grapeseed oil, a mixture of triglycerides obtained as secondary product in the wine industry, to produce resins that were compared to analogues produced from soybean and rapeseed.[98] The authors have cured the system with MTHPA and MNA in the presence of 4-methylimidazole, producing networks with high $T_g$ (62 °C) that were competitive versus the commodity oils. Also, Clark *et al.* observed an interesting balance between the rigidity of the

anhydride (reflected in the $T_g$ values) and the crosslinking density, which was negatively affected by the hardener with a bulkier backbone due to steric hindrance.

Variations in the epoxy/anhydride ratios (known as *R*) affects the network structure and consequently the mechanical performance of the resulting thermoset. Martini *et al.* demonstrated by curing linseed oil-based systems with different dicarboxylic anhydrides ratios, where the maximum cross-link density was achievable at $R = 1.0$. Higher R values could lead to reduced cross-link density, where and excess of anhydride increased the stiffness (and the $T_g$) of the cured material at the cost of chain mobility.[89] Liang *et al.* investigated the kinetics of cure for of ESO derivatives and MTHPA/MHHPA by DSC and rheology, detecting an autocatalytic behaviour with reaction order approximately 2.[99] Similarly, Boquillon *et al.* investigated and modelled the kinetics of curing of ELO with THPA catalysed by 2-methylimidazole based on DSC, which in this case revealed that the curing reaction follows first-order kinetics in this case.[100]

## 2.5 Application of Vegetable Oil-Based Chemicals

Previous sections covered some of the most significant methodologies used to introduce reactive polymerisable groups and to produce networks from triglycerides, enabling further technological applications for vegetable oils. The next sessions further expand the discussion about the application of these oils, with particular focus to literature in the polymer science field. A more extensive discussion of the use of vegetable oil-based resins for the production of composites materials is presented in Chapter 3.

### 2.5.1 Bio-Based Blends

Although the literature offers a vast collection of studies using EVO to produce thermoset polymers, structural characteristics of vegetable oils such as long aliphatic chain and low functionality directly affect the resin reactivity. These features will consequently originate thermoset polymers with lower glass transition temperature and inferior mechanical performance when compared to commercial resins.[101] To overcome these drawbacks, partially bio-based blends of EVO and commercial epoxy resins have been extensively explored to marry an increased bio-based with enhanced mechanical properties. DGEBA resins have been used due to their importance and prevalence in the epoxy resin market.[102] Structural features such as aromatic rings concede appreciable mechanical properties to thermosets produced from DGEBA, and the presence of ester bonds increases the reactivity of the terminal oxirane ring. Nowadays, nearly 90% of the world production of epoxy resins is based on the reaction between Bisphenol A. Figure 2.23 presents the chemical structure of the DGEBA along with

the curing mechanism in the presence of imidazole, which is similar to those discussed for EVO.[15]

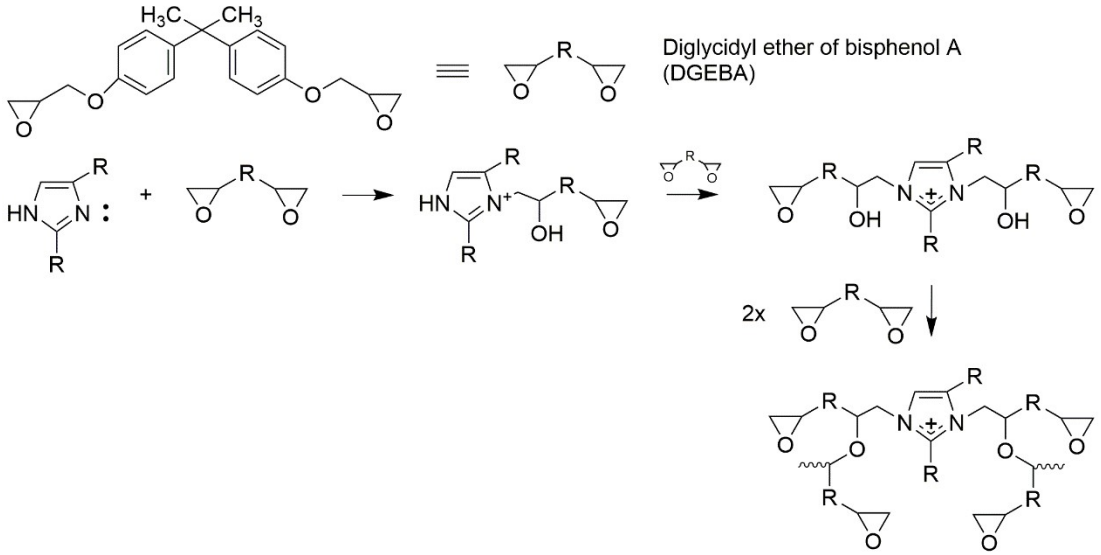


Figure 2.23: Chemical structure of the diglycidyl ether of Bisphenol A (DGEBA) along with the curing mechanism in the presence of imidazole.

Physical-chemical properties of ESO blends with DGEBA (from 0 to 60 wt%) in the presence of the cationic catalyst N-benzylpyrazinium hexafluoroantimonate (BPH) were examined by Jin and Park, who observed the influence of the oil content on impact properties and adhesive strength.[103] ESO proved to be a useful impact modifier, significantly increasing the impact strength by 58% when 60 wt% of the bio-based material was added to the formulation. Also, the bio-based epoxy is positively affected the adhesive strength, particularly at the content of 40 wt%, which was attributed to the reduced internal stress in the more flexible networks produced with ESO. ESO/DGEBA blends (from 0 to 100 wt % of bio-based epoxy resin) cured with MNA were investigated in further studies.[104] A sequential decrease in several properties (storage modulus, $T_g$ and thermal stability) was observed when a higher content of ESO was added due to the reduced rigidity of ESO backbone in comparison to DGEBA and a plasticization effect. Ratna *et al.* investigated the pre-polymerisation of ESO before blending with DGEBA with TETA hardeners as a strategy to achieve improved properties.[105] Compared to non-modified ESO, phase separation was reduced as observed by DSC and SEM. In terms of mechanical properties, this feature translated into superior impact performance, (particularly when 20 wt% of modified-ESO) since the resin did not act purely as a plasticiser.

Park *et al.* examined similar systems based on the blend of epoxidized castor oil (ECO) and DGEBA.[106] Partially bio-based networks produced in this work presented excellent thermal stability. The authors detected the influence of bio-based content on different properties, such as peak maximum temperature, cure activation energy, initial decomposition temperature and temperature of maximum degradation rate. Based on DSC studies of ESO and ECO systems, Jin *et al.* determined that the curing behaviour of blends could be drastically changed due to the difference in epoxy number and reactivity.[103] Crosslinking density, peak of maximum temperature and heat of reaction were lowered by the sequential increment of up to 80% of EVO in comparison to a DGEBA reference. With these results, the authors identified the influence of the EVO content in the phenomena behind network creation.

Blends of epoxidised crambe oil (ECRO) and epoxidized rapeseed oil (ERO) with DGEBA and DDM were prepared by Raghavachar *et al.*.[107] SEM images revealed differences in the distribution of the bio-based phase depending on which oil was used. Also, the toughness of these materials was increased by 100% when 10 wt% of ECRO was added to the blend. In an interesting approach presented by Roudsari *et al.*, DGEBA blends with ESO cured in the presence of the sebacic acid from castor oil as hardener.[108] The authors investigated the kinetics of cure and have found that this system followed an autocatalytic behaviour. In comparison to traditional amine hardeners-based systems, the blends presented lower values of $T_g$ due to reduced cross-link density and increased flexibility of the bio-based hardener.

Although less frequent, the literature also presents studies with blends produced with diglycidyl ether of bisphenol F (DGEBF, Figure 2.24) and a range of EVOs. For example, properties of DGEBF/ELO blends cured with MTHPA and poly(oxoproprylene) triamine (POPTA) were investigated by Miyagawa *et al*.[109,110] The authors observed a reduction of both storage modulus and tan δ when the bio-based content was increased due to a plasticization effect. Nevertheless, this decrease was only prominent after 20 wt% of ELO in the system, thus demonstrating the properties can be maintained by using the appropriated formulation. More interestingly, the impact strength of these blends was significantly increased with the bio-based content, which was attributed to the superior flexibility of the chains. Later, the same authors examined the fracture toughness and impact strength of blends using both ELO and ESO (in contents ranging from 0 to 50 wt%) with DGEBF.[111] These systems were cured with MTHPA in the presence of methylimidazole as an accelerator. Similarly, significant improvements were achieved in the Izod strength and fracture strength.

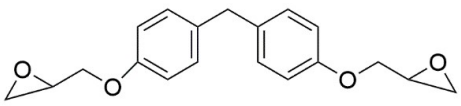

Figure 2.24: Chemical structure of diglycidyl ether of bisphenol F (DGEBF).

### 2.5.2 Functional Monomers

Thanks to their chemical versatility, modified triglycerides can also be used in other fields of polymer science other than for the production of thermoset resins, and significant efforts have been devoted to produce linear and processable thermoplastics from vegetable oils. One of the most prominent strategies is the transformation of fatty acid into bifunctional monomers to enable polycondensation and polyaddition reactions. For example, the reaction of diacids such as diesters and diacid chlorides with diols or diamines can produce respectively polyesters and polyamides, which represent polymeric systems of great commercial significance.

Several methodologies are reported for the conversion of fatty acids into diacids. Among these approaches, ozonolysis is the most industrially significant, consisting of the oxidation of the double bond to yield an acid and diacids mediated by ozone (Figure 2.25).[112] Alternatively, the oxidative cleavage of the alkene section can be performed using metallic catalysts based on tungsten, tantalum, molybdenum, zirconium, and niobium in the presence of $H_2O_2$.[113,114] Sodium hypochlorite-assisted oxidation is a third methodology commonly explored to produce these product.[4] Even though the literature presents alternative routes for the traditional ozonolysis, none of them has achieved effective commercial significance so far.

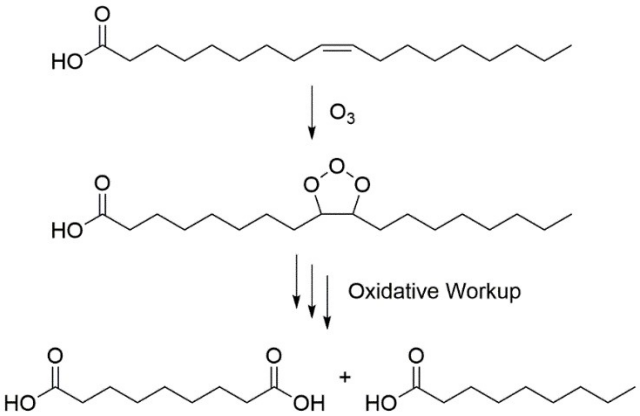


Figure 2.25: Scheme of ozonolysis of methyl oleate to produce a diacid.

Based on these transformations, bio-based polyamides are being currently produced in industrial scales from 11-amino-undecanoic acid from castor oil (Figure 2.26). These methodologies have gained rapid commercial interest because they use the same principles applied to petroleum-based equivalents.[115] Products are obtained through the cross-condensation of diacids produced from ozonolysis and diamines in a two-step mechanism. Additionally, polyamides can be obtained via self-condensation polymerisation of amino acids (*e.g.* in the case of 11-amino-undecanoic acid transformation into polyamide-11) performed directly in an autoclave where the melted reactant is polymerised under an inert atmosphere.

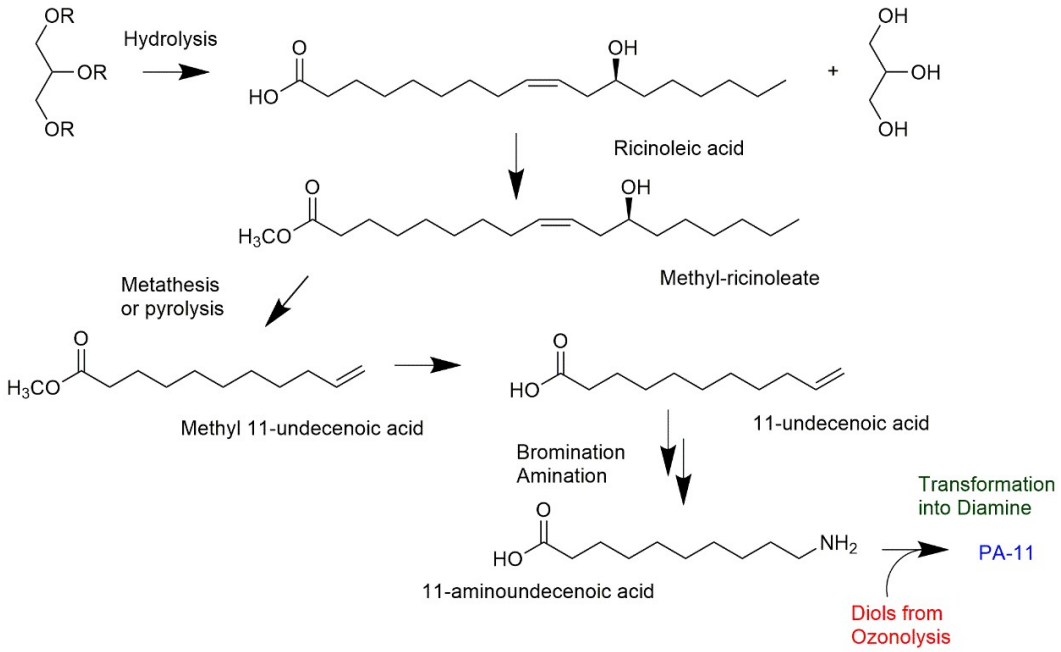


Figure 2.26: Scheme of the synthetic route for the production of PA-11 from castor oil.

Similar concepts can be explored to produce bio-based polyesters-derived polymers as presented by Hojabri *et al*.[116] Four aliphatic poly(ester-urethane)s (PEUs) were synthesised from azelaic acid, which in turn was obtained from vegetable oils through ozonolysis and oxidation. The diacid produced in this transformation is a versatile unit as it was used both in the polyester backbone by combining it with 1,9-nonadiol and in the di-isocyanate for the creation of urethane bonds, Figure 2.27. The same work demonstrated that changes in the molecular-weight of the polyesters segment affected the melting point, crystallinity and tensile properties of the resulting polymer.

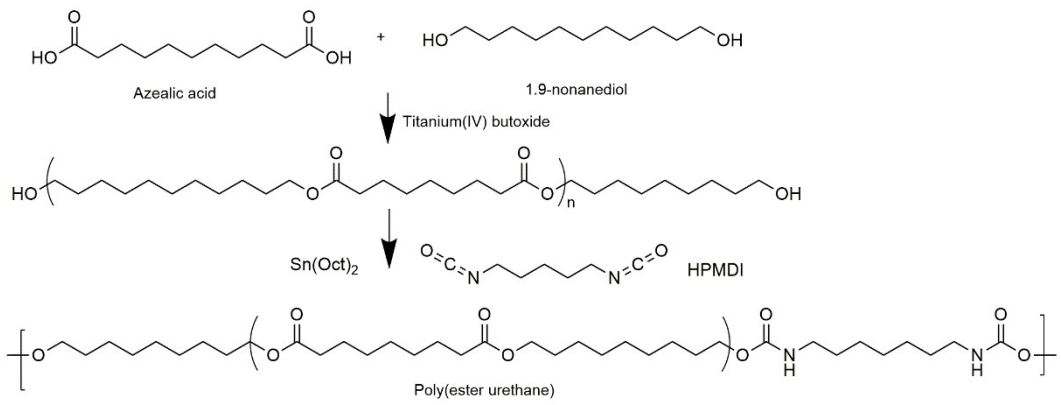


Figure 2.27: Production of bio-based poly(ester urethanes) from azelaic acid.

Monomers produced from metathesis reactions are useful building blocks for the synthesis of a variety of linear polymers, Figure 2.28. According to Meier, polymerisation techniques such as ring opening metathesis polymerisation (ROMP) and acyclic diene metathesis (ADMET) polymerisation can make use of the terminal double bonds to build up polymeric chains.[117] Warwel *et al.* reported the metathesis of FAMEs using first generation Grubbs catalyst to produce a ω-unsaturated fatty acid that was subsequently converted into polyolefins, polyesters, and polyethers via ADMET.[118] Rybak and Meier produced high-molecular-weight aliphatic α,ω-dienes from the ADMET polymerisation of 10-undecenyl-10-undecenoate from castor oil, producing ABA triblock.[119] Further studies demonstrated the synthesis of unsaturated polyamides via two different chemical routes (amidation and metathesis) that started from methyl-10-undecenoate.[120] A new level of customisation can be achieved through the direct conversion of bio-based polyesters into polyethers using gadolinium-based reduction, as recently reported by Dannecker *et al.*, further expanding the application scope of these polymers.[121]

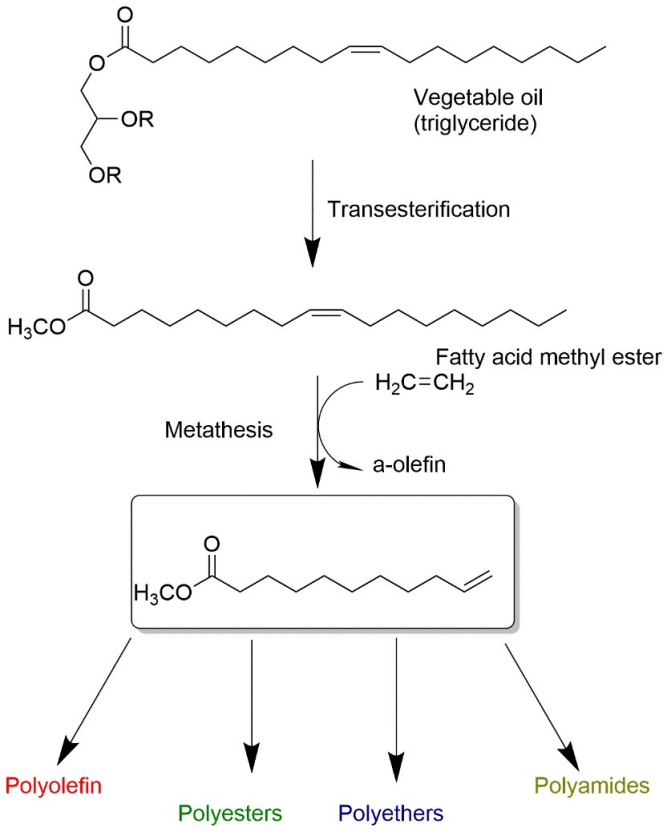


Figure 2.28: Scheme of synthetic route for the production of different polymers from metathesis products.

## 2.6 Waste Vegetable Oil: A More Sustainable Source of Triglycerides

Although significant efforts have been devoted on the creation of a new platform based on vegetable oils, the broad applicability of these materials is still restricted as their performance/cost balance is unfavourable, particularly in the thermoset resins. Additionally, data suggesting a proportional increase of the use of vegetable oil for other chemical applications (resins, plasticisers, biodiesel, *etc.*) opens space for debates about the ethical land use for growing of biomass for the food chain *versus* engineering platform.[13] Reports from organisations concerning food administration and regulations highlighted that the utilisation of fertile lands to produce biofuels compromise the land available for food crops and potentially contribute to inflated prices of feedstock (although there is no formal consensus regarding this issue).[10,122] These questions motivate the search for alternative, low-cost triglycerides sources that do not compete as feedstock to enable the development of a oleochemistry that is more sustainable and affordable. Even though some non-edible oils (karanja and jatropha oils, for example) arise as interesting alternatives to solve this dilemma, their production still confined to local production thus its production on a larger scale is limited.

In this scenario, waste vegetable oils (WVO) produced from the frying process appears as potential and yet underexplored candidates to fulfil the need for eco-friendly resources for technological application. WVO are produced in large quantities all over the world as the majority of cuisines use vegetable oils in food preparation.[123] Other sources of waste oils not linked with frying process are triglycerides treated as residual products of industrial processes, such as the WVO from grapeseed derived from wine making.[98] Nevertheless, this thesis focus only in the valorisation of oils recovered after the frying process, although the methodologies herein developed are transferable to other feedstock.

According to data from 2012, it is estimated that the E.U. is responsible for the production of approximately 700.000 tonnes of WVO from frying per year. In China, the figure reaches a total of 4.5 million tonnes per year. Meng *et al.* pointed out that roughly 50% of the Chinese WVO is potentially recoverable through the creation of an integrated collection system, which could be translated in an added-value activity.[124] As these materials are produced in abundance and are ultimately treated as waste, the costs exploring WVO is a platform of triglycerides is estimated to be approximately three times lower in comparison to the neat vegetable oil.[125,126] This is an interesting feature from the point of view of improving the balance between properties and costs of bio-derived materials since resulting materials can be more affordable.

In addition to the economic aspect, the valorisation of waste vegetable oils appears as an alternative for ecological problems associated with incorrect disposal of WVO. Common

household waste treatment procedures are not effective in removing WVO, creating "*fatbergs*" in the sewers and adding to the cost of efluents.[127,128] In developing countries, this is an even more serious problem since a large portion of these oils are disposed of incorrectly in menial ways.[129] When in contact with water, WVO forms a superficial layer due to its reduced insolubility in water and low density, decreasing the interfacial gas exchange rate between the air and the aqueous medium. Consequently, the levels of dissolved oxygen are severely affected, leading to the oxygen depletion and critically compromising the quality of aquatic life.[130,131] Also, fatty acids formed from the hydrolysis of vegetable oil in aqueous medium present considerable toxicity to some important aquatic microorganisms, for example inhibiting the growth of mussels.[132]

Apart from the environmental issues, the mishandling of WVO is a social health problem that has been growing in China and Southeast Asia.[133] The production of a material known as gutter oil is an illicit practice that consists of the reutilization of waste oil collected from restaurants or sewers as frying medium or for animal consumption. [133,134] These oils are mixed with other fats collected from grease traps and slaughterhouse waste, resulting in a material that contains high levels of toxic compounds such as polychlorinated biphenyls (PCBs) and dioxins.[135] Therefore, the creation of potential new uses for WVO through its valorisation as an added-value chemical can disincentive its incorrect disposal, bringing ecological and social benefits.

### 2.6.1 Physical and Chemical Transformations during the Frying Process.

The most significant challenge associated for the implementation of WVO as manufacturing platform is their heterogeneity, both embedded as a natural material and as a consequence degradation during frying.[136] This process causes a series of transformations triggered by the combination of heat, air, and water contained in the foods, leading to a chain of reactions that affects the physical-chemical of the oil and generate a complex mixture of compounds. Parameters such as the nature of the food being fried, the characteristics of the oil and the conditions in which the frying is conducted are closely related to the degradation process.[137] By-products of these processes range from volatiles released with steam to high-molecular-weight compounds that remain in the medium after the frying process is ceased. Over 400 different chemical species are identifiable in waste vegetable oil after the deep frying process.[138]

During frying, the viscosity and acidity of the oil increases, and the oil becomes darker and develops an unpleasant odour due to the formation of oxidised products, and these changes can be quantitatively measured by techniques such as titration and rheology. Furthermore, the accumulation of these species compromise the nutritional aspects of the oil. Despite the

complexity of this process from a chemical point of view, Choe and Min highlighted these reactions can be classified into three classes of chemical transformation: hydrolysis, oxidation and polymerisation.[139] All three degradation mechanisms are considered interconnected and superimposed, co-occurring during the frying process, Figure 2.29.

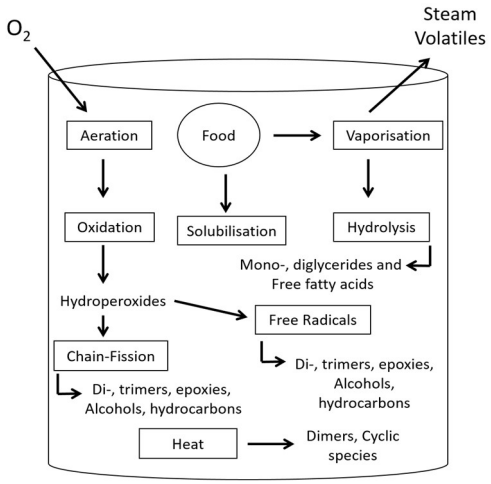


Figure 2.29: Scheme representing the simultaneous changes in the vegetable oil caused by the frying process.

### i) Hydrolysis

Water naturally contained in food or resulting from freezing generates bubbles and steam upon heating, creating a reactive atmosphere combining oxygen and water at elevated temperatures. In this scenario, the water molecules are reactive enough to act as nucleophiles, cleaving the ester groups linking the fatty acid chains to the glycerol backbone. As a result, diglycerides and free fatty acids are formed as degradation products. However, the reaction is not ceased at this point: sequential cleavage can occur at prolonged times or increased temperatures so that the ester linkages are continuously broken to yield monoglycerides and eventually the total fractionation of triglycerides into fatty acids and glycerol (Figure 2.30). Interestingly, it was observed that the steam blanket formed by during the frying process helps in the prevention of thermal oxidation.[140]

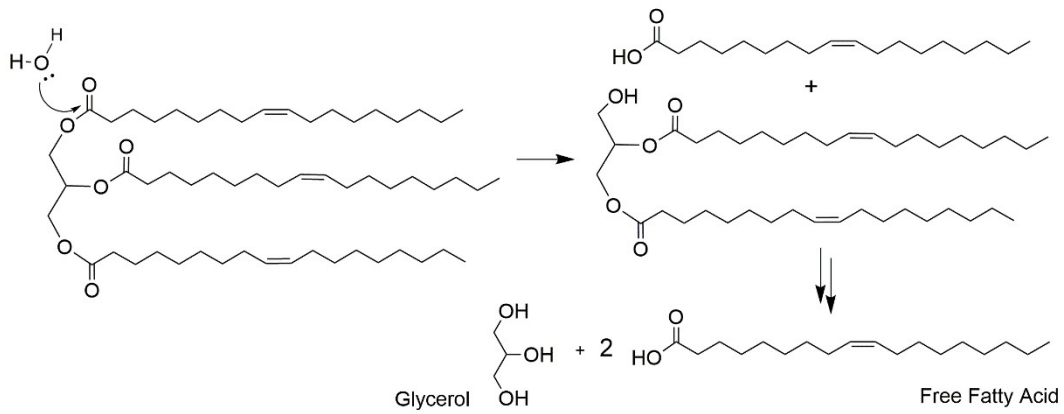


Figure 2.30: Hydrolysis of triglyceride producing free fatty acids and glycerol.

The mechanism demonstrates that the extent of the hydrolytic degradation can be tracked through the detection of mono- and diglycerides. Free fatty acids naturally accumulate due to the hydrolytic reaction, and increase the acidity and the polar content of the oil.[141] Nevertheless, it is noteworthy that some of the free fatty acids formed by this mechanism are lost during the frying process and/or are converted into different species.[142] Therefore, the acid content cannot be used as a direct parameter to follow the degradation quantitatively. As this reaction is conditioned to the presence of water in the frying medium, foods with a higher amount of water lead to an increase in the formation of hydrolysis products.[143] Choe and Min demonstrated that the formation of hydrolysis products is increased by the number of frying cycles due to the accumulation of water in the oil.[144] According to Batisda *et al.* and Paul *et at.* the formation of such compounds can be reduced by the frequent addition of fresh vegetable oil throughout the frying process.[138,145]

**ii) Oxidation**

Thermoxidative reactions take place due to the association of oxygen and temperature, following similar mechanisms to those observed in autoxidation reactions. Three distinct stages are described in transformation: initiation, followed by a step of propagation and a termination. The initiation step is dependent on the nature of the fatty acids since it is triggered by the formation of an allylic radical in a particularly labile C-H bond. This bond energy is affected by the number of unsaturations present along the fatty acid, ranging from 100 kcal $mol^{-1}$ in aliphatic bonds, to 75 kcal $mol^{-1}$ for monoallylic C-H and 50 kcal $mol^{-1}$ for bisallylic proton.[139] Once formed, allyl radicals undergo a rearrangement followed by the double bond isomerisation from *cis* to *trans* configuration. The radical reacts with atmospheric oxygen to form a peroxylic radical and subsequently a hydroperoxide group, species that is particularly unstable due to the presence of weak peroxylic bond (44 kcal $mol^{-1}$). The collapse of this bond

is the driving force for the formation of an alkoxy radical, which can interact with other radical species to form a non-radical compound that establishes the termination step, Figure 2.31.

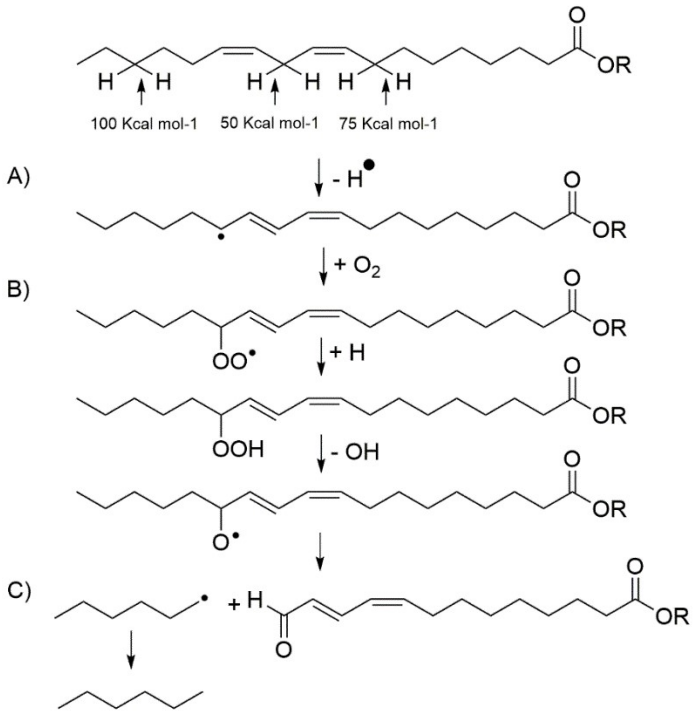


Figure 2.31: A) Initiation, B) propagating and C) termination steps in the oxidation of vegetable oil during the frying process.

Peers and Swoboda highlighted that the oil oxidation is unavoidable and always takes place independently of the type of frying (continuous, simulated or intermittent) because of the uninterrupted combination of elevated temperatures and air.[146] Consequently, the oil stability against this transformation can be extended by flushing it with other gases, such as $N_2$ and $CO_2$, or by using fryers with small surface-to-volume ratio, reducing the contact between the oil and oxygen.[139] The oxidation forms products such as aldehydes, epoxides, hydroxyketones and dicarboxylic species, which affect the original oil flavour and nutritional value. In extreme cases of reuse (gutter oil), harmful health effects can be observed due to the presence of these species, therefore the consumption of highly oxidised oils should be avoided.[147]

According to Stevenson *et al.*, factors such as temperature directly increases oxidation, especially after 200 ° C when the formation of allylic radicals is favoured.[148]. Furthermore, the reuse of the oil in frying cycles (combination of heating and cooling), a practice commonly adopted in small restaurants, increases oxidation rate and oxygen solubility when the temperature decreases.[138] The oxidation rate is also drastically affected by the nature of the oil used since highly-unsaturated oils have the initiation step facilitated by the presence of weak C-H bonds. Hydroperoxides formed during this stage may further react

to form products such as conjugated dienes, also inducing significant changes in molecular weight, organoleptic properties and biological toxicity.[149] These species can undergo fission reactions forming aldehydes alcohols, acids and hydrocarbons or dehydration to generate ketones, epoxides, alcohols and hydrocarbons.[148]

**iii) Polymerisation**

The majority of the non-volatile products accumulated throughout the frying process are dimers, trimers and polymers formed through reactions induced by the radicals formed during thermal oxidation. These compounds drastically increase viscosity, reduce the heat transfer capacity and cause foaming during frying. Moreover, these species are responsible for the brown colour of used oils, the rancid taste transmitted to the food and enhance the absorption of oil by the fried material. The combination of two allyl radicals formed by mechanisms discussed above lead to the creation of a C-C bond linking two triglyceride units.[150] This dimeric species still have alpha-allylic protons likely to be abstracted to form a macroradical, which can be further combined to generate high-molecular-weight species like trimers, oligomers and polymers in later stages of degradation.[151] Figure 2.32 schematically shows the stages of degradation leading to the formation of polymeric species from the combination of macroradicals. Similarly, an allyl (macro) radical also can be combined with an alkoxy radical leading to the formation of dimeric species linked through a C-O bond.

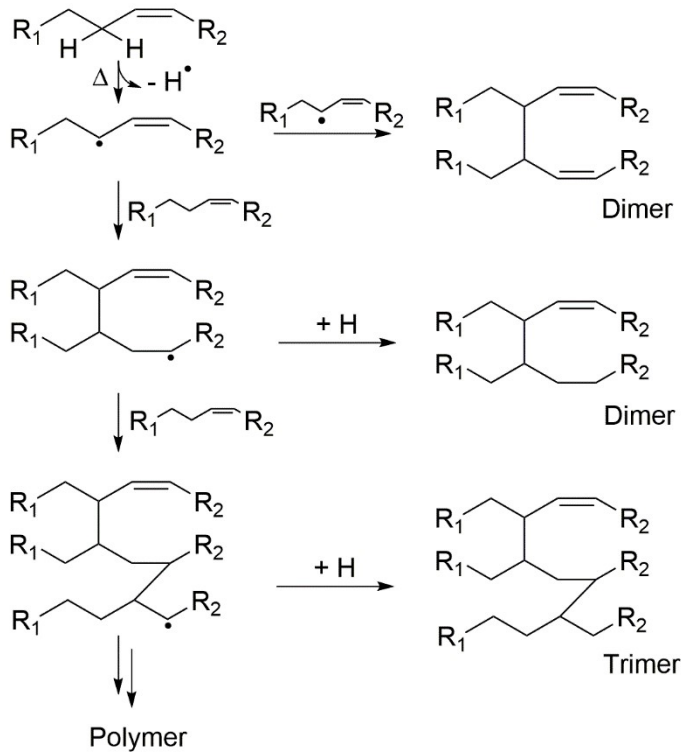


Figure 2.32: Proposed mechanism for the formation of acyclic polymers during frying.

The accumulation of dimeric and polymeric species in vegetable oil due to degradative processes is heavily dependent on parameters such as fatty acids composing the oil.[152] Tompkins and Perkins demonstrated that oils rich in linolenic acid have a higher tendency of forming high molecular-weight products due to the increased the susceptibility of forming allyl radicals. Similar findings were made by Takeoka *et al.* in studies with cotton and corn oil, which also showed that the increase of cooking temperature from 190 °C to 204 °C significantly increases polymerisation.[150] Although most of the transformations during the frying process can be classified according to these three reactions, Nawar also describes an additional case that takes place in the absence of oxygen. The action of temperature can lead to other degradation product, especially in saturated fatty acids, forming smaller alkanes, alkenes, lower fatty acids, symmetric ketones, oxopropyl esters, $CO_2$ and CO.[137]

### 2.6.2 Current Uses of WVO

Currently, scientific exploration of WVO on a large scale is typically restricted to the biodiesel production. Increasing concerns about sustainable development, environmental impacts and cost of raw materials have been attracting interest to the use of waste for fuel. This strategy is commonly known as the second generation of biofuel since it does not directly use food crops in the elaboration of the biodiesel. Nye *et al.* reported one of the earliest studies in the early 1980s exploring the transesterification of crude oil with different alcohols (methanol, ethanol, 1-propanol, 2-propanol, 1-butanol and 2-ethoxy-ethanol).[153] Fatty acids tested in high-speed diesel engine presented promising results as alternative fuels. Since then, several studies confirmed the feasibility of WVO-based biodiesel against traditional petroleum-derived diesel fuel regarding fuel consumption, emissions, engine performance and cost.[154–156] Recent studies have been focused on the development of robust and more sustainable methodologies able to improve the performance, make the production of these chemicals more competitive and safer.[157–159]

Similarly to the conversion of edible oil into biodiesel, WVO can be transesterified using acidic, alkaline or enzymatic catalysts; however, the large number of undesired compounds formed during the frying process make the direct utilisation of this material difficult. For example, the use of alkaline catalysts is limited by the presence of free fatty acids, which lead to the formation of soap and prevent the separation of the glycerol, which in turn increases the viscosity of the fuel.[149,160] Enzymatic reactions present similar difficulties as it requires more pre-treatments on the oil, demanding purer substrates. Since the heterogeneity of the waste oil is a major limitation, studies have been investigating methodologies to purify this feedstock. Generally, all investigations use filtration as a first purification step to separate solid impurities such as pieces of food from the WVO.

Water removal can also increase the yield of the transesterification as it can preclude the reaction by competing with the carbocation formed through the action of the catalyst. Demirbas have demonstrated that by heating the waste oil over 100 °C is a valid technique to reduce the water content.[161] Also, a general trend in the literature is to perform purification steps just after the transesterification, separating the methyl esters from impurities and by-products. Predojevic studied the effect of different purification methodologies based on treatment with silica gel, phosphoric acid solution and hot distilled water on the properties and yield of production of methyl esters from waste oil.[162] Although all methods proved to result in methyl ester with suitable properties, phosphoric acid treatment turned out to be the most efficient of all regarding yield. Meng *et al.* reported that purification methods based on washing the oil with hot water (60 °C) before the transesterification could provide positive results.[124] Even though other methods are reported in the literature, none of them appears to be considered a definitive methodology to purify the WVO. Also, no purification method has ever focused in preparing the oil for epoxidation.

More recently, literature has demonstrated the development of novel technologies based on the WVO valorisation. Although fewer examples are found in other areas when compared to the biodiesel area, these reports make evident that researchers are motivated to further explore the chemical value of WVO through the production of versatile products. Suzuki *et al.* reported the use of WVO as a plasticiser for PVC formulations, mimicking results previously obtained with virgin feedstocks.[163] Borugadda *et al.* presented the application of methyl esters produced from waste soybean oil as bio-based lubricants that presented suitable application in a number of industrial applications.[164] Finally, a conference paper presenting the application of surfactants synthesised with WVO for the recovery of chemicals from petroleum reservoirs was recently presented by Rabiu *et al.*[165] These materials were compared to benchmark surfactants (SDS and CTAB) and presented promising properties in this field.

### 2.6.3 Challenges and Opportunities in Exploring WVO

The production of polymers from WVO represents an opportunity to valorise this material by giving a socially and environmentally-responsible application for it, stimulating the production of new bio-based products through the creation of a more affordable oleochemical platform. Nevertheless, the frying process should always be taken into consideration when designing chemicals from WVO since it causes physical and chemical changes in the feedstock. The polymerisation and oxidation processes ultimately reduce the unsaturation degree of the vegetable oil, reducing its reactivity and potentially leading to lower levels of conversion in further the chemical modification steps. Additionally, the characteristic WVO heterogeneity can induce competing reactions due to the presence of undesired

compounds. Therefore, the development of pre-treatment to increase the purity of these triglycerides, as well as the investigation of a robust epoxidation methodology, are critical points for a consistent production of resin from this bio-based. Other features such as higher viscosity and higher water content can potentially interfere during the chemical modification step; therefore these aspects should be investigated as well.

In the best of our knowledge, the collection of studies presented in this thesis comprehends the first exploration of WVO as a platform for the synthesis of thermoset polymers and subsequent manufacture of composites. So far, literature offers no reports targeting the removal of by-products to produce substrates for this particular application, neither has investigated how chemical modification steps can be affected by the frying process. These two points are critical steps in the elaboration of engineering materials from WVO since the quality of the resin affects the mechanical properties of the final thermoset polymer/composite. By mimicking the advanced and developments achieved in the biodiesel area and general oleochemistry, this work aims to provide guidelines regarding the feasibility of production of waste vegetable oil-based resins and its applicability in the real world.

## 2.7 Summary

The concept of exploring the technological value of vegetable oils dates from many centuries; however, they have been recently rediscovered thanks to the development of new synthetic methodologies capable of manipulating the functional groups in the triglycerides and the driving force of establishing new and more sustainable chemical platforms. Among different synthetic approaches, the insertion of polymerisable groups by exploiting the reactivity of the double bonds has been prevalent in the literature, and particular attention has been given to epoxidation methodologies based on peracids. Nevertheless, novel applications have been exploring the use of enzymatic catalysis and metathesis, enabling the production of more complex units for a greener polymer chemistry.

The exploration of epoxidized vegetable oils for the formation of polymeric network was investigated, and it was revealed that the cure of these resins have been carried out preferentially with anhydride hardeners. Parameters such as the nature of the anhydride and its quantity in the formulation were found as critical parameters towards the properties of the resulting polymer. Finally, this review explored the challenges and opportunities with regards to the technological exploration of waste vegetable oil as a new platform, indicating chemical and physical changes caused by the frying process.

## 2.8 References

1 E. W. Hammond, in *Encyclopedia of Food Sciences and Nutrition*, eds. B. Caballero,

P. Finglas and F. Toldra, Academic Press, Amsterdam, 2nd edn., 2003, pp. 5899–5904.

2 F. Seniha Güner, Y. Yağcı and a. Tuncer Erciyes, *Prog. Polym. Sci.*, 2006, **31**, 633–670.

3 N. Karak, *Vegetable oil-based polymers.*, Woodhead Publishing, Cambridge, United Kingdom, 2012.

4 F. D. Gunstone, *The Chemistry of Oils and Fats: Source, Composition, Properties and Uses*, Blackwell Publishing, CRC Press, 2004.

5 T. P. Coultate, *Food: The chemistry of its components*, RSC Paperbacks, Cambridge, United Kingdom, 2002.

6 U. Biermann, U. Bornscheuer, M. a R. Meier, J. O. Metzger and H. J. Schäfer, *Angew. Chem. Int. Ed. Engl.*, 2011, **50**, 3854–71.

7 E. Galili, D. J. Stanley, J. Sharvit and M. Weinstein-Evron, *J. Archaeol. Sci.*, 1997, **24**, 1141–1150.

8 N. W. Manthey, F. Cardona, G. Francucci and T. Aravinthan, , DOI:10.1177/0731684413493030.

9 M. a. R. Meier, J. O. Metzger and U. S. Schubert, *Chem. Soc. Rev.*, 2007, **36**, 1788.

10 B. L. Axtel and R. Fairman, *Minor oil crops: FAO agricultural services bulletin numer 94*, Food and Agriculture Organization of the United Nations, Rome, 1992.

11 F. D. Gunstone, *Lipid Technol.*, 2011, **23**, 192–192.

12 *Food and Agriculture Organization (FAO) of the United - OECD Agriculture Statistics: World oilseed projections*, 2017.

13 F. D. Gunstone, *Lipid Technol.*, 2013, **25**, 72–72.

14 L. Coltro, J. B. Pitta and E. Madaleno, *Polym. Test.*, 2013, **32**, 272–278.

15 B. Ellis, *Chemistry and Technology of Epoxy Resins*, Springer-Science+Business Media, B.V, 1st Editio., 1993.

16 R. J. Gritter, in *The Ether Linkage*, John Wiley & Sons, 1967, pp. 381–391.

17 A. Streitwieser Jr and C. H. Heathcok, *Introduction to Organic Chemistry*, Macmillan Publishing, New York, United States of America, Third Edit., 1985.

18 K. M. Morgan, J. A. Ellis, J. Lee, A. Fulton, S. L. Wilson, P. S. Dupart and R. Dastoori, *J. Org. Chem.*, 2013, **78**, 4303–4311.

19 R. E. Perdue, K. D. Carlson and M. G. Gilbert, *Econ. Bot.*, 1986, **40**, 54–68.

20 J. A. Farooqui, R. Ahmad and M. Ahmad, *Eur. J. Lipid Sci. Technol.*, 1987, **89**, 30–32.

21 D. Swern, *Chem. Rev.*, 1949, **45**, 1–68.

22 U. Biermann, W. Friedt, S. Lang, W. Lühs, G. Machmüller, J. O. Metzger, M. Rüsch gen. Klaas, H. J. Schäfer and M. P. Schneider, *Angew. Chemie Int. Ed.*, 2000, **39**,

2206–2224.

23 T. W. Findley, J. T. Scanlan and D. Swern, *J. Am. Chem. Soc.*, 1945, **67**, 412–414.

24 D. Derawi and J. Salimon, *E-Journal Chem.*, 2010, **7**, 1440–1448.

25 X. Wang, H. Zhang, Z. Wang and B. Jiang, *Polymer (Guildf).*, 1997, **38**, 5407–5410.

26 G. Knothe and J. T. P. Derksen, *Recent Developments in the Synthesis of Fatty Acid Derivatives*, AOCS Publishing, Champaing, 1st edn., 1999.

27 S.-C. Chua, X. Xu and Z. Guo, *Process Biochem.*, 2012, **47**, 1439–1451.

28 J. La Scala and R. P. Wool, *J. Am. Oil Chem. Soc.*, 2002, **79**, 59–63.

29 S. Dinda, A. V Patwardhan, V. V Goud and N. C. Pradhan, *Bioresour. Technol.*, 2008, **99**, 3737–44.

30 Z. S. Petrovic, A. Zlatanic, C. C. Lava and S. Sinadinovic-Fiser, *Eur. J. Lipid Sci. Technol.*, 2002, **104**, 293–299.

31 B. M. Abdullah and J. Salimon, *J. Appl. Sci.*, 2010, **10**, 1545–1553.

32 C. Cai, H. Dai, R. Chen, C. Su, X. Xu, S. Zhang and L. Yang, *Eur. J. Lipid Sci. Technol.*, 2008, **110**, 341–346.

33 V. V. Goud, N. C. Pradhan and A. V. Patwardhan, *J. Am. Oil Chem. Soc.*, 2006, **83**, 635–640.

34 V. V. Goud, A. V. Patwardhan, S. Dinda and N. C. Pradhan, *Chem. Eng. Sci.*, 2007, **62**, 4065–4076.

35 R. L. Musante, R. J. Grau and M. a. Baltanás, *Appl. Catal. A Gen.*, 2000, **197**, 165–173.

36 V. V. Goud, A. V. Patwardhan, S. Dinda and N. C. Pradhan, *Eur. J. Lipid Sci. Technol.*, 2007, **109**, 575–584.

37 R. Mungroo, N. C. Pradhan, V. V. Goud and A. K. Dalai, *J. Am. Oil Chem. Soc.*, 2008, **85**, 887–896.

38 P. Anastas and J. C. Warner, *Green Chemistry: Theory and Practice*, Oxford University Press, New York, 1998.

39 S. Sinadinovic-Fiser, M. Jankovi and Z. S. Petrovic, *J. Am. Oil Chem. Soc.*

40 M. S. Gurbanov and B. a. Mamedov, *Russ. J. Appl. Chem.*, 2009, **82**, 1483–1487.

41 M. Rusch gen. Klass and S. Warwel, *Ind. Crops Prod.*, 1999, **9**, 125–132.

42 K. D. Carlson, R. Kleiman and M. O. Bagby, *JAOCS*, 1994, **71**, 175–182.

43 R. K. Parashar, *Reaction Mechanisms in Organic Synthesis*, John Wiley & Sons, 2009.

44 F. Bjorkling, S. E. Godtfredsen and O. Kirk, *J. Chem. Soc. Chem. Commun.*, 1990, **19**, 1301–1303.

45 I. Hilker, D. Bothe, J. Pru and H. Warnecke, *Chem. Eng. Sci.*, 2001, **56**, 427–432.

46 S. Warwel and M. R. Klaas, *J. Mol. Catal. B Enzym.*, 1995, **1**, 29–35.

47 M. Klaas and S. Warwel, *J. Am. Oil Chem. Soc.*, 1996, **73**, 9–13.

48 C. Orellana-Coca, S. Camocho, D. Adlercreutz, B. Mattiasson and R. Hatti-Kaul, *Eur. J. Lipid Sci. Technol.*, 2005, **107**, 864–870.

49 Z. S. Vlcek T, Petrovic, *J. Am. Oil Chem. Soc.*, 2006, **83**, 247–252.

50 S. Sun, X. Ke, L. Cui, G. Yang, Y. Bi, F. Song and X. Xu, *Ind. Crops Prod.*, 2011, **33**, 676–682.

51 J. Chen, J. Zhou, W. Liu, Y. Bi and D. Peng, *Chem. Pap.*, 2017, **71**, 2139–2144.

52 W. Liu, J. Chen, R. Liu and Y. Bi, *JAOCS, J. Am. Oil Chem. Soc.*, 2016, **93**, 1479–1486.

53 S. G. Tan and W. S. Chow, *Polym. Plast. Technol. Eng.*, 2010, **49**, 1581–1590.

54 W. A. Herrmann, R. W. Fischer and D. W. Marz, *Angew. Chemie Int. Ed.*, 1991, **30**, 1638–1641.

55 J. Rudolph, K. L. Reddy, J. P. Chiang and K. B. Sharpless, *J. Am. Chem. Soc.*, 1997, **119**, 6189–6190.

56 C. Coperet, H. Adolfsson and K. B. Sharpless, *Chem. Commun.*, 1997, 1565–1566.

57 H. Adolfsson, A. Converso and K. B. Sharpless, *Tetrahedron Lett.*, 1999, **40**, 3991–3994.

58 W. Herrmann, W. Scherer and M. U. Rauch, *Angew. Chemie Int. Ed.*, 1993, **32**, 1157–1160.

59 W. Adam and C. M. Mitchell, *Angew. Chemie Int. Ed.*, 1996, **35**, 533–535.

60 A. E. Gerbase, J. R. Gregório, M. Martinelli, M. C. Brasil and A. N. F. Mendes, *JAOCS*, 2002, **79**, 179–181.

61 C. Cai, H. Dai, R. Chen, C. Su, X. Xu, S. Zhang and L. Yang, *Eur. J. Lipid Sci. Technol.*, 2008, **110**, 341–346.

62 L. Daniel, A. R. Ardiyanti, B. Schuur, R. Manurung, A. a. Broekhuis and H. J. Heeres, *Eur. J. Lipid Sci. Technol.*, 2011, **113**, 18–30.

63 A. Campanella, M. A. Baltanás, M. C. Capel-sánchez and J. M. Campos-martín, *Green Chem.*, 2004, **6**, 330–334.

64 G. Venturello, E. Alneri and M. Ricci, *J. Org. Chem.*, 1983, **3**, 3831–3833.

65 I. V. Kozhevnikov, G. P. Mulder, M. C. Steverink-de Zoete and M. G. Oostwal, *J. Mol. Catal. A Chem.*, 1998, **134**, 223–228.

66 T. B. Khlebnikova, Z. P. Pai, L. A. Fedoseeva and Y. V. Mattsat, *React. Kinet. Catal. Lett.*, 2009, **98**, 9–17.

67 M. T. Benaniba, N. Belhaneche-Bensemra and G. Gelbard, *Eur. J. Lipid Sci. Technol.*, 2007, **109**, 1186–1193.

68 G. Lligadas, J. C. Ronda, M. Galia and V. Ca, *Biomacromolecules*, 2010, 2825–2835.

69 J. Scala and R. P. Wool, *J. Am. Oil Chem. Soc.*, 2002, **79**, 373–378.

70 J. Lu, S. Khot and R. P. Wool, *Polymer (Guildf).*, 2005, **46**, 71–80.

71 Wool and X. S. Sun, *Bio-based polymer and composites*, Elsevier Academic, London, 2005.

72 Y. Zhang, V. K. Thakur, Y. Li, T. F. Garrison, Z. Gao, J. Gu and M. R. Kessler, *Macromol. Mater. Eng.*, 2018, **303**, 1–10.

73 M. Skrifvars, K. Adekunle and A. Dan, *J. Appl. Polym. Sci.*, 2009, **115**, 3137–3145.

74 A. Guo, I. Javni and Z. Petrovic, *J. Appl. Polym. Sci.*, 2000, **77**, 467–473.

75 A. Zlatanic, C. Lava, W. Zhang and Z. S. Petrović, *J. Polym. Sci. Part B Polym. Phys.*, 2004, **42**, 809–819.

76 A. Guo, D. Demydov, W. Zhang and Z. S. Petrovic, *J. Polym. Environ.*, 2002, **10**, 49–52.

77 I. Javni, W. Zhang and Z. S. Petrović, *J. Appl. Polym. Sci.*, 2003, **88**, 2912–2916.

78 V. Athawale and S. Kolekar, *Polym. J.*, 1998, **30**, 813–818.

79 R. Silva, D. Spinelli, W. Bosefilho, S. Claroneto, G. Chierice and J. Tarpani, *Compos. Sci. Technol.*, 2006, **66**, 1328–1335.

80 L. B. Tavares, C. V. Boas, G. R. Schleder, A. M. Nacas, D. S. Rosa and D. J. Santos, *Express Polym. Lett.*, 2016, **10**, 927–940.

81 K. P. Somani, S. S. Kansara, N. K. Patel and A. K. Rakshit, *Int. J. Adhes. Adhes.*, 2003, **23**, 269–275.

82 P. B. van Dam, M. C. Mittelmeijer and C. Boelhouwer, *J. Chem. Soc. Chem. Commun.*, 1972, 1221.

83 T. M. Trnka and R. H. Grubbs, 2001, **34**, 18–29.

84 J. C. Mol, *Green Chem.*, 2002, **4**, 5–13.

85 F. B. H. Ahmad, S. Hamdan, M. a. Yarmo and a. Alimunir, *J. Am. Oil Chem. Soc.*, 1995, **72**, 757–758.

86 A. Zlatanic, Z. S. Petrovic and K. Dus, *Biomacromolecules*, 2002, **3**, 1048–1056.

87 A. Rybak and M. a. R. Meier, *Green Chem.*, 2007, **9**, 1356.

88 A. Rybak and M. a. R. Meier, *Green Chem.*, 2008, **10**, 1099.

89 R. Wang, Missouri University of Science & Technology, 2014.

90 R. Auvergne, S. Caillol, G. David, B. Boutevin and J. Pascault, *Chem. Rev.*, 2014, **114**, 1082–1115.

91 B. Wang, Y.-L. Cheng, Y. Liu, P. Chen, D. Li and R. Ruan, *J. Appl. Polym. Sci.*, 2013, **127**, 1458–1465.

92 N. W. Manthey, F. Cardona and T. Aravinthan, *J. Appl. Polym. Sci.*, 2012, **125**, E511–E517.

93 V. Del Río, M. P. Callao and M. S. Larrechi, *Int. J. Anal. Chem.*, 2011, **2011**,

401216.

94 a. Carbonell-Verdu, L. Bernardi, D. Garcia-Garcia, L. Sanchez-Nacher and R. Balart, *Eur. Polym. J.*, 2015, **63**, 1–10.

95 C. Ding and A. S. Matharu, *ACS Sustain. Chem. Eng.*, 2014, **2**, 2217–2236.

96 A. E. Gerbase, C. L. Petzhold and A. P. O. Costa, *J. Am. Oil Chem. Soc.*, 2002, **79**, 797–802.

97 J. Rosch and R. Mulhaupt, *Polym. Bull.*, 1993, **686**, 679–685.

98 A. J. Clark, A. H. Ross and S. A. F. Bon, *J. Polym. Environ.*, 2017, **25**, 1–10.

99 G. Liang and K. Chandrashekhara, *J. Appl. Polym. Sci.*, 2006, **102**, 3168–3180.

100 N. Boquillon and C. Fringant, *Polymer (Guildf).*, 2000, **41**, 8603–8613.

101 P. Niedermann, G. Szebényi and a. Toldy, *Compos. Sci. Technol.*, 2015, **117**, 62–68.

102 C. Scarponi, F. Sarasini, J. Tirillò, L. Lampani, T. Valente and P. Gaudenzi, *Compos. Part B Eng.*, 2016, **91**, 162–168.

103 F.-L. Jin and S.-J. Park, *Mater. Sci. Eng. A*, 2008, **478**, 402–405.

104 Y. Chen, L. Yang, J. Wu, L. Ma, D. E. Finlow, S. Lin and K. Song, *J. Therm. Anal. Calorim.*, 2012, **113**, 939–945.

105 D. Ratna, *Polym. Int.*, 2001, **184**, 179–184.

106 S.-J. Park, F.-L. Jin and J.-R. Lee, *Macromol. Chem. Phys.*, 2004, **205**, 2048–2054.

107 R. Raghavachar, R. J. Letasi, P. V. Kola, Z. Chen and J. L. Massingill, *J. Am. Oil Chem. Soc.*, 1999, **76**, 511–516.

108 G. Mashouf Roudsari, A. K. Mohanty and M. Misra, *ACS Sustain. Chem. Eng.*, 2014, **2**, 2111–2116.

109 H. Miyagawa, A. K. Mohanty, M. Misra and L. T. Drzal, *Macromol. Mater. Eng.*, 2004, **289**, 629–635.

110 H. Miyagawa, A. K. Mohanty, M. Misra and L. T. Drzal, *Macromol. Mater. Eng.*, 2004, **289**, 636–641.

111 H. Miyagawa, M. Misra, L. T. Drzal and A. K. Mohanty, *Polym. Eng. Sci.*, 2005, **45**, 487–495.

112 A. Rybak, P. a. Fokou and M. a. R. Meier, *Eur. J. Lipid Sci. Technol.*, 2008, **110**, 797–804.

113 E. Antonelli, R. D. Aloisio, M. Gambaro, T. Fiorani and C. Venturello, *J. Org. Chem.*, 1998, **1984**, 7190–7206.

114 H. Noureddini and M. Kanabur, *J. Am. Oil Chem. Soc.*, 1999, **76**, 305–312.

115 L. Martino, L. Basilissi, H. Farina, M. A. Ortenzi, E. Zini, G. Di Silvestro and M. Scandola, *Eur. Polym. J.*, 2014, **59**, 69–77.

116 L. Hojabri, J. Jose, A. L. Leao, L. Bouzidi and S. S. Narine, *Polym. (United Kingdom)*, 2012, **53**, 3762–3771.

117 M. a. R. Meier, *Macromol. Chem. Phys.*, 2009, **210**, 1073–1079.

118 C. Demes, S. Warwel, F. Br, M. Kunz and R. Mark, *Chemosphere*, 2001, **43**, 39–48.

119 A. Rybak and M. a R. Meier, *ChemSusChem*, 2008, **1**, 542–547.

120 H. Mutlu and M. a R. Meier, *Macromol. Chem. Phys.*, 2009, **210**, 1019–1025.

121 P. Dannecker, U. Biermann, M. Von Czapiewski, J. O. Metzger and M. A. R. Meier, *Angew. Chemie Int. Ed.*, 2018, 1–6.

122 M. C. Math, S. P. Kumar and S. V. Chetty, *Energy Sustain. Dev.*, 2010, **14**, 339–345.

123 J. C. J. Bart, N. Palmeri and S. Cavallaro, in *Biodiesel Science and Technology : From Soil to Oil*, CRC Press, Oxford, 2010, pp. 199–200.

124 X. Meng, G. Chen and Y. Wang, *Fuel Process. Technol.*, 2008, **89**, 851–857.

125 A. Demirbas, *Appl. Energy*, 2009, **86**, S108–S117.

126 Z. Predojevic and B. Skrbic, *J. Serbian Chem. Soc.*, 2009, **74**, 993–1007.

127 A. A. Refaat, *Int. J. Environ. Sci. Technol.*, 2009, **7**, 183–213.

128 A. Scott, *Chem. Eng. News*, 2018.

129 V. K. W. S. Araujo, S. Hamacher and L. F. Scavarda, *Bioresour. Technol.*, 2010, **101**, 4415–22.

130 D. A. Salam, N. Naik, M. T. Suidan and A. D. Venosa, *Environ. Sci. Technol.*, 2012, **46**, 2352–2359.

131 P. Campo, Y. Zhao, M. T. Suidan, A. D. Venosa and G. A. Sorial, *Chemosphere*, 2007, **68**, 2054–2062.

132 A. M. Salgado, University of Wales, 1995.

133 F. Lu and X. Wu, *Food Control*, 2014, **41**, 134–138.

134 H. Zhang, U. Aytun Ozturk, Q. Wang and Z. Zhao, *Renew. Sustain. Energy Rev.*, 2014, **38**, 677–685.

135 G. Hageman, R. Kikken, F. Ten Hoor and J. Kleinjans, *Mutat. Res.*, 1988, **204**, 593–604.

136 F. C. Fernandes, D. Lehane, K. Kirwan and S. R. Coles, *Eur. Polym. J.*, 2017, **89**, 449–460.

137 W. W. Nawar, *J. Chem. Educ.*, 1984, **61**, 299–302.

138 S. Paul, G. S. Mittal and M. S. Chinnan, *Crit. Rev. Food Sci. Nutr.*, 1997, **37**, 635–62.

139 E. Choe and D. B. Min, *J. Food Sci.*, 2007, **72**, R77-86.

140 D. Dana, M. M. Blumenthal and I. S. Saguy, *Eur. Food Res. Technol.*, 2003, **217**, 104–109.

141 C. W. Fritsch, G. Mills, J. Ford and B. Technical, *JAOCS*, 1981, **58**, 272–274.

142 C. Cuesta, F. J. Sánchez-Muniz, C. Garrido-Polonio, S. López-Varela and R. Arroyo, *J. Am. Oil Chem. Soc.*, 1993, **70**, 1069–1073.

143 H.-D. Belitz, W. Gorsch and P. Schieberle, *Food Chemistry*, Springer Berlin Heidelberg, Berlin, 4th edn., 2009.

144 E. Choe and D. B. Min, *J. Food Sci.*, 2005, **70**, 142–159.

145 S. Bastida and F. J. Sánchez-Muniz, *Food Sci. Technol. Int.*, 2001, **7**, 15–21.

146 K. E. Peers and P. a. T. Swoboda, *J. Sci. Food Agric.*, 1982, **33**, 389–395.

147 I. S. Saguy and D. Dana, *J. Food Eng.*, 2003, **56**, 143–152.

148 S. G. Stevenson, M. Vaisey-Genser and N. a. M. Eskin, *J. Am. Oil Chem. Soc.*, 1984, **61**, 1102–1108.

149 M. G. Kulkarni and A. K. Dalai, *Ind. Eng. Chem. Res.*, 2006, 45, 2901–2913.

150 G. R. Takeoka, G. H. Full and L. T. Dao, *J. Agric. Food Chem.*, 1997, **8561**, 3244–3249.

151 F. J. Sánchez-Muniz, C. Cuesta and C. Garrido-Polonio, *J. Am. Oil Chem. Soc.*, 1993, **70**, 235–240.

152 C. Tompkins and E. G. Perkins, *J. Am. Oil Chem. Soc.*, 2000, **77**, 223–229.

153 M. J. Nye, T. W. Wllliamson, S. Deshpande, J. H. Schrader, W. H. Snively and C. L. French, *J. Am. Oil Chem. Soc.*, 1983, **8**, 1598–1601.

154 M. Mittelbach and P. Tritthartb, *JAOCS*, 1988, **65**, 1185–1187.

155 M. I. Al-Widyan, G. Tashtoush and M. Abu-Qudais, *Fuel Process. Technol.*, 2002, **76**, 91–103.

156 R. Arslan and Y. Ulusoy, *Environ. Sci. Pollut. Res.*, 2018, **25**, 24520 – 24525.

157 O. Aboelazayem, M. Gadalla and B. Saha, *Renew. Energy*, 2018, **124**, 144–154.

158 F. M. Wako, A. S. Reshad, M. S. Bhalerao and V. V. Goud, *Ind. Crops Prod.*, 2018, **118**, 282–289.

159 V. C. Eze, A. N. Phan and A. P. Harvey, *Fuel*, 2018, **220**, 567–574.

160 A. Talebian-Kiakalaieh, N. A. S. Amin and H. Mazaheri, *Appl. Energy*, 2013, **104**, 683–710.

161 A. Demirbas, *Energy Convers. Manag.*, 2009, **50**, 923–927.

162 Z. J. Predojević, *Fuel*, 2008, **87**, 3522–3528.

163 A. H. Suzuki, B. G. Botelho, L. S. Oliveira and A. S. Franca, *Eur. Polym. J.*, 2018, **99**, 142–149.

164 V. B. Borugadda and V. V. Goud, *J. Clean. Prod.*, 2016, **112**, 4515–4524.

165 A. M. Rabiu, S. Elias and O. Oyekola, *Energy Procedia*, 2016, **100**, 188–192.

# Chapter 3

# Literature Review 2:

Fundaments of Sustainable Composites:
Plant Fibres and Biocomposites

## 3.1 Composites: Fundamentals, Markets and Challenges

### 3.1.1 Fundaments of Composites

A composite is defined as a material obtained from the combination of two or more components that, when joined, present improved properties compared to the originals.[1] Since these components can be distinguished regarding composition and dimension, this combination results in a multiphasic system comprised of a continuous phase, also referred as a matrix, and a dispersed phase. The dispersed phase can be incorporated into the matrix in different forms such as powders, fibres or particles of different dimensions. In composite formulations, the dispersed should be carefully selected in order either to actively change the properties of resulting material in comparison with the matrix or to be inert and merely reduce price and purely acting as a filler.[2]

Polymeric matrix composites have gained critical importance in the engineering market in the 1950's by presenting advantages over traditional metallurgical materials such as reduced price, reduced density, dimensional stability and high resistance to corrosion. Through decades of development, the industry has explored the use of a number of additives to control the properties of composites, such as chalk to reduce prices and control gloss, talc to improve impact properties and control colour, carbon black for pigmentation and UV-stability, and mica for hardness and dimension stability.[2]

Some components are added to composite formulation with the intention of modulating the mechanical properties of the resulting material. In this regard, glass fibres and carbon fibres have been traditionally selected as reinforcing agents for polymer composites application due to the high tensile performance and stress resistance associated with these agents.[34] The reinforcement effect is only observed when the stress originated by a mechanical perturbation in the polymeric matrix can be effectively transmitted without causing failure, Figure 3.1. Therefore, a material combining strong reinforcing fibres and a polymeric matrix will withstand higher mechanical stress and, consequently, will present higher properties than the unreinforced polymer.[5]

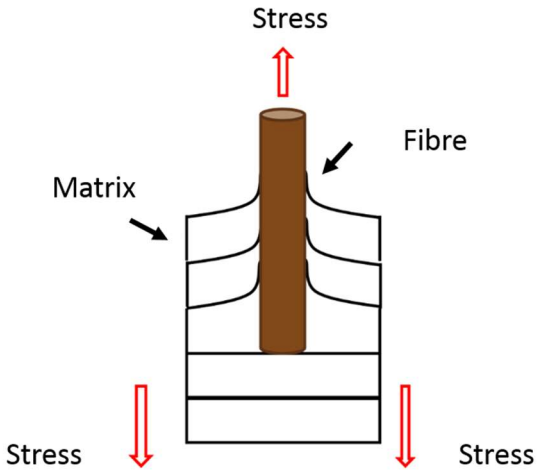


Figure 3.1: Schematic representation of the mechanical stress distribution in a fibre reinforced composite.

The reinforcing effect provided by fibres is closely linked to the adhesion between the agent and the polymeric matrix at an interfacial level. The fibre/matrix interaction interferes in the mechanical, rheological and dynamic-mechanical properties of the composites.[6] According to the literature, some of mechanisms can be used to explain the reinforcement phenomenon, as listed below.[7] Nevertheless, they act concomitantly to promote fibre adhesion and the reinforcement effect. Consequently, the individual contributions of one each mechanism towards the improvement of the mechanical properties cannot be clearly distinguishable.[8]

I. Adsorption and wetting: the wetting of the reinforcing fibre by the molten polymeric matrix or liquid resin under cure, which removes the air present in the fibre, covering all its surface.

II. Interdiffusion: the diffusion of the polymer chains in the interface. This mechanism is observed when fibres are functionalized or covered with other polymers. Adhesion will depend on the length of the polymer chains involved in the interaction and the degree of entanglement between the chains.

III. Electrostatic attraction: this mechanism occurs when there are two surfaces with opposite electric charges in the composition. The adhesion will depend on the density of electric charges, and this mechanism has a higher influence when the composite involves metallic components.

IV. Chemical bonding: occurs when functional groups on the fibre surface are able to react with chemical groups in the matrix, creating chemical bonds between the components. These bonds can be formed by naturally-occurring functionalities present on these components, or through the utilization of coupling agents.[9]

V. Mechanical adhesion: occurs when the polymer fills the grooves, cavities and other types of irregularities present on the surface of the reinforcement. Therefore, this mechanism is mainly observed in fibres with high roughness.

### 3.1.2 Composites Market

The expansion of polymeric composites to various technological sectors has been experiencing an ever-increasing rate. Market data from 2016 shows that 1,096 kt of glass fibre-reinforced composites (GFRC) were produced throughout Europe, an increase of 4.8% over the 2014 figures.[10,11] The UK and Ireland are ranked as one of the biggest manufacturers in this multimillionaire global market, being responsible for manufacturing approximately 152 kt of glass fibre reinforced polymer composites in 2016. With respect to carbon fibre reinforced composites (CFRC), approximately 58 kt of composites of this class were produced worldwide in 2016. The comparison of this value with data from 2010 shows that there was a major increase in the consumption of CFRC (47.6%) in a relatively short time. Despite the lower volume of production when compared to glass fibre composites, these materials have a higher aggregated value due to their improved mechanical properties and reduced density, therefore representing a business worth 2.15 billion dollars (as in 2015). According to estimation prepared by the *AVK Industrievereinigung Verstärkte Kunststoffe,* a German trade association, CFRC market is expected to continuously expand around 10 to 13% per year until 2020.[11]

Figure 3.2A and B represent the market shares of CFRC and GFRC according to the application area in 2016, respectively. Transport sector was the leading consumer of GFRC, closely followed by construction and electronics. In transport applications, for example, this class of composites is used in parts such as clutch disks, brake pads, headliners and automotive insulation parts. The scenario is different for carbon fibre reinforced composites, where the aerospace and defence sectors are the largest consumers. This illustrates the niche utilisation of CFRC in advanced applications where performance is the ultimate goal. Nevertheless, the transport sector is still the second largest consumer of carbon fibre reinforced composites since it is identified that the CFRC plays a key role in fuel efficiency.

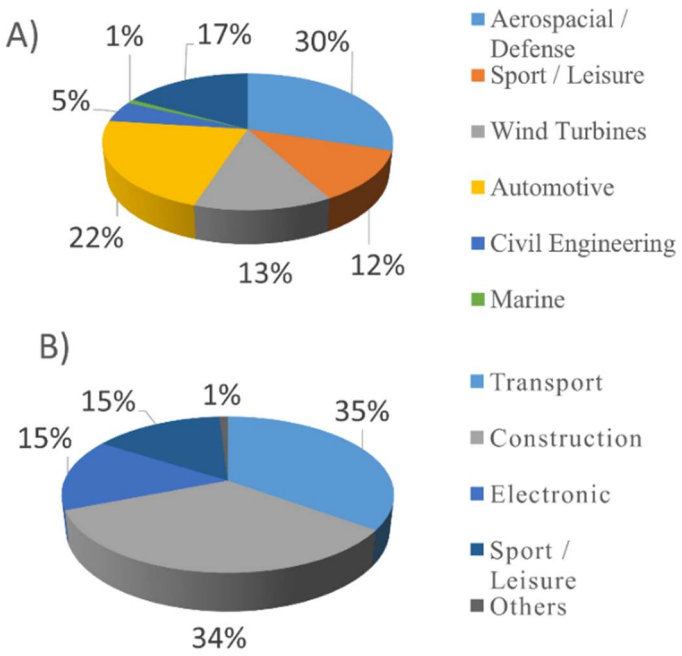


Figure 3.2: Market share of composites reinforced with A) carbon and B) glass fibres in 2016.

### 3.1.3 Challenges in the Composites Area

Despite the capacity of delivering unique performance, GFRC and CFRC suffer from limitations from the environmental point of view. The processes of producing glass fibres is based on the combination of $SiO_2$ and other oxides such as calcium, boron, sodium, iron and aluminium (depending on the grade of the fibre) at a molten stage, which is achieved at temperatures above 1200 °C.[4] Additional processes during the fibre production involves a chemical coating and a spinning process, also adding to the overall energy consumption (about 32 MJ $kg^{-1}$). The energy requirement is even more demanding for the manufacturing of carbon fibres: these materials are produced from a polyacrylonitrile (PAN) precursor, which is stretched to align the molecular chains. This highly-ordered precursor undergoes an initial heating stage to form a polymeric 6-membered ring structure, which is then heated to extreme temperatures (above 1700 °C) under a reducing atmosphere to eliminate the heteroatoms from the structure.[12] As a consequence of multiple high-temperature heating stages, the production of a kilogram of carbon fibre requires about 400 MJ of energy. Additionally, composites reinforced with these fibres present challenges related to recyclability, biodegradability and long-term impact on processing machines due to their abrasive characteristics.[13]

Furthermore, glass fibres present an additional restrictions associated with their high density (2.5 g $cm^{-3}$). Since the densities of most engineering polymer matrices are under 1.4 g $cm^{-3}$, GFRC will result in heavier components when compared to the non-reinforced polymer. This aspect is a particular challenge for components manufactured for the automotive industry, which is aiming weight-savings to meet emission targets.[14–16] Finally, latent climate changes

associated with the potential for depletion of fossil sources have raised concerns about energy-intensive manufacturing and the use of non-renewable sources, creating a driving force towards the use of eco-friendly materials in engineering.[17]

In this scenario, biocomposites have been extensively explored in recent decades to address environmentally friendly solutions for the composite market. The strategy of using renewable materials in the automotive sector is not entirely novel: back in the 1940s, Henry Ford strongly backed the utilisation of natural fibres and resins for the production of external body panels.[18] Ford`s beliefs are illustrated in Figure 3.3, which presents himself demonstrating the impact properties of a panel produced with hemp fibres and soybean oil-based resin.[19] Among different strategies, the exploration of plant fibres as reinforcing agents has stood out as one of the most successful approaches to produce environmentally friendly and competitive composites.


Figure 3.3: Henry Ford demonstrating the performance of an external body part produced with hemp fibres.[19]

## 3.2 Plant Fibres

The utilisation of natural reinforcing agents as alternative in the composites area bloomed in the early 1990s as a response to the growing demand for the incorporation renewable in the production chain.[20] Natural fibres can be classified according to their origin: animal, plant or mineral. In general, vegetal fibres have predominated over other natural fibres with respect to the application in the composites area, producing vegetable fibre reinforced composites (VFRC). However, it is possible to highlight the successful production of composites with fibres derived from animal feathers and mineral sources.[21,22] Plant fibres are extracted from different parts of plants, and are generally classified in 5 different groups, Table 3.1.[6,23] These materials are considered as low-cost and abundant raw materials, and each region of the globe can be supplied with different local fibres. Plant fibres derived from different plant parts will present slightly different properties, therefore adding a component of

versatility (and complexity) to the exploration of this technique. Natural fibres also present low density (generally < 1.5 g $cm^{-3}$), contributing to savings in weight and cheaper transport.

Table 3.1: Types of fibre according to their origin in the plant and examples.

| **Fibre Origin** | **Examples** |
|---|---|
| Leaf | Sisal, Banana, *Sansevieria metallica*, *Gladiolus X. hortuanus, Raphia ruffia,* Agave, Abaca, Pineapple, Sisal |
| Stem | Bamboo, Sugarcane Bagasse, Eucalyptus, Sun hemp, Nettle |
| Seed | Cotton, Milkweed, Kapok |
| Bast | Hemp, Jute, Flax, Kenaf |
| Miscellaneous | Banana peels, Cactus, *Panicum maximum,* Oil Palm, Coir, Broom root |

Chemically speaking, plant fibres are constituted by 4 main components: cellulose, hemicellulose, pectin and lignin. The content of each one of these components varies not only with the species but also with factors such as the cultivation site, climate and degree of maturity of the plant in the fibre extraction stage.[24] Table 3.2 shows the contents of the main components in different plant species that are commonly used in composite applications. Cellulose a highly-crystalline polymer of D-glucose with high degree of polymerization, is always the major component of cell walls, Figure 3.4A. Cellulose plays a crucial role in the application of these materials in the composite area since it is the main responsible for providing mechanical properties to plant fibres. This characteristic derives from the strong hydrogen-bond interactions between the long linear chains of cellulose, Figure 3.4A.[6] This interaction is the driving force behind the self-organization of the polymer chains, forming sheet-like structures that stack vertically and provide chemical and mechanical stability to the fibre structure. Consequently, fibres with higher mechanical properties have, in general, higher cellulose contents, increased degrees of crystallinity and higher polymerization of cellulose.[25]

Table 3.2: Main chemical components of plant fibres from different origins.

| Fibre | Cellulose (%) | Hemicellulose (%) | Pectin (%) | Lignin (%) | θ | Ref. |
|---|---|---|---|---|---|---|
| Abaca | 56-63 | 21.7 | 1 | 12-13 | - | 23,26 |
| Agave | 45.5 | 19 | - | 18.7 | - | 27 |
| Bamboo | 46.4 | 27.1 | - | 25 | - | 28 |
| Banana | 63-64 | 10 | - | 10 | 11 | 23,29 |
| Coir | 36-43 | 0.15-0.25 | 3-4 | 41-45 | 30-49 | 6,29 |
| Cottom | 85-90 | 5.7 | 0-1 | 0.7-1.6 | 20-30 | 23,29 |
| Curaua | 73.6 | 9.9 | - | 7.5 | - | 23,26 |
| Eucalyptus | 51.1 | 10.9 | - | 26.8 | - | 30 |
| Flax | 71-78 | 18.6-20.6 | 1.3 | 2.2 | 5-10 | 6,29,31 |
| Hardwood | 43-47 | 25-35 | - | 16-24 | - | 32 |
| Hemp | 70-74.4 | 17.9-22.4 | 0.9 | 3.7-5.7 | 2-6.2 | 33 |
| Henequen | 77.6 | 4-8 | 13.1 | - | - | 34 |
| Jute | 61-71.5 | 13.6-20.4 | 0.2 | 13.1 | 8 | 6,29 |
| Kenaf | 45-57 | 21.5 | 3-5 | 8-13 | - | 23,26 |
| Nettle | 86 | 4 | 0.6 | 5.4 | - | 6,29,31 |
| Pineapple | 80-83 | 15-20 | 2-4 | 8-12 | 8-15 | 26 |
| Ramie | 68.6 | 13.1 | 1.9 | 0.6 | - | 29 |
| Sisal | 67-78 | 10-14 | 10 | 8-11 | 10-22 | 6,29 |
| Softwood | 40-44 | 25-29 | - | 25-31 | - | 32 |
| Sugarcane Bagasse | 54.3-55.2 | 16.8-29.7 | - | 24-25 | - | 20 |
| Wheat Straw | 43.2 | 34.1 | - | 22 | - | 35 |

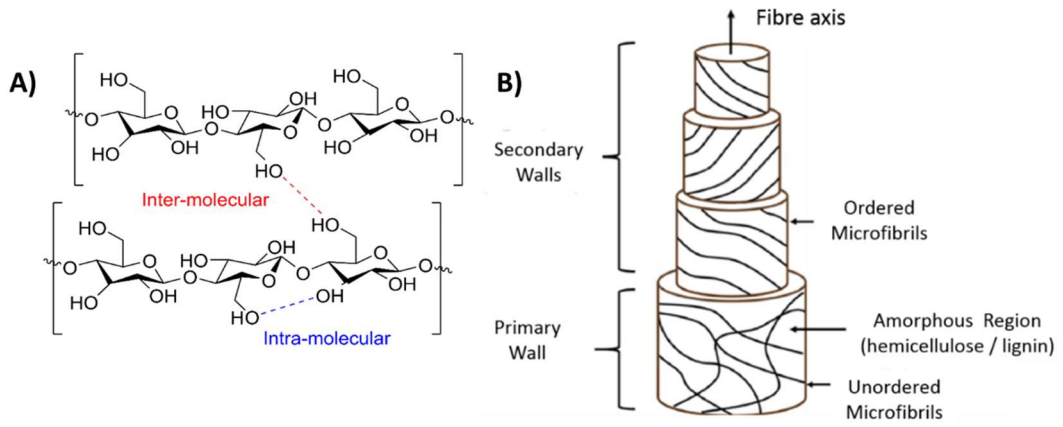


Figure 3.4: A) Chemical structure of the cellulose and the capacity of forming intra- and intermolecular hydrogen bonds and B) schematic representation of the fibre morphology.

In addition to cellulose, hemicellulose is a polysaccharide found in significant levels in plant fibres. This compound is a heteropolymer composed of several and unevenly distributed repetitive units such as xylose, glucose, and other hexoses and pentoses with a degree of polymerization near 100.[6] Since hemicellulose lacks a hierarchical structure and present a low-molecular-weight, it presents lower mechanical properties when compared to cellulose. Lignin, another significant component of plant fibres, is a complex three-dimensional and amorphous polymer with a chemically diverse backbone. Although the exact chemical structure of lignin is not fully understood, it combines aliphatic and ring-substituted phenyl units with groups such as alkyl, hydroxyl, carboxyl and methoxy units.[36,37] Lignin's function is to provide rigidity, mechanical properties and microbiological resistance to fibres. Finally, pectin is defined as a heteropolysaccharide rich in uronic acid with a degree of polymerization similar to hemicellulose; however, found in a smaller amount. Despite the low amount and the smaller mechanical properties, both hemicellulose, pectin and lignin are fundamental for the structural cohesion of the plant fibres as they act as binders.[38]

Plant fibres are hierarchically constructed by arrangements of different cell walls, as schematically presented in Figure 3.4B. These walls consist of microfibrils (internal diameter between 10 and 30 μm) formed by crystalline cellulose embedded in an amorphous matrix composed mainly by hemicellulose and lignin.[39] This mixture acts as a "cellular cement", joining the fibre bundles and providing rigidity to this mixture. Each cell wall has a different distribution of each of the components and distinct arrangements with respect to microfibrils, therefore presenting different properties. For example, the microfibrils are orderly distributed in the secondary wall in a helical arrange along the central axis of the fibre. On the other hand, microfibrils in the primary wall are randomly distributed.[39]

Structural features related to the microfibrils arrangement are also responsible for affecting the mechanical properties of plant fibres. The angle formed between the principal axis and the helical arrangement of cellulose microfibrils, known as the microfibrillar angle (θ), is responsible for determining the efficiency of the mechanical stress transference between the cell walls and the amorphous portions.[29] McLaughlin and Tait successfully modelled the mechanical performance of single fibre bundles according to a physical cylindrical cell model, demonstrating that the fibre Young's modulus followed a relationship dependent on $\cos^2\theta$. [40] Table 3.3 presents physical characteristics and mechanical properties of plant fibres of different origins in comparison to fibres traditionally used in the area of composites (aramid, carbon and glass fibres). As illustrated by the broad range of properties in Table 3.3, the combination of the structural and chemical parameters produces plant fibres with distinct and unique properties.

Table 3.3: Density (ρ), length (*l*), diameter (ϕ), elongation at break (ε), tensile strength (σ), Young`s Modulus (Y.M.), and specific properties of some plant fibres in comparison to traditional reinforcing agents.

| Fibre | ρ (g cm$^{-3}$) | *l* (mm) | ϕ (μm) | ε (%) | σ (MPa) | Y.M (GPa) | Spec. Y.M. (GPa g$^{-1}$cm$^{3}$) | Ref. |
|---|---|---|---|---|---|---|---|---|
| Abaca | 1.5 | 4.6–5.2 | 10–30 | 2.9 | 430–813 | 31.1–33.6 | n.a | 23 |
| Aramid | 1.4 | n.a | n.a | 3.3-3.7 | 3000-31500 | 63-67 | 45-48 | 6 |
| Bamboo | 0.6–1.1 | 1.5–4 | 88–25 | 1.3–8 | 140–441 | 11–36 | 18 | 33 |
| Banana | 1.35 | 0.9–0.4 | 12–30 | 5–6 | 529–914 | 27–32 | 20–24 | 23 |
| Carbon | 1.4 | n.a | n.a | 2.5 | 4000 | 230-240 | 164-171 | 6 |
| Chicken Feathers | 0.89 | n.a | n.a | n.a | 100-200 | 3-10 | 3.4-11.2 | 41 |
| Coir | 1.2 | 0.3–3.0 | 7–30 | 15–25 | 175 | 6 | 5.2 | 33 |
| Cotton | 1.21 | 15–56 | 12–35 | 2–10 | 287–597 | 6–10 | 4–6.5 | 33,42 |
| Curaua | n.a | 35 | 7-10 | 4.5-6 | 117 | 27.1 | n.a | 29 |
| E-glass | 2.5 | n.a | 15–25 | 2.5 | 2000–3500 | 70–73 | 29 | 42 |
| Flax | 1.38 | 10–65 | 5–38 | 1.2–3 | 343–1035 | 50–70 | 34–48 | 23 |
| Hardwood | 0.3–0.8 | 3.3 | 16 | n.a | 51–120.7 | 5.2–15.6 | n.a | 42 |
| Hemp | 1.35 | 5–55 | 10–51 | 1.6–4.5 | 580–1110 | 30–60 | 20–41 | 33 |
| Jute | 1.23 | 0.8–6 | 5–25 | 1.5–3.1 | 187–773 | 20–55 | 14–39 | 33 |
| Kenaf | 1.2 | 1.4–11 | 12–36 | 2.7–6.9 | 295–930 | 22–60 | 18–50 | 23 |
| Nettle | 1.51 | 5.5 | 20–80 | 1.7 | 650 | 38 | n.a | 23 |
| Pineapple | 1.5 | 3–8 | 8–41 | 1–3 | 170–1627 | 60–82 | 42–57 | 23 |
| Ramie | 1.44 | 40–250 | 18–80 | 2–4 | 400–938 | 61.4–128 | 29 | 42 |
| S-glass | 2.5 | n.a | n.a | 2.8 | 3000–3500 | 63–67 | 34.4 | 23 |
| Sisal | 1.2 | 0.8–8 | 7–47 | 1.9–3 | 507–855 | 9–22 | 6–15 | 33 |
| Softwood | 1.5 | 1 | 30 | 4.4 | 45.5–11.7 | 3.6–14.3 | n.a | 42 |
| Sugarcane Bagasse | 1.47 | 10 – 300 | 10-34 | 1.1 | 222 | 17.9-27.1 | 12.2-18.4 | 29,43 |

## 3.3 Fundamentals of the use of plant fibres in the composites area

### 3.3.1 Mechanical Performance of Plant Fibre Reinforced Composites.

The exploration of plant fibres to produce biocomposites can bring a number of advantages when compared to traditional fibres, and several authors have investigated the manufacture, use, reuse and disposal of these materials. Bledzki *et al.* compared different vegetal fibres such as cotton, jute, flax and sisal as a reinforcing agent versus of use of traditional fibres such as glass, carbon and aramid.[37] Although biocomposites presented reduced tensile properties, the plant fibres have an advantageous gain when the density of the fibres is considered. Because they have densities around 1.3 - 1.5 g cm$^{-3}$, the specific properties of these materials are competitive against glass and aramid. Nevertheless, it is essential to keep in mind that ultimate properties were still smaller than traditional composites, therefore

technical considerations should be taken when design composites reinforced with plant fibres. A summary of thermoplastic and thermoset (Table 3.4A and B) composites reinforced with vegetable fibres is presented below, illustrating the diversity of works in this area.

Table 3.4A: Composition, processing technique and maximum mechanical properties of plant fibre reinforced thermoplastic composites.

| Matrix | Fibre | Content | Processing Technique | E (GPa) | σ (MPa) | Ref. |
|---|---|---|---|---|---|---|
| HDPE | Eucalyptus | 20 - 40 wt% | Extrusion / Injection moulding | 0.97 | 20 | 44 |
| HDPE | Bamboo | 10 - 50 wt% | Extrusion | 1.4 | 29 | 45 |
| HDPE | Henequen | 20 vol% | Intensive mixer | 0.9 | 27.5 | 46 |
| HDPE | Wood | 10 - 40 wt% | Compression moulding | 3,2 | 44.5 | 47 |
| HDPE | Curaua | 20 - 40 vol% | Extrusion / Injection moulding | 1.3 | 23 | 48 |
| LDPE | Pineapple Leaf | 10-30 wt% | Melt mixing | 1.1 | 22.5 | 49 |
| LDPE | Sisal | 10-30 wt% | Melt mixing and Extrusion | 0.78 | 1.4 | 50 |
| PA-6 | Eucalyptus | 20 - 40 wt% | Extrusion / Injection moulding | 5.7 | 65 | 51 |
| PA-6 | Curaua | 20 - 40 wt% | Extrusion / Injection moulding | 5 | 82 | 52 |
| PLLA | Flax | 30 - 40 wt% | Extrusion / Compression moulding | 7.3 | 44 | 53 |
| PP | Wood flour | 20 wt% | Compression moulding | 2.0 | 25 | 54 |
| PP | Sisal | 10-30 wt% | Melt mixing and Extrusion | 1.1 | 33.8 | 55 |
| PP | Flax | 60 wt% | Compression moulding | 14.3 | 164 | 56 |
| PP | Flax | 20 - 40 vol% | Extrusion | 8.4 | 68 | 57 |
| PP | Hemp | 30 - 50 wt% | Extrusion / Injection moulding | 4.88 | 47.2 | 58 |
| PP | Hemp | 10 - 20 wt% | Internal Mixing | 3.1 | 27.8 | 59 |
| PP | Jute | 10-30 wt% | Extrusion / Injection moulding | 4.5 | 47 | 60 |
| PP | Kenaf | 30 - 40 wt% | Compression moulding | 4.8 | 45 | 61 |
| PP | Cotton | 18 – 23 vol% | Compression moulding | 1.9 | 39 | 62 |
| PP | Flax | 30 - 40 wt% | Extrusion / Compression moulding | 7.6 | 29 | 53 |
| PS | Sisal | 10-30 wt% | Solution mixing | * | * | 63 |
| PVC | Bamboo | 50 - 70 wt% | Compression moulding | 1.3 | 7.5 | 64 |

*: Only dynamic-mechanical properties were explored.

Table 3.4B: Composition, processing technique and maximum mechanical properties of plant fibre reinforced thermoplastic composites.

| Matrix | Fibre | Content | Processing Technique | E (GPa) | σ (MPa) | Ref. |
|---|---|---|---|---|---|---|
| Epoxy | Sisal | 30 - 80 vol% | Compression moulding | 25 | 200 | 65 |
| Epoxy | Flax | 40 wt% | Autoclave | 28 | 133 | 66 |
| Epoxy | Sisal | 20 wt% | Wet Lay-up | 2 | 37 | 67 |
| Epoxy | Hemp | 20 wt% | Wet Lay-up | 2,2 | 37 | 67 |
| Epoxy | Nettle | 20 wt% | Wet Lay-up | 2 | 35 | 67 |
| Epoxy | Flax | 50 - 80 vol % | Wet Lay-up | 10 | 156 | 67 |
| Epoxy | *Lantana camara* | 10 - 40 wt% | Wet Lay-up | n.a | 55.5 | 68 |
| Phenolic | Sisal | 33 wt% | Compression moulding | n.a | 25 | 69 |
| Phenolic | Bamboo | 25 vol% | Compression moulding | n.a | n.a | 70 |
| Phenolic | Jute/cotton | 17 - 40 wt% | Compression moulding | 7.1 | 59.4 | 71 |
| Phenolic | Pine needle | 10 – 40 wt% | Compression moulding | 0.6 | 31 | 72 |
| Phenolic | Flax | 50 - 80 vol% | Wet Lay-up | 6.5 | 62 | 73 |
| Urea | *Grewia Optiva* | 10 – 40 wt% | Compression moulding | 0.3 | 10 | 74 |
| Polyester | Pineapple Leaf | 10 - 40 wt% | Wet Lay-up | 2.3 | 52 | 75 |
| Polyester | Hemp | 16 - 44 wt% | Wet Lay-up | 6.2 | 53 | 76 |
| Polyester | Date palm | 6 - 10 wt% | Wet Lay-up | 7* | 70* | 77 |
| Polyester | Banana and Sisal | 40 wt% | Wet Lay-up | 1,5 | 59 | 78 |
| Polyester | Vakka Palm | 37 vol% | Wet Lay-up | 1,8 | 50 | 79 |
| Polyester | Sisal | 10 - 40 wt% | Wet Lay-up | n.a | 120 | 80 |
| Polyester | Sisal | 45 - 65 vol% | Wet Lay-up | † | † | 81 |

*Flexural properties †: Impact Properties

### 3.3.2 Environmental Performance of Plant Fibre Reinforced Composites.

In addition to studies related to the comparison of the mechanical properties of traditional and plant fibre reinforced composite, several papers focused on the elucidation of the environmental impact caused by the utilisation of these materials. Among several tools, life cycle assessment (LCA) allows the computation of all inputs/outputs of matter and energy in the life of a material, including the production of each of the components (extraction of raw material, transportation, *etc*.), manufacture and use of the final piece, Figure 3.5. This evaluation is also known as "from the cradle to the grave" since it accounts for reuse and disposal stages. Each LCA inputs/outputs are translated into environmental indicators according to a database, in order to calculate the net impacts of the entire process that are expressed in different categories (greenhouse gas emissions, damage the ozone layer, ecotoxicity, *etc*.)[82]

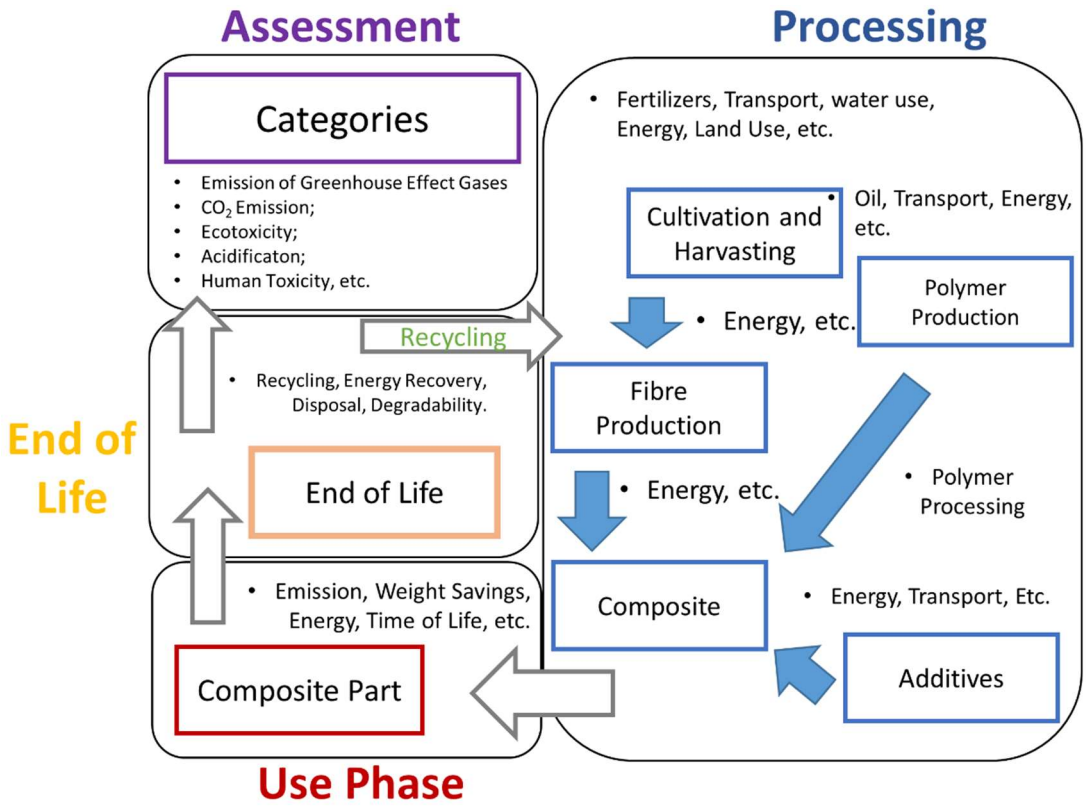


Figure 3.5: Representation of the inventory and boundaries of a "cradle to grave" life cycle assessment of a plant fibre reinforced composite.

In an early work in this area, Wotzel *et al.* investigated the impacts of the production of epoxy matrix composites reinforced with hemp fibres.[83] These materials were used as a replacement for injection moulded parts produced with ABS (acrylonitrile butadiene styrene) used as panels in the Audi A3. The authors used LCA to model the composite production, revealing that epoxy resin and curing agent were responsible for 77.5% of the total primary energy required, while the cultivation of hemp fibre corresponded to only 0.7% of the total energy. Comparing the epoxy/hemp composite with the material produced with ABS, the authors report a reduction of 45% in energy consumption followed by a reduction of parameters related to the emission of pollutants to the air.

The reduction of environmental indicators can be also associated with the decrease in the amount of polymer derived from petrochemical sources in the formulation. For example, composites reinforced with plant fibres usually require a higher content of reinforcing agent to reach the same properties of the analogous GFRC.[9] Consequently, plant fibres permit achieving a greater substitution of the polymeric matrix in the formulation, thus reducing the quantity of petroleum derivatives in their composition.

Corbiere-Nicollier *et al.* modelled the impacts associated with the production of polypropylene (PP) composites reinforced with *Miscanthus sinensis* (Chinese silver grass)

fibres as a substitute for GFRC.[82] The study compared the burdens of fibreglass production versus the cultivation, processing and transport of *Miscanthus sinensis*, followed by the manufacture of the functional unit (a transport pallet). Also, the authors also considered the use of the pallets and disposal through energy recovery to close the life-cycle. In this model, the production of composites using plant fibres led to a significant decrease (49%) in the use of non-renewable primary energy due to energy reduction, less use of PP and reduced density. In addition, emission of pollutants such as CO, $CO_2$, methane, $NO_x$, $SO_x$ and lead was reduced by replacing of glass by vegetable fibres. On the other hand, the study revealed an increase in emissions of $N_2O$ and $NH_3$ associated with fertilizers used during the plant cultivation. Overall, the use of plant fibres reduced the human toxicity factor by 57%, eutrophication by 8%, acidification by 34%, and GHG by 36%. Similar results were trends were observed by Joshi *et al*. when reviewing trends in this area. [13]

More recently, Luz *et al.* studied the impact of using sugarcane bagasse fibres as a substitute for talc in the production of composites for the automotive area.[84] Moving away from talc is particularly interesting for automotive makers as it has high density, while bagasse fibres are abundant in some areas in Brazil. The authors investigated the production of a panel of 1 $m^2$ (functional unit) produced with PP matrix by extrusion and injection moulding in cradle to the grave approach. The authors identified the importance of the transport distance of the fibre and composite samples, since it involves the consumption of fossil fuel and can alter the results in the sensitivity analysis. Calculations demonstrated that the use of sugarcane bagasse could lead to a reduction of the total energy required by approximately 20%, with economies observed mainly in the transport phase. A reduction of up to 5% was observed in all factors analysed (acidification, global warming potential, *etc.*). In addition, the authors showed that the combination of production and recycling stages of talc composites could lead to an increase of up to 25% in $CO_2$ emissions, further supporting the use of plant fibres.

Studies presented by Le Duigou and Baley contributed to the area by combining LCA technique with micromechanical analysis for an eco-design of automotive structural automotive parts produced from PP composite.[85] This approach integrated environmental and mechanical performance in one single analysis. In this study, the authors considered as a structural part used as support for the engine produced by extrusion and injection moulding as a functional unit. Prior to the calculation of the environmental impact, the authors had to model the changes in tensile modulus and fibre aspect ratio caused by the processing steps.

The replacement of glass fibres with flax fibres led a 5% density reduction, which positively affected the emissions in the use phase. In the boundaries defined by the authors, the materials were destined to incineration as a method of disposal, which led to energy recovery. The environmental impact analysis of these materials revealed that the replacement of glass fibres with flax fibres was responsible for 12% decrease in primary energy

consumption (96.5 MJ $kg^{-1}$ for flax composite versus 109.8 MJ $kg^{-1}$ for GFRC equivalents). Consequently, several of the environmental parameters investigated were favourable to the use of the bio-based fibre in the preparation of composites.

Since the mechanical performance of the composite could be adjusted according to the amount of reinforcing agent in the system, the authors established a relationship between fibre content, the variation of the properties and changes in the environmental impact categories. Therefore, Le Duigou and Baley demonstrated that the effect of eutrophication increases directly with the fibre content due to cultivation and spinning stages. In conclusion, the authors reported that the best formulation from the point of view of the balance between mechanical performance and environmental impact would be that with 30 wt% fibre in the formulation.

The processing steps used for the fibre production can have a direct influence in the environmental performance of the resulting composite.[86] For example, Dissanayake has extensively analysed different methodologies for extraction (water retting, dew retting and bio-retting) and post-processing of flax fibres (hackling, carding and spinning), and demonstrated that the selection of the correct method for the fibre extraction has major implications on acidification, entropification and aquatic toxicity.[87] Regarding the separation process, fibre spinning is the most energetically intensive stage as the spinning of 1 t of flax fibres consumes quantities of primary energy comparable to the production of 1 t of glass fibres. Therefore, this approach partially invalidates the advantages the use of natural fibres. Consequently, the authors suggest that the use of sliver (product of carding) is more advised than that of yarn from the point of view of energy consumption. [87]

The sustainable production of composites should focus not only look at the technological performance, but also considerate socio-economic impacts of their life cycle. Satyanarayana *et al.* discussed that the technological exploitation of plant fibres could contribute positively to the development and growth of local areas of cultivation, increasing the income of small producers and communities.[20] In this regard, Alves *et al.* studied the production of bonnets with jute fibres for off-road cars used by Brazilian communities in touristic area.[88] After modelling the impact, authors demonstrated the benefits of this approach from the environmental point of view. In addition, the study identified barriers related to the transportation of raw materials and recycling of the parts after the use phase since the region in which the composites are produced/used have a limited technological park ready for these processes. Finally, Alves *et al.* demonstrated that the production of these composites could contribute to the local economy since it incentives regional farmers involved with fibre cultivation, reduces manufacturing costs and attract more investment to the local industry.

Given these benefits, large automotive conglomerates such as Daimler AG, Volkswagen AG, BMW, Ford and Opel have been exploring the application of VFRC within

several car parts.[18,39,89,90] Nevertheless, it should be noted that there are still many challenges that prevent the application of VFRC in a broader context. Manufacturers have restricted the utilisation of these materials to interior parts since these parts suffer from moisture related problems. The cellulose found in the plant fibres is a highly polar component, therefore these materials tend to absorb water, which results in problems of dimensional stability, impairment of the surface finish and, finally, reduction of the mechanical properties.[25] The addition of plant fibres to composites also compromises their thermal stability. Plant fibres have a small resistance to combustion, and its thermal degradation temperature (ca. 220 °C) is low when compared to the processing temperature of most thermoplastics.[20] Consequently, the processing stage of VFRC deserves special attention since the conditions must be adequated to minimize the thermal degradation. Finally, the incompatibility between the hydrophilic character of the cellulosic fibres and the hydrophobic nature of the vast majority of polymer matrices is a great challenge to be uptake.[8] In this regard, section 3.5 covers strategies developed to uptake this barrier.

## 3.4 Green Materials: Composites from Renewable Matrices

Although plant fibres present themselves to the composites market as an ecologically-viable alternative, the polymer matrices used to produce these same materials are still mostly derived from petroleum and non-biodegradable. These characteristics prevent the further reduction of the environmental impact related to the production of VFRC. Consequently, academia and industry have been investigating the development of polymers from renewable sources for the development of chemical platforms able to produce fully bio-based composites. In this regard, thermoplastics produced from biological matrices and thermoset polymers from vegetable sources are the most commonly reported strategies in the literature. For example, materials such as polylactic acid (PLA) and polyhydroxyalkanoates (PHA) are currently commercially available bio-based matrices and applied in a range technologies[91] A more in-depth discussion of the role of bio-based thermoplastics in terms of their applicability was presented by Babu *et al.*.[92]

The combination of plant fibres and polymers from renewable sources can produce materials that marry high content of bio-based content and competitive mechanical properties. In this regard, polymer composites can be classified according to the nature of the polymer matrix and the reinforcing fibre.[93] Figure 3.6 illustrates a general classification used herein according to origin of the fibre and the polymer matrix. Green composites can be defined as those that offer more sustainable alternatives to traditional composites through the utilization of environmentally-friendly solutions, such as bio-based polymers and reinforcing effects. On the other hand, biocomposites can be defined as those in which all components are bio-based,

whilst some other authors even consider the biocompatibility aspect to define a material as biocomposite or not.[26,94] Nevertheless, there is no consensus in literature about this definition, and authors often interchange these terms.

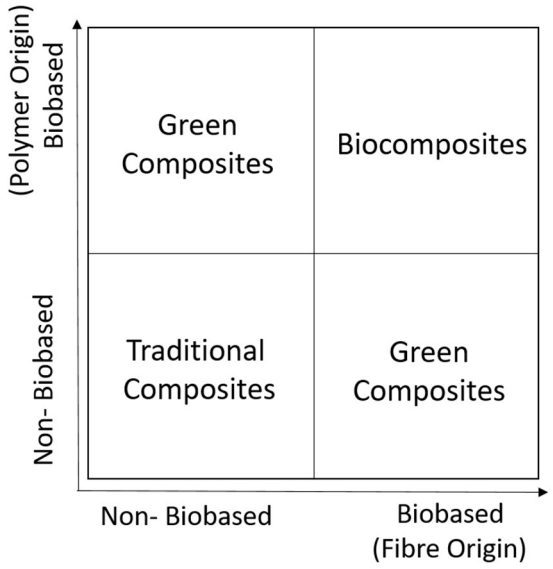


Figure 3.6: Schematic representation of the classification of composites according to their origin.

Vegetable oils have been receiving attention over the last two decades for the production of bio-based resins that are converted into thermosetting polymers. The transformation of vegetable oils into polymers is typically achieved through the chemical modification of triglycerides, inserting polymerizable groups as previously discussed in Chapter 2. An increasing number of studies and products have been incorporating EVO to produce polymers and composites. For example, Boquillon *et al.* produced a series of hemp fibre reinforced composites with epoxidized linseed oil (also known as ELO) by hot press technique using MTHPA as a curing agent and 2-methyl-imidazole as a catalyst.[95] The authors produced materials with up to 65 vol% of the reinforcing agent and observed a strong dependence of performance with fibre loading, which significantly increased the storage modulus and the $T_g$, indicating favourable interfacial interactions between the fibre and matrix.

Erhan *et al.* explored epoxidized soybean oil (ESO) resins to produce composites by freeform technique with glass, carbon, mineral and plant fibres.[96,97] Through the utilization of different polyamines as a hardener for the system, the authors demonstrated that mechanical properties of the resulting composite could be severely influenced by the fibre origin, the curing agents and curing temperature. Consequently, the study produced materials that ranged from elastomers to rigid materials. Also, the fibre loading and fibre alignment proved to affect the performance of the composites.

Tran *et al.* continued the exploration of the ESO-based composites reinforced with different natural fibres such as kenaf, kayocell, protein grits, and solka-floc.[98] The authors explored the resin transfer moulding (RTM) technique to produce materials with good resin infusion through fibres. Further chemical modification of ESO demonstrated the ability of controling parameters such as resin viscosity, gel time and mechanical properties without having to use petrochemicals additives. Among all formulations, kenaf fibres produced materials with the best tensile performance in all matrices investigated. Liu *et al.* reported the fabrication of composites combining ESO resin and flax fibres produced by compression moulding through the use of 1,1-tris(p-hydroxyphenyl)ethane triglycidyl ether (THPE-GE), which acts as hardener.[99] Scanning Electronic Microscopy (SEM) pictures confirmed excellent adhesion of the fibres onto the polymeric matrix, resulting in composites with good flexural properties. Maximum flexural properties were obtained with a reinforcing content of 13.5 wt% and fibres length of 3.6 mm.

Composites prepared with epoxidized linseed oil (ELO), cured with anhydrides and amines (in stoichiometric ratios) and reinforced with flax fibres were investigated by Fejos *et al.*[100] Different fibre textiles (twill, non-woven and unidirectional yarns) were used for the preparation of the composites by compression moulding to investigate the effect of the fibre alignment. Also, the authors varied the fibre ratio (from 33 to 61 wt%) to understand the wetting capacity of the resin and the efficiency of the stress transference phenomenon. Dynamic-mechanical studies demonstrated that anhydrides could produce matrices with higher $T_g$ versus amine hardeners. In addition, $T_g$ was reduced with increments in the fibre weight ratio, demonstrating the limitations in the stress-transference phenomenon and side reactions between the anhydride and the cellulose. The reinforcing effect proved to be highly dependent on the fibre alignment, where unidirectional yarns led to composites with superior storage modulus when tested on that direction. Finally, the authors revealed that these composites present a moderate shape-memory ability.

The production of matrices obtained with alternative polymerization techniques was investigated by Pfister and Larock.[101] EVOs produced from corn, soybean, fish and linseed oil were cationically polymerised and reinforced with agricultural sourced fibres such as corn flour, wheat straw and grass fibres. Composites with up to 75 wt% of fibres, tensile moduli ranging from 1.6 to 2.3 GPa and tension strength from 5.5 to 11.3 MPa were obtained. The authors identified that highly unsaturated oils such as linseed oil were able to produce composites with superior mechanical performance, reflecting the ability of these oils of having a greater substitution per unit and consequently allowing the formation of denser crosslinks. Regarding the effect of the fibres, wheat straw-reinforced composites demonstrated the best properties among all systems tested. Although the authors pointed out that these composites have limited mechanical properties compared to the analogues from petrochemical resins, they

emphasize that such materials can still find market application as non-structural parts in the automotive and construction areas such as door panels, ceilings, window frames and furniture.

The literature also presents a collection of works on the production of composites from the post-modified EVO resins, which were introduced in the previous chapter.[102] Acrylated epoxidised soybean oil (AESO) based composites reinforced with glass fibres were initially investigated as a strategy to produce materials with improved the mechanical properties at the cost of bio-based content in the final formulation. Based on this study, the same group developed hybrid composites combining glass-flax to maximise the advantages of each system.[103] This approach permitted obtaining a wide range of properties based on the content of each fibre in the formulation. AESO resin was blended with low-molecular-weight reactive diluents such as styrene to reduce the viscosity of the system, promoting better processability, reducing the costs of manufacturing, but increasing the environmental impact. AESO matrices were also reinforced with flax and hemp fibres, as demonstrated later by Williams and Wool.[104] In this work, the authors manufactured composites by RTM and observed superior mechanical performances in the 30 to 40 vol % of fibre load, which were comparable synthetic resins such as DGEBA and polyesters resins.

Further developments in the area of composites AESO resins were accomplished through the use of cellulose, flax, newspaper and recycled paper fibres, as presented by O'Donnel *et al.*[105] In this work, vacuum-assisted resin transfer moulding (VARTM) was used to produce the composites, exploring negative pressure to improve fibre impregnation. Among the different fibres tested in the study, recycled paper presented the best mechanical properties, achieving tensile modulus of 4.5 GPa with a reinforcing content of 55 wt%. The authors attributed this superior performance to the higher porosity of the recycled paper in comparison to other plant fibres investigated.

Interestingly, animal-derived natural fibres composites were also produced combining AESO resins with keratin fibres from avian feather, which were used both in their natural state and after a pyrolysis treatment.[106,107] Keratins fibres are good reinforcing agents due to its low-cost and lightweight as a consequence of its tubular and hollow structure, presenting density of approximately 1 g $cm^{-3}$. Also, these fibres are hydrophobic consequently being more chemically compatible with resins from vegetable oil and causing an enhanced fibre/matrix interaction. In this work, the authors produced composites with up to 30 vol % of avian fibres through the VARTM technique and observed a progressive reduction in the density of the resulting pieces of up to 8% with the fibre increment in comparison to the polymer matrix. In terms of thermal and mechanical performance, keratin-reinforced AESO composites presented a high glass transition temperature (70 °C) with flexural moduli of 1.9 GPa. In addition, keratin fibres improved the impact properties of the composites as a consequence of the unique

microscopic structure of the reinforcing fibres investigated in this study. The same group demonstrated the use of these composites in the construction of electronic circuits, as potential substituents for epoxy and polyester resins.[22]

More recently, a sequence of works developed by Skrifvars *et al.* examined the preparation of composites combining ESO modified with methacrylic and acetic anhydrides, introduced in the last chapter.[108,109] Flax fibres were stacked randomly and clockwise (0° and 90°) to investigate the effect of fibre orientation and manually impregnated with the resin. Composites presented good flexural and impact properties, and resins modified with methacrylic anhydride presented flexural strength and modulus of 90 MPa and 4.8 GPa, respectively. The addition of styrene as reactive diluent increased values to 118 MPa and 6.1 GPa due to its increased stiffness, but drastically reduced the renewable content and increased the environmental impact of the material, as previously discussed. Regarding the impact properties, modified resins resulted in the highest impact strength when blended with styrene (62 kJ $m^{-2}$) due to improvements in fibre/matrix interaction, as identified by SEM images.

In subsequent studies, the same authors prepared composites with jute and Lyocell fibres (regenerated cellulose fibre), as well as hybrid materials by hand-spraying technique.[108] The advantage of this methodology relies on its simplicity, reduced cost and the possibility of integrating higher volumes/longer fibres than wet lay-up. A dependence between the mechanical performance and the fibre architecture was found in jute-reinforced composites. Also, hybridization trough the addition of Lyocell resulted in further improvements in comparison with composites prepared only with jute, which was attributed to the inherent differences in the fibre structure and interaction with matrix.

The constant search for reducing the environmental impacts associated with the production of biocomposites has led to studies to investigate improvements from the point of view of the curing agent. Recently, Liu *et al.* demonstrated the production of composites reinforced with flax fibres, where the AESO-based matrix was cured with N-vinyl-2-pyrrolidone (NVP, Figure 3.7) as a styrene substituent.[110] Despite the widely utilisation of styrene as a reactive diluent, it is highly volatile and toxic. The authors demonstrated that AESO/NVP formulations presented a viscosity two times higher than that observed for the analogous system with styrene. Nevertheless, materials presented a maximum cure rate temperature 42 °C lower than styrene, demonstrating that the reactivity of the system requires lower cure temperatures, therefore being viable from a processing perspective. From the mechanical point of view, the substitution of styrene by NVP did not lead to any sacrifice in tensile, flexural and impact properties, thus evidencing the competitiveness of this molecule as a styrene substitute.

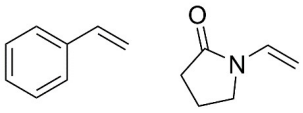

Figure 3.7: Chemical structures of styrene (left) and N-vinyl-2-pyrrolidone (right).

Another strategy to reduce the environmental impact is the use dicarboxylic acids as hardeners. These functionalities can be reacted with the oxirane rings present in EVOs to form networks through the formation of β-hydroxyester type bonds via ring-opening reactions as seen in Figure 3.8[111] One of the first demonstrations of this strategy was presented by Shogren *et al.*, who investigated the biodegradability behaviour of polymers produced from the citric acid, other dicarboxylic acids (adipic acid, succinic acid and sebacic acid) and diamines.[112] Citric acid is a particularly promising curing agent because of its high degree of functionality, wide availability and low-price. In this study, the authors observed that although polymers produced from the dicarboxylic acids were mineralised in approximately 30 days, the higher crosslink density provided by the citric acid was responsible for reducing the speed of the degradation. Nevertheless, denser crosslinks are able to provide better mechanical properties to the thermoset network, presenting a trade-off situation.

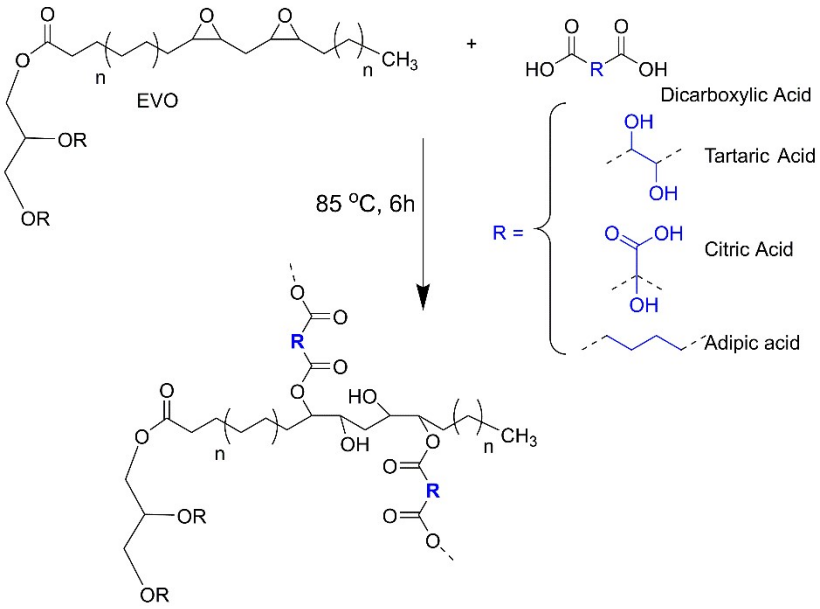


Figure 3.8: Representation of the crosslink formation through the cure of epoxidized vegetable oil (EVO) with dicarboxylic acids.

The production of polymers and composites from citric acid has been gaining attention following recent publications presented by Altuna and collaborators, which demonstrated the production of fully bioderived networks with adhesive and self-repair properties.[111] Despite the advances in the area of biopolymers[113] , the application of this strategy for the production

of composites has been only explored recently.[114–116] Recently, Gogoi *et al.* reported the production of green composites with ESO matrix cured with citric acid and reinforced with functionalized carbon nanotubes.[117] The introduction of carboxyl groups on the walls of carbon nanotubes (multiple walls) improved the interaction with the matrix as well and assisted the dispersion of the reinforcing agent. The authors used the FTIR technique to track the formation of the polymer network, and identified that the presence of functional groups on the nanotube accelerated the reaction of cure. The insertion of the reinforcing agent in contents up to 3 wt% increased the thermal stability of the composites to by 38 °C and the tensile strength by four times compared to the polymers without functionalized nanotubes.

Literature also shows a range of green composites that were prepared from the further modification of EVO into other resin systems. Dutta *et al.* investigated the production of jute fibre-reinforced composites with partially bio-based polyurethanes produced from the oil of the *Mesua ferrea L*. blended with commercial curing agents and epoxy resins (DGEBA) by hand lay-up.[118] Materials presented mechanical properties that were strongly dependent on the ratio of each component, where composites with higher bio-based content presented inferior performance. However, the alkali fibre treatment proved to improve the matrix/reinforcement interaction as evaluated by FTIR, SEM and TGA.[119] Castor-oil derived polyurethanes were used for the production of banana fibre reinforced composites by Merlini *et al.*[120] Randomly distributed mats of alkali-treated short fibres were processed with polyurethane resin though hand lay-up followed by compression moulding at room temperature at various fibre volume. The authors observed an increase in mechanical properties as a consequence of the fibre treatment, and the optimum fibre content and length in terms of chemical performance were found to be 15 vol% and 30 mm, respectively. Also, bio-based polyols were used in a mixture with polycaprolactone diol to produce castor oil-based polyurethanes films with controlled mechanical properties by Lee *et al.*[121] The polymeric matrix was reinforced with hemp fibres modified with isocyanate in an attempt to improve the interfacial adhesion of the components through the creation of superficial urethane bonds, which were confirmed through ATR-FTIR and proved to increase the mechanical properties of the composites in comparison to non-modified composite analogous.

The range of examples combining bio-based resins and plant fibres have demonstrated the versatility of this strategy to produce materials with high renewable content and lower carbon footprint when compared to traditional composites, also adding with novel and unique properties. Nonetheless, the application of these materials as structural parts demands systems with elevated glass transition temperature and highly crosslinked thermoset network, which is not achievable in most of the reported systems due to the chemical nature of the triglycerides.[96,122,123] Literature acknowledge this limitation, as this can be seen as one of the main challenges to make EVO-based composites not only viable when high performance is

not required.[122] Therefore, when designing this class of bio-based composites, one should consider as the primary goal to maximise the reactivity between the EVO resin and the hardener to produce dense networks and consequently polymers/composites with superior mechanical performance. Also, the resin/hardener system should be carefully designed to select molecular structures with rigid backbones, which will contribute to the creation of a stiff and strong thermoset.

### 3.5 Plant Fibre Modification

The abundance of polar molecules on the surface of plant fibres results in a highly hydrophilic character that conflicts with the hydrophobic nature of the polymer matrixes. Consequently, these materials will present a reduced interfacial interaction, reduced transfer of mechanical stress from the matrix to the reinforcing agent and consequently the resulting composite will presen limited mechanical properties.[124] Since compatibilization between these components is one of the most significant challenges in the area; literature has concentrated efforts in tackling this problem by modifying the chemical characteristics of the components. Although some methodologies are based on the modification of the matrix itself, this review will focus on methodologies that alter the chemical and physical properties of the plant fibres.

#### 3.5.1 Chemical Treatments

Figure 3.9 illustrates methodologies that have been utilised to modify the chemical characteristics of vegetable fibres. These procedures explore the reactivity of the pendant hydroxyl group found in the cellulose units to insert new chemical functionalities, enabling new forms of interaction with the polymer chain. Therefore, the versatility of cellulose as a chemical platform is demonstrated by the flexibility of the reactions performed in this particular site. The following sections explore in more depth the most common approaches listed on literature to promote a better fibre/matrix interaction.

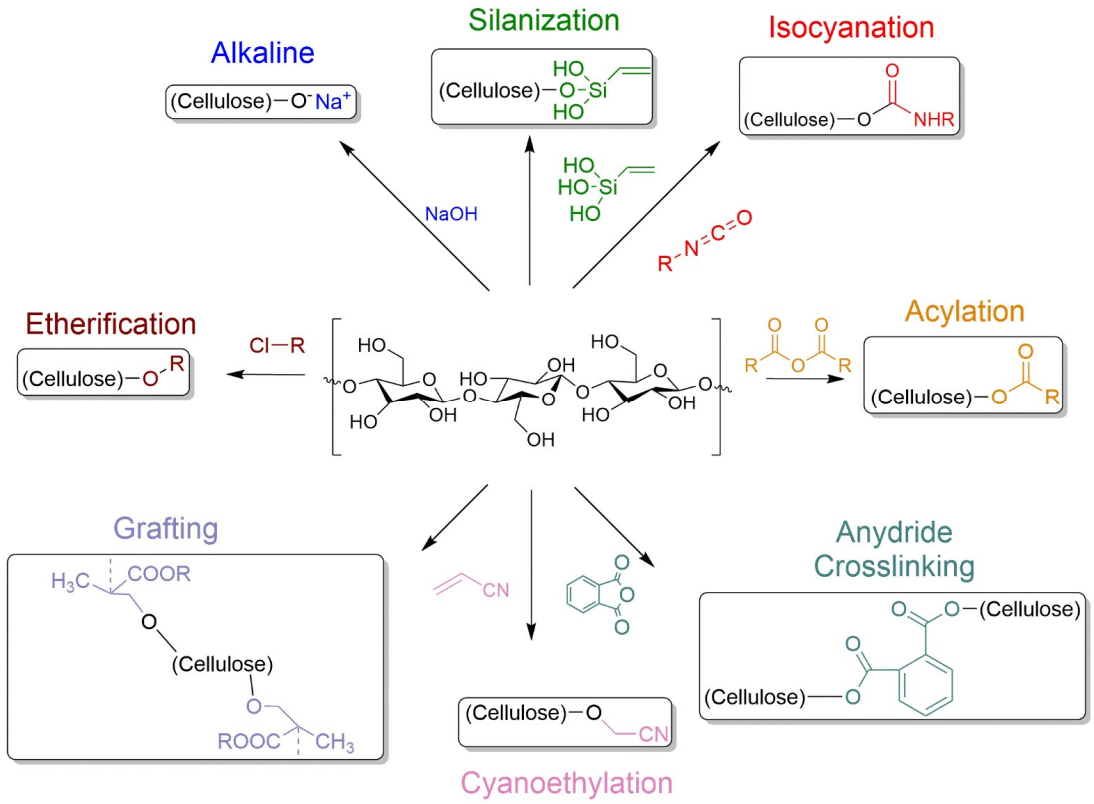


Figure 3.9: Representation of the different chemical pathways towards plant fibre modification.[23]

## a) Alkaline

Alkali treatment, also described as mercerisation, is one of the most commonly explored methodologies to chemically modify fibres due to its low-cost, effectiveness and simplicity. An extensive list of studies combining different alkali-treated fibres and matrices are reported in the literature. [66,125–131] The principle behind mercerisation is the chemical extraction of lignin and hemicellulose from the surface of the fibres, consequently increasing the relative content of cellulose in the reinforcing agent. Furthermore, waxes and oils present on the surface of plant fibres are also efficiently eliminated through this process.[8] Alkali treatment also has as the secondary effect of breaking the hydrogen bonds in the fibrillar arrangement in some extension through the ionisation of the hydroxyl groups. Consequently, the fibre bundles undergo fibrillation, increasing the surface area and aspect ratio of the plant fibres.[132]

The removal of lignin from the fibres due to mercerisation also provokes the reorientation of the cellulose crystallites, changing the directional properties of the fibres, the overall degree of crystallinity and the microfibrillar angle. From a chemical point of view, mercerisation can be represented according to the overall reaction represented by Scheme 3.1.[125] Nevertheless, the treatment can adversely affect the mechanical properties of the plant

fibre through cellulose depolymerisation, which can occur if the fibres are exposed to the alkaline medium for prolonged periods or to solutions with very high alkali concentration.[119]

$$\text{Cellulose-OH} + \text{NaOH} \rightarrow \text{Cellulose-O}^{-}\text{Na}^{+} + \text{H}_2\text{O} + \text{Impurities}$$

Scheme 3.1: Representation of the chemical transformations during the process of alkaline treatment of vegetal fibres.

Given the importance of finding the best balance between reaction time, the concentration of the NaOH solution, functionality and the occurrence of side-reactions during the alkaline surface treatment, different studies concentrated on optimising the reaction conditions.[37] Ray *et al.* subjected jute fibres to different treatment times ranging from 2 to 8 h at a constant reaction temperature and solution concentration (30 °C and 5 wt% NaOH).[133] These fibres were added as reinforcing agents to polyester resin in fibre fractions varying from 8 to 35 wt%, therefore the authors investigated both the effect of these both variables at the same time. The increase of the fibre modulus was proportional with the treatment time, with the best results being observed after 8 h (79%). This investigation revealed that a 4 h treatment was the optimum to promote the best balance in terms of performance, time of reaction and insertion of defects.

**b) Silanization**

Silane agents have been explored to improve the fibre/matrix adhesion since the early developments of glass fibre reinforced composites, proving to be a versatile methodology to couple a variety of polymeric matrices and fibres.[37] Organosilanes generally present the chemical formula R-$(CH_2)_n$-Si(OR')$_3$, where OR' is the hydrolysable group that allows the attachment to the plant fibre and R is an organic function responsible for interacting with the matrix. The nature of the organic group R can be manipulated to copolymerize with the matrix, forming an interpenetrating network.

Different theories were formulated to describe the interfacial bonding mechanism promoted by silane agents in composites.[132] Since chemical bonding is considered the principal mechanism that contributes towards the improvement in mechanical properties, silanization can be interpreted as the coupling phenomenon caused by the utilisation of bifunctional silanes. In the presence of moisture, the hydrolysable OR' groups react to form silanols (Figure 3.10A), which consequently can interact with the hydroxyl groups to create a stable siloxane covalent link (Figure 3.10B). Once immobilised, the organic functions attached to the silane can interact with the polymer network, providing the interaction enhancement. The extension of this functionalisation through this approach is dependent on the hydrolysis

step, nature of the functionalities attached to the silane, pH and temperature used in the methodology.[124,134] Nevertheless, unreacted groups are still able to interact with the cellulose through hydrogen bonds, as illustrated in Figure 3.10B, also contributing to the improvement of the fibre adhesion.

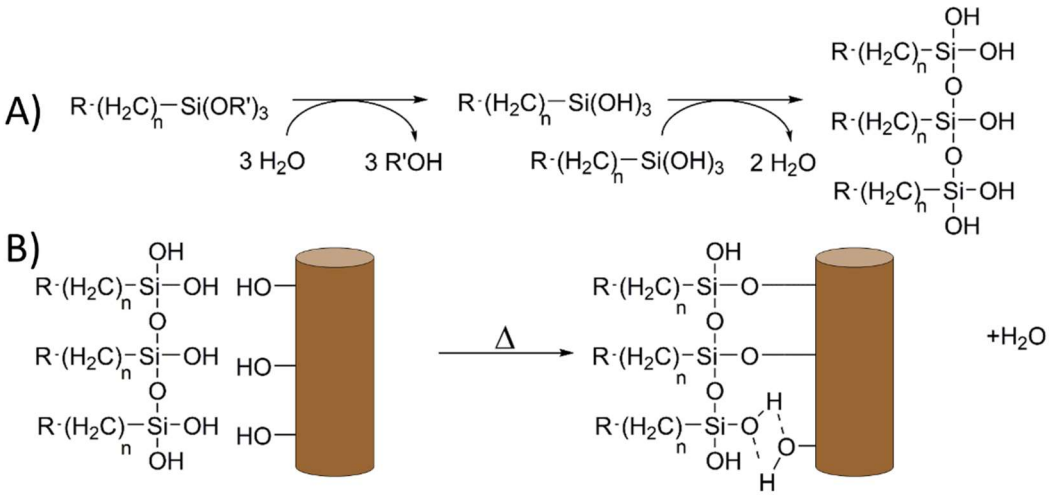


Figure 3.10: Schematic representation of the silanization through A) formation of silanol and B) creation of siloxane bonds.

One of the earliest reports of this strategy for VFRC comes was published by Bisanda and Ansell, who investigated sisal/epoxy composites prepared by compression moulding.[135] The treatment consisted in submerging the fibres in a 5% silane methanolic solution, preceded by an alkaline pre-treatment. A comparative study of the water uptake behaviour of these composites revealed that the silane treatment was capable of reducing the weight gain by caused by water absorption by nearly 68% whilst improving the flexural modulus and strength by 35% and 7%, respectively.

A similar approach was reported by Seki, who combined the mercerization and silanization to treat jute fibres used in epoxy and polyester resin composites.[136] Apart from improvements of 12% and 7% in tensile modulus and strength (respectively) in comparison to alkali treated equivalents, the author also observed an improvement of 42% in the interlaminar shear strength, demonstrating the improvement in the fibres adhesion onto the matrix. Further optimisations regarding the type and concentration of the silane were published by the same group, demonstrating further improvements in the mechanical performance of the composites reinforced with jute fibres.[137] Recently, Suwanruji *et al.* demonstrated the application of silane coupling agents for the modification of pineapple leaf fibres (PALF) used to reinforce LDPE and PP.[138] For both systems, chemically-treated fibres

were responsible for improving the tensile strength of the resulting composites. Similar results were obtained by Sepe *et al.* in investigations with hemp fibres and epoxy resin.[129]

**c) Stearic Acid**

Stearic acid can be used to modify the surface of the fibre through esterification between the hydroxyl groups present in the cellulose and carboxyl groups present in the fatty acid, Figure 3.11.[124] Additionally, the same treatment is responsible for removing non-crystalline materials such as pectin and waxes from the fibre since it is usually performed in ethanolic solution. This approach can also be considered as environmentally friendly since it is based on the exploration of a renewable compatibilizing agent. The combination of the consumption of the hydroxyl groups on the fibre surface and the attachment of long aliphatic chains ($C_{17}$) is responsible for significantly reducing the polarity of the material.

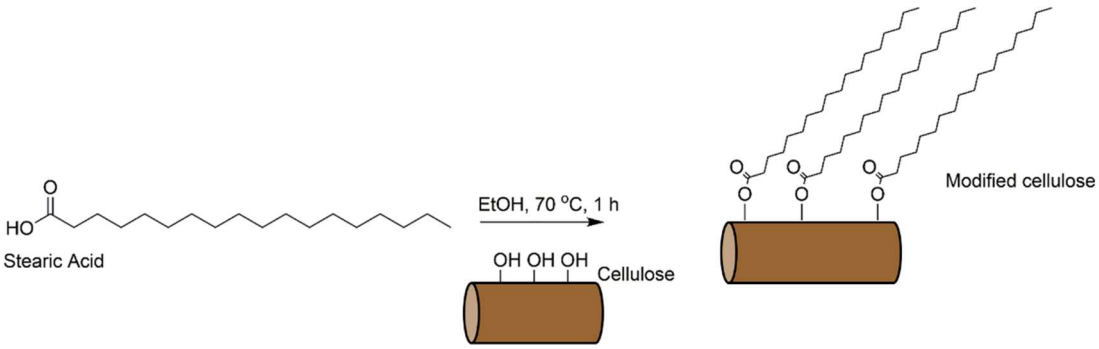


Figure 3.11: Representation of the functionalisation of plant fibres with stearic acid.

Kalaprasad *et al.* examined stearic acid treatment to chemically modify sisal fibres in the production of composites with LDPE.[139] A similar study was conducted by Torres and Cubillas, who developed polyethylene composites reinforced with treated sisal fibres by compression moulding.[140] Images obtained by SEM illustrated the improved adhesion between the fibres and the matrix through the reduction of fibre pull-out and better fibre dispersion. The improved interaction was also demonstrated by an increase in interfacial shear strength (23%) in comparison to analogues produced with untreated fibre.

Fibre polarity change caused by the treatment was further investigated by Paul *et al.* through the calculation of Kamlet–Taft solvatochromic polarity parameters.[141] This methodology is based on the characterisation of the fibre surface through the use of a set of three dyes and UV-Vis measurements, permitting the calculation of the hydrogen bond donating ability (α), hydrogen bond accepting ability (β) and dipolarity ($\pi^*$) parameters that can be related to the surface polarity. The authors demonstrated that stearic acid treatment was

the most efficient in reducing the polarity of banana fibres when compared to alkaline treatment, benzoylation, silanization and $KMnO_4$ treatment in the preparation of composites with PP by compression moulding. Paul *et al.* also investigated the thermal stability of these composites, demonstrating that the chemical modification with stearic acid was responsible for improving the thermal stability of the materials by improving the fibre/matrix interaction.[142]

The application of stearic acid treatment has also been demonstrated by Zafeiropoulos *et al.* for the production of composites with PP and flax fibres.[143] Initial studies about the fibre surface revealed that the treatment was capable of increasing the crystallinity of the cellulose, as observed by x-ray diffraction (XRD). SEM images revealed changes in the fibres topography, and that they were heterogeneously covered with the sizing agent. These findings were later confirmed by X-ray photoelectron spectroscopy (XPS) and time-of-flight secondary ion mass spectrometry (ToF-SIMS).[144] An investigation of the interface of these systems by single fibre fragmentation test revealed that stearic acid treatment was able to improve the stress transfer efficiency at the interface.[145] Finally, the study demonstrated optimisation of the stearation time, since excessively long reaction times were responsible for reducing the fibre strength and causing a lubricant effect, ultimately reducing the fibre/matrix adhesion.

**d) Etherification**

The etherification of plant fibres is a versatile methodology that permits the insertion of a range of functionalities through the utilisation of different electrophiles. This methodology is typically combined with pre-treatment of NaOH that exposes the hydroxyl groups of the cellulose and forms a charged intermediate that acts as an effective nucleophile.[124] Groups commonly utilised in this approach are epoxides, alkyl halides, benzyl chloride, acrylonitrile, and formaldehyde.[132]

In addition, alkyl chlorides and bromides facilitates this step through the use of existing groups, forming an anionic species and the giving the functionalised fibre. The use of benzoyl chloride (Figure 3.12) to chemically modify plant fibres has gained attention in the composites sector due to its ability to decrease the hydrophilicity of the plant replacing the superficial hydroxyl groups by benzoyl groups. This approach was already demonstrated in 1989 by Hon and Ou in the modification of pine wood.[146] Later, this methodology was demonstrated by Nair *et al.* for the production of PS composites with chemically modified sisal fibres.[63] The authors observed the changes in the chemical structure of the fibres caused by benzoylation by using FTIR and demonstrated the increase in thermal stability of the fibres, which surpassed other methodologies of functionalization due to a superior fibre/matrix

interaction. The improvement in adhesion also resulted in an increase of 12.8 °C in the $T_g$, superior damping properties and higher storage modulus.

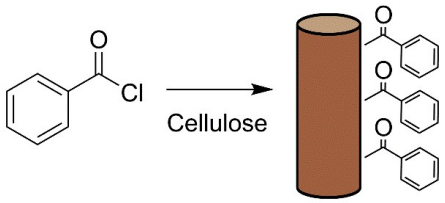


Figure 3.12: Chemical structure of benzoyl chloride and representation of the functionalisation of cellulose.

Similarly, Joseph *et al.* investigated the tensile properties of LDPE composites reinforced with sisal fibres treated with benzoyl chloride, and authors have observed that the methodology was more efficient in improving the mechanical performance in comparison to the traditional alkali treatment.[147] Overall, the benzoylation improved the tensile strength by 31% and the tensile modulus by 30%, confirming the improvement in adhesion between the reinforcing agent and the matrix. In another work, Wang *et al.* utilised of benzoylated flax fibres and rotational moulding as a processing technique.[130] Despite the reduction of the properties of the individual fibre bundles, composites prepared with treated fibres presented an improvement of 6% in tensile strength when compared to analogues produced with untreated flax. Most interestingly, benzoylation was responsible for reducing the water uptake of the composites by up to 19% due to the hydrophobisation of the fibre surface, outperforming other functionalisation methodologies.

An alternative approach to etherify plant fibres is the cyanoethylation with acrylonitrile.[125] This methodology is performed in the presence of NaOH, which deprotonates the hydroxyl groups from the cellulose and enables the reaction of these sites with acrylonitrile to form the ether bond, Figure 3.13.[148] In this regard, the cyanoethylation of non-woven jute fibres was explored by Saha *et al.* to produce composites with polyester resin by wet lay-up.[149] Longer treatment times reduced hydrophilicity of the fibres but also reduced their strength.[150] Dynamic-mechanical characterisation of the composites demonstrated the superiority of the modified fibres in comparison to unmodified fibres due to the improved adhesion. Consequently, authors detected higher values of storage modulus, an increase of approximately 20 °C in $T_g$ and an increase of the damping proprieties that corroborated the better fibre/matrix interaction. Similar results have also been reported for other plant fibres, such as sisal[65,80] abaca, [151] and pineapple leaf fibres.[152]

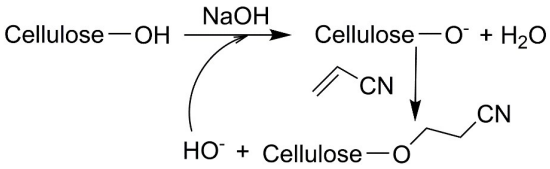


Figure 3.13: Representation of the etherification of plant fibres through cyanoethylation.

**e) Permanganate Treatment**

The oxidising nature of potassium permanganate ($KMnO_4$) has also been explored to induce new functionalities into cellulose in natural fibres. The highly reactive permanganate (VII) ions are capable of initiating a graft copolymerization involving the matrix and the cellulose, according to the proposed mechanism demonstrated in Figure 3.14.[153,154] Consequently, the grafting phenomenon leads to interfacial interlocking and better adhesion between the fibre and the matrix.[155] Secondary effects of the treatment with permanganate involve solubilisation and functionalisation of lignin.

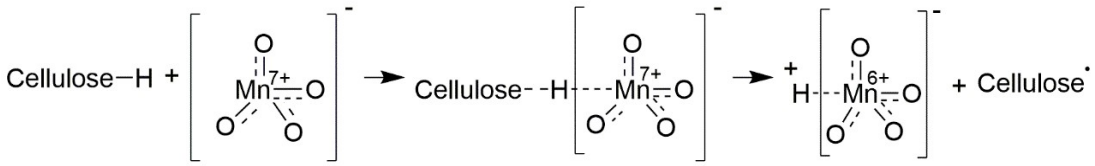


Figure 3.14: Creation of reactive cellulose species due to oxidation caused by permanganate.

The functionalisation with $KMnO_4$ has been demonstrated to different plant fibre systems on literature. For example, treated banana fibres were applied for the manufacturing of composites with PP.[141] The comparison of this methodology with others such as benzoyl chloride, stearic acid and silanization demonstrated that $KMnO_4$ could produce the stronger fibre/matrix adhesion. Paul *et al.* also reported the application of this treatment for sisal fibres used to produce composites with LDPE.[153] A study of the concentration of the permanganate solution (0.033, 0.0625, and 0.125% in acetone) revealed that concentrated solutions were able to reduce the hydrophilic nature of the fibres more effectively. However, the authors found that treatments performed with solutions of concentration above 1% led to an increase in the water uptake due to the formation of polar groups on the surface. Similar studies conducted by Joseph *et al.* and Kalaprasad *et al.* with sisal/LDPE confirmed the reinforcing effect observed by the permanganate treatment.[139,147]

This strategy has also been applied in the area of thermoset composites, as demonstrated by Sreekala *et al.* in the production of phenol-formaldehyde resins with different fibres.[156] In comparison to treatments such as mercerisation, acetylation, peroxide and corona,

the one based on $KMnO_4$ resulted in composites with the highest tensile strength (40 MPa). Similarly, polyester reinforced with permanganate-treated fibres investigated by Sreekumar, who demonstrated the effectiveness of the fibre modification on properties such as thermal conductivity, diffusivity, permittivity, specific heat, and tensile properties.[157]

More recently, Khan *et al.* explored the oxidation via $KMnO_4$ to chemically modify jute fibres used to reinforce PP by compression moulding.[158] The authors investigated different conditions for the chemical modification such as oxidation in solutions of oxalic acid, $H_2SO_4$ and NaOH. The medium proved to interfere with the level of fibre oxidation observed after the treatment, consequently affecting the reinforcing effect. In this regard, the authors reported that the treatment in oxalic acid solution led to composites with the best mechanical properties (1.28 GPa of tensile modulus and 69.8 MPa of tensile strength). Interestingly, the medium had little influence on properties such as water uptake and thermal stability. Despite the popularity of the $KMnO_4$ treatment, a recent study reported by Bulut and Aksit demonstrated that other oxidising agents, such as sodium perborate trihydrate, can lead to better improvements in performance.[159]

### 3.5.2 Physical Treatments

Alternatively to surface treatments based on the insertion of new chemical functionalities, physical methodologies can be explored to change the characteristics of plant fibres without changing their chemical composition.[37] These methods are responsible for modifying structural and surface properties, consequently influencing the resulting reinforcing effect. Physical treatments are considered as more environmentally friendly approaches to manipulate the fibre properties since they do not rely on the use of chemicals, changing the surface of fibre without affecting the bulk of the fibre.[160] However, these methodologies generally require more advanced equipment, adding costs to the treatment. Literature has a number of methodologies such as corona, plasma, ultraviolet (UV) and electron radiation that are capable of manipulating the fibre surface in order to improve adhesion into the polymeric matrix, and the most relevant ones are reviewed in the following sections.

#### a) Corona Treatment

Corona treatments utilise high voltage to generate a plasma at electrode tips, atmospheric pressure and in the presence of oxygen-containing species. This methodology changes the properties of the fibre surface by the inserting charges, changing in the surface polarity and increasing the fibre roughness, consequently facilitating the mechanical interlocking with the polymer. A proposed mechanism of how the cellulose units are transformed by this methodology is presented in Figure 3.15. One of the earlier application of

this methodology was reported by Belgacem *et al.* in the production of hardwood/PP composites, demonstrating that the increase of the plasma treatment time could linearly improve the strength of the samples.[161]

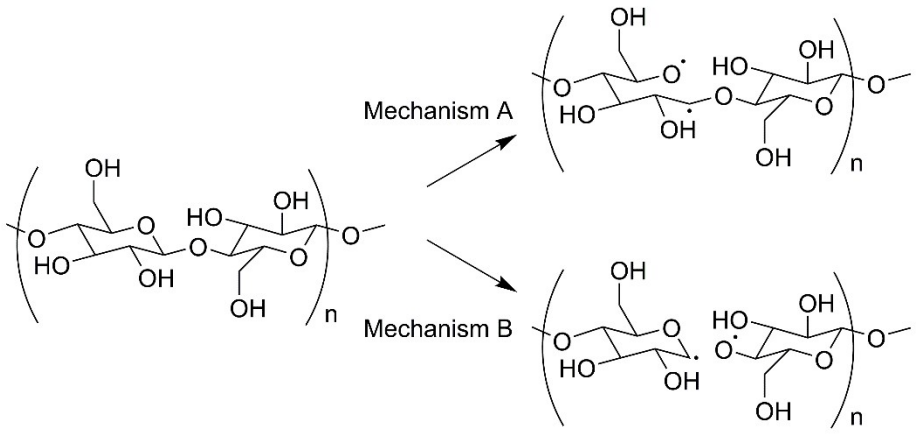


Figure 3.15: Mechanisms of functionalisation of cellulose via corona treatment. [162]

Further studies presented by Gassan and Gutowski explored the corona treatment to modify the surfaces of jute fibres used in epoxy resin composites.[163] After investigating different treatment conditions, the authors demonstrated an increase of the free surface energy with the use of more energetic plasma and improvements in storage moduli. Nevertheless, prolonged treatment times resulted in the reduction of the fibre strength due to excessive superficial oxidation, therefore limiting the reinforcing capacity. The same study investigated the utilisation of UV treatment to modify the properties of the fibres, which is based on the susceptibility of the components such as cellulose and lignin in undergoing oxidation under UV light.[164] The optimisation of the exposition time permitted balancing the increase in surface energy and a decrease in fibre strength due to oxidation, and consequently an improvement of 30% in the flexural strength of the composites.

A recent demonstration of the application of corona treated-fibres was reported by de Almeida Mesquita *et al.* for the reinforcement of polyester resins.[165] Pine, eucalyptus and sugarcane bagasse fibres were treated by alkaline method and with corona discharge of 12 kV. The authors demonstrated the improvement of the fibre/matrix interaction in through a water uptake test, which demonstrated a reduction of 10% in weight gain, and SEM images. Among the different systems tested, eucalyptus fibre reinforced composites presented the best mechanical properties due to the higher content of cellulose present in these fibres. Despite the improved impact performance, all formulations presented a compromise in flexural strength due to oxidation caused by the treatment.

**b) Cold Plasma**

A similar methodology explored to modify the fibre surface is cold plasma treatment, and is based on the formation of a plasma with high voltage, but in this case under an atmosphere of inert gases such as argon.[9] Sinha and Panigrahi explored this methodology to produce polyester resins reinforced with cold plasma treated jute fibres by wet lay-up.[160] The authors demonstrated that this treatment was capable of increasing the hydrophobicity of fibre surface whilst increasing the fibre area, as observed by contact angle determinations and confirmed by FTIR. The spectroscopy technique also revealed that the plasma treatment was capable of reducing the presence of hydroxyls and carbonyls groups in the fibre surface. In terms of mechanical properties, the treatment was able to increase the flexural strength of the composites by 14% compared to the raw fibre.

Ma and Joo investigated the utilisation of cold plasma as a pre-treatment to produce PLA composites.[166] Following the cold plasma methodology, a silane coupling agent was added to the system to act as a compatibilizer. Therefore, the authors could combine the physical change of the fibres and change of polarity with the addition of new functionalities. The authors detected changes in the crystallinity of the cellulose caused by the treatment, but no significant changes in mechanical properties since only part of the surface was modified. The interfacial shear strength was investigated, demonstrating that changes in the fibre surface energy could promote a stronger adhesion onto the matrix. The cold plasma treatment was also investigated by Bozaci *et al.* for the modification of flax fibres used to manufacture HDPE and polyester composites.[167] SEM images confirmed topological transformations caused by these treatments and the consequent increase in fibre surface area that could be correlated with the power of the plasma source. Cracks and grooves formed on the fibre by the treatment allow better mechanical interlocking with the matrix, improving adhesion. Nevertheless, these modifications resulted in fibres with reduced strength, a drawback commonly observed in this kind of treatment. Nevertheless, the treatment also improved the interfacial shear strength (IFSS) in comparison with analogues produced with untreated fibres. Interestingly, air plasma treatment resulted in higher IFSS for the HDPE composites, whereas argon plasma resulted in better adhesion properties in the polyester composites.

**c) Heat Treatment**

Thermal treatment can be also explored to modify the chemical, physical and mechanical properties of plant fibres.[9] These transformations are associated with a change in the water content in the fibre, which consequently changes in the crystalline structure and degree of polymerisation of cellulose and make the fibres stiffer. Additionally, the

combination of high temperatures and oxygen have a secondary effect of forming carbonyl, carboxyl and peroxide groups on the fibre surface.[168]

Rong *et al.* applied heat treatments for the preparation of epoxy resin composites reinforced with unidirectional sisal fibres.[65] Thermally-modified fibres (5 h at 150 °C) were compared to chemical methodologies such as mercerisation, acetylation and silanization. Among all treatments, the heat provided the best increase in crystallinity (3.4%) and tensile modulus (36.8%), but a modest change in Young`s modulus (3.3%). Further investigations demonstrated the positive impact of this methodology in properties such as damping and impact properties of modified-sisal fibre epoxy composites.[169] Thermally-treated sisal fibres were also applied to produce composites with polyester resins, as reported by Sreekumar *et al.*[170] The authors revealed that other modification strategies such as mercerisation and silanization could outperformed the heat treatment in terms of improving mechanical properties. However, this work explored milder conditions for the heat treatment (4 h at 100 °C) in comparison to the studies, which can explain the poorer performance of this methodology.

Ariawan *et al.* recently explored heat treatment to modify non-woven kenaf fibres used to produce polyester resin composites by RTM.[171] In this work, the authors exposed the kenaf mats to different lengths of thermal treatment (from 2.5 to 12.5 h) at 140 °C, and observed the maximum degree of cellulose crystallinity in the fibres after the 10 h treatment. Change in the chemical composition of the fibre surface was confirmed by XPS, demonstrating the oxidation caused by the combination of temperature and oxygen. Although the addition of fibre to the polyester resin significantly increased the water uptake (due to the fibre hydrophilicity), this process could be mitigated by the heat treatment. The modification was responsible for increasing the tensile modulus of the neat resin from 3.55 to 5.19 GPa, offering a 6% extra reinforcement effect in comparison to untreated fibres.

## 3.6 Summary

This review chapter identified the scale of the current composite market and the main challenges that are driving towards the exploration of plant fibres as reinforcing agents. Studies reviewed in this chapter presented how the chemical and structural features present in plant fibres contribute towards the production of materials with unique and novel properties in comparison to traditional materials, which depend on the selection of the matrix and the reinforcing fibre. The review also demonstrated the advantages of this approach from the environmental point of view, reducing the use of primary energy during production, recovery energy at the end of the life cycle and reduced consumption of resources during the end phase, consequently leading to significantly lower carbon footprints. Current, literature has also

embraced the utilization of bio-based polymers to produce composites entirely derived from natural sources, push the sustainability aspect further. Investigations reviewed in this chapter also identify that one of the main limitations of the area is to bring the property of biocomposites to the same level as engineering materials. In this regards, a range of chemical and physical methodologies have been explored to improve the fibre/matrix interaction.

## 3.7 References


1 W. R. Hibbard Jr, in *Fiber Composite Materials*, 1965, pp. 1–5.

2 H.-G. Elias, in *An Introduction to Plastics*, Wiley-VCH, Weinheim, Second., 2003, pp. 291–294.

3 A. K. Mohanty, M. Misra and L. T. Drzal, 2002, **10**, 19–26.

4 D. Hull and T. W. Clyne, *An Introduction to Composite Materials*, Cambridge Univerisity Press, Cambridge, United Kingdom, Second., 1996.

5 N. S. Enikolopyan, M. L. Fridman, I. O. Stalnova and V. L. Popov, in *Filler Polymers I: Science and Technology*, Springer-Verlag, Berlin, Germany, 1990, pp. 1–69.

6 A. K. Bledzki, S. Reihmane and J. Gassan, *J. Appl. Polym. Sci.*, 1996, **59**, 1329–1336.

7 M. S. Rabello, *Aditivação de Polímeros*, Artiliber, São Paulo, 1st edn., 2000.

8 J. George, M. S. Sreekala and S. Thomas, *Polym. Eng. Sci.*, 2001, **41**, 1471–1485.

9 K. L. Pickering, M. G. A. Efendy and T. M. Le, *Compos. - Part A Appl. Sci. Manuf.*, 2016, **83**, 98–112.

10 E. Witten, T. Kraus and M. Kuhnel, *Composites Market Report 2014*, 2014.

11 E. Witten, T. Kraus and M. Kühnel, *Composites Market Report 2016*, 2016.

12 L. Shen and M. K. Patel, *J. Polym. Environ.*, 2008, **16**, 154–167.

13 S. . V Joshi, L. . T. Drzal, a. . K. Mohanty and S. Arora, *Compos. Part A Appl. Sci. Manuf.*, 2004, **35**, 371–376.

14 H. Ku, H. Wang, N. Pattarachaiyakoop and M. Trada, *Compos. Part B Eng.*, 2011, **42**, 856–873.

15 Directive 2000/53/EC of the European Parliament and of the Council of 18 September 2000 on End-of-life vehicles., http://eur-lex.europa.eu/legal-content/EN/TXT, (accessed 16 October 2017).

16 Directive 2008/112/EC of the European Parliament and of the Council of 16 December 2008 amending Council Directives 76/768/EEC, 88/378/EEC, 1999/13/EC and Directives 2000/53/EC, 2002/96/EC and 2004/42/EC of the European Parliament and of the Council in or, http://eur-lex.europa.eu/legal-

content/EN/TXT/?uri=celex:32008L0112.

17 V. K. Thakur, M. K. Thakur, R. K. Gupta, R. Prasanth and M. R. Kessler, in *Green Composites from Natural Resources*, ed. V. K. Thakur, CRC Press, Florida, 2014, pp. 2–3.

18 J. Holbery and D. Houston, *JOM*, 2006, **November**, 80–86.

19 J. Smits, *Engineering*, 2016, **2**, 518–527.

20 K. G. Satyanarayana, J. L. Guimarães and F. Wypych, *Compos. Part A Appl. Sci. Manuf.*, 2007, **38**, 1694–1709.

21 Y. Zhang, C. Yu, P. K. Chu, F. Lv, C. Zhang, J. Ji, R. Zhang and H. Wang, *Mater. Chem. Phys.*, 2012, **133**, 845–849.

22 M. Zhan and R. P. Wool, *Compos. Part A Appl. Sci. Manuf.*, 2013, **47**, 22–30.

23 T. Gurunathan, S. Mohanty and S. K. Nayak, *Compos. Part A Appl. Sci. Manuf.*, 2015, **77**, 1–25.

24 G. Koronis, A. Silva and M. Fontul, *Compos. Part B Eng.*, 2013, **44**, 120–127.

25 Z. N. Azwa, B. F. Yousif, a. C. Manalo and W. Karunasena, *Mater. Des.*, 2013, **47**, 424–442.

26 O. Faruk, A. K. Bledzki, H.-P. Fink and M. Sain, *Prog. Polym. Sci.*, 2012, **37**, 1552–1596.

27 E. Espino, M. Cakir, S. Domenek, A. D. Román-Gutiérrez, N. Belgacem and J. Bras, *Ind. Crops Prod.*, 2014, **62**, 552–559.

28 W. Chen, H. Yu, Y. Liu, Y. Hai, M. Zhang and P. Chen, *Cellulose*, 2011, **18**, 433–442.

29 K. G. Satyanarayana, G. G. C. Arizaga and F. Wypych, *Prog. Polym. Sci.*, 2009, **34**, 982–1021.

30 M. C. Silva, O. R. Lopes, J. L. Colodette, A. O. Porto, J. Rieumont, D. Chaussy, M. N. Belgacem and G. G. Silva, *Ind. Crops Prod.*, 2008, **27**, 288–295.

31 M. A. Fuqua, S. Huo and C. A. Ulven, *Polym. Rev.*, 2012, **52**, 259–320.

32 M. Jawaid and H. P. S. Abdul Khalil, *Carbohydr. Polym.*, 2011, **86**, 1–18.

33 M. P. M. Dicker, P. F. Duckworth, A. B. Baker, G. Francois, M. K. Hazzard and P. M. Weaver, *Compos. Part A Appl. Sci. Manuf.*, 2014, **56**, 280–289.

34 X. Li, L. G. Tabil and S. Panigrahi, *J. Polym. Environ.*, 2007, **15**, 25–33.

35 A. Kaushik and M. Singh, *Carbohydr. Res.*, 2011, **346**, 76–85.

36 K. V Sarkanen, *Lignins: occurence, formation, structure and reactions*, Wiley Interscience, New York, USA, 1971.

37 A. K. Bledzki and J. Gassan, *Prog. Polym. Sci.*, 1999, **24**, 221–274.

38 S. Mishra, A. K. Mohanty, L. T. Drzal, M. Misra and G. Hinrichsen, *Macromol. Mater. Eng.*, 2004, 955–974.

39 M. John and S. Thomas, *Carbohydr. Polym.*, 2008, **71**, 343–364.

40 E. C. McLaughlin and R. A. Tait, *J. Mater. Sci.*, 1980, **15**, 89–95.

41 D. N. Saheb and J. P. Jog, *Adv. Polym. Technol.*, 1999, **18**, 351–363.

42 E. Zini and M. Scandola, *Polym. Compos.*, 2011, **32**, 1905–1915.

43 V. Rudolph, M. G. Rasul, V. Rudolph and M. Carsky, 1999, **2361**, 905–910.

44 A. Guilhen, R. Gadioli, F. C. Fernandes, W. R. Waldman and M. A. De Paoli, *J. Appl. Polym. Sci.*, 2017, **45219**, 1–10.

45 W. Ren, D. Zhang, G. Wang and H. Cheng, *BioResources*, 2014, **9**, 4117–4127.

46 P. J. Herrera-Franco and A. Valadez-González, *Compos. Part B Eng.*, 2005, **36**, 597–608.

47 X. Colom, F. Carrasco, P. Pagès and J. Canavate, *Compos. Sci. Technol.*, 2003, **63**, 161–169.

48 J. A. De Morais, R. Gadioli and M.-A. De Paoli, *Polímeros*, 2016, **26**, 115–122.

49 J. George and S. Thomas, *J. Appl. Polym. Sci.*, 1995, 843–854.

50 K. Joseph, S. Thomas, C. Pavithran and M. Brahmakumar, *J. Appl. Polym. Sci.*, 1993, **47**, 1731–1739.

51 F. C. Fernandes, R. Gadioli, E. Yassitepe and M.-A. De Paoli, *Polym. Compos.*, 2017, **38**, 299–308.

52 P. A. Santos, Universidade Estadual de Campinas (UNICAMP), 2009.

53 K. Oksman, M. Skrifvars and J.-F. Selin, *Compos. Sci. Technol.*, 2003, **63**, 1317–1324.

54 L. Dányádi, J. Móczó and B. Pukánszky, *Compos. Part A*, 2010, **41**, 199–206.

55 P. V Joseph, K. Joseph and S. Thomas, 1999, **59**, 1625–1640.

56 K. Van de Velde and P. Kiekens, *Compos. Struct.*, 2003, **62**, 443–448.

57 H. L. Bos, J. Müssig and M. J. A. van den Oever, *Compos. Part A Appl. Sci. Manuf.*, 2006, **37**, 1591–1604.

58 K. L. Pickering, G. W. Beckermann, S. N. Alam and N. J. Foreman, *Compos. Part A Appl. Sci. Manuf.*, 2007, **38**, 461–468.

59 M. Pracella, D. Chionna, I. Anguillesi, Z. Kulinski and E. Piorkowska, *Compos. Sci. Technol.*, 2006, **66**, 2218–2230.

60 T. T. L. Doan, S. L. Gao and E. Mäder, *Compos. Sci. Technol.*, 2006, **66**, 952–963.

61 M. Zampaloni, F. Pourboghrat, S. a. Yankovich, B. N. Rodgers, J. Moore, L. T. Drzal, a. K. Mohanty and M. Misra, *Compos. Part A Appl. Sci. Manuf.*, 2007, **38**, 1569–1580.

62 L. Y. Mwaikambo, E. Martuscelli and M. Avella, *Polym. Test.*, 2000, **19**, 905–918.

63 K. C. Manikandan Nair, S. Thomas and G. Groeninckx, *Compos. Sci. Technol.*, 2001, **61**, 2519–2529.

64 H. Wang, R. Chang, K. chuan Sheng, M. Adl and X. qun Qian, *J. Bionic Eng.*, 2008, **5**, 28–33.

65 M. Z. Rong, M. Q. Zhang, Y. Liu, G. C. Yang and H. M. Zeng, *Compos. Sci. Technol.*, 2001, **61**, 1437–1447.

66 I. Van De Weyenberg, J. Ivens, A. De Coster, B. Kino, E. Baetens and I. Verpoest, *Compos. Sci. Technol.*, 2003, **63**, 1241–1246.

67 M. K. Lila, G. K. Saini, M. Kannan and I. Singh, *Fibers Polym.*, 2017, **18**, 806–810.

68 C. Deo and S. K. Acharya, *J. Reinf. Plast. Compos.*, 2010, **29**, 2513–2521.

69 A. C. Milanese, M. O. H. Cioffi and H. J. C. Voorwald, *Compos. Part B Eng.*, 2012, **43**, 2843–2850.

70 M. Das and D. Chakraborty, *J. Reinf. Plast. Compos.*, 2009, **28**, 1339–1348.

71 E. S. De Medeiros, J. A. M. Agnelli, K. Joseph, L. H. De Carvalho and L. H. C. Mattoso, *Polym. Compos.*, 2005, **26**, 1–11.

72 V. K. Thakur and A. S. Singha, *Int. J. Polym. Anal. Charact.*, 2011, **16**, 390–398.

73 D. G. Hepworth, D. M. Bruce, J. F. V Vincent and G. Jeronimidis, *J. Mater. Sci.*, 2000, **35**, 293–298.

74 A. S. Singha and V. K. Thakur, *Polym. Compos.*, 2009, **116**, 459–470.

75 L. Devi, S. S. Bhagawan and S. Thomas, *J. Appl. Sci.*, 1996, **64**, 1739–1748.

76 T. Yuanjian and D. H. Isaac, *Compos. Sci. Technol.*, 2007, **67**, 3300–3307.

77 K. Al-Kaabi, A. Al-Khanbashi and A. Hammami, *Polym. Compos.*, 2005, **26**, 604–613.

78 M. Idicula, N. R. Neelakantan, Z. Oommen, K. Joseph and S. Thomas, *J. Appl. Polym. Sci.*, 2005, **96**, 1699–1709.

79 K. Murali Mohan Rao, K. Mohana Rao and A. V. Ratna Prasad, *Mater. Des.*, 2010, **31**, 508–513.

80 S. Mishra, M. Misra, S. S. Tripathy, S. K. Nayak and A. K. Mohanty, *Polym. Compos.*, 2002, **23**, 164.

81 C. Pavithran, P. S. Mukherjee, M. Brahmakumar and A. D. Damodaran, *J. Mater. Sci. Lett.*, 1988, **7**, 825–826.

82 T. Corbiere-Nicollier, B. Gfeller Laban, L. Lundquist, Y. Leterrier, J.-A. Manson and O. Jolliet, *Resour. Conserv. Recycl.*, 2001, **33**, 267–287.

83 K. Wotzel, R. Wirth and M. Flake, *Die Angew. Makromol. Chemie*, 1999, **272**, 121–127.

84 S. M. Luz, A. Caldeira-pires and P. M. C. Ferrão, *"Resources, Conserv. Recycl.*, 2010, **54**, 1135–1144.

85 A. Le Duigou and C. Baley, *J. Clean. Prod.*, 2014, **83**, 61–69.

86 N. P. J. Dissanayake and J. Summerscales, in *Green Composites from Natural*

*Resources*, ed. V. K. Thakur, CRC Press, Florida, 2014, pp. 157–158.

87 N. J. Dissanayake, University of Plymouth, 2011.

88 C. Alves, P. M. C. Ferrão, A. J. Silva, L. G. Reis, M. Freitas, L. B. Rodrigues and D. E. Alves, *J. Clean. Prod.*, 2010, **18**, 313–327.

89 J. Sloan, The making of the BMW i3, https://www.compositesworld.com/blog/post/the-making-of-the-bmw-i3, (accessed 31 October 2018).

90 D. M. Yazan, V. A. Romano and V. Albino, *J. Clean. Prod.*, 2016, **129**, 537–547.

91 M. R. Yates and C. Y. Barlow, *Resour. Conserv. Recycl.*, 2013, **78**, 54–66.

92 R. P. Babu, K. O'Connor and R. Seeram, *Prog. Biomater.*, 2013, **2**, 8.

93 F. M. Al-Oqqla and M. A. Omari, in *Green Energy and Technology*, Spinger International Publishing AG, Cham, Switzerland, 2017, pp. 13–29.

94 K. Haraguchi, *Encyclopedia of Polymeric Nanomaterials*, Springer, 2017.

95 N. Boquillon, *J. Appl. Polym. Sci.*, 2006, **101**, 4037–4043.

96 Z. S. Liu, S. Z. Erhan, J. Xu and P. D. Calvert, *J. Appl. Polym. Sci.*, 2002, **85**, 2100–2107.

97 Z. Liu, S. Z. Erhan and P. D. Calvert, *J. Am. Oil Chem. Soc.*, 2004, **81**, 605–610.

98 P. Tran, D. Graiver and R. Narayan, *J. Appl. Polym. Sci.*, 2006, **102**, 69–75.

99 Z. Liu, S. Z. Erhan, D. E. Akin and F. E. Barton, *J. Agric. Food Chem.*, 2006, **54**, 2134–2137.

100 M. Fejős, J. Karger-Kocsis and S. Grishchuk, *J. Reinf. Plast. Compos.*, 2013, **32**, 1879–1886.

101 D. P. Pfister and R. C. Larock, *J. Appl. Polym. Sci.*, 2011, **123**, 1392–1400.

102 S. N. Khot, J. J. Lascala, E. Can, S. S. Morye, G. I. Williams, G. R. Palmese, S. H. Kusefoglu and R. P. Wool, *J. Appl. Polym. Sci.*, 2001, **82**, 703–723.

103 S. S. Morye and R. P. Wool, *Polym. Compos.*, 2005, **26**, 407–416.

104 G. I. Williams and R. P. Wool, *Appl. Compos. Mater.*, 2000, **7**, 421–432.

105 A. O'Donnell, M. . Dweib and R. . Wool, *Compos. Sci. Technol.*, 2004, **64**, 1135–1145.

106 M. a. Dweib, B. Hu, a. O'Donnell, H. W. Shenton and R. P. Wool, *Compos. Struct.*, 2004, **63**, 147–157.

107 C. K. Hong and R. P. Wool, *J. Appl. Polym. Sci.*, 2005, **95**, 1524–1538.

108 K. Adekunle, C. Patzelt, A. Kalantar and M. Skrifvars, *J. Appl. Polym. Sci.*, 2011, **122**, 2855–2863.

109 M. Skrifvars, K. Adekunle and A. Dan, *J. Appl. Polym. Sci.*, 2009, **115**, 3137–3145.

110 W. Liu, T. Chen, T. Xie and R. Qiu, *Compos. Part A Appl. Sci. Manuf.*, 2016, **82**, 1–7.

111 F. I. Altuna, V. Pettarin and R. J. J. Williams, *Green Chem.*, 2013, **15**, 3360.

112 R. L. Shogren, Z. Petrovic, Z. Liu and S. Z. Erhan, *J. Polym. Environ.*, 2004, **12**, 173–178.

113 A. Li and K. Li, *ACS Sustain. Chem. Eng.*, 2014, **2**, 2090–2096.

114 M. Pawar, A. Kadam, O. Yemul, V. Thamke and K. Kodam, *Ind. Crops Prod.*, 2016, **89**, 434–447.

115 S. Ma and D. C. Webster, *Macromolecules*, 2015, **48**, 7127–7137.

116 R. T. Zeng, Y. Wu, Y. D. Li, M. Wang and J. B. Zeng, *Polym. Test.*, 2017, **57**, 281–287.

117 P. Gogoi, H. Horo, M. Khannam and S. K. Dolui, *Ind. Crops Prod.*, 2015, **76**, 346–354.

118 S. Dutta, N. Karak and S. Baruah, *J. Appl. Polym. Sci.*, , DOI:10.1002/app.

119 N. Moigne and P. Navard, *Cellulose*, 2009, **17**, 31–45.

120 C. Merlini, V. Soldi and G. M. O. Barra, *Polym. Test.*, 2011, **30**, 833–840.

121 N. Lee, O.-J. Kwon, B. C. Chun, J. W. Cho and J. S. Park, *Fibers Polym.*, 2009, **10**, 154–160.

122 A. Paramarta and D. C. Webster, *React. Funct. Polym.*, 2016, **105**, 140–149.

123 R. Wang and T. P. Schuman, *Express Polym. Lett.*, 2013, **7**, 272–292.

124 M. M. Kabir, H. Wang, K. T. Lau and F. Cardona, *Compos. Part B*, 2012, **43**, 2883–2892.

125 A. K. Mohanty, M. Misra and L. T. Drzal, *Compos. Interfaces*, 2001, **8**, 313–343.

126 A. C. H. Barreto, D. S. Rosa, P. B. A. Fechine and S. E. Mazzetto, *Compos. Part A Appl. Sci. Manuf.*, 2011, **42**, 492–500.

127 A. Gomes, T. Matsuo, K. Goda and J. Ohgi, *Compos. Part A Appl. Sci. Manuf.*, 2007, **38**, 1811–1820.

128 V. Fiore, G. Di Bella and A. Valenza, *Compos. Part B Eng.*, 2015, **68**, 14–21.

129 R. Sepe, F. Bollino, L. Boccarusso and F. Caputo, *Compos. Part B Eng.*, 2018, **133**, 210–217.

130 B. Wang, S. Panigrahi, L. Tabil and W. Crerar, *J. Reinf. Plast. Compos.*, 2007, **26**, 447–463.

131 M. S. Sreekala, M. G. Kumaran and S. Thomas, *Compos. - Part A Appl. Sci. Manuf.*, 2002, **33**, 763–777.

132 S. Kalia, B. S. Kaith and I. Kaur, *Polym. Eng. Sci.*, , DOI:10.1002/pen.

133 D. Ray, B. K. Sarkar, A. K. Rana and N. R. Bose, *Bull. Mater. Sci.*, 2001, **24**, 129–135.

134 A. Ashori, in *Hybrid Polymer Composite Materials: Properties and Characterisation*, eds. V. K. Thakur, M. K. Thakur and A. Pappu, Elsevier Ltd, 2017,

pp. 39–56.

135 E. T. N. Bisanda and M. P. Ansell, *Compos. Sci. Technol.*, 1991, **41**, 165–178.

136 Y. Seki, *Mater. Sci. Eng. A*, 2009, **508**, 247–252.

137 K. Sever, M. Sarikanat, Y. Seki, G. Erkan and U. H. Erdogan, 2010, 1913–1924.

138 P. Suwanruji, T. Tuechart, W. Smitthipong and R. Chollakup, *J. Thermoplast. Compos. Mater.*, 2017, **30**, 1344–1360.

139 G. Kalaprasad, B. Francis, S. Thomas, C. R. Kumar, C. Pavithran, G. Groeninckx and S. Thomas, *Polym. Int.*, 2004, **1638**, 1624–1638.

140 F. G. Torres and M. L. Cubillas, *Polym. Test.*, 2005, **24**, 694–698.

141 S. Annie, K. Joseph, G. D. G. Mathew, L. A. Pothen and S. Thomas, *Compos. Part A*, 2010, **41**, 1380–1387.

142 S. A. Paul, C. Oommen, K. Joseph, G. Mathew and S. Thomas, *Polym. Compos.*, 2010, **31**, 1113–1123.

143 N. E. Zafeiropoulos, C. A. Baillie and J. M. Hodgkinson, *Compos. Part A Appl. Sci. Manuf.*, 2002, **33**, 1083–1093.

144 N. E. Zafeiropoulos, P. E. Vickers and C. A. Baillie, *J. Mater. Sci.*, 2003, **8**, 3903–3914.

145 N. E. Zafeiropoulos, D. R. Williams, C. A. Baillie and F. L. Matthews, *Compos. Part A*, 2002, **33**, 1185–1190.

146 D. N. S. Hon and J. M. S. Luis, *J. Polym. Sci. Part a-Polymer Chem.*, 1989, **27**, 4143–4160.

147 K. Joseph and S. Thomast, 1996, **37**, 5139–5149.

148 G. C. Daul, R. M. Reinhardt and J. D. Reid, *Text. Res. J.*, 1955, 246–253.

149 a K. Saha, S. Das, D. Bhatta and B. C. Mitra, *J. Appl. Polym. Sci.*, 1999, **71**, 1505–1513.

150 A. K. Saha and B. C. Mitra, *J. Appl. Polym. Sci.*, 1996, **62**, 733–742.

151 M. Shibata, K. Ozawa, N. Teramoto, R. Yosomiya and H. Takeishi, *Macromol. Mater. Eng.*, 2003, **288**, 35–43.

152 S. Mishra, M. Misra, S. S. TripathyY, S. K. Nayak and A. K. Mohanty, *J. Reinf. Plast. Compos.*, 2001, **20**, 321–334.

153 A. Paul, K. Joseph and S. Thomas, *Compos. Sci. Technol.*, 1997, **57**, 67–79.

154 S. S. Tripathy, S. Jena, S. B. Misra, N. P. Padhi and B. C. Singh, *J. Appl. Polym. Sci.*, 1985, **30**, 1399–1406.

155 M. M. Rahman, A. K. Mallik and M. A. Khan, *J. ofApplied Polym. Sci.*, 2007, **105**, 3077–3086.

156 M. S. Sreekala, M. G. Kumaran, S. Joseph, M. Jacob and S. Thomas, *Appl. Compos. Mater.*, 2000, **7**, 295–329.

157 P. A. Sreekumar, B. Agoudjil, A. Boudenne, G. Unnikrishnan, L. Ibos, M. Fois and S. Thomas, *J. Reinf. Plast. Compos.*, 2012, **31**, 117–127.

158 J. A. Khan, M. A. Khan and R. Islam, *Polym. Compos.*, , DOI:10.1002/pc.

159 Y. Bulut and A. Aksit, *Cellulose*, 2013, **20**, 3155–3164.

160 E. Sinha and S. Panigrahi, *J. Compos. Mater.*, 2009, **43**, 1791–1802.

161 M. N. Belgacem, P. Bataille and S. Sapieha, *J. Appl. Polym. Sci.*, 1994, **53**, 379–385.

162 M. Ragoubi, D. Bienaimé, S. Molina, B. George and A. Merlin, *Ind. Crops Prod.*, 2010, **31**, 344–349.

163 J. Gassan and V. S. Gutowski, *Compos. Sci. Technol.*, 2000, **60**, 2857–2863.

164 D. N. Hon, *Wood Fiber Sci.*, 1994, **2**, 185–191.

165 R. G. de A. Mesquita, A. A. da S. César, R. F. Mendes, L. M. Mendes, J. M. Marconcini, G. Glenn and G. H. D. Tonoli, *J. Polym. Environ.*, 2017, **25**, 800–811.

166 H. Ma and C. Whan Joo, *J. Compos. Mater.*, 2011, **45**, 2455–2463.

167 E. Bozaci, K. Sever, M. Sarikanat, Y. Seki, A. Demir, E. Ozdogan and I. Tavman, *Compos. Part B Eng.*, 2013, **45**, 565–572.

168 Y. Cao, S. Sakamoto and K. Goda, *16Th Int. Conf. Compos. Mater.*, 2007, 1–4.

169 M. Z. Rong, M. Q. Zhang, Y. Liu, H. M. Yan, G. C. Yang and H. M. Zeng, *Polym. Compos.*, 2002, **23**, 182–192.

170 P. A. Sreekumar, K. Joseph, G. Unnikrishnan and S. Thomast, *Polym. Compos.*, 2011, **32**, 131–138.

171 D. Ariawan, M. S. Salim, R. M. Taib, M. Z. A. Thirmizir and Z. A. M. Ishak, *Compos. Interfaces*, 2017, **25**, 1–17.

# Chapter 4

# Bio-based Epoxy Resins from Waste Vegetable Oil:

## Purification, Chemical Modification and Application as a Reactive Diluent in Blends/Composites

Contents of this chapter have been published at:

F. C. Fernandes, D. Lehane, K. Kirwan and S. R. Coles, *Eur. Polym. J.*, 2017, **89**, 449–460.

## 4.1 Introduction

Currently, epoxidation represents the most commercially relevant chemical manipulation of vegetable oils (VO), producing bio-based epoxy resins that are used as adhesives, plasticisers and in polymer applications.[1,2] Despite many benefits from environmental and economic standpoints, structural characteristics of triglycerides such as their long aliphatic chains can negatively affect the application of these materials for engineering purposes. Typically, thermoset polymers originated from these resins exhibit inferior mechanical performance when compared to commercial resins based on diglycidyl ether of bisphenol A (DGEBA) due to differences in the stiffness of the molecular backbone and reactivity.[3] Consequently, there is still resistance towards the adoption of these materials as a replacement for petrochemical-based epoxies. Due to this limitation, partially bio-based blends combining epoxidized vegetable oils (EVOs) with DGEBA have been extensively explored to overcome these technical drawbacks, producing materials marrying bio-based content and enhanced mechanical properties. Examples of the production of DGEBA/epoxidized soybean oil (ESO) blends cured in the presence of methyl nadic anhydride (MNA), and phthalic anhydride (PA) are reported in several studies.[4–9] Overall these investigations demonstrated that the bio-based materials could lead to increased impact properties and adhesive strength in comparison to DGEBA formulations.

Nevertheless, the cost of these materials has restricted the industrial application of these materials as they remain uncompetitive in comparison to the petroleum-based resins.[10] Moreover, the use of edible oil for engineering raise discussions about the ethical use of land, the exclusion of VOs from the food chain and how it can negatively affect the price of staple markets.[11] Consequently, the production of bio-based materials from non-edible sources have been chased in a number of studies to overcome these barriers.[12,13] An alternative source of triglycerides that are yet to be exploited is waste vegetable oils (WVO), which can potential to satisfy the need for low-cost materials that also do not compete as food crops.[14,15] The technological valorisation of WVO also addresses the severe environmental and social problems associated with the incorrect disposal of cooking oil, which severely compromises aquatic life (as a result of oxygen depletion).[16,17] Nonetheless, the biggest challenge to implement WVO as a manufacturing platform is their heterogeneity; both embedded as a natural material and as a consequence of the by-products formed by thermal degradation and hydrolysis during the frying process. [18–21] A review of the most common reactions taking place during the use-phase of cooking oil was presented in Chapter 2.

In this chapter, the incorporation of epoxy resins from WVOs in DGEBA formulations was studied to evaluate the feasibility of these triglycerides in the production of thermoset polymers. Purification methodologies were firstly developed targeting the

elimination/reduction of by-products formed during frying to produce cleaner fatty acids from waste. WVO (and analogues) were epoxidized via different methodologies to comprehend factors that could affect the creation of oxirane rings, characteristic that is crucial to obtain materials with satisfactory mechanical properties. Therefore, studies herein presented establish a protocol to produce added-value chemicals from after-use vegetable oil efficiently. Blends were cured with different bio-based contents and characterised according to their mechanical and thermal properties. Later, milled recycled carbon fibres (MCF) were added to the blends to promote the recovery of mechanical properties and further reinforcement to demonstrate the first application of these materials.

## 4.2 Experimental

### 4.2.1 Materials

Virgin and waste vegetable oil samples (used in deep fat fryers for 4 days) were collected from food outlets at the University of Warwick, Coventry, UK. The samples were a blend of rapeseed and palm oil (approx. 3:1 vol.). Hydrogen peroxide (30% v/v), *m*-chloroperbenzoic acid (mCBPA, 77 wt%), toluene (puriss. p.a.>99.7%), dichloromethane (CHROMASOLV Plus) were supplied by Sigma-Aldrich UK. Activated carbon, $HNO_3$, $MgSO_4$ were supplied by VWR International. Super Sap CLR® was used as the epoxy part A (DGEBA, Entropy Resins, United States) and a part B of hardener (a mixture of isophorone diamine and 1,3-benzenedimethanamine, Entropy Resins, United States). Recycled carbon fibres (Carbiso™ MF, thermally recycled) were supplied by ELG Carbon Fibre Ltd. With a nominal average diameter of 7.5 μm and an average length of 80 μm. All chemicals, except WVOs samples, were used as received.

### 4.2.2 Purification of WVOs

#### 4.2.2.1 Single Extraction

WVO (50 mL) was filtered to remove solid impurities and subsequently diluted in $CH_2Cl_2$ (25 mL) to reduce the viscosity. The solution was washed once with a saturated solution of NaCl (100 mL) at 60 °C. The mixture was separated, and the organic phase was dried over $MgSO_4$, filtered and the solvent was removed using a rotatory evaporator. A clear brown oil was obtained (90 % yield).[22]

#### 4.2.2.2 Multiple Extractions

WVO (50 mL) was filtrated to remove solid impurities and subsequently diluted in $CH_2Cl_2$ (25 mL) to reduce the viscosity and facilitate the separation process. The solution was

washed with a saturated solution of NaCl (25 mL) at 60 °C. The mixture was left until phase separation, the organic phase was collected, and the procedure repeated four more times. The crude oil was dried over $MgSO_4$, filtered to remove the drying agent, and the solvent was removed using a rotatory evaporator. A clear brown oil was obtained (84 % yield).

### 4.2.3 Purification with Activated Carbon and Chemically Modified Activated Carbon.

The chemical modification step and purification followed the procedures optimised by de Castro Vasques *et al.*.[23] For that, activated carbon (5 g) was added in a beaker with concentrated $HNO_3$ solution (10 mL, 70 %) at 60ºC and stirred for 1 h. The mixture was filtered and the solid washed with water until the pH of the washed solution reached 7. The resulting black solid was left drying for 1 h at 110 °C in an oven with a yield of 86%. Chemically-modified activated carbon (3 g) was added to WVO (50 mL) in a round bottom flask and maintained under stirring for 24 h at 50 ºC. The mixture was subsequently filtered to separate the activated carbon from the purified oil, resulting in a brownish oil (62% yield). The same procedure was carried out using activated carbon without any prior modification for comparison proposes, resulting in a brownish oil with 67% of yield.

### 4.2.3 Epoxidation Methodologies

#### 4.2.3.1 Epoxidation with Peracetic Acid (Methodologies A and B)

WVO (50 mL, $5.6\times10^{-2}$ mol, $1.2\times10^{-1}$ mol of double bonds, 1 equiv.) was added in a round bottom flask with toluene (25 mL), acetic acid (3.5 mL, $6.4\times10^{-2}$ mol, 0.5 equiv.) and Amberlyst 15® (11 g, 22 wt % in relation to the oil content) as an acidic ion-exchange resin (AIER). The mixture was kept under stirring at 60 °C for 30 min and then $H_2O_2$ 30 % v/v (29 mL, $2.5\times10^{-1}$ mol, 2 equiv.) was added dropwise over 30 min. The reaction was left for 6 h under these conditions; then, the resulting product was filtered to remove the ion-exchange resin catalyst. The mixture was washed with a solution of 5 wt % $NaHCO_3$ and 5 wt % NaCl until all acid residues were removed (as identified by the pH). The crude oil was dried over $MgSO_4$, filtered to remove the drying agent and the solvent was removed using a rotatory evaporator.[24] The product was a yellow oily solid (71% yield). The same procedure was repeated substituting the AIER catalyst by catalytic amounts of $H_2SO_4$.

#### 4.2.3.2 Epoxidation with *m*-Chloroperbenzoic Acid (mCPBA, Methodology C).

WVO (25 mL, $2.8\times10^{-2}$ mol, $6\times10^{-2}$ mol of double bonds, 1 equiv.) was added to a round bottom flask and dissolved in $CHCl_3$ (150 mL). mCPBA (17.4 g, $6.6\times10^{-2}$ mol, 1.1 equiv.) was dissolved in $CHCl_3$ (100 mL) and slowly added (over 10 min) while the reaction

flask was kept in an ice bath ($T < 25$ °C). Once finished the addition, the ice bath was removed to permit the temperature to be raised to room temperature and stirring was continued under these conditions for 1.5 h. The resulting solution was filtered to remove by-products and washed with a solution of 5 wt% of $Na_2S_2O_5$ and 5 wt% of $NaHCO_3$. The resulting oil was dried over $MgSO_4$, filtered to remove the drying agent and the solvent was removed using a rotatory evaporator. The final product was a white oily solid (68% yield).

### 4.2.4 Preparation of Blends and Composites

Super Sap CLR® commercial resin was used as the foundation to produce the thermosets. The bio-based resin was added to the commercial epoxy resin (Part A) in a beaker according to the targeted formulation so the sum of both parts would be approximately 10 g. Formulations were prepared with bio-based resin contents of 0 wt%, 5 wt%, 10 wt%, 15 wt%, 20 wt% and 30 wt% of bio-based epoxy. Any contents beyond this point resulted in uncured polymers. Blends were prepared using epoxidized neat, waste and purified vegetable oils (total of 16 formulations counting the reference material). Sequentially, 47 wt% (concerning the total weight of the mixture) of the amine hardener (Part B) was added to the solution, and the blend was carefully stirred for 2 min ensuring proper infusion of the hardener into the epoxy resin and avoiding the formation of air bubbles. The resulting mixture was poured into dog bone shaped silicone moulds and left curing at room temperature for 24 h and post-cured in an oven at 50 °C for 2 h. Composites were prepared similarly, and the reinforcing agent (milled recycled carbon fibres, MCF) was added after part B was blended to the epoxy part in a weight percentage in regard to the total mass of the mixture. Formulations with 1 wt%, 5 wt%, 10 wt%, 20 wt% and 30 wt% were prepared using a fixed bio-based content of purified oil at 10 wt% (10EPVO).

### 4.2.5 Characterisations

Infrared spectra (ATR-FTIR; Cary Tensor 27) were obtained from 4000–500 $cm^{-1}$, accumulating 24 scans with a resolution of 4 $cm^{-1}$. $^1H$ NMR spectra were recorded on Bruker spectrometers HD Avance III 300 MHz & Bruker Avance III 400 MHz (300.129 MHz and 400.047 MHz, respectively) from samples of approximately 0.2 g dissolved in 500 µL of $CDCl_3$ with tetramethylsilane (Sigma-Aldrich, UK). Regarding the moisture content, approximately 1 g of the samples was added to an Ohaus MB45 balance programmed to heat the samples to 105 °C. The moisture content was measured according to the weight difference after 15 min at these conditions. The average and the standard deviation were calculated based on the analysis of three samples of each oil.

Dynamic mechanical analysis (DMA) was carried using a Triton Tritec DMTA in the dual cantilever mode, oscillatory frequency of 1.0 Hz, from -20 to 120 °C, heating rate of 2 °C $min^{-1}$ and displacement of 0.02 mm. Specimens were rectangles of the nominal size of 1.5 x 5 x 24 mm and glass transition temperature ($T_g$) was defined from tan δ peak. Weight-loss curves were measured by thermogravimetric analysis (TGA) using a Mettler Toledo TGA 1 STAR$^e$ System, from 25 to 600 °C, a heating rate of 10 ºC $min^{-1}$ under an $N_2$ flow of 100 mL $min^{-1}$. Curing behaviour was analysed by differential scanning calorimetry (DSC) using a Mettler Toledo DSC 1 STAR$^e$ System, from 25 to 350 °C, a heating rate of 10 ºC $min^{-1}$ under an $N_2$ flow of 100 mL $min^{-1}$. Tensile tests were carried out on an Instron 30 kN with samples in a scaled version (50%) of the ASTM D638, test velocity of 2 mm $min^{-1}$. Mechanical parameters were calculated based on the average of a minimum of seven specimens.

## 4.3 Results and Discussion

### 4.3.1 Vegetable Oil Characterisation

Initial studies were concentrated on the characterisation of the chemical structure of the oil feedstock, with particular attention to alterations caused by the frying process, which took place at 180 – 190 °C. The degree of unsaturation is a critical factor since double bonds are the reactive sites explored for the insertion of polymerisable groups. Therefore, the more double bonds present in the VO, the more oxirane groups can be inserted and consequently the denser the polymeric network will be after the cure. In this regard, $^1$H NMR analysis was used to investigate the chemical structure of the starting materials, to calculate the unsaturation degree and to identify by-products derived from the frying process. In this procedure, peak integration was calculated through relationship between the area of the signal of interest and of the signal *d*, assigned to six protons in α-position to the carbonyl per triglyceride unit.

Changes in the unsaturation degree of NVO and WVO caused by the thermal oxidation were identified through the reduction of resonance peaks in 1.94 – 2.14 and 5.26-5.40 ppm, assigned with α-allylic and allylic protons, respectively (Figure 4.1).[25] The integration of the peak associated with allylic protons (*e*) permitted the calculation of the average number of double bonds present per triglyceride unit. In this regard, a significant reduction (approximately 20%) in the average number of double bonds, from 2.88 to 2.28, could be detected by $^1$H NMR when comparing NVO and WVO samples. This evidenced the degradation triggered by allylic radicals, resulting in products with fewer reactive sites.[19,26] Although these oils present a lower degree of unsaturation in comparison to other VO typically used for the production of epoxy resins (e.g. linseed oil – 6.6 double bonds per triglyceride), the rapeseed/palm blend is a realistic representation of oils commonly used for cooking worldwide and therefore are ideal models for the scope of this study.[27,28] The full attribution

of other major $^{1}$H NMR peaks in these spectra are presented in Table 4.1, and values of coupling constants are presented in the Appendix.

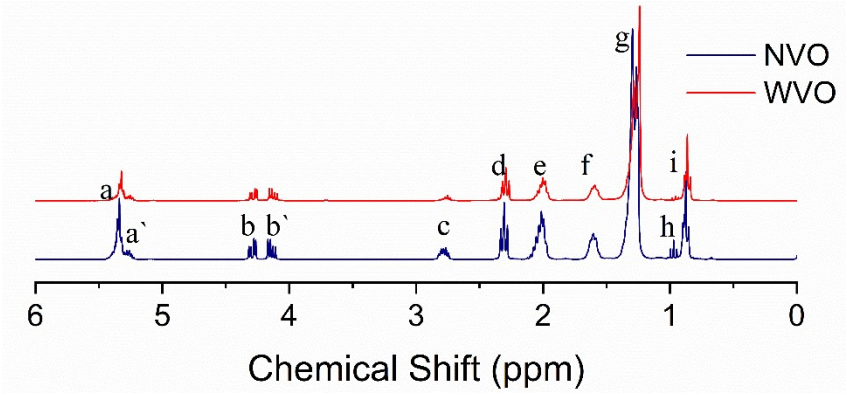


Figure 4.1: $^{1}$H NMR spectra of the neat (NVO) and waste vegetable oil (WVO) samples and assignment of the major resonance peaks.

Table 4.1: Major signals detected in $^{1}$H NMR spectra of the samples of neat (NVO) and waste vegetable oil (WVO) samples.

| Chemical Shift (ppm) | Proton | Functional Group |
|---|---|---|
| 0.83 – 0.93 | *i* | C**H**$_3$ (saturated, oleic and linoleic acyl group) |
| 0.98 | *h* | C**H**$_3$ (linolenic acyl group) |
| 1.22 – 1.42 | *g* | (C**H**$_2$)n- (acyl group) |
| 1.52 – 1.70 | *f* | OCO-CH$_2$-C**H**$_2$- (acyl group) |
| 1.94 – 2.14 | *e* | C**H**$_2$-CH=CH- (acyl groups) |
| 2.30 | *d* | OCO-C**H**$_2$- (acyl group) |
| 2.77 | *c* | HC-C**H**$_2$-CH= (acyl groups) |
| 4.10 | *b`* | C**H**$_2$OCOR (glyceryl group) |
| 4.29 | *b* | C**H**$_2$OCOR (glyceryl group) |
| 5.20 – 5.26 | *a`* | C**H**OCOR (glyceryl group) |
| 5.26–5.40 | *a* | C**H**=C**H**- (acyl group) |

Additionally, the signal *h* assigned to the terminal methyl groups in linolenic acids chains was significantly reduced from NVO to WVO. This observation is consistent with the increase of the signal *I*, assigned to protons in terminal methyl groups found in chains of reduced degree of unsaturation. Despite the chemical similarity, protons associated with signals *h* and *i* presented different chemical shift because they are at different distances to the nearest double bond. Therefore, these atoms experienced different chemical environments, which was affected by the chemical shielding caused by the double bond. In conclusion, these

two spectral changes demonstrated that highly unsaturated fatty acid chains are being degraded during the frying process to form less unsaturated units.

The presence of by-products from the frying process was also confirmed by multiple $^{1}$H NMR signals. The spectrum obtained from WVO revealed minor resonance peaks at 3.72 ppm and 5.08 ppm assigned to the glycerol group exclusively found in by-products of hydrolyses such as 1,2-diglycerides.[29] The analysis of resonance peaks between 4.00 and 4.35 ppm in the NVO spectrum revealed a well-defined double duplet associated with protons of the glycerol backbone of the triglyceride. However, the frying process was responsible for broadening these signals, introducing shoulders only found in the WVO spectrum. According to Nieva-Echevarria *et al.*, this effect is associated with the presence of 1,3-diglycerides in the sample, another hydrolysis by-product.[30] The same authors associated the peak at 4.18 ppm found in WVO with 1-glycerides, a product of two-step hydrolysis. Additionally, signals in 9.75 and 9.5 ppm were exclusively found in the WVO spectrum and associated with highly oxidised products such as n-alkanals, (*E*)-2-alkenals and (*E*,*E*)-2,4-alkadienals.[29,31]

The chemical structure was further analysed by ATR-FTIR spectroscopy. This technique was explored to investigate the creation of new bonds through the appearance of unique vibrational modes in the infrared energetic range. Spectra obtained from NVO and WVO (Figure 4.2) presented remarkable similarity since the by-products formed during the frying process present very similar chemical bonds.[32] Nevertheless, small changes could still be observed in the NVO versus WVO comparison. For example, the appearance of a new absorption peak in 1116 cm$^{-1}$ (ν C-O-C) in the WVO spectrum indicated the formation of ether bonds. This observation suggested the formation of thermal oxidation products triggered by the allylic radicals, which form this kind of bond during the termination step.[26]

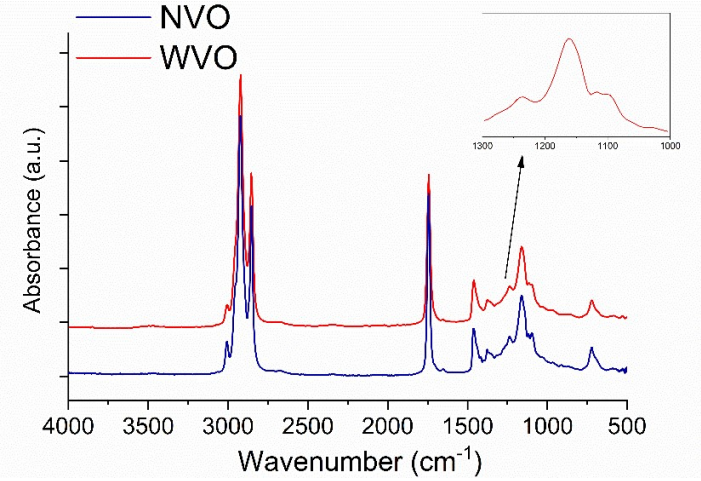


Figure 4.2: ATR- FTIR spectra of the NVO and WVO samples, from 4000 to 500 cm$^{-1}$.

The ATR-FTIR spectra provided more information through the analysis of the region associated with the unsaturated bonds. The absorption band in assigned to ν C-H in double bonds (3006 $cm^{-1}$) is visually reduced after the frying process. The normalisation of this band permitted the direct comparison of variation of this signal across different samples, and the band associated with ν C-H (2856 $cm^{-1}$) was selected as the reference since it is unaffected by the degradation processes during frying.[26] The calculation of the ratio between the intensity of the referential band and the band in ν C-H (double bonds) confirmed the relative decrease in the number of double bonds as the ratio value goes from 4.9 to 6.3. Furthermore, the reduction of the signal in 1652 $cm^{-1}$ associated with ν C=C *cis* from the NVO to WVO spectra revealed the isomerisation phenomenon that took place during frying.[33,34] A detailed assignment of key signals of absorption in the infrared region is found in Table 4.2. The information collected by ATR-FTIR complemented and supported the $^{1}H$ NMR data regarding the degradative reactions that took place during the frying process.

Table 4.2: Assignment of the major absorbance peaks found in the infrared spectra of neat (NVO) and waste vegetable oil (WVO) samples

| **Wavenumber ($cm^{-1}$)** | **Assignment** |
|---|---|
| 3009 | ν C-H in *cis* double bonds |
| 2947 - 2954 | ν $CH_3$ Symmetric |
| 2926 and 2854 | ν $CH_2$ Symmetric and asymmetric |
| 1745 | ν C=O |
| 1654 | ν C=C *cis* |
| 1465 to 1458 | δ $CH_3$ and $CH_2$ |
| 1377 | δ $CH_2$ |
| 1238, 1163, 1116, 1099 | ν C-O in ester group |

Transformations were also analysed by GC-MS, providing information regarding the fatty acid distribution, Figure 4.3. The fatty acid composition was obtained through the detection of major methyl esters (ratio higher than 1%) produced via transesterification. Compositional analysis of the NVO demonstrated high levels of unsaturated fatty acids, such as linolenic acid (C18:3, 20.8%); linoleic acid (C18:2, 3.2%); oleic acid (C18:1, 58.1% *cis* and 1.5% *trans*) and eicosadienoic acid (C20:1, 1.3%). From the total amount of fatty acids, only 12.9% presented saturated chains (mainly palmitic and stearic acids), which do not contribute towards the creation of the network since the insertion of oxirane ring is impossible. These long aliphatic segments found in the sample derive from the palm oil in blend used in the study, which is added to improve the thermal stability and reduce prices.[35]

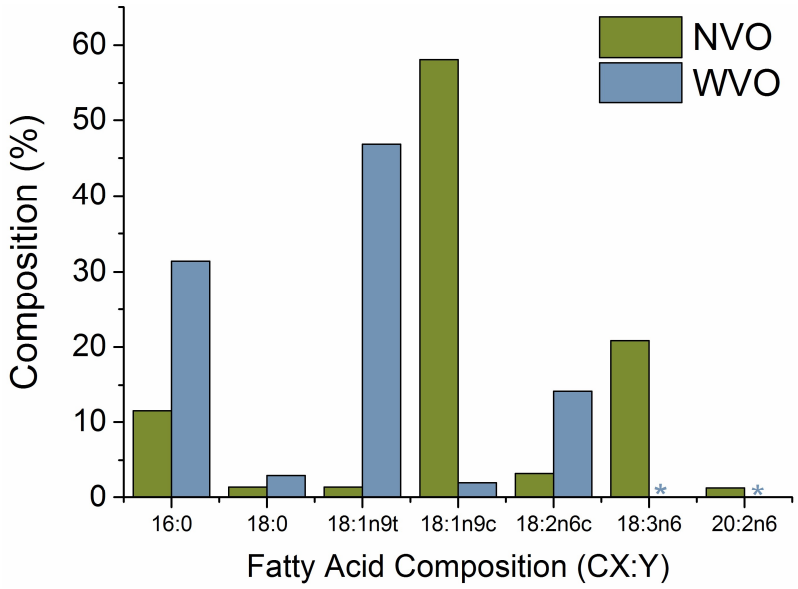


Figure 4.3: Fatty acids profile NVO and WVO samples as detected by gas chromatography–mass spectrometry (GC-MS). Stars represent no observable content.

Figure 4.3 also presents the fatty acid profile observed for WVO samples, demonstrating that the presence of linolenic acid chains (C18:3) was reduced to zero after the frying process. This observation reiterated the information gathered by $^{1}$H NMR, which demonstrated that highly unsaturated chains suffered with thermal oxidation.[20] Interestingly, the decrease in the levels of linolenic acid was accompanied by the increase of linoleic acid chains (C18:2, from 3.2% to 14.2%). This suggests the partial conversion of the chains of a higher degree of unsaturation into smaller ones. The consumption of the double bonds was also detected by the relative increase in the presence of stearic (C18:0, 3.0%) and palmitic acid (C16:0, 31.4%). The isomerisation process was also detected by GC-MS, where *cis*-oleic acid chains were partially converted into *trans*-oleic (58% and 47% in NVO and WVO, respectively).[33,34] Nevertheless, it is important to highlight that these values can in some cases represent a scenario different from reality since the standards used for calibration do not contain all isomers formed during the frying process.

### 4.3.2 Purification of Waste Vegetable oil

The characterisation of NVO and WVO have identified the main changes caused by the frying step from a chemical standpoint. These results provided the technical background required for the development of techniques to remove the impurities from the oil, obtaining a clean triglyceride source. As there was no literature focusing on the purification of WVO for the production of resins, different procedures were tested based on existing methodologies reported for the biodiesel area.[22,23] Despite the differences in each approach, all methodologies targeted the removal of highly oxidised compounds formed by the frying process (such as

aldehydes, epoxystearyl groups, primary and secondary alcohol) and products of hydrolysis such as mono- and diglycerides. The removal of these compounds is an essential step since functionalities that cannot be directly converted into reactive epoxy groups would contribute to the heterogeneity of the final product, reducing the selectivity and the control in the polymerisation steps.

Methodologies selected to purify WVOs consisted of the extraction of polar by-products with water at 60 °C by single and multiple extractions processes, as well as adsorption of the impurities using both activated carbon and activated carbon chemically modified with nitric ions.[23,36] These four approaches (described in Table 4.3) were previously successful in reducing the number of impurities present in WVOs. Figure 4.4 exemplifies the principle behind each purification methodology, schematically demonstrating how the separation between substrate and impurity occurs based on chemical affinity. In this study, these purification methodologies were responsible for introducing a new class of samples denominated as purified waste vegetable oil (PVO).

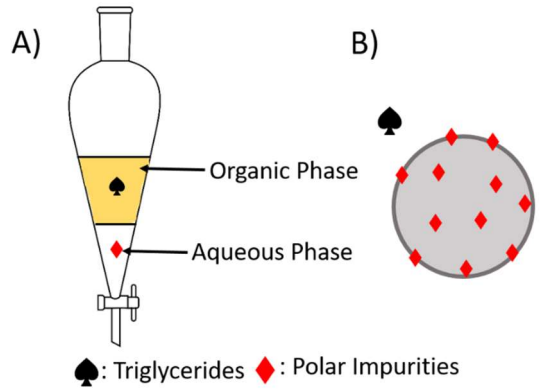


Figure 4.4: Representation of purification methodologies A) aqueous extraction of polar impurities and B) adsorption of impurities with activated carbon.

Table 4.3: Summary of the purification methodologies investigated in this study.

| **Technique** | **Methodology** |
|---|---|
| Extraction | Single-Step Aqueous Extraction<br>Multiple-Step Aqueous Extraction |
| Adsorption | Activated Carbon<br>$NO_3$-modified Activated Carbon |

The selection criteria behind the choice of these purification methodologies were the scalability, practicality (use of simple and readily applicable techniques) and the environmental impact associated with them. Although methods such as recrystallisation,

distillation and column chromatography are also reported in the literature for the manipulation of triglycerides, none of them proved were satisfactory in terms of purification due to low efficiency and use of high temperatures/large volumes of solvent.[37] These characteristics would compromise the scalability of the procedure and partially nullify the environmental benefits of using WVO as feedstock. Despite the water content being one of the main concerns in the purification of WVO for biodiesel, this is not as critical for the production of EVO.[38] The presence of water is considered a problem only once the oxirane ring is formed as it can perform a nucleophilic attack and ring-open the heterocycle.

At this stage, $^{1}$H NMR analyses were used to track the removal of by-products. The comparison between the spectra obtained before and after the multiple extraction processes illustrated changes caused by the purification step, Figure 4.5. All methodologies proved to be efficient in removing highly oxidised compounds as resonance peaks in the 9–10 ppm region were eliminated entirely from the PVO spectra. Therefore, all PVO samples were free of compounds such as n-alkanals and aldehydes. On the other hand, the elimination of compounds such as mono- and diglycerides (as evidenced by the reduction of signals in 3.72 and 4.18 ppm) was exclusively identified in the aqueous extraction procedures.

Comparing both extraction methodologies, the best results were observed for the multiple extractions with water at 60 °C, as previously optimised in literature.[22] In this regard, a higher extraction efficiency was expected for the procedure when executed multiple times with smaller solvent volume over a single extraction with a higher (but equivalent) solvent volume as the process is ruled by one single equilibrium constants. Spectra from samples purified with activated carbon presented the same observable peaks in the vegetable oil before any purification. The reduced efficiency of adsorption-based procedures could be associated with the fact that they were adapted from the purification of fatty acid methyl esters, which present reduced viscosity in comparison to WVO. Consequently, the increased viscosity hinders the adsorption process and result in an unsuccessful reduction of some of the by-products.[39,40]

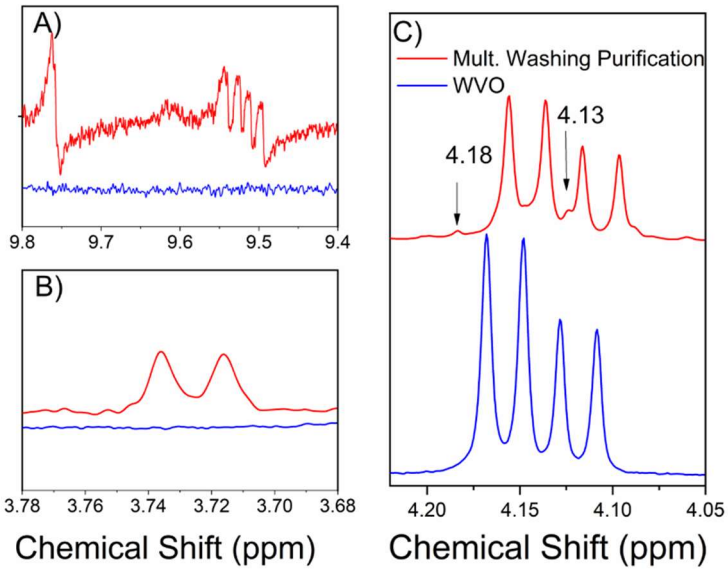


Figure 4.5: $^{1}$H NMR signals affected by the purification procedure: A) the region of aldehydic compounds, B) and C) regions associated mono- and diglycerides.

ATR-FTIR spectroscopy was also employed to track the elimination of thermal oxidation products, revealing again the similarity between spectra obtained by PVO and the other oil samples. Although the limited sensitivity of the technique in this regard, hydroperoxides were observed in the 3100 – 3600 $cm^{-1}$ spectral region, which are important to understand the degradation phenomena. Accumulated hydroperoxides can form alkoxy and hydroxyl radicals that can further degrade the oil and reduce the degree of unsaturation.[41]

In terms of how ATR-FTIR can be explored to comprehend the degradation associated with peroxides, the ratio between the areas of a reference band (ν C-H, 2856 $cm^{-1}$) and the band related to the hydroperoxides (ν O-H) can be used to compare the presence of these species in different oil samples.[25] $A_{2856}/A_{3100\text{-}3600}$ ratios were calculated for all purification methodologies investigated in this study, Figure 4.6. A smaller value of this ratio represented a relative increase of the 3100 – 3600 $cm^{-1}$ spectral band in comparison to the reference band, therefore an increased presence of by-products. For example, the drop in $A_{2856}/A_{3100\text{-}3600}$ ratio represented the formation peroxide by-products in WVO. Among all procedures, aqueous extractions once again proved to remove these degradation by-products more efficiently since the ratios presented the highest values, particularly for multiple aqueous extractions. Moreover, the ratio between the reference band and the ν C-H in double bonds (3006 $cm^{-1}$) was also investigated to identify possible alterations in the unsaturation degree caused by the purifications. Nevertheless, as also revealed in Figure 4.6, these ratios were not significantly altered by any of the purification procedures.

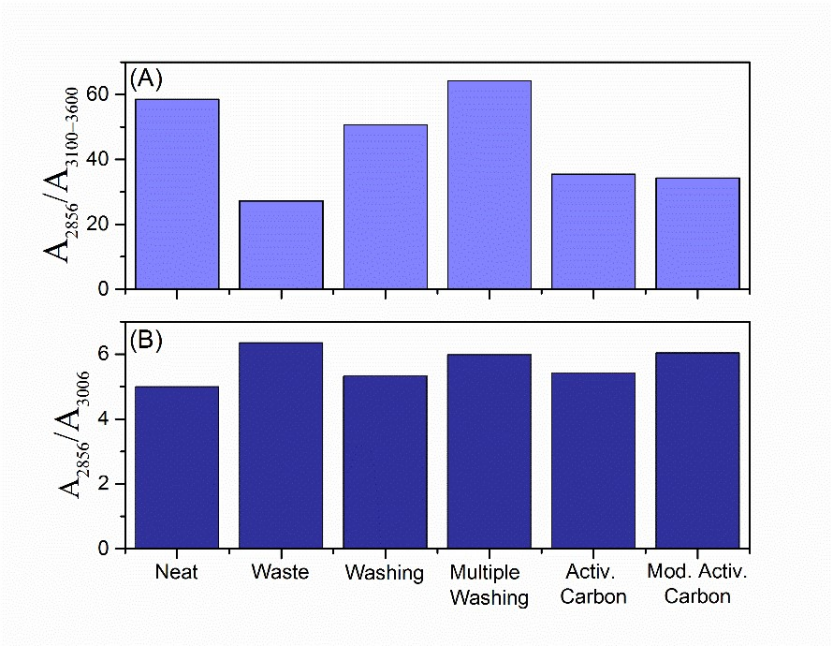


Figure 4.6: Ratios between the bands of the infrared spectra of the samples purified by the different methodologies: A) $A_{2856}/A_{3100-3600}$ and B) $A_{2856}/A_{3006}$.

Another critical alteration caused by the frying process is the increase of the water content in the oil.[19] Although it is not expected that water causes any significant interference during the epoxidation process, water can lead to premature hydrolysis after prolonged storage to form mono- and diglycerides.[18] In turn, these molecules can potentially create less tightly-connected networks, reducing mechanical properties. Therefore, it is critical to monitor the moisture content in the oil samples at all stages since two of purification methods take place in aqueous solutions.

Moisture content analyses was used to inspect the initial water content in NVO, WVO as well as the levels after the purification methodologies. However, as this methodology relies on the detection of weight loss as a function of temperature to determine the moisture content, thermogravimetric analyses were first employed to examine the thermal stability of the VO, ensuring their thermal stability in the experimental range. In this regard, thermogravimetric curves of NVO, WVO and the purified samples revealed that all samples presented an initial temperature of degradation higher than 350 °C, Figure 4.7. Interestingly, neat and purified oils presented higher stability than WVO, Table 4.4. This observation is a consequence of the presence of low-molecular-weight by-products formed during the frying process, which are eliminated by the purification methodologies.[42] Therefore, the purification is responsible for bringing the oil thermal stability closer to what is observed for the virgin sample. Nevertheless, some studies highlighted that the initial temperature of degradation of WVO can increases in some cases when the virgin oil is exposed to very harsh frying conditions (*i.e.* longer frying

times, higher temperature, repeated cycles, *etc.*), favouring the formation of height-molecular-weight species.[43]

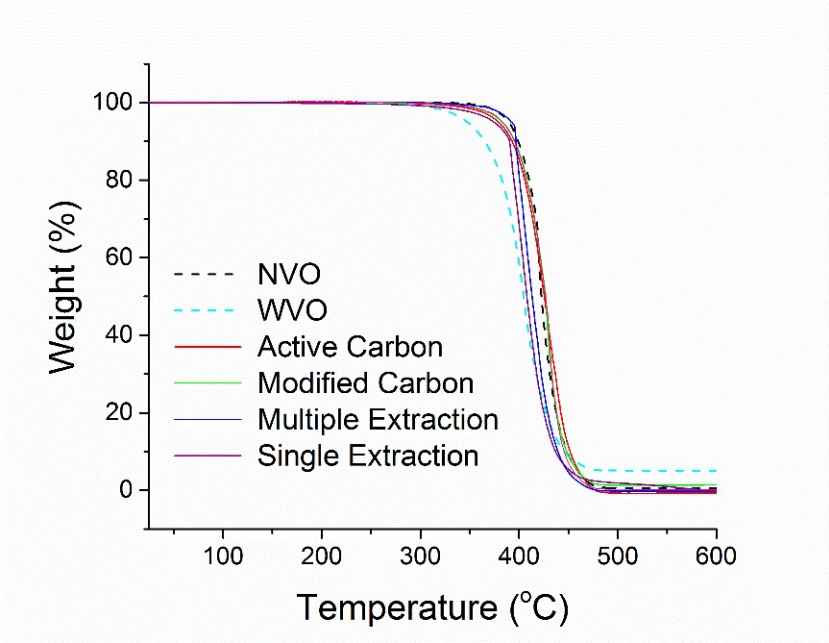


Figure 4.7: Thermograms of NVO, WVO and purified samples from 25 °C to 600 °C, heating rate of 10 °C $min^{-1}$, under an inert atmosphere.

Curves of the first derivative of the weight-loss percentage with respect to temperature (Figure 4.8) enabled a more detailed inspection of each sample. The comparison between WVO and NVO curves indicated that the degradation processes started at lower temperatures in the waste-derived sample. Also, the temperature of maximum degradation rate ($T_{Max}$) revealed that PVO samples obtained from the methods based on activated carbon presented the loss of volatile molecules very similar to what observed for WVO, indicating a poor purification performance. On the other hand, samples presented reduced quantity of volatiles in the triglyceride mixture. Consequently, these same samples presented a degradation profile that is much more similar to NVO.

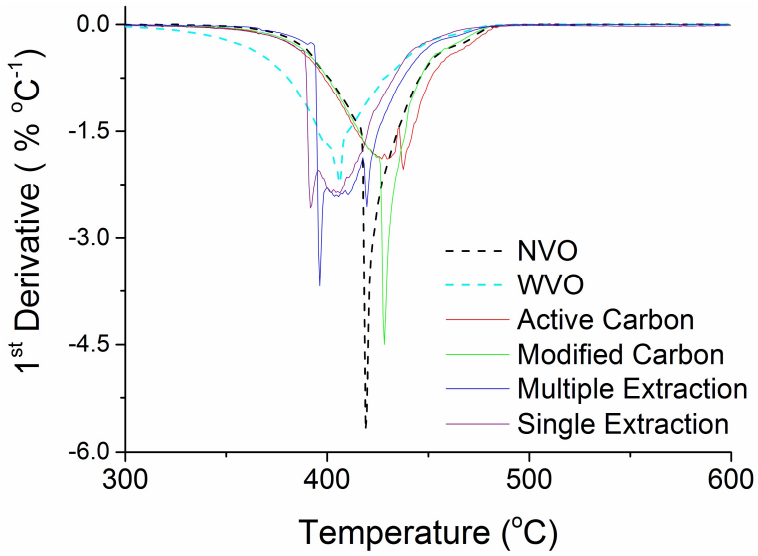


Figure 4.8: Curves of first derivative of the weight loss with respect to temperature of NVO, WVO and purified samples from 25 °C to 600 °C, heating rate of 10 °C $min^{-1}$, under an inert atmosphere.

Table 4.4: Initial temperature of degradation ($T_{Onset}$) and of maximum rate of degradation ($T_{Max}$) of neat (NVO), waste (WVO) and purified samples.

| **Sample** | $T_{Onset}$ **(°C)** | $T_{Max}$ **(°C)** |
|---|---|---|
| NVO | 382.4 | 419.0 |
| WVO | 350.7 | 405.0 |
| Active carbon | 388.6 | 437.0 |
| Chemically modified activated carbon | 395.0 | 428.3 |
| Single aqueous extraction | 393.3 | 396.3 |
| Multiple aqueous extractions | 388.0 | 391.7 |

Since results from thermogravimetric analyses demonstrated that no significant thermal degradation event took place before 350 °C the utilisation of a moisture balance to calculate the water content was validated. In this regard, these values were obtained by heating each oil samples to 105 °C for 15 min and calculating the weight difference, Table 4.5. As expected, the frying process increased the water content in the WVO by approximately 23% when compared to NVO. Potential sources of incorporation of water are the natural moisture found in food and from frying frozen food.[44] Despite the initial concern about the moisture content caused by the purification process in aqueous media, these methodologies effectively decreased the moisture content of WVO to the same levels observed to NVO. This reduction was associated with the drying step using $MgSO_4$ performed in all methods that eliminated

any additional moisture. Therefore, it can be said that none of the methodologies introduced risks of premature hydrolysis despite being conducted in water.

Table 4.5: Moisture content in of neat (NVO), waste (WVO) and purified samples.

| Sample | Moisture Content (%) |
|---|---|
| NVO | 0.74 ± 0.03 |
| WVO | 0.91 ± 0.03 |
| Single aqueous extraction | 0.75 ± 0.05 |
| Multiple aqueous extraction | 0.76 ± 0.02 |
| Activated carbon | 0.76 ± 0.02 |
| Chemically modified activated carbon | 0.77 ± 0.04 |

Overall, findings associated with the investigation of the purification processes demonstrated that the methodology based on multiple aqueous extractions at 60 °C was the most efficient in terms of reducing the polar impurities in the oil. At the same time, this methodology proved not to lead to not compromises in other qualities of the samples, such as the moisture content and degradation of unsaturation sites. Therefore, this multiple extraction approach was selected as the standard procedure for purifying WVOs throughout the investigations in this study.

### 4.3.3 Chemical Modification of Bio-Based Epoxy Resins

The selection of the most suitable methodology requires balancing between selectivity, cost and environmental impact to allow the sustainable production of bio-based epoxy resins.[1] After reviewing the methodologies presented previously, three epoxidation routes were pre-selected for a screening test based on the methodologies reviewed in Chapter 2. Therefore, vegetable oil samples were epoxidized through methodologies based on peracids (A: Acid catalysed, B: ion exchange resin (AIER) catalysed) and with *m*-chloroperbenzoic acid (C: mCPBA), Figure 4.9. Also, resins were prepared from WVO before and after the purification process to investigate the impact of the purification in the chemical modification step and of the frying stage. These investigations prepared new samples denominated as epoxidized neat vegetable oil (ENVO), epoxidized waste vegetable oil (EWVO), and epoxidized purified waste vegetable oil (EPVO).

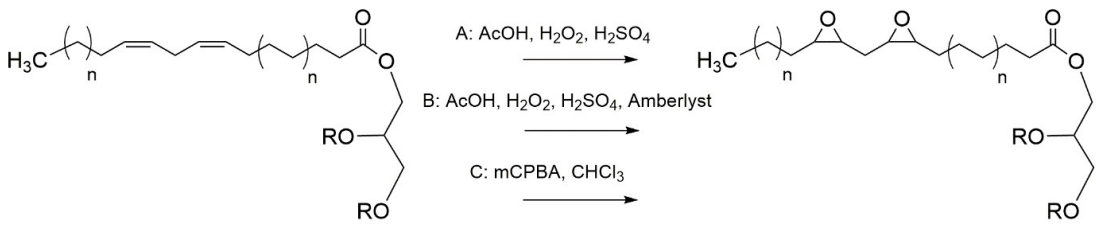


Figure 4.9: Schematic representation of the epoxidation methodologies explored in this study.

As presented in Chapter 2, the molar ratio between the oxygen donor and the oxygen carrier plays an important role regarding control and selectivity since they create the highly-reactive intermediate that interacts with the substrate.[45] In the current study, the oxygen donor employed was $H_2O_2$ and the oxygen carrier was acetic acid. This combination led to the formation of peracetic acid, intermediate that is capable of reacting rapidly with unsaturation sites due to the presence of a labile hydroperoxide bond. Once the peracid reacts with the substrate, the oxygen carrier could be regenerated and participate again in the oxygen atom transport process. Therefore, quantities required of oxygen carrier were always smaller than the number of molar equivalents of oxygen donor.[46]

One potential limitation observed in peracid-mediated epoxidations is the susceptibility to nucleophilic attacks triggered by the organic acid, forming ring-opening by-products with a reduced capacity of polymerisation that can compromise the properties of the resulting thermoset. Therefore, it is crucial to find the right balance between parameters such as reaction time, temperature and concentration of the oxygen carrier to achieve a successful result. For example, too much carrier and long reaction times will eventually lead to ring-opening reactions and by-products, whereas few carrier molecules and short reaction times will result in poor conversion values. In this regard, the current study was based on previous reports by Dinda *et al.*, who investigated and optimised the yields in the conversion of vegetable oils into epoxy resins.[45] In this study, authors observed the best results through the utilisation of molar ratios of (1:2:0.5) with respect to the double bond equivalent, oxygen donor and oxygen carrier. Also, the same study provided important guidelines regarding the temperature and time of reaction.

Apart from the oxygen donor/carrier, peracid-based methodologies often utilise acidic ion exchange resins (AIER) as a catalyst. The presence of this agent is critical to transport active species (peracids) from the aqueous phase to the organic layer, facilitating the contact between the species by presenting an amphipathic nature (*i.e.* interacting with both polar and non-polar groups). Therefore, this approached was also tested in the present study as an alternative to the $H_2SO_4$-based system, and the AIER load utilised in the current study was based in optimisations presented by Mungroo *et al.*.[47] Finally, a methodology using mCPBA was also investigated due to the unique ability of this molecule of acting both as a highly

reactive carrier and oxygen donor. mCPBA is also known for leading to reduced reaction times when compared to peracidic procedures. Another advantage of the methodology based on mCPBA is that all species are present in the organic phase, therefore this methodology dismisses the utilization of phase-transfer agents.

Based on studies presented by Dinda *et al.*, the reaction time was optimised for WVO-based systems by tracking the formation of the EVO through thin layer chromatography (TLC).[45] These tests revealed that no further conversion was achieved after 6 h for methodology B and 1 h for C. Surprisingly, only traces of the desired product were formed even after 12 h of reaction through methodology A. ATR-FTIR spectrum of samples produced by this methodology revealed no conversion (no reduction of ν C-H in cis double bonds), suggesting that the transference of reactive species was strictly regulated by the limited miscibility between these two phases.[48,49] Consequently, a very poor conversion was achieved by this methodology. Similarly, no significant conversion was observed by $^{1}$H NMR. These findings demonstrated that despite the success of this methodology for other VO-based substrates, WVO was not reactive enough to undergo an epoxidation process mediated by $H_2SO_4$.

Products obtained by methodologies B and C were initially characterised by ATR-FTIR to identify the formation of the critical structural aspects that defined the epoxidized product, Figure 4.10A. The disappearance of absorbance peaks in 3006 and 1654 $cm^{-1}$ evidenced the consumption of double bonds. Additionally, the incomplete disappearance of these absorbance bands suggested a partial conversion of unsaturations to into oxirane rings, leading to conversions diverting from 100%. The attribution of the most significant signals of the ATR-FTIR spectra is found in Table 4.6 and Figure 4.10B.[49]

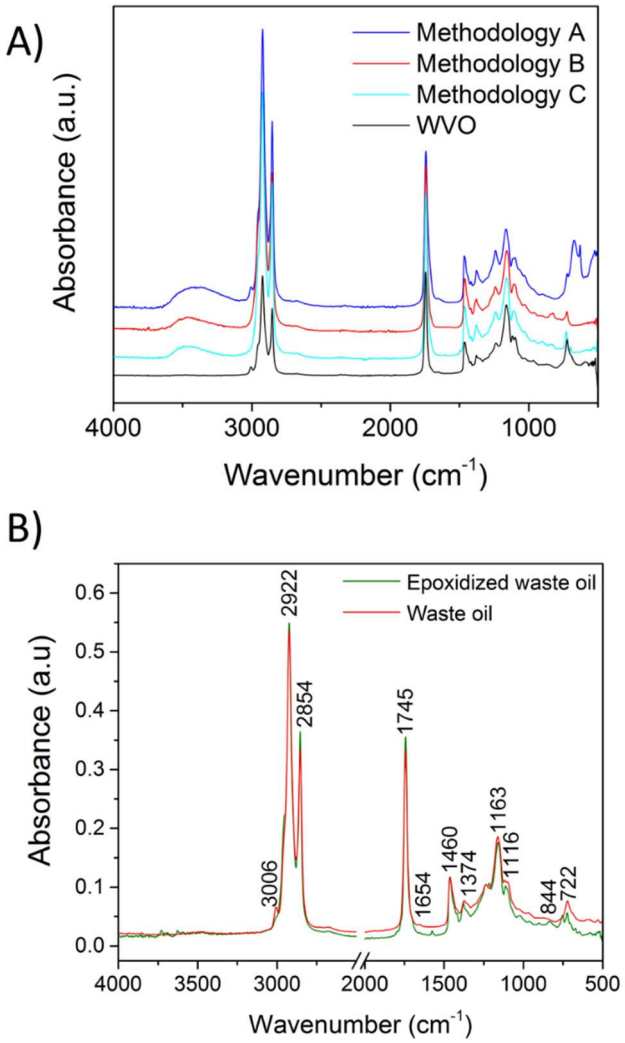


Figure 4.10: A) ATR-FTIR spectra of products obtained from WVO through Methodologies A-C and B) Assignment of the most relevant peaks.

Table 4.6: Wavenumber and assignment of the principal bands in the ATR-FTIR spectrum of vegetable oil samples.

| **Wavenumber ($cm^{-1}$)** | **Attribution** |
|---|---|
| 3006 | ν C-H in *cis*-double bonds |
| 2925 and 2858 | ν $CH_2$, $CH_3$ symmetric and asymmetric |
| 1740 | ν C=O |
| 1654 | ν C=C in *cis*-double bonds |
| 1460 | Scissoring $CH_2$, asymmetric δ $CH_3$ |
| 1372 | Symmetric δ $CH_2$ |
| 1163, 1116, 1099 | ν C-O in group ester |
| 844 | Oxirane ring |
| 722 | In-phase rocking of $(CH_2)_n$, n>3 |

The reduction of bands associated with the double bonds was accompanied the appearance of a new absorption peak in 844 $cm^{-1}$, assigned to ν C-O-C in the epoxy ring, which indicated the conversion of the unsaturated sites to the desired epoxy rings.[50] The appearance of a broad band in the 3100 – 3400 $cm^{-1}$ range, associated with ν O-H, could be assigned with the presence of residual water, acetic acid or ring-opening by-products in the crude oil. The comparison between epoxy resins produced from different oil sources revealed no observable differences within the sensitivity of the equipment, which demonstrated that the products obtained from WVO, NVO and PVO were chemically similar.

Changes in chemical structure caused by the epoxidation procedure were further comprehended by $^{1}H$ NMR, Figure 4.11. Similarly to ATR-FTIR, the disappearance of resonance peaks in 5.26 – 5.40 ppm (signal *a*) and 1.94 – 2.14 (signal *e*) were clear indications that double bonds were being consumed during the reaction. New signals in the 2.9 – 3.2 ppm region, as well as signals in 1.45 ppm, were assigned to protons in α-position to one oxirane. The resonance peak in 1.75 ppm, assigned to protons in α-position to two oxirane rings also confirmed the formation of products with more than one epoxy ring per fatty acid. Nonetheless, signals *m* and *k* were exclusively found in products derived from NVO due to its highly unsaturated nature. A complete assignment of the principal peaks found the spectra is shown in Table 4.7, and coupling constants are presented in the Appendix.

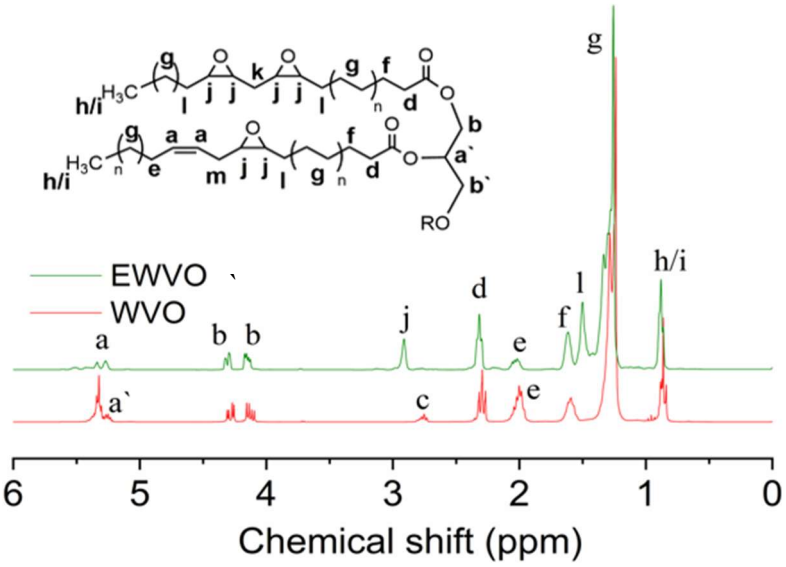


Figure 4.11: $^{1}H$ NMR spectra of waste vegetable oil before and after the epoxidation procedure (Methodology B) and assignment of the principal signals.

Table 4.7: Assignment of the principal resonance peaks in the $^{1}$H NMR spectra of epoxidized vegetable oils.

| Chemical Shift (ppm) | Proton | Functional Group |
|---|---|---|
| 0.83 – 0.93 | *i* | C**H**$_3$ (saturated, oleic and linoleic acyl group) |
| 0.98 | *h* | C**H**$_3$ (linolenic acyl group) |
| 1.20 – 1.42 | *g* | (C**H**$_2$)$_n$- (acyl group) |
| 1.47 | *l* | C**H**$_2$ adjacent to one oxirane ring |
| 1.51 – 1.70 | *f* | OCO-CH$_2$-C**H**$_2$- (acyl group) |
| 1.71 – 1.80 | *k* | C**H**$_2$ adjacent to two oxirane rings |
| 1.94 – 2.14 | *e* | C**H**$_2$-CH=CH- (acyl groups) |
| 2.10 | *m* | C**H**$_2$ adjacent to an oxirane ring and C=C |
| 2.30 | *d* | OCO-C**H**$_2$- (acyl group) |
| 2.77 | *c* | HC-C**H**$_2$-CH= (acyl groups) |
| 2.9 – 3.2 | *j* | C**H**-O-C**H** in oxirane ring |
| 4.10 | *b`* | C**H**$_2$OCOR (glyceryl group) |
| 4.30 | *b* | C**H**$_2$OCOR (glyceryl group) |
| 5.20 – 5.25 | *a'* | C**H**OCOR (glyceryl group) |
| 5.28–5.42 | *a* | C**H**=C**H**- (acyl group) |

Caption: dd: double duplet, dt: double triplet, t: triplet, m: multiplet

Conversion and selectivity were calculated from the $^{1}$H NMR spectra and presented in Table 4.8. Values were calculated taking the resonance peak associated with signal *d* as reference for the integration (2 protons) the reduction of the area of signal *e* (α-allylic protons) used to calculate the conversion and the increase of the area of signal *j* (exclusive to oxirane rings, two protons per ring) explored to obtain values of selectivity. The production of molecules with a high degree of functionalization is crucial for the formation of materials with superior mechanical properties as this characteristic is conceded by the crosslinks formed from the oxirane rings. In this study, conversion was defined as the proportion between the initial number of double bonds and amount consumed as detected through the resonance peak of allylic protons. On the other hand, selectivity established the relationship between the number of oxirane rings formed in comparison to the number of double bonds initially present in the structure.[51] These parameters, while similar, were complementary since the analysis of the pair conversion/selectivity provides information on the extent of secondary reactions and by-product formation.

Table 4.8: Conversion, number of oxirane rings per unit and selectivity of epoxidations with different oil under three methodologies

| **Methodology A** | | | |
|---|---|---|---|
| No conversion observed. | | | |
| **Methodology B** | | | |
| **Oil sample** | **Conversion (%)** | **Oxirane per Unit** | **Selectivity (%)** |
| Neat | 93 | 2.66 | 93 |
| Waste | 89 | 1.70 | 74 |
| Purified | 93 | 1.82 | 78 |
| **Methodology C** | | | |
| **Sample** | **Conversion (%)** | **Oxirane per Unit** | **Selectivity (%)** |
| Neat | 86 | 2.46 | 85 |
| Waste | 74 | 1.68 | 73 |
| Purified | 90 | 2.03 | 89 |

Difference between conversion and selectivity observed in methodology B indicated the partial transformation of double bonds to other functionalities rather than epoxy rings due to side-reactions.[24] However, Methodology C exhibited a remarkable correlation between conversion and selectivity, indicating the creation of fewer ring-opening by-products as a consequence of the formation of less nucleophilic species (chlorobenzoic acid) in this synthetic strategy. Consequently, this approach avoided side-reactions and formed comparatively more of the desired products.

Regarding the effect of the purification in the epoxidation step, findings from Methodology B showed that it had small impact on the reaction parameters as products from waste and purified oils presented very similar selectivity (4% difference). On the other hand, data from Methodology C demonstrated that the purification had a more significant effect on the formation of the desired products, increasing both conversion (*i.e.* the number of oxirane rings) and selectivity by 16%. This observation indicated that the impurities removed by this process could, in fact, interfere with the epoxidation by either disturbing the mechanism through the promotion of competitive reactions or merely preventing the conversion of the double bonds into the desired products. In conclusion, we selected the epoxy resins produced via methodology C for the preparation of the blends due to its higher number of oxirane rings per triglyceride unit, which consequently leads to increased formation of crosslinks and finally thermoset polymers with higher mechanical properties.

### 4.3.4 Production of Partially Bio-Based Blends

Chemically modified oils prepared by methodology C were selected for the preparation of blends due to its higher number of oxirane rings per triglyceride unit. A total of 15 blend formulations were prepared by combining EVOs produced from neat, waste and purified waste vegetable oil with DGEBA resin. This strategy permitted assessing the impact of the use-phase in the properties of the resulting polymer. Bio-based epoxies were added to DGEBA at different contents (from 5 to 30 wt%) and cured with SuperSap hardener, Table 4.9. Properties were compared to a control sample prepared from DGEBA to comprehend the effect of the bio-based content.

Table 4.9: Composition of partially bio-blends prepared in this study.

| Formulation | Bio-based Content (%) | Epoxy Resin Origin |
|---|---|---|
| 5ENVO | 5 | Neat Vegetable Oil (ENVO) |
| 10ENVO | 10 | |
| 15ENVO | 15 | |
| 20ENVO | 20 | |
| 30ENVO | 30 | |
| 5EWVO | 5 | Waste Vegetable Oil (EWVO) |
| 10EWVO | 10 | |
| 15EWVO | 15 | |
| 20EWVO | 20 | |
| 30EWVO | 30 | |
| 5EPVO | 5 | Purified Waste Vegetable Oil (EPVO) |
| 10EPVO | 10 | |
| 15EPVO | 15 | |
| 20EPVO | 20 | |
| 30EPVO | 30 | |
| DGEBA | 0 | Super Sap® |

Figure 4.12 presents the visual aspect of blends prepared with increasing EWVO content. A noticeable reduction in transparency of the cured samples was detected when the bio-based content was increased from 10 to 15%. This increase in opaqueness indicated a reduced solubility of the triglyceride-based resin in the DGEBA system when added in higher contents and/or a mixture of refraction indices. Similar behaviours were detected in samples cured with EPCO and ENVO resins, indicating a limitation of the DGEBA system in this regard. This phenomenon can also be associated with the reduced reactivity of the EVO

systems with the amine hardener found in the formulation.[52] Therefore, part of the chemically-modified triglycerides failed to get actively incorporated in the network, being trapped between the crosslinks as unreacted resin instead.

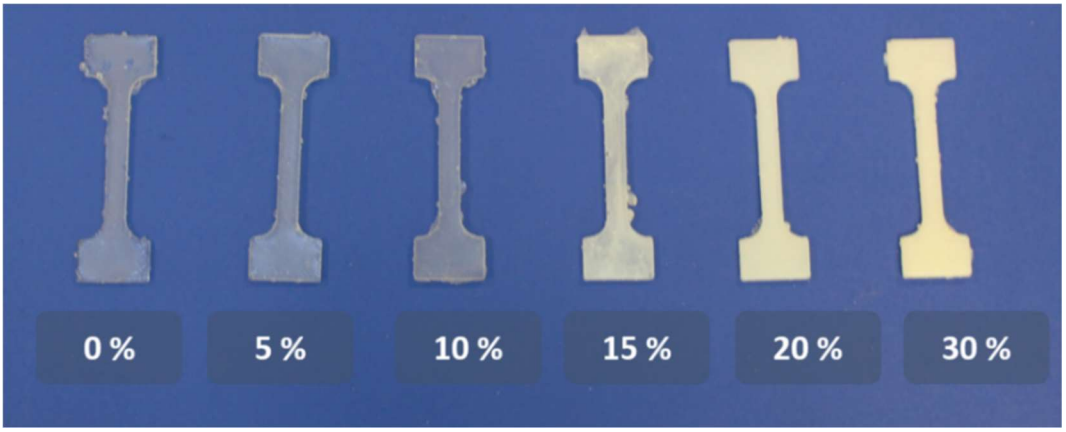


Figure 4.12: Tensile test samples prepared with 0, 5, 10, 15, 20 and 30 wt% of EWVO with respect to the epoxy resin part.

DSC analyses investigated the cure behaviour according to the addition of bio-based epoxy in the formulation. Enthalpy of cure ($\Delta H_c$) was calculated from the calorimetric curves through the integration of exothermic curing peaks present in Figure 4.13, with maximum ranging from 88 to 96 ºC, forming fewer crosslinks and released less heat of reaction. Values of $\Delta H_c$ remained similar along the experimental range until the transition from 20 wt% to 30 wt% of bio-based content, which presented a significant drop (32%) in the enthalpy of curing again. From the phenomenological point of view, this observation represented the point where the crosslinking process was mostly affected by the presence of the less reactive sites and drop in solubility between the components, as previously described in the literature.[5]

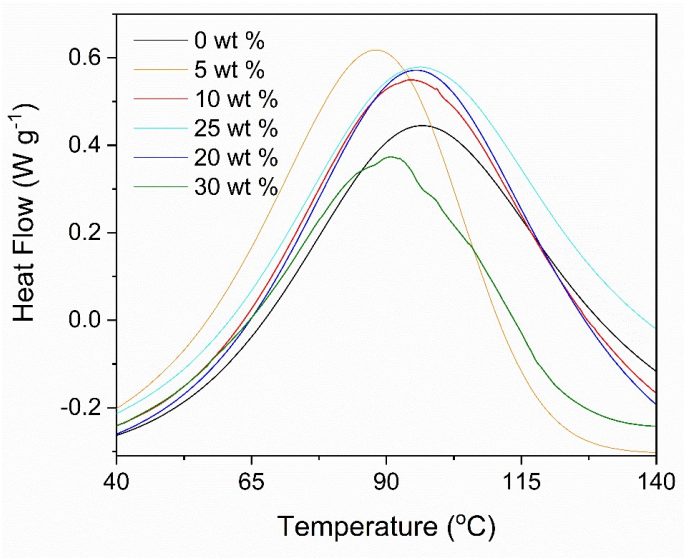


Figure 4.13: Maxima of calorimetric curves obtained from dynamic DSC of blends with EPVO with different bio-based content, heating rate of 10 °C $min^{-1}$.

Table 4.10: Maximum curing temperature and enthalpy of curing of samples with different epoxidized oil content.

| EPVO content | Max. Curing Temperature (°C) | Enthalpy of Curing (J $g^{-1}$) |
|---|---|---|
| **0 wt %** | 97.2 | 338.4 |
| **5 wt %** | 88.3 | 250.1 |
| **10 wt %** | 95.2 | 250.0 |
| **15 wt %** | 96.6 | 257.8 |
| **20 wt %** | 96.2 | 249.5 |
| **30 wt %** | 92.4 | 170.2 |

In addition to challenges regarding the functionality and the solubility, the reduced reactivity between the amine hardener and the oxirane ring present in the EVO resins further hindered the process of network formation. This class of curing presented limited reactivity because the ring-opening reaction that triggered the formation of the crosslinks was driven by nucleophilic attacks. In EVO resins, this process was severely limited by steric hindrance and the high electronic density effects promoted by the vicinal aliphatic chains.[53] Despite the changes in ΔH, the maximum curing temperature remained significantly unaffected by the oil content, evidencing that the bio-based resin caused no change in the curing mechanism.

Next steps were concentrated on the mechanical characterisation of thermoset polymers produced from these blends. Representative stress *versus* strain curves obtained from samples with different contents of bio-based epoxy (Figure 4.14) clearly illustrated the variation in tensile behaviour caused by the EVO content. Samples shifted from the rigid

structures with small values of elongation at break and high ultimate strength to solids with distinguished elongation but very low strength when a high amount of EVO was added to the system.

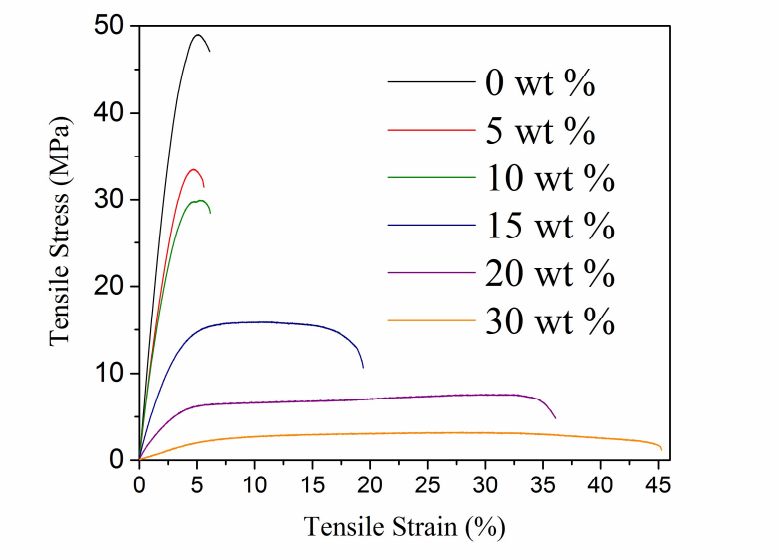


Figure 4.14: Stress/strain curves of samples with different EPVO content.

The analysis of the Young's moduli (Figure 4.15A) of these networks revealed that the gradual addition of bio-based resin led to a progressive decrease in this property, independently of origin of the bio-based resin. The addition of 5 wt% of EPVO decreased the tensile elastic modulus from 1.5 GPa in the non-bio-based formulation to 1.2 GPa and subsequently to 1.0 GPa when the bio-based content is increased to 10 wt%. Interestingly, a greater decline (approximately 50%) was detected from 15 wt%. Such behaviour was not exclusively observed for WVO-base systems; in fact, similar findings were described in previous studies with EVO-based resins prepared from soybean oil.[54] Therefore, this phenomenon cannot be associated with the reduced functionality of the resins herein explored, but in reality, demonstrated intrinsic differences between the bio-based and the commercial system. This tensile behaviour was associated with the reduced rigidity of the molecular backbone of compounds derived from VO, which were comprised of long aliphatic chains, in comparison with the DGEBA.

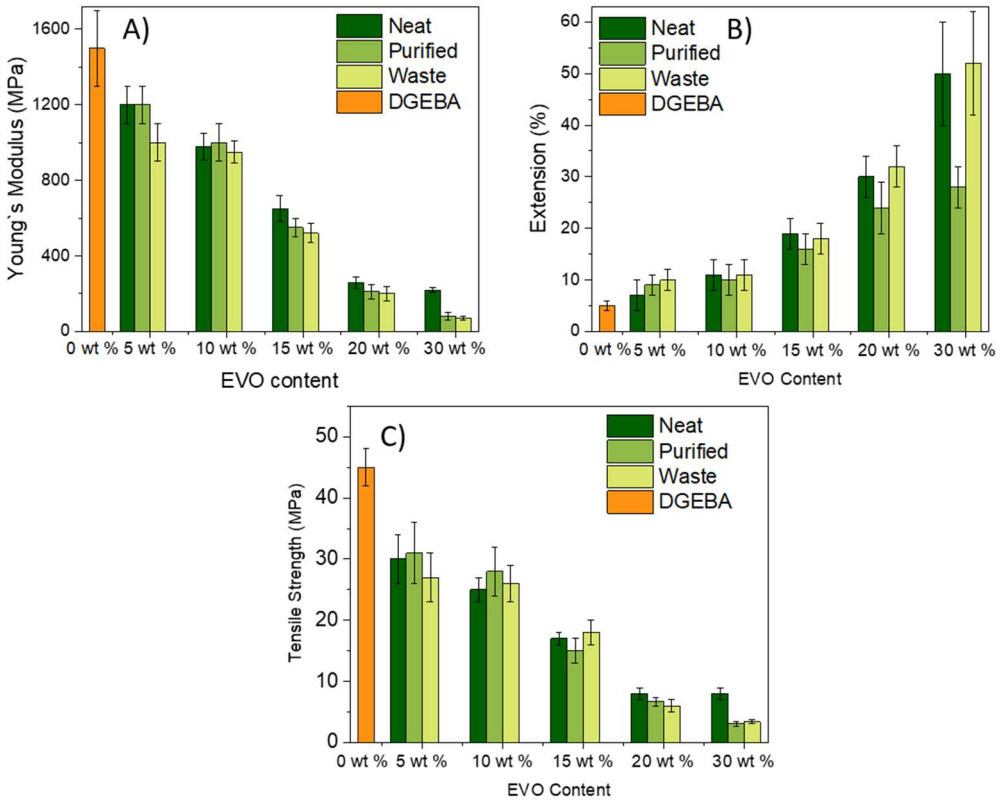


Figure 4.15: A) Young's Moduli, B) elongation and C) tensile strength of specimens with different EVO content and different origins.

Elongation at break and tensile strength properties of blends are presented in Figure 4.15B and C, respectively. A significant increase in the elongation property was observed in response to the decrease in tensile modulus, and an increase of up to one order of magnitude was detected when 30 wt% of EPVO was used to replace DGEBA. As discussed in previous works, these observations were consequences of the creation of loosely-connected networks due to the lower number of oxirane rings in these EVO resins.[8] Consequently, these networks were capable of presenting higher values of elongation before the losing physical integrity. According to Miyagawa *et al.*, this additional elongation is typically manifested more actively from bio-based contents of 15 wt%, which is aligned with finding in this study. From this point, EVOs began to act primarily as plasticisers since these molecules were incapable of being inserted in the polymeric network. In terms of tensile strength, the reduction of the overall aromaticity of the system due to the replacement of DGEBA by EVO directly reduces the "intermolecular" forces present in the network. Consequently, thermoset polymers presented reduced strength at break.

With respect to the origin of the bio-based resin, materials produced from WVO presented lower mechanical properties (from 5 to 30%) when compared to formulations from

neat or purified oil, Table 4.11. This observation was associated with the lower degree of substitution achieved during the epoxidation reactions using this substrate. Consequently, fewer crosslinks were being formed during the cure and the material presented poorer mechanical properties. On the other hand, thermosets prepared with purified oil displayed tensile properties equivalent to those obtained from neat oil when added in contents up to 10 wt%. This analysis supported the purification step in terms of mechanical performance. From 15 wt% onwards, the elastic modulus of EPVO-derived samples diverged from values found in analogous produced from neat oil and gradually became more similar to EWVO-based samples due to the plastification effect. Therefore, these results established a critical point in the formulations range in which the effect of reduced reactivity becomes more significant from the tensile properties standpoint.

Table 4.11: Tensile properties of the thermosets prepared with partially bio-based blends.

| ***EPVO*** | ***Young's Modulus (MPa)*** | ***Elongation (%)*** | ***Tensile Strength (MPa)*** |
|---|---|---|---|
| 0 wt % | 1500 ± 200 | 5 ± 1 | 45 ± 3 |
| 5 wt % | 1200 ± 100 | 9 ± 2 | 31 ± 5 |
| 10 wt % | 1000 ± 100 | 10 ± 3 | 28 ± 4 |
| 15 wt % | 550 ± 50 | 16 ± 3 | 15 ± 2 |
| 20 wt % | 210 ± 40 | 24 ± 5 | 6.7 ± 0.7 |
| 30 wt % | 80 ± 20 | 38 ± 4 | 3.1 ± 0.4 |
| **ENVO** | **Young's Modulus (MPa)** | **Elongation (%)** | **Tensile Strength (MPa)** |
| 5 wt % | 1200 ± 100 | 7 ± 3 | 30 ± 4 |
| 10 wt % | 980 ± 70 | 11 ± 3 | 25 ± 2 |
| 15 wt % | 650 ± 70 | 19 ± 3 | 17 ± 1 |
| 20 wt % | 260 ± 30 | 30 ± 4 | 8 ± 1 |
| 30 wt % | 220 ± 15 | 50 ± 10 | 8 ± 1 |
| **EWVO** | **Young's Modulus (MPa)** | **Elongation (%)** | **Tensile Strength (MPa)** |
| 5 wt % | 1000 ± 100 | 10 ± 2 | 27 ± 4 |
| 10 wt % | 950 ± 60 | 11 ± 3 | 26 ± 3 |
| 15 wt % | 520 ± 50 | 18 ± 3 | 18 ± 2 |
| 20 wt % | 200 ± 40 | 32 ± 4 | 6 ± 1 |
| 30 wt % | 70 ± 10 | 52 ± 10 | 3.4 ± 0.3 |

Changes in mechanical response were further comprehended by dynamic-mechanical analyses (DMA). DMA was also able to provide specific information about the plasticising effect since this technique can detect phenomena related to chain mobility. A more detailed exploration of DMA for the characterisation of thermoset polymers is found in Chapter 5. Storage modulus (E′) curves obtained from temperature scans (Figure 4.16A) demonstrated the reduction of E′ in all samples when the bio-epoxy was added, which was associated with the progressively higher chain mobility due to the temperature. The comparison of E′ for different formulations revealed that the elastic response decreased when more EPVO was added to the system. In this regard, the combination of the progressively more aliphatic molecules with reduced rigidity in the network and the creation of fewer networks due to the reduced reactivity negatively affected the overall dynamic mechanical response of the polymers. An additional way to observe the reduction in elastic response was through the analysis of E′ at room temperature (25 ºC), Table 4.12. It illustrated changes in the order of magnitude of the elastic behaviour of the network as the EPVO content was increased.

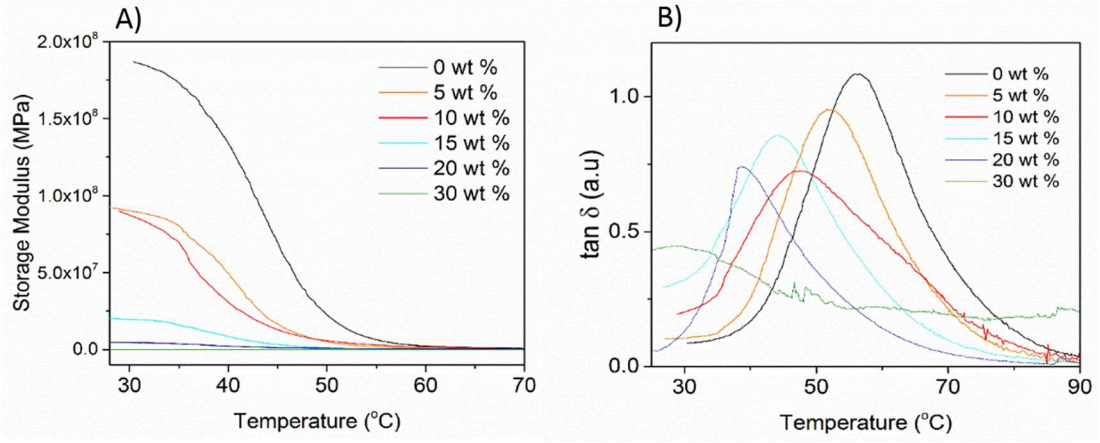


Figure 4.16: Curves of A) Storage modulus and B) tan δ versus temperature for samples with different EPVO oil content.

Table 4.12: Storage Modulus (E′) at room temperature and glass transition temperature ($T_g$) of formulations produced from purified waste vegetable oil (WVO).

| EPVO Content (wt%) | E′ (25 °C) (MPa) | $T_g$ (°C) |
|---|---|---|
| 0 | 186.7 | 56.3 |
| 5 | 89.5 | 51.9 |
| 10 | 86.6 | 47.4 |
| 15 | 19.4 | 44.0 |
| 20 | 4.4 | 38.6 |
| 30 | 4.2 | 27.4 |

Curves of tan δ versus temperature were also examined to inspect changes in the glass transition temperature ($T_g$) of these networks caused by the addition of bio-based epoxy to the blend (Figure 4.16B). The analysis of the tan δ maximum peak demonstrated a shift towards lower temperatures with the addition of EPVO to the formulation. Consequently, the $T_g$ values were reduced from 56.3 °C in the non-bio-based formulation to 27.4 °C in the sample with the highest EPVO concentration (30 wt%), Table 4.12. The transition phenomenon characterised by the tan δ also became progressively broader, which was associated with the formation of highly heterogeneous networks due to the presence of unincorporated segments.[55] In addition, the increasing presence of long aliphatic contributes to relative mobility of the network, therefore further facilitating the phenomenon of glassy transition. The combination of these characteristics resulted in less tight networks that conceded additional mobility to the macromolecules and, ultimately, reduced the storage moduli and the $T_g$ of the polymers.[56]

Blends were also analysed with respect to their thermal stability under inert atmosphere by TGA. Thermogravimetric curves of EPVO-based formulations and their first derivatives are shown in Figure 4.17, and parameters such as the initial temperature of degradation ($T_{Onset}$) and maximum degradation rate ($T_{Max}$) extracted from those curves are shown in Table 4.13. The gradual addition of EVO to the blend made it progressively less thermally stable, which was consistent with previous observations regarding the thermal stability of the triglyceride-based moieties. Two main degradation events were observed in the weight-loss curve: the first event was associated with the release of low molecular weight species disconnected to the network such as unreacted curing agent.

.

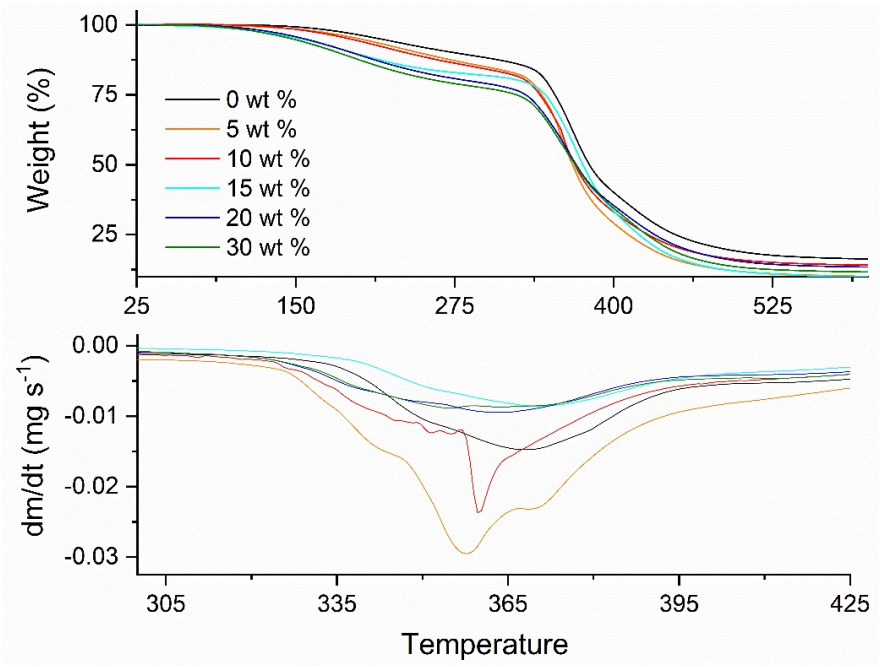


Figure 4.17: Thermograms of epoxidized purified vegetable oil (EPVO) -based resins from 25 °C to 600 °C (top), heating rate of 10 °C $min^{-1}$, under an inert atmosphere, and their respective first derivative curve (bottom).

The first event was directly affected by the EVO content, demonstrating that fewer molecules of the curing agent reacted, consequently resulting in a reduced degree of cure. The latter event was associated with the decomposition of the network itself, which is de-bonded by the action of thermo-oxidative reactions.[57] Nevertheless, the analysis of the blends' thermal stability revealed the utilisation of waste oil-based resins led to no significant sacrifice in this property in comparison with equivalent materials produced from virgin oil. Therefore, the quantity of the EVO in the system has proved to be more critical than the origin of the resin itself, supporting the substitution of neat oil as a reactive diluent.

Table 4.13: Initial temperature of degradation ($T_{Onset}$) of degradation events and of maximum rate of degradation ($T_{Max}$) of samples produced from different epoxidized oils.

| **EPVO** | **1st Weight-loss Event (°C)** | **2nd Weight-loss Event (°C)** | ***T*Max (°C)** |
|---|---|---|---|
| 0 wt % | 153.4 | 345.6 | 369.0 |
| 5 wt % | 134.5 | 342.1 | 357.7 |
| 10 wt % | 139.5 | 345.7 | 362.3 |
| 15 wt % | 129.6 | 345.7 | 367.7 |
| 20 wt % | 125.4 | 334.2 | 363.6 |
| 30 wt % | 112.2 | 328.6 | 355.6 |
| **ENVO** | **1st Weight-loss Event (°C)** | **2nd Weight-loss Event (°C)** | ***T*Max (ºC)** |
| 5 wt % | 161.8 | 348.2 | 368.3 |
| 10 wt % | 154.8 | 344.0 | 368.0 |
| 15 wt % | 136.7 | 339.1 | 366.3 |
| 20 wt % | 138.4 | 335.2 | 360.7 |
| 30 wt % | 123.6 | 334.4 | 357.7 |
| **EWVO** | **1st Weight-loss Event (°C)** | **2nd Weight-loss Event (°C)** | ***T*Max (°C)** |
| 5 wt % | 161.2 | 346.0 | 373.0 |
| 10 wt % | 160.3 | 342.4 | 369.1 |
| 15 wt % | 132.4 | 341.6 | 368.3 |
| 20 wt % | 129.1 | 336.5 | 360.3 |
| 30 wt % | 119.1 | 331.6 | 364.3 |

### 4.3.5 Demonstrating the Concept: Using the Blends in Sustainable Composites.

Since the addition of bio-based resins to DGEBA formulations resulted in thermoset polymers with reduced tensile properties, the production of composites using these polymers as a matrix was idealised as a strategy to recover the original performance. Among the range of formulations investigate in the study, the blend of DGEBA with 10 wt% of EPVO (10EPVO) was selected as model matrix since it demonstrated the most promising balance between tensile properties and the bio-based fraction from all waste-based formulations. In order to produce these materials more sustainably, composites were manufactured using milled carbon fibres (MCF) obtained from recycled streams (Carbiso™ MF supplied by *ELG*

*Carbon Fibre Ltd.*), Figure 4.18. Therefore, this approach was designed to enable the combination of two waste streams (waste oil and waste carbon fibre) in one single material.

Figure 4.18: Aspect of the milled carbon fibre (Carbiso™ MF) used for the preparation of composites

Formulations with MCF contents varying from 1 to 30 wt% were prepared and characterised according to their tensile properties, Figure 4.19A-C. Properties of MCF-reinforced composites were compared with the original blend (10EPVO) to understand the relative reinforcing effect and with the commercial DGEBA resin, both with and without any reinforcing effect. This approach permitted an understanding of how the formulations prepared in this study compared to benchmark formulations. The initial properties of the commercial control (DGEBA) could be promptly re-achieved using MCF as a reinforcing agent, and an increase of approximately 10% in modulus was observed when only 1 wt% of fibre was added to the formulation. Composites containing 5 wt% of recycled fibres presented tensile modulus that exceeded the level of performance observed in the DGEBA control.

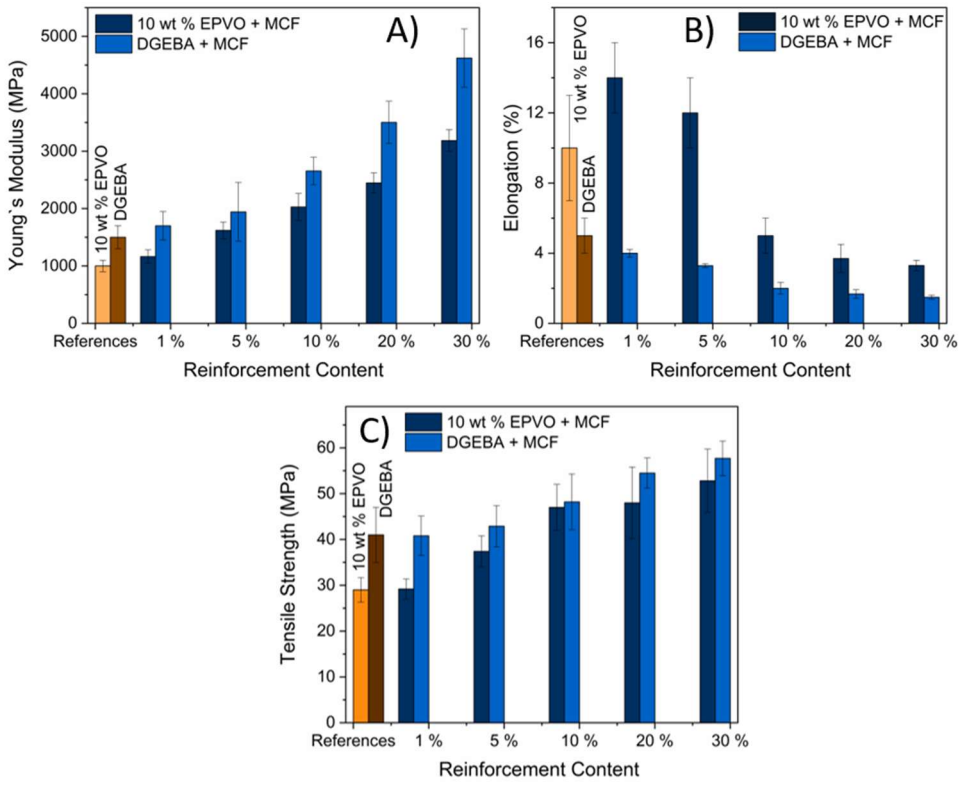


Figure 4.19: A) Young's moduli, B) elongation at break and C) tensile strength of composites with different milled carbon fibre (MCF) contents in comparison to DGEBA reference

MCF-reinforced composites presented a continuous increase in tensile properties throughout the experimental range, achieving a maximum tensile modulus of 3.2 ± 0.2 GPa and tensile strength of 53 ± 7 MPa when 30 wt% of fibre was added to the system, an improvement of 113% and 17% against the commercial formulation, respectively. Values of extension at the breaking point a demonstrated a gradual shift towards more rigid samples, decreasing over the formulation range and reaching a minimum of 3.3% when 30 wt% of MCF was added in the formulation. The successful reinforcing effect demonstrated the good interaction achieved between the fibre and the matrix, supporting the utilisation of this partially bio-based blend for composite applications. Table 4.14 presents the tensile properties for all formulations investigated in this part of the study. Therefore, these results demonstrated that it was possible to introduce waste-based components to replace DGEBA in thermoset formulations whilst adding tensile to the resulting materials.

Table 4.14: Tensile properties of the composites prepared with epoxidized purified vegetable oil (EPVO) -based matrix reinforced with recycled carbon fibres.

| **MCF Content** | **Young's Modulus (GPa)** | **Elongation at Break (%)** | **Tensile Strength (MPa)** |
|---|---|---|---|
| DGEBA | 1.5 ± 0.2 | 5 ± 1 | 45 ± 3 |
| 1 wt% | 1.7 ± 0.2 | 4.0 ± 0.2 | 41 ± 4 |
| 5 wt% | 1.9 ± 0.5 | 3.3 ± 0.1 | 43 ± 6 |
| 10 wt% | 2.6 ± 0.2 | 2.0 ± 0.3 | 54 ± 3 |
| 20 wt% | 3.5 ± 0.4 | 1.7 ± 0.2 | 58 ± 4 |
| 30 wt% | 4.6 ± 0.5 | 1.5 ± 0.1 | 53 ± 7 |
| 10EPVO | 1.0 ± 0.1 | 10 ± 3 | 28 ± 4 |
| 1 wt% | 1.2 ± 0.1 | 9 ± 2 | 29 ± 2 |
| 5 wt% | 1.6 ± 0.1 | 10 ± 3 | 37 ± 3 |
| 10 wt% | 2.0 ± 0.2 | 16 ± 3 | 47 ± 5 |
| 20 wt% | 2.5 ± 0.2 | 24 ± 5 | 48 ± 8 |
| 30 wt% | 3.2 ± 0.2 | 38 ± 4 | 53 ± 7 |

Scanning electronic microscopy (SEM) images were used to comprehend the reinforcement effect from the fibre/matrix interaction point of view. As presented in Figure 4.20A, the matrix could effectively cover the MCF fibres, resulting in a good transference of mechanical stress. Nevertheless, images obtained at lower magnifications (Figure 4.20B and C) demonstrated that fibre pull-out could also be observed after the fracture. Interestingly, the same images demonstrated that MCF is not homogeneously dispersed along the composite. Since the cure takes up to 24 h, MCF had time to migrate to the bottom of the mould due to gravity. Therefore, one side of the sample presented more MCF (Figure 4.20B) than the other (Figure 4.20C). These findings demonstrated the limitations of the methodology and technique selected to manufacture these composites, which could receive refinements to increase the properties of the resulting materials further. For example, a faster cure cycle through the use of temperature would have significantly reduced the gel time and consequently reduced the fibre migration effect.

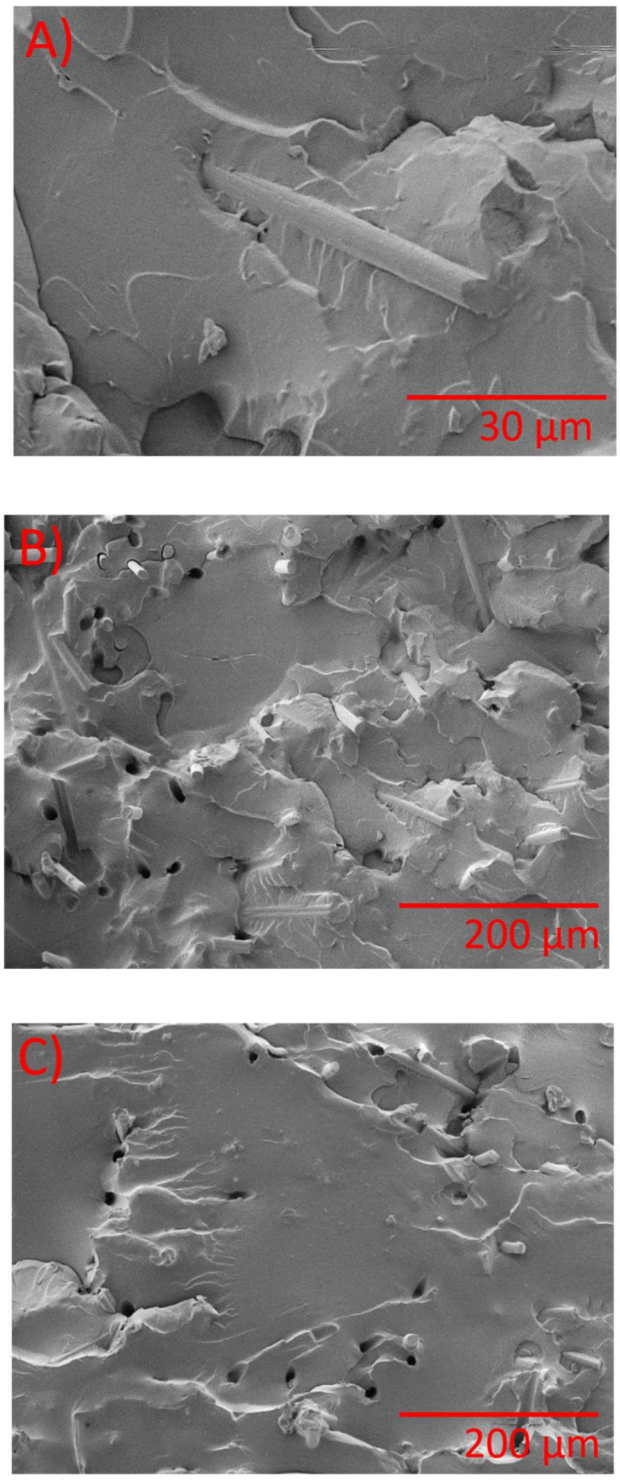


Figure 4.20: SEM images of composites prepared with MCF obtained in A) high magnification (3000×) and low magnification (500×) of the B) lower and C) top cross-section of fractured samples.

The effect of the addition of MCF was also investigated from the dynamic-mechanical properties point of view. As presented in Figure 4.21A, a sequential increase in storage

modulus was observed when more MCF was added to the formulations. Similarly to what observed for the tensile tests, the superior storage modulus demonstrated the improvement of rigidity when the MCF was incorporated to the formulations. This phenomenon was also tracked through the values of E′ at room temperature (Table 4.15), which demonstrated the magnitude of the impact caused by the addition of MCF. Moreover, curves of tan δ versus temperature demonstrated that composites prepared with MCF presented $T_g$s ranging from 49.2 °C to 51.8 °C, Figure 4.21B. These results illustrated a modest increase in $T_g$ in comparison with the original bio-based blend (46.7 °C) due to the partial immobilization of the polymeric matrix caused by a favourable interfacial interaction with the fibre. Consequently, the mobility of the polymeric network is reduced and a higher temperature is necessary to cause the glass transition. The same effect is evidenced by the reduction of the values of the tan δ maximum with the increase of the fibre content, illustrating the increase of the damping properties.[58]

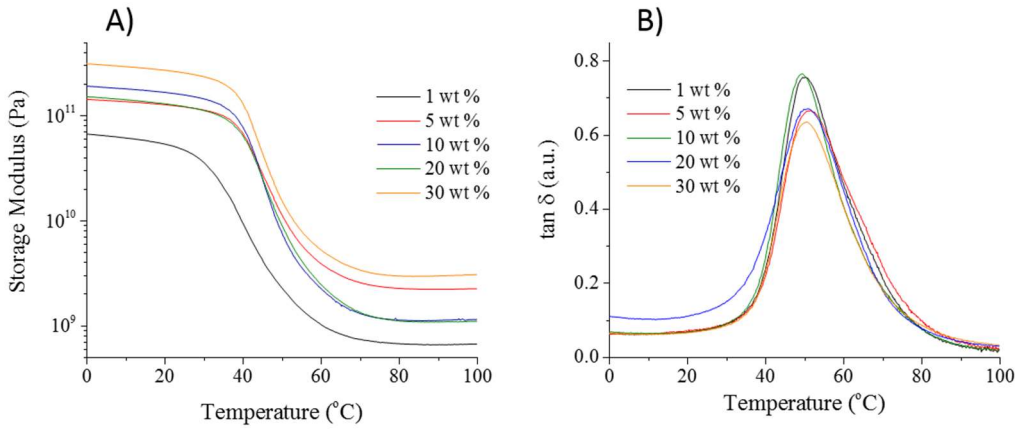


Figure 4.21: Curves of A) Storage modulus and B) tan δ versus temperature for composites with different MCF contents.

Table 4.15: Storage Modulus (E′) at room temperature and glass transition temperature ($T_g$) of formulations produced from purified waste vegetable oil.

| **MCF Content** | **E′ (25 °C) (GPa)** | **$T_g$ (°C)** |
|---|---|---|
| DGEBA | 1.9 | 56.3 |
| 10EPVO | 0.9 | 47.4 |
| 1 wt% | 3.52 | 49.9 |
| 5 wt% | 11.0 | 51.4 |
| 10 wt% | 11.2 | 49.9 |
| 20 wt% | 14.2 | 50.7 |
| 30 wt% | 23.1 | 51.1 |

Thermal stability of the composites was evaluated by TGA, and the weight-loss curves for each composite formulation are presented in Figure 4.22. The initial weight-loss event associated with the low-molecular-weight compounds and the second event at higher temperatures related to the thermal decomposition of the cross-links were again observed in the same temperature range as the unreinforced polymers, Table 4.16. On the other hand, composites demonstrated an exclusive accumulation of non-volatile residues after the main decomposition events, which was directly proportional to the MCF content. These findings result from the higher thermal stability of the reinforcing fibres in comparison to the matrix, which does not degrade in this temperature range. In fact, carbon fibres are known for presenting distinguished thermal resistance due to the strength and stability of the C-C bonds that molecularly describe this material, achieved after an energy-intensive production process.[59] Furthermore, the similarity between values of $T_{Onset}$ and $T_{Max}$ observed in both composites, and unreinforced polymer demonstrated that the addition of MCF did not cause any significant changes in the thermal degradation mechanism experimented by the polymeric matrix when it degrades.

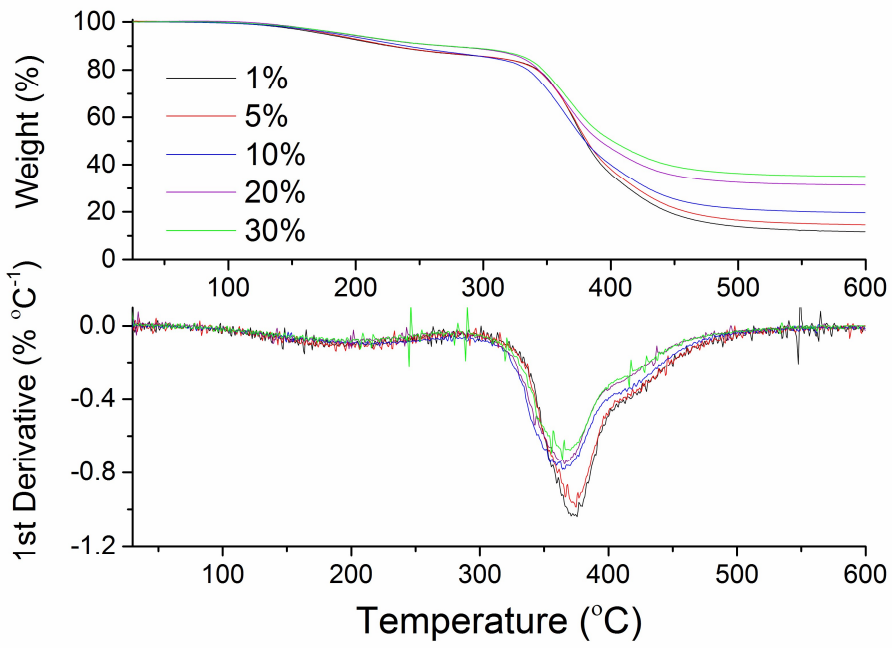


Figure 4.22: Thermograms of composite reinforced with MCF, from 25 °C to 600 °C (top), heating rate of 10 °C $min^{-1}$, under an inert atmosphere, and their respective first derivative curve (bottom).

Table 4.16: Initial temperature of degradation ($T_{Onset}$) of the degradation events and of maximum rate of degradation ($T_{Max}$) of composites produced with different milled carbon fibre contents.

| MCF Content | 1st Weight-loss Event (ºC) | 2nd Weight-loss Event (ºC) | $T_{Max}$ (ºC) |
|---|---|---|---|
| DGEBA | 153.4 | 345.6 | 369.0 |
| 10EPVO | 139.5 | 345.7 | 362.3 |
| 1 wt% | 133.5 | 344.3 | 371.7 |
| 5 wt % | 134.5 | 342.1 | 375.0 |
| 10 wt % | 139.5 | 345.7 | 366.3 |
| 15 wt % | 129.6 | 345.7 | 367.7 |
| 20 wt % | 125.4 | 343.2 | 366.6 |
| 30 wt % | 132.2 | 341.6 | 364.3 |

## 4.4 Summary

Thermoset polymers were successfully prepared with bio-based epoxy resins prepared in this chapter using virgin, waste and purified vegetable oil samples blended with commercial DGEBA resin and cured with amine hardener. These materials characterised the first successful application of waste vegetable oil for the production of this class of materials. Extensive characterization of the oil samples permitted understanding of changes caused by the frying process from the chemical point of view, allowing the development of purification and chemical modification methodologies to produce highly-functional resins. Although waste oil-based polymers presented poorer tensile properties than analogues produced from neat oil, the use of purified oil-based resins proved to cause no significant sacrifice in tensile properties when added to the formulations in contents up to 10 wt%. Levels above 15 wt% caused a plasticising effect due to proportionally fewer and less reactive oxirane rings that ended up not being incorporated into the network, as confirmed by DMA and TGA. The addition of recycled carbon fibres to the partially bio-based blends permitted re-achieving and further improving the tensile properties of the commercial resin that were initially lost with the addition of bio-based epoxy. Best tensile properties (3.2 ± 0.2 GPa of Young's modulus and 53 ± 7 MPa of tensile strength) were observed when 30 wt% of recycled fibres were added to the formulation.

Therefore, studies in this chapter demonstrated the possibility of valorising WVO as an alternative source of triglycerides for the production of epoxy resins. At the same time, these results identified potential limitations regarding the reactivity of these resins, particularly with amine hardeners. This particular aspect also hindered maximum quantity of WVO

incorporated in the networks, holding back the bio-based content of the final network Therefore, studies presented in the next chapter focused on strategies to improve the bio-based content and the mechanical performance of the resulting thermosets by exploring different formulations.

## 4.5 References


1 U. Biermann, W. Friedt, S. Lang, W. Lühs, G. Machmüller, J. O. Metzger, M. Rüsch gen. Klaas, H. J. Schäfer and M. P. Schneider, *Angew. Chemie Int. Ed.*, 2000, **39**, 2206–2224.

2 S. Miao, P. Wang, Z. Su and S. Zhang, *Acta Biomater.*, 2014, **10**, 1692–704.

3 P. Niedermann, G. Szebényi and a. Toldy, *Compos. Sci. Technol.*, 2015, **117**, 62–68.

4 F.-L. Jin and S.-J. Park, *Mater. Sci. Eng. A*, 2008, **478**, 402–405.

5 Y. Chen, L. Yang, J. Wu, L. Ma, D. E. Finlow, S. Lin and K. Song, *J. Therm. Anal. Calorim.*, 2012, **113**, 939–945.

6 S.-J. Park, F.-L. Jin and J.-R. Lee, *Macromol. Chem. Phys.*, 2004, **205**, 2048–2054.

7 R. Raghavachar, R. J. Letasi, P. V. Kola, Z. Chen and J. L. Massingill, *J. Am. Oil Chem. Soc.*, 1999, **76**, 511–516.

8 H. Miyagawa, A. K. Mohanty, M. Misra and L. T. Drzal, *Macromol. Mater. Eng.*, 2004, **289**, 636–641.

9 H. Miyagawa, M. Misra, L. T. Drzal and A. K. Mohanty, *Polym. Eng. Sci.*, 2005, **45**, 487–495.

10 F. P. La Mantia and M. Morreale, *Compos. Part A Appl. Sci. Manuf.*, 2011, **42**, 579–588.

11 J. Osborne, Bioenergy growth must be carefully managed, http://www.fao.org/newsroom/en/news/2007/1000702/index.html, (accessed 7 November 2018).

12 G. Lligadas, J. C. Ronda, M. Galia and V. Ca, *Biomacromolecules*, 2010, 2825–2835.

13 C. Zhang, R. Ding and M. R. Kessler, *Macromol. Rapid Commun.*, 2014, **35**, 1068–74.

14 X. Meng, G. Chen and Y. Wang, *Fuel Process. Technol.*, 2008, **89**, 851–857.

15 M. G. Kulkarni and A. K. Dalai, *Ind. Eng. Chem. Res.*, 2006, 45, 2901–2913.

16 D. A. Salam, N. Naik, M. T. Suidan and A. D. Venosa, *Environ. Sci. Technol.*, 2012, **46**, 2352–2359.

17 P. Campo, Y. Zhao, M. T. Suidan, A. D. Venosa and G. a. Sorial, *Chemosphere*, 2007, **68**, 2054–2062.

18 S. Paul, G. S. Mittal and M. S. Chinnan, *Crit. Rev. Food Sci. Nutr.*, 1997, **37**, 635–62.

19 E. Choe and D. B. Min, *J. Food Sci.*, 2007, **72**, R77-86.

20 E. Choe and D. B. Min, *J. Food Sci.*, 2005, **70**, 142–159.

21 W. W. Nawar, *J. Chem. Educ.*, 1984, **61**, 299–302.

22 Z. J. Predojević, *Fuel*, 2008, **87**, 3522–3528.

23 É. de Castro Vasques, C. R. Granhen Tavares, C. Itsuo Yamamoto, M. Rogério Mafra and L. Igarashi-Mafra, *Environ. Technol.*, 2013, **34**, 2361–2369.

24 Z. S. Petrovic, A. Zlatanic, C. C. Lava and S. Sinadinovic-Fiser, *Eur. J. Lipid Sci. Technol.*, 2002, **104**, 293–299.

25 M. D. Guillén and N. Cabo, *J. Sci. Food Agric.*, 2000, **80**, 2028–2036.

26 M. D. Guillén and E. Goicoechea, *J. Agric. Food Chem.*, 2007, **55**, 10729–10736.

27 S. N. Khot, J. J. Lascala, E. Can, S. S. Morye, G. I. Williams, G. R. Palmese, S. H. Kusefoglu and R. P. Wool, *J. Appl. Polym. Sci.*, 2001, **82**, 703–723.

28 Z. Yaakob, M. Mohammad, M. Alherbawi, Z. Alam and K. Sopian, *Renew. Sustain. Energy Rev.*, 2013, **18**, 184–193.

29 A. Martínez-Yusta, E. Goicoechea and M. D. Guillén, *Compr. Rev. Food Sci. Food Saf.*, 2014, **13**, 838–859.

30 B. Nieva-Echevarría, E. Goicoechea, M. J. Manzanos and M. D. Guillén, *Food Res. Int.*, 2014, **66**, 379–387.

31 G. R. Takeoka, R. G. Buttery and C. T. Perrino, *J. Agric. Food Chem*, 1995, **43**, 22–26.

32 W. Tsuzuki, A. Matsuoka and K. Ushida, *Food Chem.*, 2010, **123**, 976–982.

33 Q. Zhang, A. S. M. Saleh, J. Chen and Q. Shen, *Chem. Phys. Lipids*, 2012, **165**, 662–681.

34 V. K. Tyagi and a. K. Vasishtha, *J. Am. Oil Chem. Soc.*, 1996, **73**, 499–506.

35 M. J. Crosa, V. Skerl, M. Cadenazzi, L. Olazábal, R. Silva, G. Suburú and M. Torres, *Food Chem.*, 2014, **146**, 603–7.

36 P. Felizardo, M. J. Neiva Correia, I. Raposo, J. F. Mendes, R. Berkemeier and J. M. Bordado, *Waste Manag.*, 2006, **26**, 487–494.

37 S. R. Coles, G. Barker, A. J. Clark, K. Kirwan, D. Jacobs, K. Makenji and D. Pink, *Macromol. Biosci.*, 2008, **8**, 526–32.

38 D. Y. C. Leung and Y. Guo, *Fuel Process. Technol.*, 2006, **87**, 883–890.

39 H. Noureddini, B. C. Teoh and L. Davis Clements, *J. Am. Oil Chem. Soc.*, 1992, **69**, 1189–1191.

40 M. J. Pratas, S. Freitas, M. B. Oliveira, S. C. Monteiro, A. S. Lima and J. a. P. Coutinho, *J. Chem. Eng. Data*, 2010, **55**, 3983–3990.

41 F. R. van de Voort, a. a. Ismail, J. Sedman, J. Dubois and T. Nicodemo, *J. Am. Oil Chem. Soc.*, 1994, **71**, 921–926.

42 K. Warner and T. L. Mounts, *J. Am. Oil Chem. Soc.*, 1993, **70**, 983–988.

43 M. D. Guillén and A. Ruiz, *Eur. J. Lipid Sci. Technol.*, 2008, **110**, 52–60.

44 S. Bastida and F. J. Sánchez-Muniz, *Food Sci. Technol. Int.*, 2001, **7**, 15–21.

45 S. Dinda, A. V Patwardhan, V. V Goud and N. C. Pradhan, *Bioresour. Technol.*, 2008, **99**, 3737–44.

46 J. La Scala and R. P. Wool, *Polymer (Guildf).*, 2005, **46**, 61–69.

47 R. Mungroo, N. C. Pradhan, V. V. Goud and A. K. Dalai, *J. Am. Oil Chem. Soc.*, 2008, **85**, 887–896.

48 R. L. Musante, R. J. Grau and M. a. Baltanás, *Appl. Catal. A Gen.*, 2000, **197**, 165–173.

49 J. Chen, M. D. Soucek, W. J. Simonsick and R. W. Celikay, *Polymer (Guildf).*, 2002, **43**, 5379–5389.

50 P. Saithai, J. Lecomte, E. Dubreucq and V. Tanrattanakul, *Express Polym. Lett.*, 2013, **7**, 910–924.

51 A. E. Gerbase, J. R. Gregório, M. Martinelli, M. C. Brasil and A. N. F. Mendes, *JAOCS*, 2002, **79**, 179–181.

52 B. Ellis, *Chemistry and Technology of Epoxy Resins*, Springer-Science+Business Media, B.V, 1st Editio., 1993.

53 R. Wang and T. P. Schuman, *Express Polym. Lett.*, 2013, **7**, 272–292.

54 D. Ratna, *Polym. Int.*, 2001, **184**, 179–184.

55 A. Paramarta and D. C. Webster, *React. Funct. Polym.*, 2016, **105**, 140–149.

56 A. E. Gerbase, C. L. Petzhold and A. P. O. Costa, *J. Am. Oil Chem. Soc.*, 2002, **79**, 797–802.

57 S. G. Tan, Z. Ahmad and W. S. Chow, *Polym. Int.*, 2014, **63**, 273–279.

58 D. Shanmugam and M. Thiruchitrambalam, *Mater. Des.*, 2013, **50**, 533–542.

59 D. Hull and T. W. Clyne, *An Introduction to Composite Materials*, Cambridge Univerisity Press, Cambridge, United Kingdom, Second., 1996.

# Chapter 5

# Thermoset Polymers from Waste Vegetable Oil:

## Optimisation of the Formulations towards High $T_g$ Polymers

Contents of this chapter have been published at:

F. C. Fernandes, K. Kirwan, P. R. Wilson and S. R. Coles, *Green Mater.*, 2018, **6**, 38–46.

## 5.1 Introduction

Although previous investigations produced polymers and composites with satisfactory performance, these systems still presented DGEBA as the major component in the formulation, in some cases as high as 90 wt%. Therefore, the aim of this chapter to maximise the renewable content of these thermoset polymers by investigating the production of systems exclusively formed with WVO (*i.e.* in the absence of DGEBA). To achieve this milestone while also getting the most out of the mechanical performance, the study targeted the creation of an optimised formulation tailored according to WVO's reactivity. In this regard, four experimental parameters were systematically explored to identify the best relationship between factors that are known for affecting the properties of EVO-derived polymers: the curing agent (also referred to as hardener), its quantity, the catalyst and the nature of the oil used to produce the resin.[1–3]

Regarding the hardener selection, previous systems made clear the challenges associated with choice of curing agents with limited reactivity.[4] Therefore, aromatic and cycloaliphatic anhydrides have been preferred for curing EVO because of their reactivity with internal epoxide groups.[1] In the presence of tertiary amines (or imidazoles), the mechanism is accelerated through the formation of a carboxylate ion that results in epoxy ring-opening forming an alkoxide ion. From that point, the propagation step can yield both esterification and etherification products.[5] The alkoxide ion can react first with an anhydride molecule to form a monoester, and thereafter a diester by reacting with the carboxylate from the opening of the anhydride linkage. Alternatively, the same alkoxide ion can promote the oxirane ring-opening to produce an ether linkage. However, according to Park *et al*., the esterification process is much faster than etherification, so it is accepted that the first process is the dominant one.[6]

Chapter 2 presented a collection of studies that have explored different molecules in this class (and analogues), such as hexahydrophthalic anhydride, phthalic anhydride, maleic anhydride, maleic anhydride and dodecenylsuccinic anhydride.[2,7–12] Overall, these studies have demonstrated the ability of creating formulations resulting in tight network, with control over the mechanical properties given by the hardener selected once these molecules get actively incorporated in the network.[13] Moreover, the quantity of the hardener has been identified by different authors as another critical parameter towards the construction of rigid networks. For example Omonov *et al.* investigated the effect of the hardener molar ratio in networks obtained with epoxidized canola oil (ECO) cured with PA.[14] In this study, thermosets were produced with hardener molar ratios (PA: ECO) ranging from 1.0:1.0 to 2.0:1.0, and the authors observed a continuous rise in dynamic-mechanical properties and $T_g$ with the increase anhydride in the system. These improvements were then attributed to the formation of denser,

more connected polymeric networks. The same study demonstrated that the molar ratio could influence the kinetics of the cure. Despite these changes, this study demonstrated that the molar ratio had little impact on the curing temperature.

Investigations conducted by Gupta *et al.* investigated the production of thermosets using EVO resins synthesised from soybean oil and PA as curing agent in molar ratios varying from 0.7:1.0 to 1.3:1.0 (epoxy resin : anhydride ratio).[15] The influence of the hardener content was observed by dynamic mechanical analysis (DMA), where an increase both in the $T_g$ and the material storage modulus was observed when the molar ratio was increased from 0.7 to 1.0. However, the authors identified that successive increases of PA (up to a molar ratio of 1.3:1.0) led to networks with reduced properties. This observation was attributed to a phase separation effect, which was confirmed through scanning electron microscopy (SEM) images. Therefore, Gupta *et al.* demonstrated that the anhydride could also negatively impact the formulation. Similarly, Clark *et al.* have established a relationship between both the molar ratio and the chemical nature of the anhydride with the resulting crosslinking density when investigating the preparation of bio-based polyesters from waste grapeseed oil, so that bulky hardeners should be avoid to favour tightly connected networks.[16]

In addition to the hardener type and the molar ratio between epoxy groups and hardener, two curing catalysts were investigated as external factors. Despite the known influence of this parameter over the creation of the network formation, not many studies focus on directly comparisons between different catalytic systems.[9] Finally, the origin of the oil feedstock was considered as the fourth and final parameter investigated in this chapter. Literature has demonstrated a connection between the degree of unsaturation of a given oil and the properties of the resulting thermoset polymer.[17,18] Therefore, WVO-based formulations were compared to analogues from neat VO to assess the impact in performance caused by replacing the edible triglycerides with waste materials due to the frying procedure. Thermal, chemical and dynamic mechanical properties of the resulting polymers were characterised in this present chapter to understand and optimise the relationships between the factors, creating guidelines for further investigations in this thesis and the area of bio-based resins.

## 5.2 Methodology

### 5.2.1 Materials and Characterisations

WVO (used as a deep frying medium for 4 days, blend of rapeseed/palm oil approximately 3:1) and the virgin vegetable oil equivalent were collected from one of the food outlets at University of Warwick, Coventry, UK. Hydrogen peroxide (30% v/v), toluene (puriss. p.a. >99.7%), dichloromethane (puriss. 99%), phthalic anhydride (PA, 99%), methyl-

hexahydrophthalic anhydride (MHHPA, 96 %, mixture of isomers cis and trans), DMF, and 2-methylimidazole (99%) were supplied by Sigma-Aldrich. $MgSO_4$ (dried), triethylamine (99%), toluene (analytical grade), MeOH, HCl (37%), sucrose, NaOH (pellets), $NaHCO_3$ and $K_2CO_3$ were supplied by VWR International. All chemicals except the WVO samples were used as received.

ATR-FTIR and $^1H$ NMR analysis were carried out according to the methodology presented in Chapter 4. Dynamic mechanical analysis (DMA, Triton Tritec Dynamic Mechanical Thermal Analyser) was performed using a dual cantilever bending setup with an oscillating frequency of 1.0 Hz, displacement of 0.05 mm from -60 to 100 °C at a heating rate of 2 °C $min^{-1}$. Specimens were in the rectangular form of a nominal size of 1.5 x 5 x 24 mm. Glass transition temperature ($T_g$) was obtained from the maximum of the tan δ peak in curves of tan δ versus temperature.

Weight-loss curves were measured by thermogravimetric analysis (TGA) using a Mettler Toledo TGA 1 STARe System programmed, 25 to 600 °C, heating rate of 10 °C $min^{-1}$, under an $N_2$ flow of 100 mL $min^{-1}$. This heating rate was selected for a better balance between time of analysis and reduction of thermal gradients. The temperature of initial degradation ($T_{Onset}$) was defined from the onset of the degradation temperature of the main thermal event and temperature of maximum degradation ($T_{Max}$) was determined from the curve of 1st derivative of weight loss with respect to temperature. Network formation was analysed by differential scanning calorimetry (DSC) using a Mettler Toledo DSC 1 STARe System, from 25 to 350 °C, using a heating rate of 10 °C $min^{-1}$ and under an $N_2$ flow of 100 mL $min^{-1}$. For the curing kinetics, curves of conversion were obtained from isothermal runs at 160, 150 and 140 °C for 60 min. Samples were then cooled down to 25 °C at 20 °C $min^{-1}$ and again heated to 350 °C at 10 °C $min^{-1}$ for the calculation of the residual cure. Chemical resistance test was performed by immersing rectangular samples of approximately 1 g of each formulation in vials containing 20 ml of water, NaOH (1 M), $H_2SO_4$ (1 M) and toluene. These vials were left at room temperature for 7 days, and changes in the weight and physical aspects were calculated for each pair of formulation/solution.

### 5.2.2 Preparation of the bio-based epoxy resins

WVO was purified by multiple liquid extraction according to the procedure presented in section 4.2.2.2 (Chapter 4), and the bio-based epoxy resins was synthesised from purified WVO and neat vegetable oil according to Methodology B presented in section 4.2.3.1. The stoichiometry was adjusted to use 200 mL of each oil as starting quantity. Epoxy resins synthesised from WVO were denominated by epoxidized purified waste vegetable oil (EPVO) and analogues from neat oil by epoxidized neat vegetable oil (ENVO).

### 5.2.3 Preparation of the thermoset polymers

Approximately 10 g of bio-based epoxy resin, originated either from EPVO or epoxidized ENVO, were added to a round bottom flask. Hardener to epoxy resin (H:E) ratio was varied from 0.8:1.0 to 1.4:1.0, producing resin systems given in Table 5.1. When PA was used as curing agent, the mixture was heated to 140 °C in order to facilitate solubilization and ensure proper homogenisation. In contrast, MHHPA was added to the system at room temperature since it is a liquid at normal conditions. In sequence, 3 mol% (in relation to the epoxy amount) of the curing catalyst (triethylamine or 2-methylimidazole) were added to the flask. The system was stirred for 3 minutes to ensure homogeneity, and then the content was poured into dog bone-shaped silicone moulds. The formulations were placed in an oven (Fistreem Vacuum Oven) at 140 °C for 16 h, and thermoset polymers were post-cured at 160 °C for 2 h. The description of the formulations is presented in Table 5.1

Table 5.1: Range of formulations created from vegetable oil-based resins and anhydrides cured with tetraethylammonium (TEA) and 2-methylimidazole (2-MI).

| Resin Origin | Curing Agent | Molar Ratio (H:E) | Entry (TEA) | Entry (2-MI) |
|---|---|---|---|---|
| ENVO | MHHPA | 0.8:1.0 | 1 | 17 |
| | | 1.0:1.0 | 2 | 18 |
| | | 1.2:1.0 | 3 | 19 |
| | | 1.4:1.0 | 4 | 20 |
| | PA | 0.8:1.0 | 5 | 21 |
| | | 1.0:1.0 | 6 | 22 |
| | | 1.2:1.0 | 7 | 23 |
| | | 1.4:1.0 | 8 | 24 |
| EPVO | MHHPA | 0.8:1.0 | 9 | 25 |
| | | 1.0:1.0 | 10 | 26 |
| | | 1.2:1.0 | 11 | 27 |
| | | 1.4:1.0 | 12 | 28 |
| | PA | 0.8:1.0 | 13 | 29 |
| | | 1.0:1.0 | 14 | 30 |
| | | 1.2:1.0 | 15 | 31 |
| | | 1.4:1.0 | 16 | 32 |

### 5.2.4 Synthesis of Sucrose Ester Fatty Acids (SEFAs)-based resins

The first step to produce epoxidized SEFAs resins was the synthesis of fatty acid methyl esters (FAME). For that, 100 mL of purified WVO ($1.01\times10^{-1}$ mol, 1 equiv.) were added in a round bottom flask and transesterified with 12.4 ml of MeOH ($3.03\times10^{-1}$ mol, 3 equiv.) and 30% NaOH solution at 65°C for 3 h under constant agitation. The crude product was acidulated using HCl until pH neutrality. The resulting fatty acid layer was separated from the glycerol phase and repeatedly washed with water to eliminate traces of mineral acids, methanol and glycerol. FAMEs were dried under $MgSO_4$ and filtered for separation of the drying agent. A yellow oily solid was obtained with a yield of 82%.

For the synthesis of SEFAs, 10g of sucrose ($2.92\times10^{-2}$ mol, 1 equiv.) were dissolved in 200 mL of DMF in a round bottom flask at 120 °C and an excess amount of FAME (70 g, $2.37\times10^{-1}$ mol, 8 equiv.) was added together with $K_2CO_3$ (1 wt%) as catalyst. The mixture was cooled to room temperature and kept under these conditions for 2h under stirring. The pH of the reactional medium was neutralised with $NaHCO_3$ and the crude product, and unreacted sucrose was separated by precipitation with toluene. The resulting product was washed with water for removal of polar impurities, and subsequently, the solvent was removed using a rotary vacuum evaporator. A yellow oil was obtained with a yield of 64%. Finally, the epoxidation of SEFA into ESEFA was envisioned through the repetition of the epoxidation procedure applied to WVO (section 4.2.3.1).

## 5.3 Results and Discussions

### 5.3.1 General Considerations

Figure 5.1 illustrates all experimental steps towards the preparation of the thermoset polymers from waste oil, from the purification of the WVO, epoxidation to produce the resins and cure with cyclic anhydrides. Features such as the unsaturation degree of NVO and PVO (2.88 and 2.18, respectively), as well as the number of epoxy rings per triglyceride unit (2.66 and 2.08, respectively), were defined by $^1$H NMR as discussed in Chapter 4. Also, this image demonstrates the extra complexity added by the curing step in comparison with the systems investigated in the previous chapter.

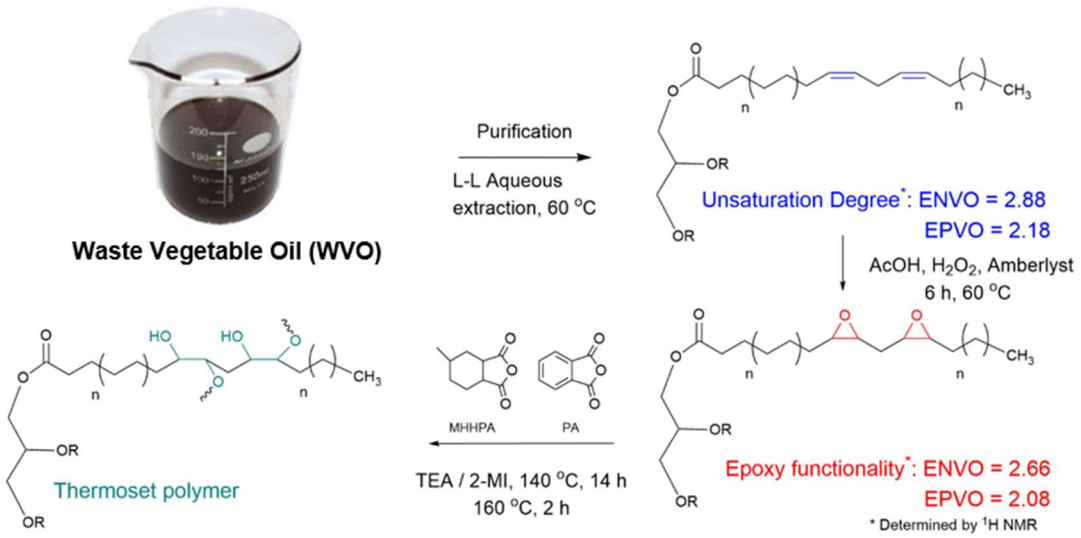


Figure 5.1: Production of bio-based thermoset polymers from waste vegetable oil.

At this stage, considerations regarding the environmental impact were made for the selection of the most appropriated methodology to prepare the EVOs. The epoxidation with $H_2O_2$ was selected as standard procedure to prepare the bio-based resins due to the combination of satisfactory conversions, greater atom economy in comparison to *m*-chloroperbenzoic acid (mCPBA) and scalability.[4] In this regard, for every double bond that is transformed into an oxirane ring, the epoxidation with mCPBA generates one molecule of chlorobenzoic acid, representing a relative atom efficiency of only 9%. To illustrate this concept, the E-Factor for each procedure was calculated based on the methodology introduced by R.A. Sheldon in the early 90's.[19,20] The E Factor is a simple way to analyse the ratio between the amount of waste generated and the product synthesised according to the following relationship:

Equation 5.1 $$\text{E Factor} = \frac{Mass_{\,Total\,Waste}}{Mass_{\,Product}}$$

Considering the amount of organic waste and organic solvent used by both competing procedures, the one based on mCPBA scored a E-Factor = 6 while the peracid methodology accounted for a E-Factor = 1.72. These findings illustrated clearly the advantage of using the acetic acid / $H_2O_2$ system from the environmental and scalability point of view. Therefore, all resins synthesised in Chapter 5 were produced according to this method.

Also in terms of environmental impacts of this methodology, the waste vegetable oil can be considered a burden-free starting material from a life cycle assessment perspective as the impacts associated with deep-frying are included in the production of chemicals from food

waste.[21] Consequently, the production of materials from waste oil streams mitigate all the impact of the VO production. Finally, the $CH_2Cl_2$ consumed in the purification step and the toluene used in the synthesis were recuperated by rotatory evaporation and recycled into the system, therefore reducing the impact associated with solvent consumption.

The investigation of four formulation parameters (origin of the VO, hardener, quantity of hardener and catalyst) was envisioned to optimise the properties of the resulting thermoset and to create guidelines supporting future investigations on how to improve the performance of thermoset polymers from WVO. Nevertheless, the commutation of these parameters into actual formulations would result in a situation in which individual contributions could be masked by other factors varying at the same time. In other words, achieving a single conclusion about how each parameter influenced the physical properties of the thermoset formulation would be not trivial because there were too many responses combining different factors (formulation parameters), as illustrated in Figure 5.2.

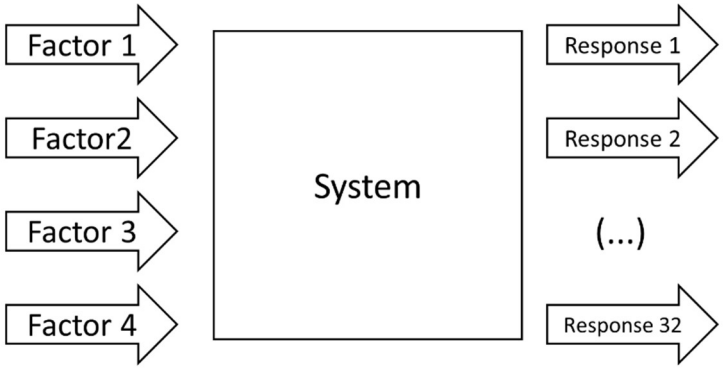


Figure 5.2: Combination of factors and responses in the current study.

This scenario was ideal for the application of statistical methodologies that calculate the significance of each experimental factor, such as the Design of Experiments (DOE). A DOE is a systematic approach that defines the statistical relationships between factors and responses. This strategy calculates the effect of primary factors (directly investigated by the experiment) and their interactions (also known as secondary factors).[22] Therefore; one can understand not only how the factors influence the system, but also if factors influence each other both synergistically or antagonistically. DOE is commonly applied by experimentalists in academia and industry to reduce the development time of a new product or process, improve performance and achieve process robustness.[22]

In the scope of this work, the DOE permitted classifying each parameter according to its contribution towards increasing the $T_g$ of the networks. Regarding this property, literature discusses that EVO-based formulations should be designed with the maximized $T_g$ and rigidity

in order to attend the technical specifications required in structural applications.[23] Therefore, the maximization of these criteria has been adopted by many authors since bio-based epoxy networks tend to have challenges in rivalling with petrochemical equivalents in terms of $T_g$. Therefore, the identification of the most effective ways to improve the $T_g$ of biopolymers is mandatory to enable the successful application of these systems. Factors and responses were organised according to a $2^4$ factorial experiment according to the positive and negative levels presented in Table 5.2.[22] For the purpose of building a symmetric factorial, the four levels of anhydride molar ratio were clustered as into low (non-stoichiometric and stoichiometric levels, 0.8:1.0 and 1.0:1.0) and high (stoichiometric excess, 1.4:1.0 and 1.2:1.0) levels.

Table 5.2: Factors and levels used in the design of experiments.

| Factor | Positive Level | Negative Level |
|---|---|---|
| Oil Origin (A) | ENVO | EPVO |
| Hardener (B) | PA | MHHPA |
| Molar Ratio (C) | High (1.4 and 1.2:1) | Low (1.0 and 0.8:1) |
| Catalyst (D) | 2-MI | TEA |

The following sessions investigate parameters associated with the creation of the network from a thermal and chemical point of view. Once the phenomena behind the cure are elucidated, a more detailed investigation of the $T_g$ in terms of the formulation and the application of the DOE is presented in section 5.3.4.

### 5.3.2 Investigation of curing behaviour

Investigations of the curing process by DSC permitted the calculation of the enthalpy of cure ($\Delta H_{Cure}$) through the integration of the main exothermic peak found in the 120 – 150 °C. Results presented in Table 5.3 demonstrated that higher anhydride molar ratios led to increased heat of reaction in all scenarios as a consequence of the increased stoichiometric ratio. In other words, there are more hardener molecules available to promote the polymerization through the ring opening of the oxirane groups, which in turn releases the strain energy of the 3-member ring species.[24]

Table 5.3: Thermodynamic parameters of the curing of formulations 1-32.

| Entry | $\Delta H_{Cure}$ (kJ mol$^{-1}$) | $\Delta H_{Cure}$ (J g$^{-1}$) | Entry | $\Delta H_{Cure}$ (kJ mol$^{-1}$) | $\Delta H_{Cure}$ (J g$^{-1}$) |
|---|---|---|---|---|---|
| **1** | 48.4 | 133.7 | **17** | 51.3 | 166.7 |
| **2** | 51.1 | 156.2 | **18** | 53.8 | 174.9 |
| **3** | 57.4 | 186.5 | **19** | 55.2 | 179.4 |
| **4** | 64.9 | 211.0 | **20** | 55.6 | 180.8 |
| **5** | 39.2 | 110.1 | **21** | 52.2 | 132.7 |
| **6** | 45.5 | 132.7 | **22** | 54.1 | 133.2 |
| **7** | 49.3 | 160.2 | **23** | 56.3 | 135.2 |
| **8** | 52.0 | 169.1 | **24** | 63.5 | 175.3 |
| **9** | 41.1 | 113.7 | **25** | 22.3 | 52.3 |
| **10** | 48.1 | 120.1 | **26** | 42.7 | 100.3 |
| **11** | 51.7 | 121.6 | **27** | 43.7 | 102.3 |
| **12** | 57.9 | 136.1 | **28** | 44.6 | 104.9 |
| **13** | 33.9 | 92.1 | **29** | 40.8 | 122.7 |
| **14** | 40.8 | 107.0 | **30** | 41.0 | 127.2 |
| **15** | 48.3 | 113.5 | **31** | 41.6 | 132.2 |
| **16** | 51.5 | 121.9 | **32** | 53.9 | 149.3 |

However, the same data demonstrated that some formulations presented a non-linear relationship between the molar ratio and the $\Delta H_{Cure}$, particularly for systems produced with 2-MI, Figure 5.3. This observation demonstrated the complexity of the mechanism behind the cure, and has been previously reported in literature and discussed in Chapter 2.[12,25] Regarding samples prepared with resins from different origins, ENVO-based systems (**1-8/17-24**) presented a higher heat of reaction per gramme of resin when compared to EPVO analogues (**9-16/25-32**) due to the increased number of oxirane rings (2.66 versus 2.08, respectively). The analysis of this property versus the values of enthalpy per mol permitted a direct observation of effect associated with the epoxy equivalent. Nevertheless, this reduction also meant that drawbacks associated with the exothermicity of this reaction can be reduced by the use of EPVO. Also, these findings confirmed the anticipated hypothesis that EPVO presents reduced reactivity compared to ENVO. Despite polymers formed with MHHPA presented higher $\Delta H_{Cure}$ than PA analogues when TEA was used as catalyst, the same behaviour was not observed for 2-MI catalysed systems. In these cases, the unsaturation degree proved to be the major factor controlling the heat of reaction.

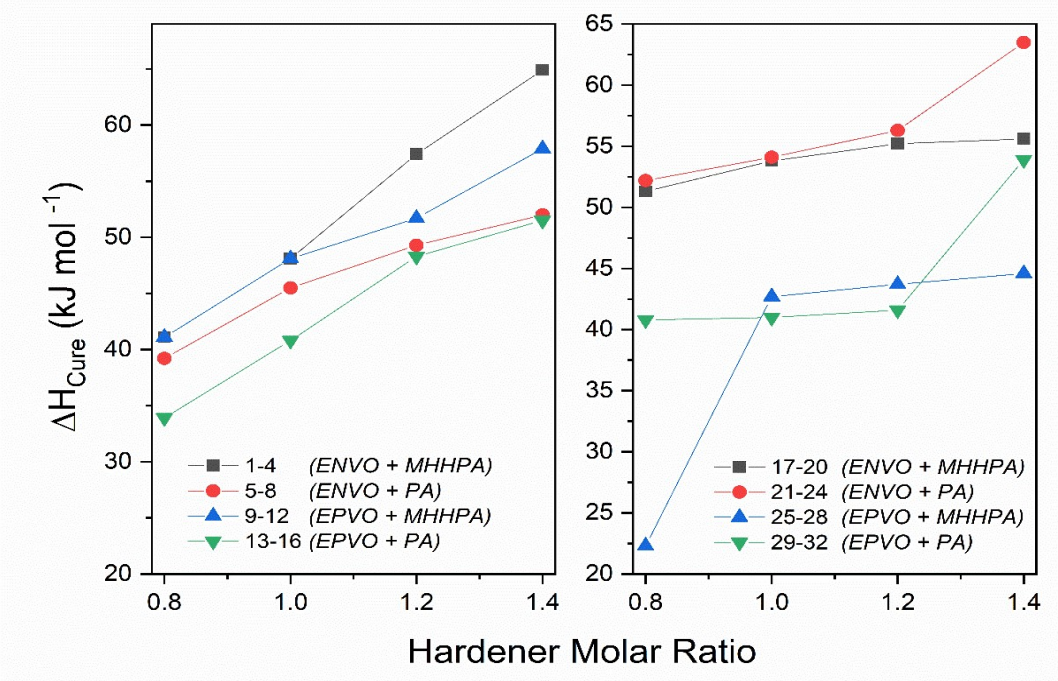


Figure 5.3: Relationship between the molar ratio and the enthalpy of cure ($\Delta H_{Cure}$) for formulations cured with tetraethylammonium (TEA, left) and 2-methylimidazole (2-MI, right).

At this point, the curing phenomenon was further investigated from the kinetic point of view by isothermal DSC runs. The basic understanding of the kinetic starts with the description of conversion rate by a reaction rate constant that by definition is temperature-dependent and the concentration of one species (Equation 5.2).[26,27] The reaction rate constant can be described according to an Arrhenius expression (Equation 5.3).

Equation 5.2 $$\frac{d\alpha}{dt} = K(T).f(\alpha)$$

Equation 5.3 $$K(T) = A\,exp\left(\frac{-Ea}{RT}\right)$$

The degree of cure, also described as the conversion (α), can be calculated from the relationship between the partial heat of reaction (H (*t*) accumulated at a given moment) and the total enthalpy (ΔH), as given by Equation 5.4. In this scenario, the conversion ranges from α = 0 (fully uncured resin) to α = 1 (fully cured thermoset) during the curing phenomenon.

Equation 5.4 $$\alpha(t) = \frac{H(t)}{\Delta H_{Cure}}$$

From these definitions, kinetic models are constructed through the combination of the previous equations, describing that the reaction rate (dα /dt) is directly related to the heat flux rate (dH / dt) according to what is described in Equation 5.5. Equations 5.2 and 5.5 can be

rearranged in a single expression described by Equation 5.6. This single equation represents the foundation for all kinetic models based on the use of a reaction constant.[8] Throughout the decades, one of the major challenges in the area has been finding mathematical expressions equivalents to $f(\alpha)$ that can adequately describe the network formation from a physical point of view.

Equation 5.5 $$\frac{d\alpha}{dt} = \frac{1}{\Delta H_{cure}}\left(\frac{dH}{dt}\right)$$

Equation 5.6 $$\frac{d\alpha}{dt} = A\,exp\left(\frac{-E\alpha}{RT}\right)f(\alpha)$$

Experimentally, a set of thermograms was obtained for each formulation in three different temperatures (140, 150 and 160 ° C), enabling the calculation of kinetic parameters. Figure 5.4 illustrates one of the 32 sets of thermograms obtained from the isothermal experiments, exemplifying how the heat of reaction was released during the isothermal process. The calorimetric profile is a crucial since it can be directly related to the mechanism in which the curing phenomenon occurs, therefore providing evidence of the kinetics parameters. In this regard, all thermograms presented very similar behaviour, in which the main exothermic peak was developed at the very beginning of the curing phenomenon. From this point, the heat release was rapidly reduced to the point that no significant heat is released after the 25 min mark.

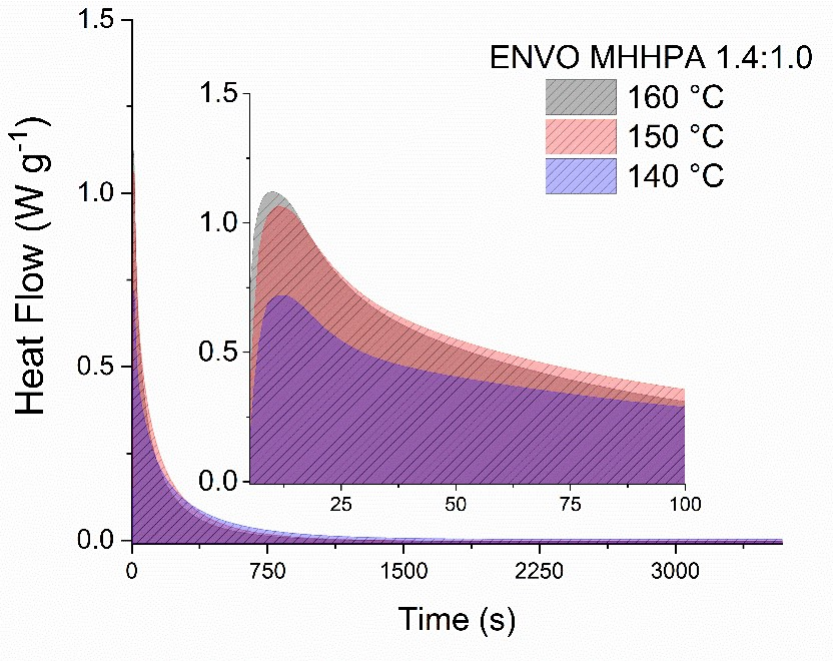


Figure 5.4: Curves of heat flow as a function of time for curing one of the formulations of epoxidized vegetable oil cured with methylhexahydrophthalic anhydride (MHHPA) at different temperatures. Insert shows detail of the curve.

Conversion was calculated through the integration of the heat flow in relation to the total enthalpy of reaction. The total enthalpy of reaction considers the enthalpy of cure obtained from the dynamic studies, and the residual cure calculated from the dynamic segment after the isothermal process. Figure 5.5 and Figure 5.6 show the evolution of α for formulations **1-16**, revealing the evolution of α with the curing temperature. Thermograms obtained at the highest curing temperature (160 °C) reached the steady state (where the conversion reached a maximum and invariant value) more rapidly than at 140 °C. In this regard, the temperature was responsible for providing molecular mobility, facilitating the propagation stage and overcoming the energetic barrier of this transformation. Nevertheless, it is worth mentioning that Zhang *et al.* demonstrated that α could be negatively affected by the temperature in cases where vitrification is observed.[28] Vitrification is a thermo-reversible phenomenon that occurs when the $T_g$ of a given network in the process of cure reaches the temperature of cure, changing a viscous liquid into a glassy state and drastically reducing the cure kinetics.[29] However, systems based on vegetable oils generally have $T_g$ smaller than the temperature required to form the network when anhydrides are used, therefore not displaying a vitrification effect.[2] A discussion in more depth about the $T_g$ of the networks produces in this study can be found in section 5.3.5, and curves associated with formulations 17-32 can be found in the Appendix section.

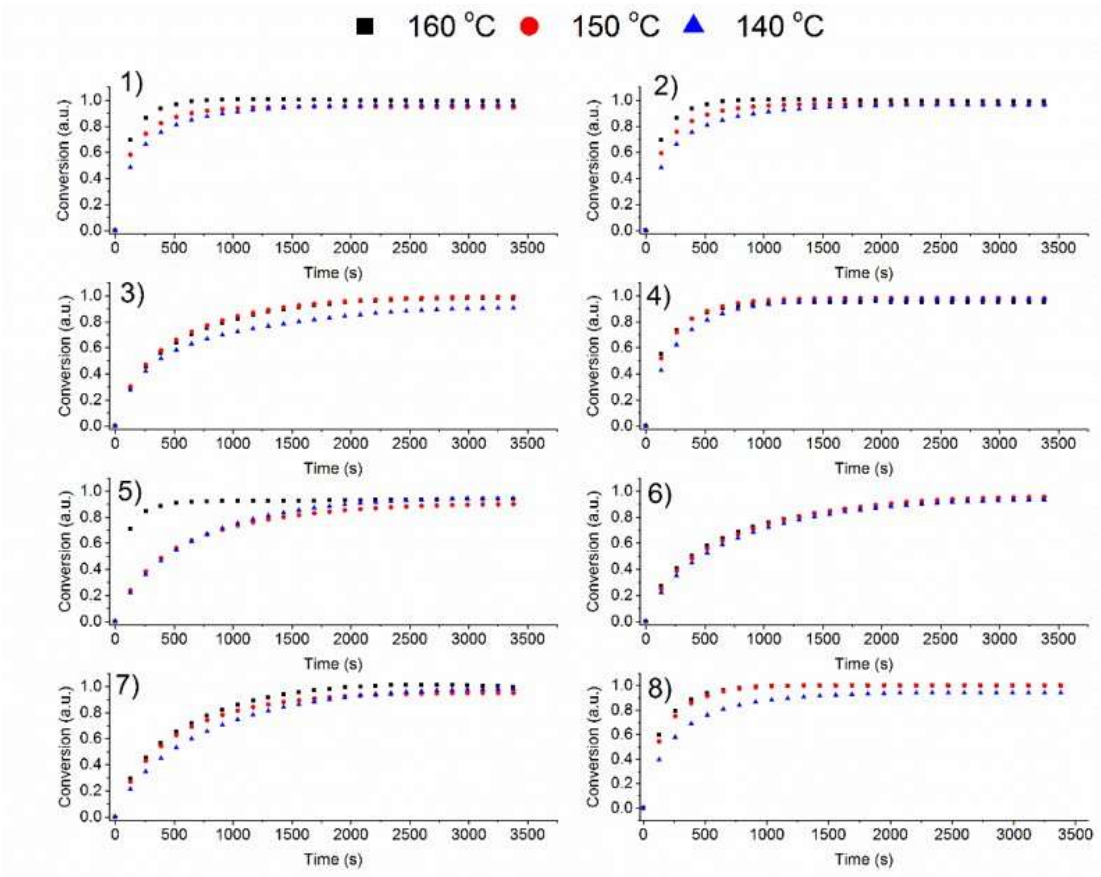


Figure 5.5**:** Curves of conversion (α) versus time of the isothermal experiments of formulations 1-8.

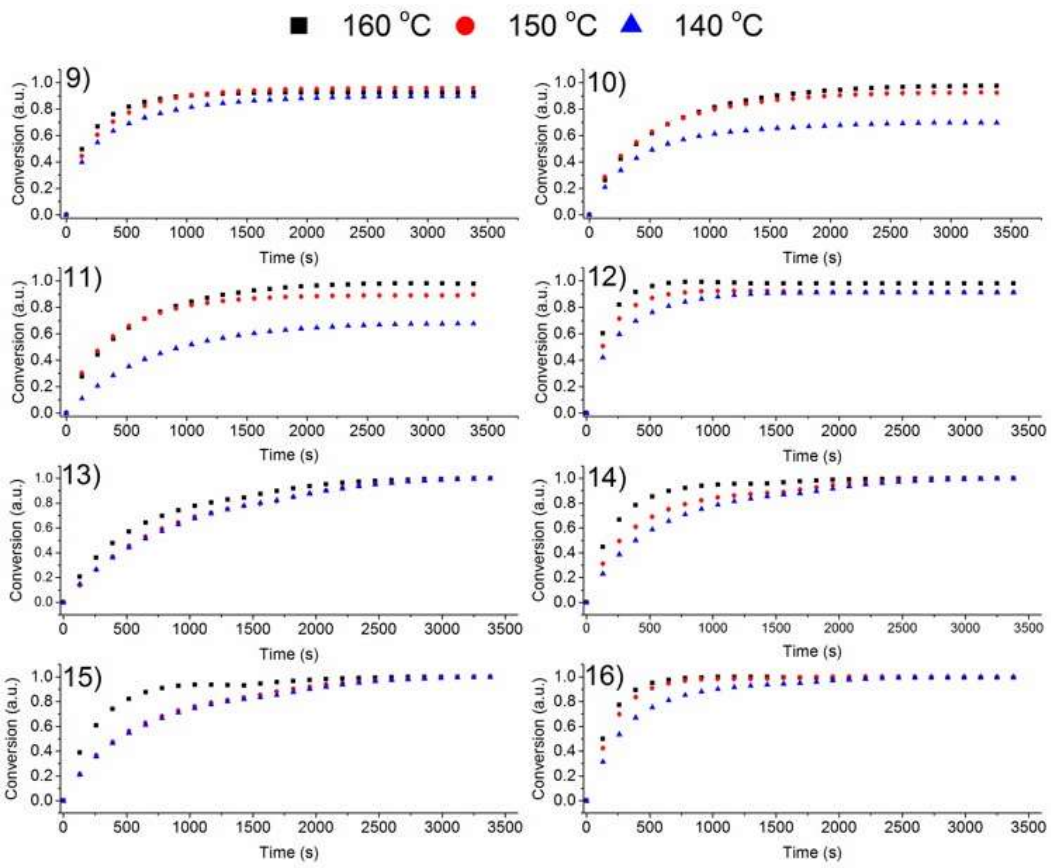


Figure 5.6: Curves of conversion (α) versus time of the isothermal experiments of formulations 9-16.

The shape of the conversion curves illustrated that the curing agent could influence the network creation, mainly in the experiments performed at 140 °C. Formulations produced with PA showed a slower conversion rate when compared to the analogues with MHHPA, either taking longer to reach the steady state of displaying reduced values of α. Since PA has a melting temperature close to 140 °C, the reaction of cure can experience an additional diffusional limitation as a consequence of the high viscosity of the hardener. Consequently, the reduced conversion led to thermoset networks with a high residual cure.[30] This effect was not observed when the cure was carried out at higher temperature because the viscosity could be reduced to a level where the diffusional hindrance was negligible.

Appropriate data treatment allowed a quantitative description of the kinetics of cure through the adjustment of the conversion curves to mathematical models. The selection of the correct equation to describe the data is a critical step in the modelling since all kinetic parameters are derived from this fitting.[31] Consequently, attention was given to the shape of the heat flow curves since it can provide evidence of how the cure phenomena are being mechanistically controlled. In this regard, experimental curves did not present the

characteristic profile of an autocatalytic phenomenon, which is typically described by a slow initiation with maximum reaction rate at around $0.3 \leq \alpha \leq 0.4$.[32] Therefore, autocatalytic equations were eliminated from the pool of mathematical expressions capable of describing the data.

An additional expression commonly explored to describe the kinetics of cure of EVOs is Kamal's model. This approach is a special model that accounts for the presence of interactions during the phenomenon through the use of more than one reaction constant.[31]. This strategy was investigated through the application of the Kamal equation as described by Equation 5.7. In this expression, $K_1$ can be calculated from scenarios where $\alpha \rightarrow 0$ while parameters *n, m* and $K_2$ are obtained from the linearization of $f(\alpha)$. The elucidation of the kinetic parameters would then enable the calculation of activation energies $E_1$ and $E_2$ associated with the competing mechanisms. Despite the successful calculation of parameters associated with phenomenon 1 ($K_1$ and *n*), *m* and $K_2$ proved impossible to be accurately calculated since the responses of ln (α) with respect to $\ln\left\{\left[\frac{d\alpha/dt}{(1-\alpha)^n}\right] - K_1\right\}$ were not linear. Therefore, the data treatment through the application of the Kamal model was abandoned and alternative methods were explored.

Equation 5.7 $$\frac{d\alpha}{dt} = (k_1 + k_2\alpha^m)(1-\alpha)^n$$

Considering the lack of fit observed for both autocatalytic models, a new approach was investigated nth order expressions. This mathematical model, described by Equation 5.8, is known for its simplicity since it can approximate the cure phenomenon to a transformation of fractional order. Literature has previously demonstrated successful applications of this kind of expression to describe the cure of EVOs, validating this approach. The linearization of Equation 5.8 resulted into Equation 5.9, which allowed the calculation of the reaction order constant (n) and the reaction constant (K) for each curve of α from the plot of log(dα⁄dt) as a function of log(1-α). The pre-exponential factor (A) and the activation energy (Ea) were calculated from the set of three temperature-dependent constant K(T) obtained for each formulation. This approach was used to successfully calculate the kinetic model parameters for all thermoset formulations. Table 5.4 and Table 5.5 present the parameters obtained for formulations 1-16 while the remaining formulations are presented in the Appendix section.

Equation 5.8 $$\frac{d\alpha}{dt} = K(T)(1-\alpha)^n$$

Equation 5.9 $$log\left(\frac{d\alpha}{dt}\right) = log\,K(T) + nlog(1-\alpha)$$

Table 5.4: Parameters of the n$^{th}$ order kinetic model from the conversion curves representing formulations 1-8.

| Entry | $T_{cure}$ (°C) | K $(1/mol\ L^{-'}\ s)$ | n | $E_a$ (kJ mol$^{-1}$) | A $(1/mol\ L^{-'}\ s)$ |
|---|---|---|---|---|---|
| **1** | 160 | 0.85 | 1.07 | 31.4 | 4.32 |
| | 150 | 0.76 | 1.66 | | |
| | 140 | 0.67 | 1.75 | | |
| **2** | 160 | 0.85 | 1.07 | 31.9 | 4.48 |
| | 150 | 0.77 | 1.49 | | |
| | 140 | 0.67 | 1.67 | | |
| **3** | 160 | 0.22 | 1.02 | 34.5 | 0.45 |
| | 150 | 0.20 | 1.08 | | |
| | 140 | 0.19 | 1.11 | | |
| **4** | 160 | 0.80 | 1.34 | 21.8 | 12.02 |
| | 150 | 0.69 | 1.37 | | |
| | 140 | 0.55 | 1.48 | | |
| **5** | 160 | 0.32 | 1.20 | 53.9 | 5.68 |
| | 150 | 0.27 | 1.30 | | |
| | 140 | 0.21 | 1.51 | | |
| **6** | 160 | 0.19 | 1.18 | 24.0 | 0.66 |
| | 150 | 0.17 | 1.34 | | |
| | 140 | 0.16 | 1.45 | | |
| **7** | 160 | 0.16 | 0.72 | 14.4 | 0.34 |
| | 150 | 0.15 | 0.97 | | |
| | 140 | 0.14 | 1.38 | | |
| **8** | 160 | 0.46 | 0.81 | 53.1 | 7.25 |
| | 150 | 0.38 | 0.86 | | |
| | 140 | 0.31 | 1.76 | | |

Table 5.5: Parameters of the n$^{th}$ order kinetic model from the conversion curves representing formulations 9-16.

| Entry | $T_{cure}$ (°C) | K $(1/mol\,L^{-'}\,s)$ | n | $E_a$ (kJ mol$^{-1}$) | A $(1/mol\,L^{-'}\,s)$ |
|---|---|---|---|---|---|
| **9** | 160 | 1.19 | 1.92 | 95.1 | 15.53 |
| | 150 | 0.63 | 1.61 | | |
| | 140 | 0.60 | 2.07 | | |
| **10** | 160 | 0.58 | 1.43 | 117.9 | 26.25 |
| | 150 | 0.38 | 1.50 | | |
| | 140 | 0.24 | 1.70 | | |
| **11** | 160 | 0.53 | 1.02 | 109.1 | 15.35 |
| | 150 | 0.37 | 1.22 | | |
| | 140 | 0.24 | 1.61 | | |
| **12** | 160 | 0.80 | 1.02 | 44.7 | 8.42 |
| | 150 | 0.69 | 1.12 | | |
| | 140 | 0.55 | 1.75 | | |
| **13** | 160 | 0.22 | 1.21 | 96.8 | 12.07 |
| | 150 | 0.15 | 1.09 | | |
| | 140 | 0.11 | 0.98 | | |
| **14** | 160 | 0.66 | 1.37 | 120.3 | 37.3 |
| | 150 | 0.56 | 1.45 | | |
| | 140 | 0.27 | 1.58 | | |
| **15** | 160 | 0.47 | 1.16 | 179.4 | 8.6 |
| | 150 | 0.24 | 1.41 | | |
| | 140 | 0.13 | 1.46 | | |
| **16** | 160 | 0.65 | 0.93 | 59.3 | 14.3 |
| | 150 | 0.55 | 0.99 | | |
| | 140 | 0.42 | 1.33 | | |

Kinetic data from formulations prepared with TEA as catalyst (**1-16**) demonstrated that the increase of temperature (from 140 to 160 °C) led to decreased reaction orders, as well as to increased reaction constant, resulting in a quicker cure.[33] This results is alligned with the fact that temperature is reponsible for providing the energy and mobility required to the form the network crosslinks. Despite the influence on the molar ratio in the dynamic DSC studies, no clear trend was observed from the kinetic point of view since parameters fluctuated with no particular tendency. The lack of relationship between the kinetic model and the H:E ratio

is in accordance with studies previous studies.[34] Also ENVO-derived formulations presented in general reduced $E_a$ when compared to the EPVO analogues, suggesting that the increased degree of functionalization of the first resin facilitated the formation the network.

Results obtained from formulations with 2-MI (Appendix) demonstrated that the catalyst played an essential role in the kinetics of cure. As opposed to what observed for TEA-catalysed systems, the decrease in temperature led to the reduction of both the reaction order and reaction constant. This observation evidenced that mechanisms of cure promoted by 2-MI and TEA follow different kinetic regime, as discussed by Supanchaiyamat *et al.* in the production of ELO-based systems with different catalysts.[35] In fact, imidazoles present higher catalytic activity in comparison to tertiary amines for the creation of networks with anhydrides. Despite the action of the catalyst, other parameters such as the hardener content and the oil origin followed the same trend previously observed for formulations 1-16.

Overall, investigations elucidated the principal effects associating the kinetic phenomena and parameter such as the catalyst and the degree of functionality of the resins, which is directly linked with the use of WVO as platform. In terms of the catalyst, the study demonstrated the advantages of using 2-MI from the network formation point of view. Also, the kinetic model can be used as a tool to simplify the complex curing process, providing predictability to the reaction and establishing a relationship between optimized cure conditions and the properties of the final thermosetting polymer.[36,37]. Therefore, such information can be used to determine optimised steps to the process cycle.[38,39] In the case of the presented in this study, kinetic studies demonstrated that the minimum temperature of cure had to be 140 °C, with 150 °C reducing diffusional effects associated with the use of PA.

It is noteworthy discussing the limitations of the kinetic model constructed in this study Data related to higher levels of conversion (above $\alpha = 0.7$) did not meet the conditions imposed by the linear model due to the effects of gelation. This scenario has been previously demonstrated by Ampudia *et al.* and Boquillon & Frigant in studies with anhydride-cure epoxies, and is accepted when discussing the application of simple kinect models reactions of this complexicity.[40–42] Despite these approximations, the study still have drawn important conclusions about the formation of the network, supporting future studies in the area of thermosets from WVO.

### 5.3.3 Spectroscopic Investigations

ATR-FTIR spectroscopy was used to investigate the network formation from the chemical perspective since wet analyses are not efficient in accurately tracking the creation and consumption of functional groups. After the gel point, these sites become sterically hindered and eventually inaccessible.[43] Therefore, only a limited number of techniques are

capable of examining the chemical characteristics of the thermoset polymer after formation of the crosslinking.

Figure 5.7 presents the spectra obtained from hardeners prior to the reaction of cure. The most notable difference between these spectra the presence of the observation of the aromatic ring in PA (740 $cm^{-1}$, ν C-H), and the absorbance peak at 1600 $cm^{-1}$ associated with the aromatic ring stretching vibrational modes. On the other hand, the cycloaliphatic ring present in the MHHPA structure was observable by the absorption peaks at 2954 (ν $C-H_3$) and 2871 $cm^{-1}$ (ν $C-H_2$). Additionally, the absorbance peaks in 904 $cm^{-1}$ (ν C-O-C) was found in both curing agents, characterising the anhydride linkage. In this regards, this signal and of the one found at 1850 $cm^{-1}$ (ν C=O) are crucial to comprehend the formation of the network since they are the ones mainly affected by the network formation.[44] A complete assignment of the absorption peaks found in the ATR-FTIR spectra of both hardeners is presented in Table 5.6.[45]

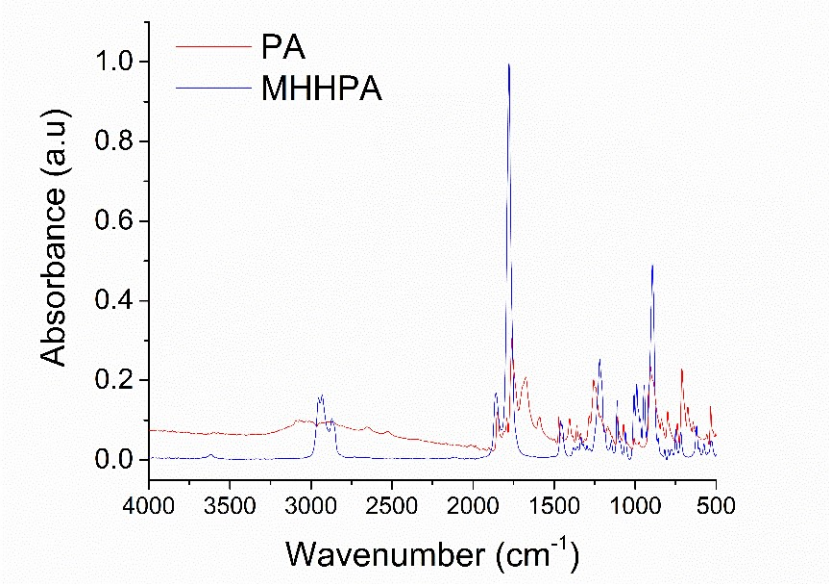


Figure 5.7: ATR-FTIR spectra of phthalic anhydride (PA) and methylhexahydrophthalic anhydride (MHHPA), from 4000 to 500 $cm^{-1}$.

Table 5.6: Wavenumber and assignment of the principal bands in the ATR-FTIR spectrum of vegetable oil samples.

| **Wavenumber (cm-1)** | **Assignment** |
|---|---|
| 2954 | ν C-$H_3$ in MHHPA backbone |
| 2931 and 2871 | ν $CH_2$ Symmetric and asymmetric |
| 1857 | ν C=O in PA |
| 1847 | ν C=O in MHHPA |
| 1670 | ν C=C *cis* in PA |
| 1600 | ν Aromatic Ring in PA |
| 1469 and 1458 | δ $CH_2$ in MHHPA/PA |
| 1099 | ν C-O in MHHPA/PA |
| 904 | ν C-O-C in MHHPA/PA |

ATR-FTIR spectra of the polymers **1-16** (Figure 5.8) demonstrated that all formulations showed a remarkable reduction of the ν C-O in 844 $cm^{-1}$, illustrating the consumption of oxirane rings during the cure. The ring-opening reaction could also be evidenced by the appearance of a broad band centred in 3450 $cm^{-1}$ (ν O-H). These groups are formed by the reaction site that opens for the creation of the ester linkage between the moieties. Simultaneously, a new absorption peak at 1069 $cm^{-1}$ (as highwas detected in the cured polymers, demonstrating that the creation took place mainly through the esterification.

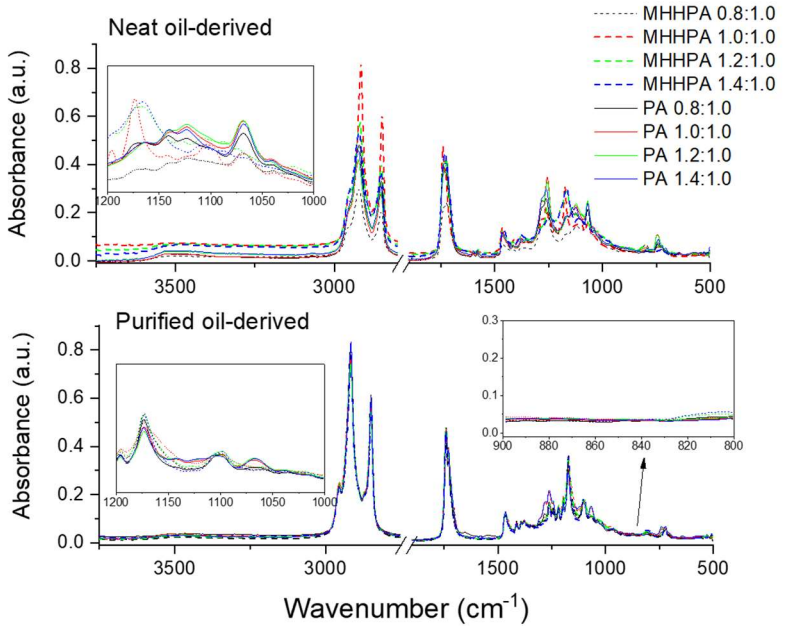


Figure 5.8: ATR-FTIR spectra of formulations 1-8 (above) and 9-16 (below), from 3750 to 500 $cm^{-1}$.

Transformations on the hardener moiety were observed in the 1700-1800 $cm^{-1}$ spectral region. Peaks initially present at 1800 $cm^{-1}$ (ν C=O in cyclic anhydride) were reduced while a new peak at 1730 $cm^{-1}$ appeared in the spectra of cured polymers. This observation indicated that the dicarboxylic ring was opened during the cross-linking process, supporting the reaction mechanism previously suggested in the literature. Other absorbance appearing as a shoulder at 1740$cm^{-1}$, associated with the ester group in the fatty acids backbone, remained unchanged during the curing process. Although the absorption peaks exclusively associated with the presence of aromatic rings were detectable in PA-based polymers, signals of the ν C-$H_3$ and ν C-$H_2$ associated with the cycloaliphatic ring of MHHPA were suppressed by the absorption bands derived from the aliphatic chains.

The utilisation of waste oil-based caused no observable differences in the spectra within the sensitivity of the technique. Also, the choice of catalyst caused no significant changes since the two series of polymers (**1-16** and **17-32**) have spectra with no distinguishable features, Figure 5.8 and Figure 5.9. Even though differences were observed in the kinetic studies, it can be established that both catalysts also led the network formation through esterification reaction over etherification. Despite its simplicity, ATR-FTIR provided evidence about the mechanistic details of the cure reaction and to elucidate the chemical aspects of the network.

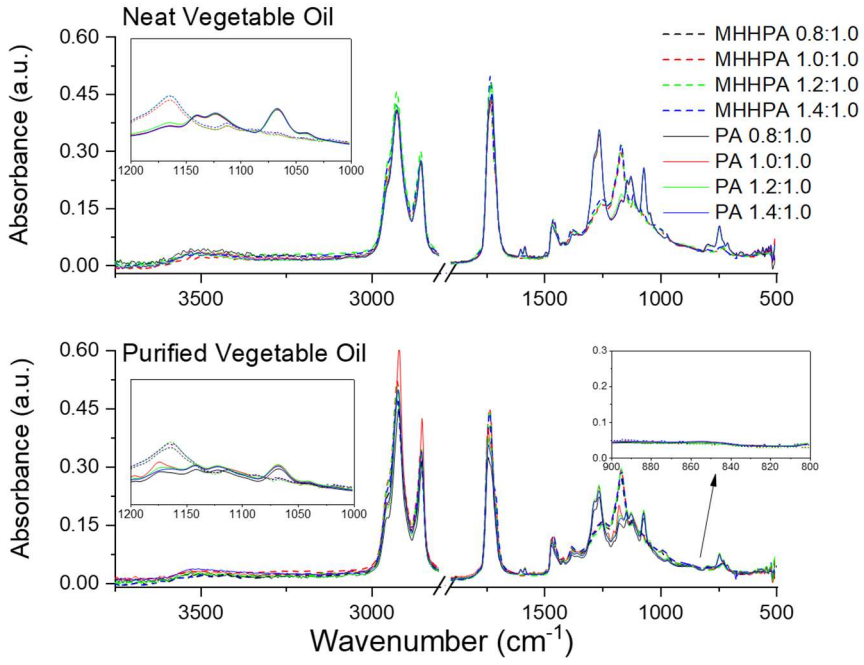


Figure 5.9: ATR-FTIR spectra of formulations 17-24 (above) and 25-32 (below), from 3750 to 500 $cm^{-1}$.

### 5.3.4 Dynamic Mechanical Properties and Optimisation of $T_g$

Dynamic mechanical analyses (DMA) were performed to measure the viscoelastic response and the mechanical properties of the polymeric network in a range of temperatures, comprehending the effects of formulation parameters. DMA also allowed the determination of the thermal phenomena that are followed by changes in mechanical behaviour (or vice versa), such as glass transition, crystallization, degradation, and healing and post-cure events.[46] Therefore, data collected by DMA permitted establishing relationships between transformations in the microscopic scale like as polymer chain rearrangements, medium scale properties such as fibre/matrix interaction and, finally, at the macroscopic mechanical performance of the material.

Curves of storage modulus (E′) versus temperature of formulations **1-16** and **17-32** (Figure 5.10A and B, respectively) are shown in logarithmic scale for better visualisation. The behaviour of storage moduli with the increase in temperature demonstrated gains in chain mobility due to the higher system energy, which enabled quick relaxations.[47] More importantly, curves revealed the dependence between maximum E′, the hardener molar ratio and the anhydride selection. For example, anhydride-rich formulations produced polymers with superior E′ because of the higher molecular rigidity of these hardeners in comparison with the aliphatic backbone of the EVOs. Also, EVO-rich polymers reached the rubbery plateau at lower temperatures in comparison to anhydride-rich formulations, demonstrating a secondary effect of the mobility gain provided by the aliphatic moieties. These findings illustrated the ability of controlling the properties of the polymeric network according to the H:E molar ratio. Additionally, as the formulations do not show any significant increase in the modulus of elasticity in this temperature range, it can be concluded that the samples do not show residual cure under these conditions.

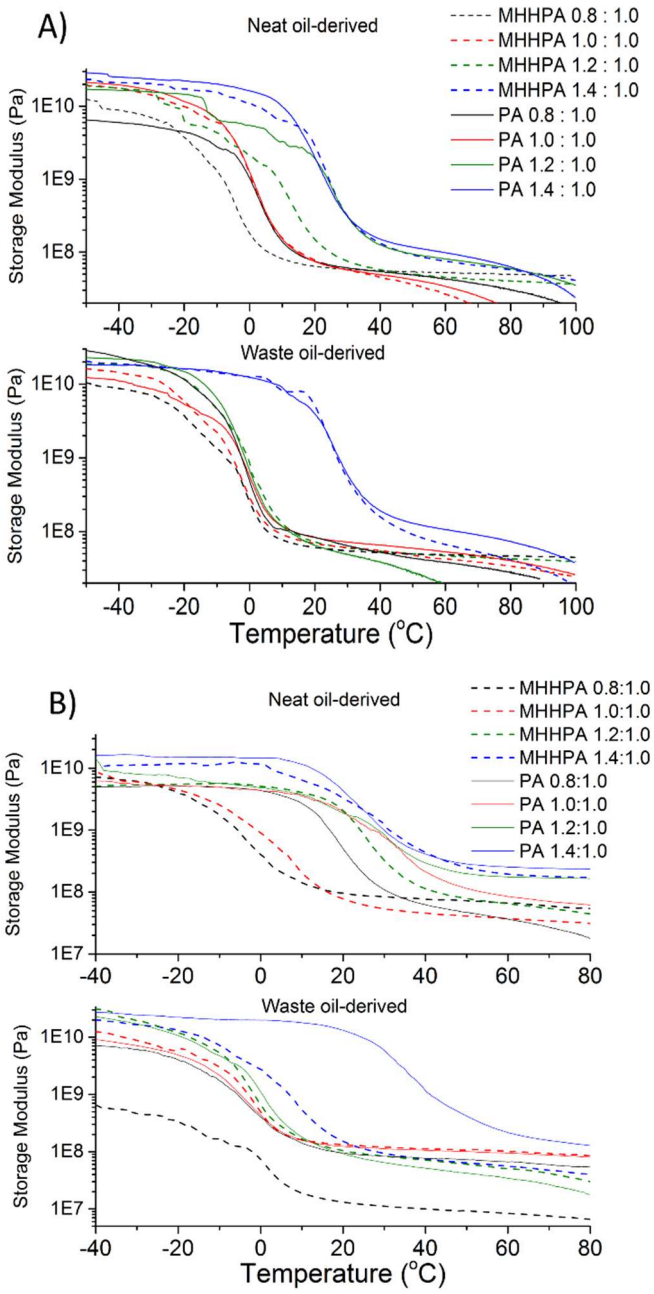


Figure 5.10: Curves of storage modulus versus temperature for polymers produced with A) tetraethylammonium (TEA) and B) 2-methylimidazole (2-MI) as the catalyst. Top curves derive from neat oil-based resins and bottom curves from waste oil-based resins.

Regarding the choice of hardener, formulations produced with PA presented higher E′ in comparison to MHHPA because of the superior rigidity of the PA molecular structure, which displays an aromatic structure versus the cycloaliphatic backbone found in MHHPA. Double bonds in the PA backbone introduces additional mobility restriction when compared to the cycloaliphatic ring of the MHHPA, resulting in more rigid networks. Additionally, the aromaticity present in PA contributed to stronger intermolecular forces, consequently increasing the molecular stiffness of the crosslinks. Interestingly, no relationship regarding

the oil origin and the initial E′ was observed in these curves despite the reduced reactivity observed for these resins.

Other relationships were investigated at room temperature through the analysis of E′ at 25 °C as a function of the anhydride type and its molar ratio (Figure 5.11). The use of PA resulted in polymers with higher storage modulus (from 4% to 700%) compared to similar formulations with MHHPA at this temperature. This observation reflected again features associated with the superior molecular stiffness of the aromatic ring in the PA structure. Also, at this temperature range, polymers produced with ENVO resin presented slightly higher E′ at 25 °C when compared to EPVO equivalent due to the hypothetical creation of more cross-links. Regarding the effect of molar ratio, the relationship between the network stiffness and the amount of hardener was replicated at conditions close to the temperature of use. Finally, networks produced in the presence of 2-MI as a catalyst followed the same set of behaviours observed for those materials produced with TEA.

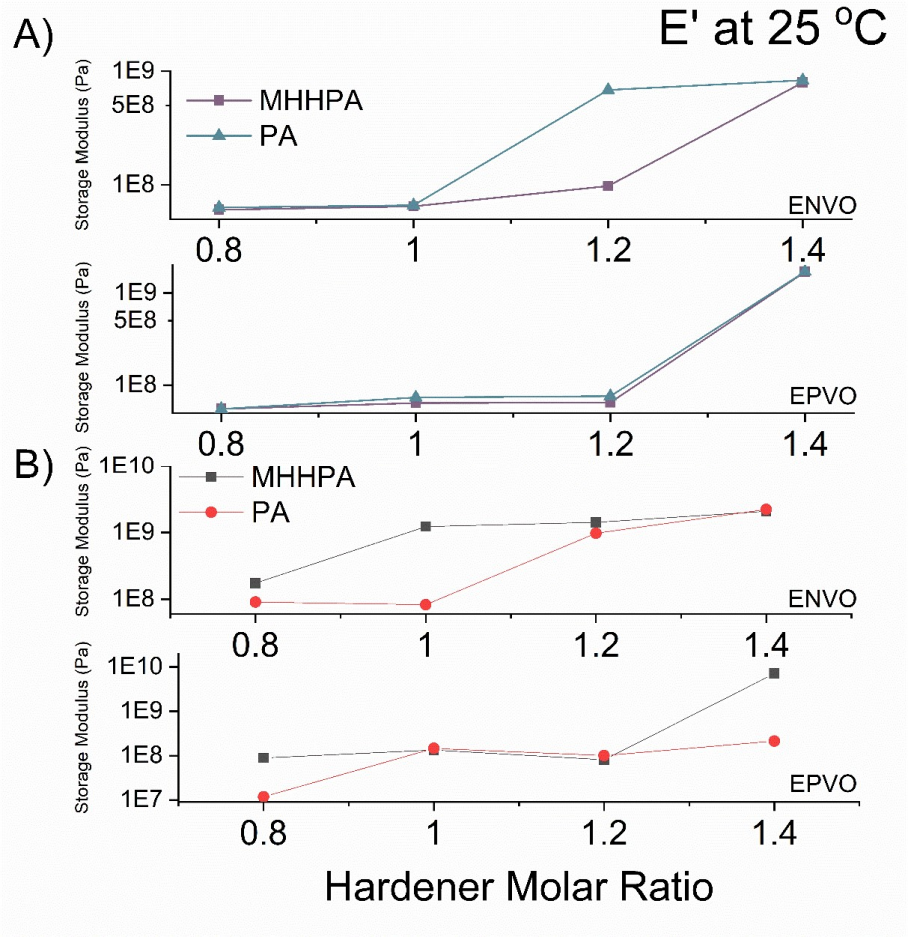


Figure 5.11: Storage moduli at room temperature (25 ° C) versus anhydride molar ratio of the polymers produced from formulations cured with A) TEA and B) 2MI.

Furthermore, the $T_g$ was investigated to understand additional changes in the network caused by temperature. Initially rigid, the network transitions to an elastic state due to the sudden increase of mobility and coordinated movement of both lateral groups and crosslinks.[48] Typically, polymer derived from epoxy resins have the $T_g$ identified through DMA rather than DSC because these systems present minimal changes in the specific heat (also known as $C_P$) during the transition.[48] Consequently, the calorimetric peak observed in dynamic DSC runs is often too small to be clearly identified. On the other hand, the mobility gain caused by the same phenomenon is clearty evidenced in temperature scan DMA runs by different parameters. Therefore, the $T_g$ was examined from the maximum peak of tan δ curves. At the $T_g$ point, the network experiences a sharp decrease in storage modulus (E'), followed by an increase of the plastic component, described by the loss modulus (E"), resulting in a characteristic peak.

In this regard, the viscoelastic theory that describes the DMA technique defines that tanδ is dependent on both E′ and E", as demonstrated by the Equations 5.10 A-C. This sequence of mathematical steps demonstrates how tan δ is originated on the dependence between the elastic and plastic moduli the stress, strain and the phase angle δ.[49] Therefore, the maximum value of tan δ is a valid form to identify the glass transition since it coincides with the inflexion of the E′ decrease, *i.e.* the region where transformation is imminent.[50] It is important to note that, since the glass transition phenomenon results in a number of changes in the physical/mechanical behaviour of a material, the literature offers different methodologies for the description and identification of this relaxation.[51] Consequently, discrepancies between different studies are often observed if authors compared values obtained by different approaches.

Equation 5.10A $$\mathrm{E`}(t) = \frac{\sigma_0}{\varepsilon_0}\cos(\delta)$$

Equation 5.10B $$\mathrm{E``}(t) = \frac{\sigma_0}{\varepsilon_0}\sin(\delta)$$

Equation 5.10C $$\tan\delta = \frac{E``}{E`}$$

Figure 5.12A and B present tanδ curves obtained for all thermoset formulations, and the values of $T_g$ are shown in Table 5.7. Results revealed the dependence of $T_g$ with all parameters covered in this study (hardener, molar ratio, oil source and catalyst), with values ranging from -3.4 to 42.5 °C. Although these $T_g$ values are smaller in comparison with DGEBA (SuperSap CLR®, 56.3 °C, Chapter 4), they are comparable to thermosets previously reported in literature deriving form similar formulations (from -8 to 65 °C, Gerbase *et al.*, and from -17 to 62 °C, Clark *et al.)*[2,16] In addition, all curves presented broad tanδ peaks,

evidencing the formation of heterogeneous networks.[52] In the context of EVO-based thermosets, this observation is a consequence of the distribution of oxirane groups across the triglyceride backbone, which produces a statistical distribution of double bonds since the starting materials derive from mixed triglycerides.[53]

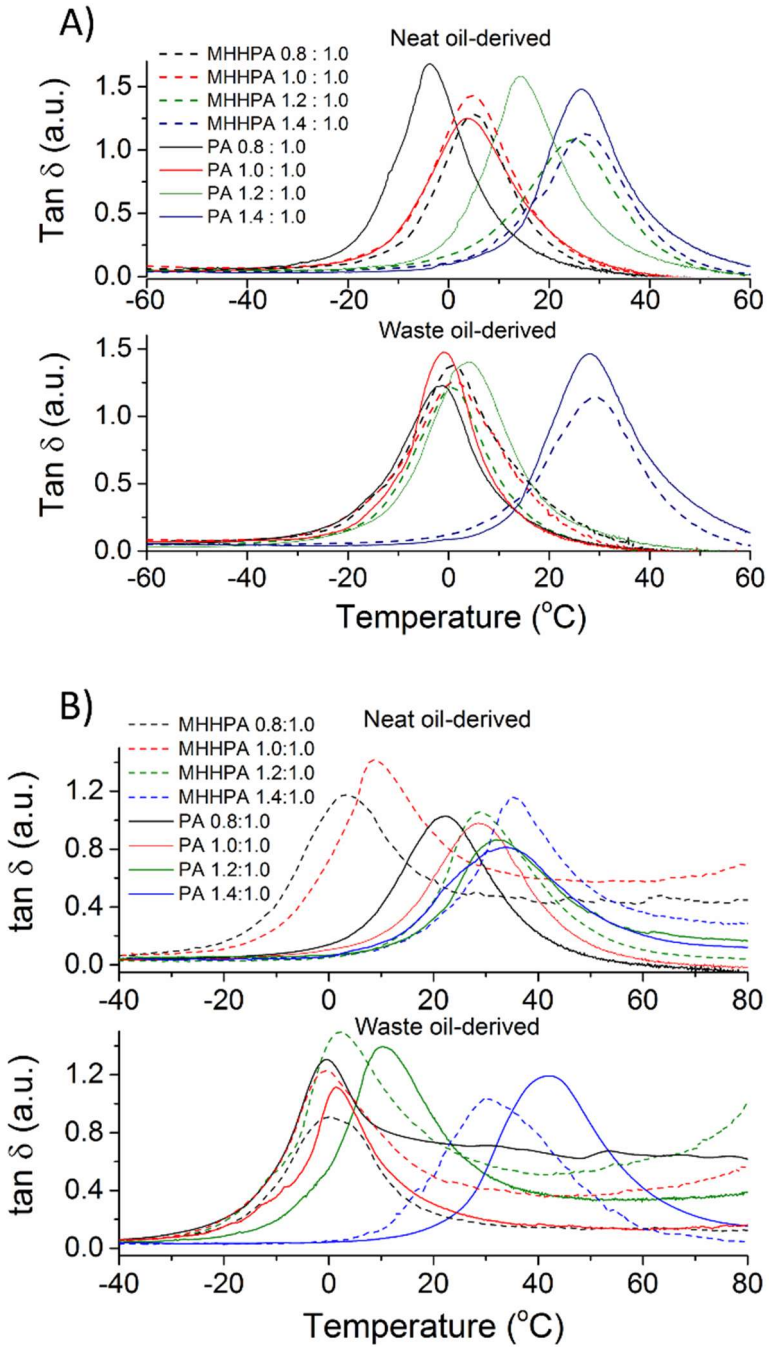


Figure 5.12: Curves of tan δ versus temperature for polymers produced with A) TEA and B) 2-MI as the catalyst. Top curves derive from neat oil-based resins and bottom curves from waste oil-based resins.

Table 5.7: Glass transition temperature ($T_g$) and cross-link density ($\nu_e$) of formulations 1-32

| Entry | $T_g$ (°C) | $\nu_e$ ($10^{-3}$ mol cm$^{-3}$) | Entry | $T_g$ (°C) | $\nu_e$ ($10^{-3}$ mol cm$^{-3}$) |
|---|---|---|---|---|---|
| **1** | 4.3 | 0.068 | **17** | 3.0 | 0.051 |
| **2** | 4.8 | 0.069 | **18** | 9.1 | 0.065 |
| **3** | 24.4 | 0.071 | **19** | 28.8 | 0.073 |
| **4** | 27.4 | 0.082 | **20** | 35.2 | 0.203 |
| **5** | -3.4 | 0.072 | **21** | 22.2 | 0.081 |
| **6** | 5.6 | 0.084 | **22** | 28.8 | 0.087 |
| **7** | 14.5 | 0.100 | **23** | 31.7 | 0.196 |
| **8** | 27.2 | 0.108 | **24** | 34.6 | 0.274 |
| **9** | 0.8 | 0.051 | **25** | 0.1 | 0.054 |
| **10** | 1.1 | 0.053 | **26** | 2.5 | 0.060 |
| **11** | 3.6 | 0.061 | **27** | 27.0 | 0.064 |
| **12** | 28.9 | 0.064 | **28** | 30.6 | 0.071 |
| **13** | -1.3 | 0.052 | **29** | 0.6 | 0.097 |
| **14** | -0.5 | 0.067 | **30** | 2.3 | 0.141 |
| **15** | 3.9 | 0.076 | **31** | 10.4 | 0.153 |
| **16** | 28.1 | 0.106 | **32** | 42.5 | 0.169 |

Tan δ curves revealed that formulations with high anhydride molar ratio led to polymers with higher $T_g$. This effect attenuated the contribution of the aliphatic chains towards increasing the overall mobility of the system, which would negatively influence this value. Nevertheless, chain flexibility played a more critical role at formulation produced with lower anhydride ratio levels. In these systems, unreacted aliphatic chains plasticised the network and further reduced the $T_g$.[54] Therefore, the combination of both effects resulted in the final dynamic-mechanical properties being the sum of the contributions of hardener rigidity and the plasticizing effect; therefore, the $T_g$ values presented a non-linear increase with the anhydride molar ratio.

The comparison between the feedstock demonstrated that WVO (**9-16/ 25-32**) led to polymers with lower $T_g$ than the analogous from neat oil (**1-8/ 17-24**) as consequence of the reduced number of oxirane rings per unit. Therefore, it was assumed that these networks have fewer interconnections between the epoxy and anhydride moieties and are more prone to gain coordinate molecular mobility, presenting these transitions at lower temperatures. Previous studies have already demonstrated that epoxy resins produced from highly-unsaturated oils (such as linseed oil) are capable of producing polymers with increased $T_g$ when compared to

less unsaturated oils[50]. Moreover, tanδ curves demonstrated that the polymers had identifiable no secondary transitions (*e.g.* $T_\beta$) at the low-end temperature range

Since a relationship between the degree of functionality and the $T_g$ was detected, the crosslink density ($\nu_e$) was investigated in more depth through the relationship presented in Equation 5.11.[2] In this expression, E' is the storage modulus at a given temperature, R is the universal gas constant ($8{,}314\times10^3$ cm$^3$ MPa K$^{-1}$ mol$^{-1}$) and T is the temperature of the rubbery plateau, described as ($T_g$+40) K. The $\nu_e$ of a thermoset polymer not only influences the $T_g$ but also plays a significant role in characteristics such as the hardness, impact strength and brittleness.

Equation 5.11 $$\nu_e = \frac{E`}{3RT}$$

The $\nu_e$ values (Table 5.7) demonstrated that higher molar ratios led to a denser network in all systems. There results meet previous observations showing that more connections between the moieties are formed in the presence of excess hardener.[40] Also, polymers obtained from WVO-based resin (**9-16/25-32**) presented smaller values of $\nu_e$ when compared to analogues produced from ENVO, supporting the hypothesis that fewer crosslinks are formed in these formulations due to the lower functionality of the resin. More interestingly, calculations demonstrated that thermosets produced with 2-MI presented higher $\nu_e$ than those produced from TEA, corroborating the values of $T_g$ observed for **17-32** in comparison to **1-16**. These differences can be associated with the higher catalytic activity of imidazoles in contrast to tertiary amines for promoting the anhydrides ring-opening that triggers the polymerisation, therefore facilitating the creation of the network.[35]

The understanding about the relationships between the formulation parameters and the $T_g$ responses permitted the application of the DOE aiming at maximising this property. $T_g$ values were compiled and analysed in Minitab 17 (Minitab Ltd, UK) using a stepwise analysis to produce a DOE model containing factors over a 95 % confidence interval. A Pareto chart (Figure 5.13) was constructed from the statistical analysis, demonstrating that the molar ratio (factor C) was the most statistically significant parameter regulating the $T_g$ of these polymers. Other factors such as the choice of catalyst (factor D) and the oil origin (factor A) had smaller (but significant) contributions. Figure 5.13 also presented the main effects plots, demonstrating how the $T_g$ varied between the low and high-level factors. Interactions plots were omitted since they demonstrated no statistical effect. The increase in $T_g$ caused by the high level of the molar ratio is a consequence of the increased stiffness of the anhydrides and a higher crosslink density observed in these formulations. Therefore, this test demonstrated that the use high anhydride ratios was significant enough to mitigate the $T_g$ reduction caused

by the lower functionality of WVO-based resins (Factor A). The DOE also confirmed the importance of the catalyst selection (Factor D, second most important) since the increased reactivity of 2-MI produced polymers with superior $T_g$. Interestingly, the choice of hardener (Factor B) proved to have no significant impact on the $T_g$ despite the impact observed in the storage modulus curves.

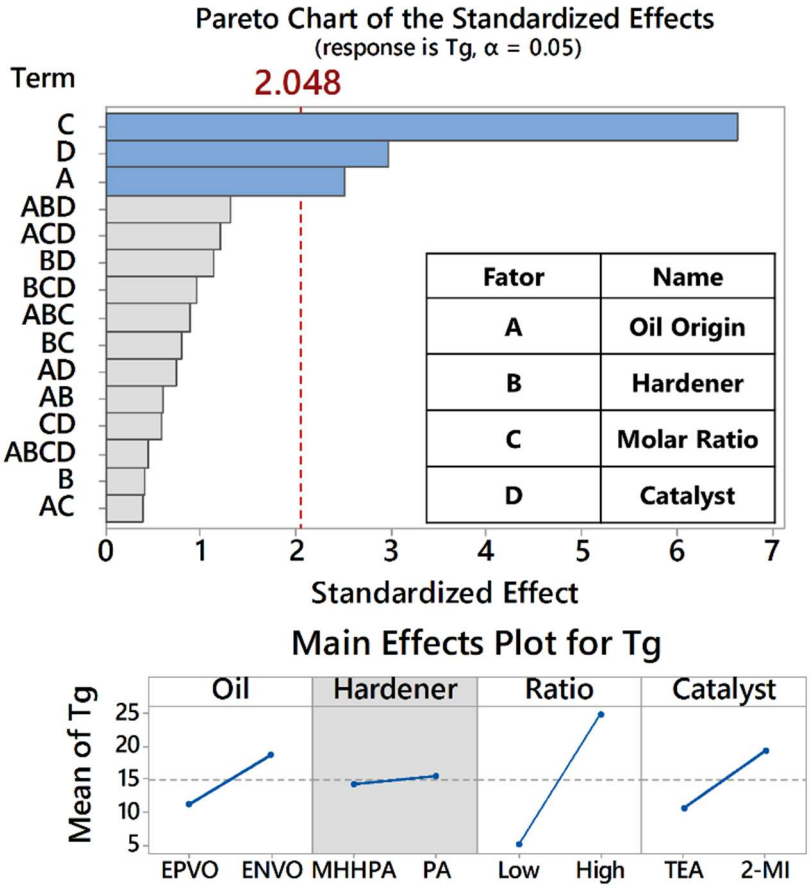


Figure 5.13: Pareto charts and main effects plot for standardised experimental conditions for the $T_g$ of bio-based epoxies. Greyed out factors represent removed factors due to a significance valve lower than 95%.

Based on the statistical analysis above, DMA data demonstrated that factors such as the anhydride molar ratio and the catalyst could be exploited to tune the properties of the resulting networks despite the compromise in mechanical properties caused by the reduced functionality of WVO-based. These adjustments can therefore mitigate losses and drawbacks caused by the use of WVO, which can be explored to reach a favourable balance in performance. Now that the formation and properties of the networks were comprehended, the next sections focus on the stability of these systems against temperture and different chemical environments.

### 5.3.5 Network thermal stability

The exceptional thermal stability found in thermoset materials is one of the main features that differentiate them from thermoplastics polymers, defining some of their unique applications. Therefore, the thermal stability of polymers produced in this study was benchmarked with analogues from neat oil and commercial DGEBA samples, defining features such as the upper limit temperature of use. Although previous studies demonstrated that EVO-based polymers can thermally degrade in a single-step, formulations investigated in this study presented a two-stage decomposition (Figure 5.14A and B).[2,55]

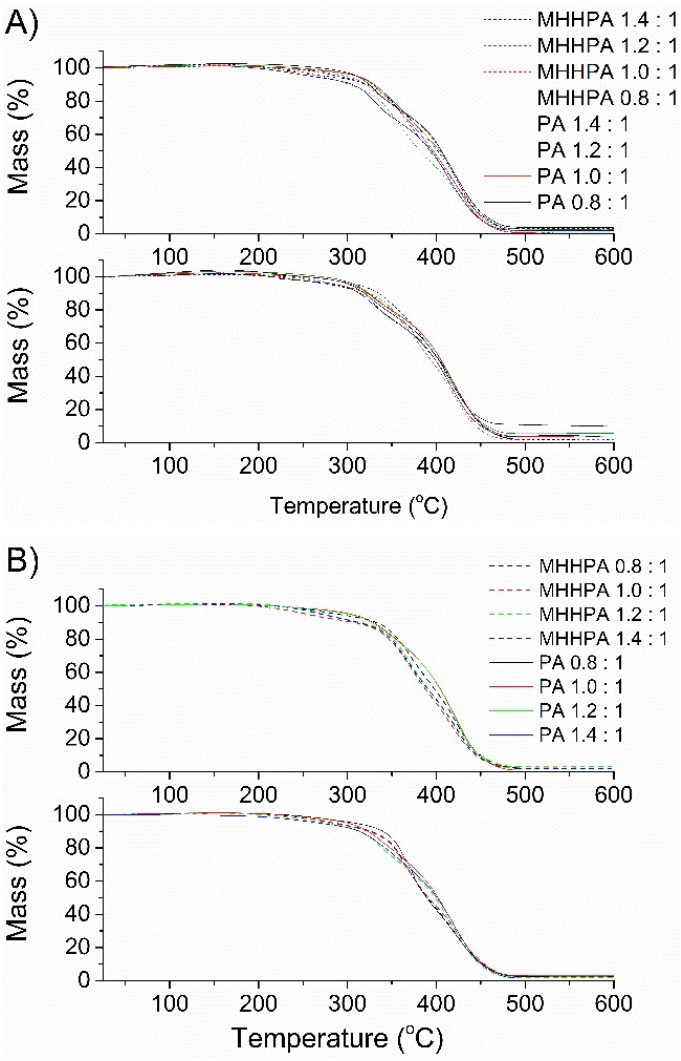


Figure 5.14: Thermograms of the polymers from formulations A) 1-8 (top) and 9-16 (bottom) and B), 17-24 (top) and 25-32 (bottom), from 25 °C to 600 °C, under $N_2$ atmosphere.

The first thermal event (at approximately 215 °C) was a minor weight-loss correspondent to the thermal decomposition of low-molecular-weight molecules not structurally incorporated by the crosslinks. In other words, this event illustrated the presence

of unreacted curing agents in some formulations since it coincided with the thermal decomposition of the hardeners (213.9 and 230.6 °C for PA and MHHPA, respectively). The following event was observed at *circa* 310 °C and represented a major degradation step, which was attributed to the combined thermal decomposition of triglycerides and the ester moieties. This simultaneous degradation phenomenon is commonly observed for thermosets produced from EVO and has been evidenced through TGA/FTIR/GCMS studies. [54,56]

Table 5.8 presents values of $T_{Onset}$ and $T_{Max}$ for formulations **1-32**, comparing them with the stability of the starting materials. The anhydride content (given by the molar ratio) proved to be the primary agent influencing $T_{Onset}$ since networks richer in anhydride had reduced thermal stability, which can be seen by the variation of this value along the series **1** to **4**, **5** to **8**, and so on. This observation is a consequence of the reduced thermal stability of the anhydride moiety in comparison with the triglycerides moiety, and can be also observed in Figure 5.15. In other words, the network becomes gradually more abundant in the less thermally-stable component, therefore degrading at reduced temperatures. Moreover, it is detected that the minor degradation event observed at lower temperatures became gradually more significant at higher molar ratios, meaning that an increasing proportion of unreacted anhydrides were not incorporated into the network.

Table 5.8: Initial degradation temperature ($T_{Onset}$) and maximum degradation temperature ($T_{Max}$) of polymer produced from formulations 1-32 and their components.

| Entry | $T_{Onset}$ (°C) | $T_{Max}$ (°C) | Entry | $T_{Onset}$ (°C) | $T_{Max}$ (°C) |
|---|---|---|---|---|---|
| **1** | 323.5 | 447.4 | **17** | 310.1 | 427.6 |
| **2** | 304.6 | 425.2 | **18** | 309.2 | 435.3 |
| **3** | 289.9 | 423.9 | **19** | 302.0 | 432.4 |
| **4** | 290.4 | 425.1 | **20** | 295.5 | 420.8 |
| **5** | 316.7 | 415.1 | **21** | 310.5 | 415.8 |
| **6** | 308.2 | 410.9 | **22** | 305.4 | 413.4 |
| **7** | 306.9 | 420.7 | **23** | 303.6 | 413.3 |
| **8** | 304.6 | 414.5 | **24** | 300.1 | 414.0 |
| **9** | 314.5 | 422.8 | **25** | 321.2 | 423.2 |
| **10** | 312.6 | 424.6 | **26** | 317.9 | 437.4 |
| **11** | 306.6 | 423.6 | **27** | 310.4 | 423.6 |
| **12** | 302.8 | 427.2 | **28** | 308.4 | 422.0 |
| **13** | 302.0 | 414.3 | **29** | 318.5 | 422.9 |
| **14** | 300.2 | 423.4 | **30** | 315.9 | 424.6 |
| **15** | 298.3 | 421.0 | **31** | 310.2 | 423.6 |
| **16** | 293.8 | 419.5 | **32** | 308.6 | 427.2 |
| **MHHPA** | 230.6 | 272.3 | **PA** | 213.9 | 245.4 |
| **ENVO** | 365.7 | 405.22 | **EPVO** | 364.0 | 406.7 |

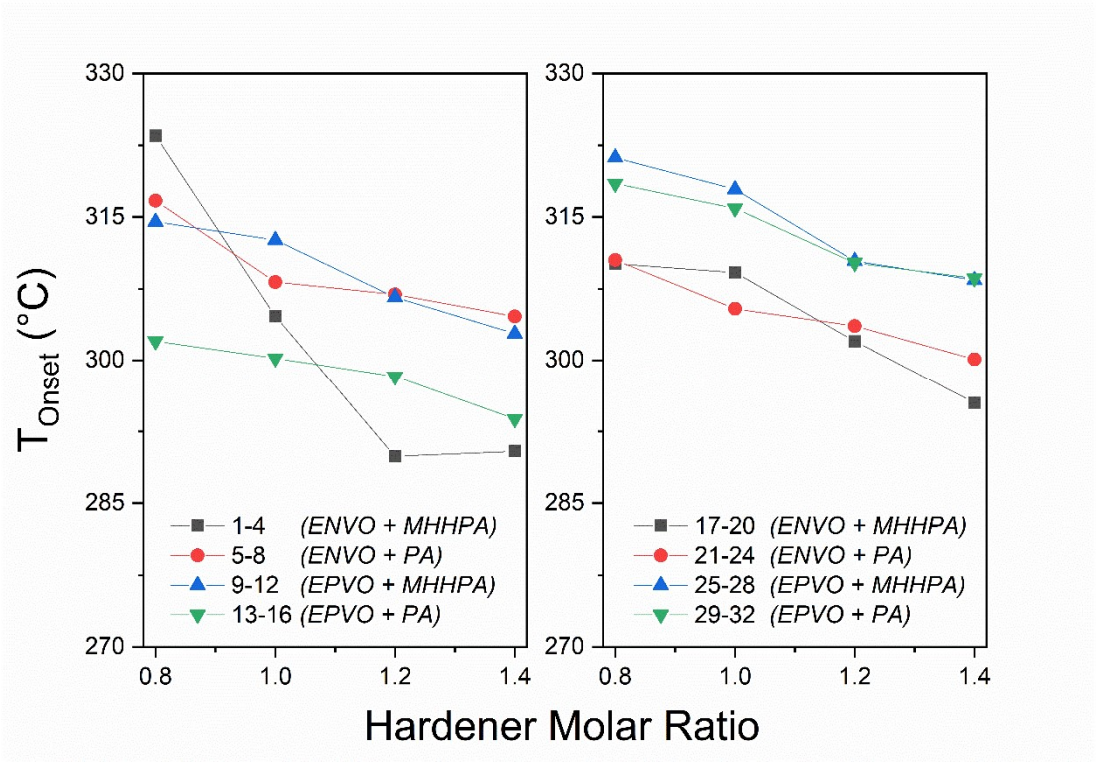


Figure 5.15: Relationship between the molar ratio and the $T_{Onset}$ for formulations cured with tetraethylammonium (TEA, left) and 2-methylimidazole (2-MI, right).

The strategy of using WVO to replace neat oil in thermoset formulations demonstrated to cause no significant effect in terms of thermal stability since $T_{Onset}$ and $T_{Max}$ presented no relationship with the origin of the resin (comparison of **1-8** series with **9-16** series, for example). This finding is aligned with previous reports that revealed no direct connection between the degree of functionality of EVO and the thermal stability of the cured polymer.[54] Similarly, the choice of the curing catalyst also demonstrated no particular tendency. Therefore, TGA data supported the utilization of WVO-based epoxy resins from the thermal stability point of view in comparison to analogues produced from virgin oil. Nevertheless, these bio-based networks were less thermally stable than commercial DGEBA polymers, despite presenting higher $T_{Max}$ values.

### 5.3.6 Chemical Resistance

The exceptional solvent resistance of thermoset polymers results from the tightly connected network formed during the curing process, and this characteristic is responsible for defining several applications for these systems in areas such as coatings and sealers. In order to comprehend this behaviour in WVO-based systems, the chemical resistance of polymers produced from formulations **1-32** was evaluated according to their relative resistance in water, NaOH (1 M), $H_2SO_4$ (1 M) and toluene. As presented in Table 5.9, all formulations were stable

in aqueous and acidic media as no significant changes were observed in volume, weight or physical aspect. On the other hand, samples immersed in toluene swelled and presented weight gains between five and seven times the initial weight. Nevertheless, none of the samples was completed dissolved in these conditions. Precise volume changes were not recorded for these samples since their dimension changed irregularly.

Table 5.9: Chemical resistance of polymers produced from 1-32 in water, NaOH (1 M), $H_2SO_4$ (1 M) and toluene, 7 days at room temperature.

| Entry | $H_2O$ | NaOH | $H_2SO_4$ | Toluene | Entry | $H_2O$ | NaOH | $H_2SO_4$ | Toluene |
|---|---|---|---|---|---|---|---|---|---|
| **1** | - | + | - | * | **17** | - | + | - | * |
| **2** | - | + | - | * | **18** | - | + | - | * |
| **3** | - | + | - | * | **19** | - | + | - | * |
| **4** | - | + | - | * | **20** | - | * | - | * |
| **5** | - | + | - | * | **21** | - | + | - | * |
| **6** | - | * | - | * | **22** | - | * | - | * |
| **7** | - | * | - | * | **23** | - | * | - | * |
| **8** | - | * | - | * | **24** | - | * | - | * |
| **9** | - | + | - | * | **25** | - | + | - | * |
| **10** | - | * | - | * | **26** | - | + | - | * |
| **11** | - | * | - | * | **27** | - | + | - | * |
| **12** | - | * | - | * | **28** | - | * | - | * |
| **13** | - | + | - | * | **29** | - | + | - | * |
| **14** | - | + | - | * | **30** | - | + | - | * |
| **15** | - | + | - | * | **31** | - | * | - | * |
| **16** | - | * | - | * | **32** | - | * | - | * |

Caption: +: soluble, -: insoluble and *: swelling

Despite the resistance in previous conditions, thermoset polymers behaved very differently in NaOH: some polymers swelled after immersion for seven days while the same conditions led to the complete dissolution of another group of formulations. This behaviour is similar to what was reported for polymers produced from Karanja oil and *Mesua ferrea L.* seed oil.[55,57] The particularly poor chemical resistance of EVO-based thermosets in alkali medium is a consequence of hydrolysable ester bonds in the network.[31] In strongly basic conditions, bonds that connect the EVO and anhydride moieties can be attacked, consequently deconstructing the network and leading to the polymer solubilisation.

In this regard, the next step was to understand why some formulations presented resistance to NaOH (*i.e.* just swelled) while others were susceptible to hydrolysis. At this point, a comparison between the chemical resistance and the $\nu_e$ could be established to understand these observations. As demonstrated by Narute *et al.,* thermosets with higher $\nu_e$ possess superior chemical resistance as denser and tighter crosslinks to hinder the solvent penetration.[58] By comparing Table 5.7 and 5.9, it was observed that samples that resistant to hydrolysus displayed $\nu_e$ above $0.076\times10^{-3}$ mol $cm^{-3}$, while all those that degraded presented $\nu_e$ smaller than this. Consequently, formulations produced with increased anhydride molar ratio and cured in the presence of 2-MI presented the most satisfactory performance in chemical resistance tests. Also, this test demonstrated that the origin of the bio-based epoxy resin played no significant role in defining the chemical resistance of the polymer, therefore supporting the utilization of WVO concerning this property. In fact, this empirical threshold can be used for future predictions of the chemical resistance of similar materials.

### 5.3.7 Sucrose esters

Giving the importance of the relationship between $T_g$ and the final properties of the networks, and the restricted performance achieved by epoxidised WVO as resin, this study explored alternative strategies to produce thermoset polymers with denser and more rigid networks. In this regard, the syntheses of sucrose ester-based resins from WVO was envisioned as an approach to prepare more reactive resins and consequently polymers with enhanced mechanical performance. Sucrose ester fatty acids (SEFA) are bio-based molecules obtained from the combination of sucrose and fatty acids that have been firstly explored in the 1960s as coating resins. However, this material presented limited success due to the reduced degree of substitution, restricting the mechanical properties of SEFA-derived films. Nevertheless, SEFA have found application as non-ionic surfactants and have been explored for decades as food additives, acting as emulsifiers in cookies, cakes and bread .[59–61] In early 2000, these materials were rediscovered when industrial processes expanded achieved superior degrees of substitution (up to 7.7 fatty acids per sucrose unit).

Commonly, these units are synthesised using soybean oil, producing a material that is also known in the literature as sucrose soyate.[62] Furthermore, the production of epoxidized sucrose ester fatty acids (ESEFA or epoxidized sucrose soyate, Figure 5.16) is a more recent approach developed by Webster and collaborators to produce alternatives to of traditional epoxy resins from vegetable.[62,63] The advantage of ESEFA over EVO is the higher degree of functionality, enabling the creating of highly connected networks. Also, the sucrose moiety that anchors the fatty acids also contributes towards improving the rigidity of the resulting

polymer. These molecules present a very similar reactivity in comparison with EVOs, therefore networks are preferentially formed through the cure of these resins with anhydrides.

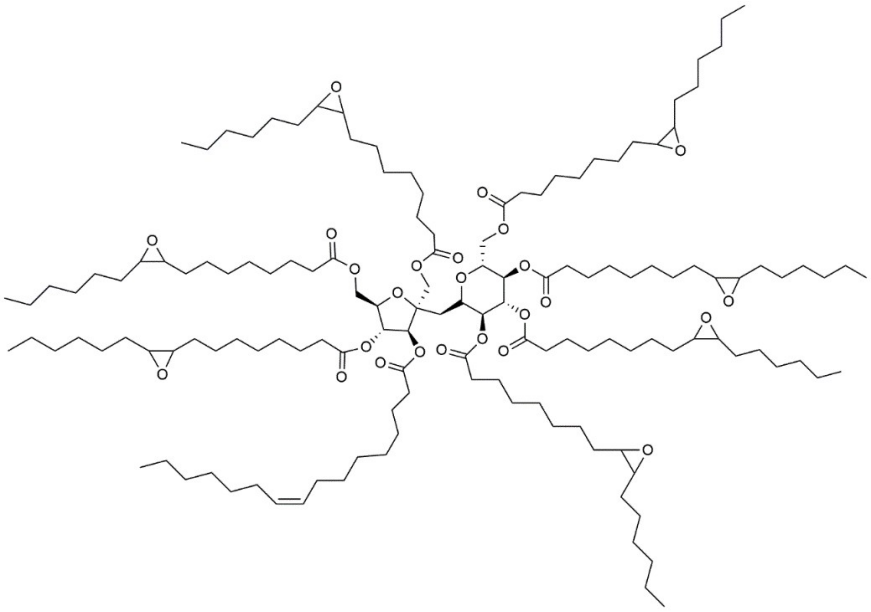

Figure 5.16: Proposed chemical structure for an epoxidized sucrose ester fatty acid (ESEFA).

The preparation of ESEFA from WVO was proposed as a strategy to produce more reactive resins capable of producing networks with superior $T_g$ whilst improving the sustainability of the ESEFA production. According to the combination of methodologies presented by Hass *et al.*, Deshpande *et al.* and Webster *et al.* (Figure 5.17), the first step to prepare the product was the synthesis of FAME from WVO.[59,64–66] Following optimised procedures presented by Wang *et al.*, FAME were successfully synthesised (Step 1) as determined by the reduction of the signals associated with the glycerol backbone (as determined by $^1$H NMR analysis).[67] Nevertheless, the crude product still presented traces of methanol that persisted even after purifying the product.

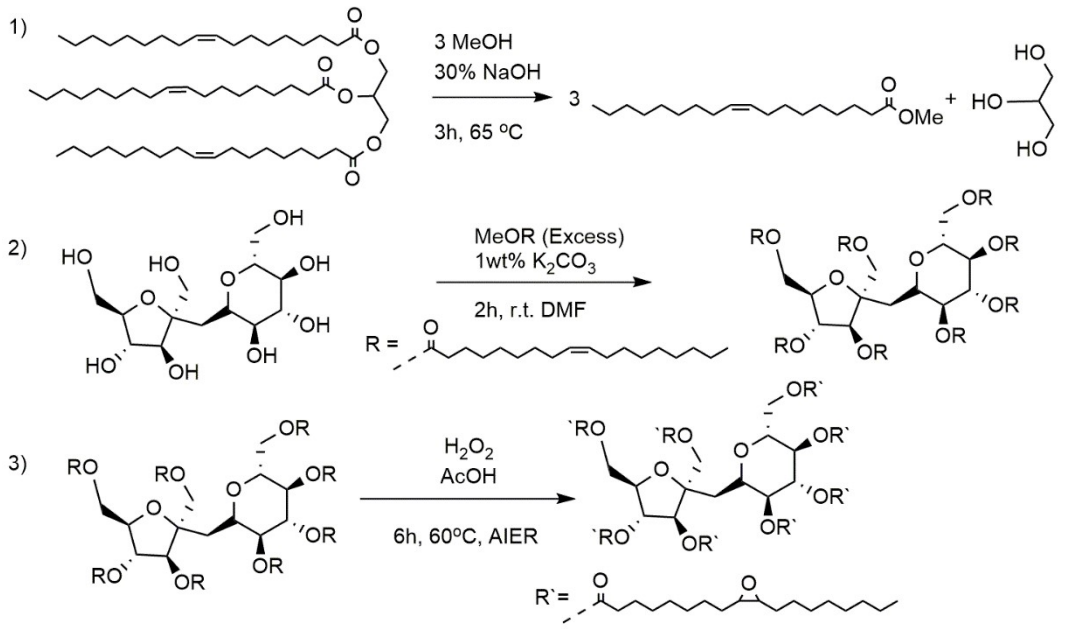


Figure 5.17: Representation of the synthetic pathway to produce ESEFAs from WVO. 1) Transesterification of triglycerides; 2) formation of sucrose ester and 3) formation of epoxidized sucrose ester.

The following step consisted on the transesterification of the sucrose with the FAME to obtain the SEFA, precursor of the ESEFA resin. (Step 2).[66] Products with low degrees of substitution were obtained by this approach as detected by the reduced formation of ester linkages between the sucrose moiety and the FAME approximately 2 fatty acids inserted per sucrose unit, as calculated through the reduction of NMR signals associated with the methyl groups initially attached to the fatty acid backbone. Consequently, conditions were changed to reflect the reduced reactivity between the fatty acids and the sucrose moieties. Increased reaction times (from 2 h to 6 h) and temperatures (from room temperature to 120 °C) were explored to produce more functional products (however, these approaches were unsuccessful in improving the quality of the SEFAs.) In fact, this reproduced the early limitations of producing molecules with reduced capacity of inserting reactive groups in the sucrose moiety. The analysis of recent publications investigating the synthesis of SEFA revealed that special conditions such as the use of enzymatic systems had been preferred in literature.[68,69] No information regarding the details of the industrial process explored to synthesise the Sefose 1618UC™ or Sefa Soyate™ were found. Nevertheless, it was clear that ordinary conditions were not sufficient for the synthesis of highly-functional products.

In conclusion, the exploration of additional reaction parameters to produce SEFA demonstrated to be out of the scope of this thesis: the degree of substitution was not high enough to justify the extra synthetic steps that would add time, cost and waste. Consequently,

it was decided to keep using EVO-based systems as core materials to produce thermoset polymers and composites in the next steps of this study.

## 5.4 Summary

Thermoset polymers were successfully produced with bio-based epoxy resins entirely prepared from WVO and cyclic anhydrides in the presence of two different catalytic systems. The comparison of these formulations with analogous networks produced with neat vegetable oil revealed that both resins produced thermosets with similar thermal stability and chemical resistance. Differences in mechanical performance were observed due to the degree of functionality of EPVO resins in comparison with EPVO equivalents. Nevertheless, the statistical analysis identified and classified the most critical parameters with regards to the $T_g$ of the polymer, demonstrating that the anhydride molar ratio can mitigate the reductions caused by WVO. The inspection of other parameters revealed that the use of 2-MI as catalyst resulted in polymers with increased $T_g$ and higher crosslink density. Furthermore, increased anhydride/epoxy molar ratio produced thermosets with superior storage modulus, but reduced thermal stability. Attempts of producing a new class of resins based on sucrose ester were unsuccessful, hence EVO-based systems were used to carry out the next steps.

In conclusion, optimisation studies presented in this chapter overcame the limited reactivity of WVO-based resins and opened space for the application of this new class of bio-based epoxy resins to fabricate composites. The next chapters of this thesis are concentrated on the creation of a library of materials with the guidelines created in this chapter in mind, inspecting the best opportunities to incorporate WVO-based resins in real-life systems and explore the potential benefits brought by this strategy.

## 5.5 References

1 R. Auvergne, S. Caillol, G. David, B. Boutevin and J. Pascault, *Chem. Rev.*, 2014, **114**, 1082–1115.

2 A. E. Gerbase, C. L. Petzhold and A. P. O. Costa, *J. Am. Oil Chem. Soc.*, 2002, **79**, 797–802.

3 R. Wang, Missouri University of Science & Technology, 2014.

4 F. C. Fernandes, D. Lehane, K. Kirwan and S. R. Coles, *Eur. Polym. J.*, 2017, **89**, 449–460.

5 J. Berger and F. Lohse, *J. Appl. Polym. Sci.*, 1985, **30**, 531–546.

6 S. J. Park, F. L. Jin, J. R. Lee and J. S. Shin, *Eur. Polym. J.*, 2005, **41**, 231–237.

7 J. Rosch and R. Mulhaupt, *Polym. Bull.*, 1993, **686**, 679–685.

8 G. Liang and K. Chandrashekhara, *J. Appl. Polym. Sci.*, 2006, **102**, 3168–3180.

9 C. Ding and A. S. Matharu, *ACS Sustain. Chem. Eng.*, 2014, **2**, 2217–2236.

10 W. S. Port, L. L. Gelb and W. C. Ault, *US Pat. 2975149*.

11 J. M. España, L. Sánchez-Nacher, T. Boronat, V. Fombuena and R. Balart, *J. Am. Oil Chem. Soc.*, 2012, **89**, 2067–2075.

12 D. D. S. Martini, B. A. Braga and D. Samios, *Polymer (Guildf).*, 2009, **50**, 2919–2925.

13 A. Maiorana, L. Yue, Manas-Zloczower and R. Gross, *J. Appl. Polym. Sci.*, , DOI:10.1002/app.44212.

14 T. S. Omonov and J. M. Curtis, *J. Appl. Polym. Sci.*, 2014, **131**, 40142–40151.

15 A. P. Gupta, S. Ahmad and A. Dev, *Polym. Plast. Technol. Eng.*, 2010, **49**, 657–661.

16 A. J. Clark, A. H. Ross and S. A. F. Bon, *J. Polym. Environ.*, 2017, **25**, 1–10.

17 M. D. Samper, V. Fombuena, T. Boronat, D. García-Sanoguera and R. Balart, *J. Am. Oil Chem. Soc.*, 2012, **89**, 1521–1528.

18 M. Pawar, A. Kadam, O. Yemul, V. Thamke and K. Kodam, *Ind. Crops Prod.*, 2016, **89**, 434–447.

19 R. A. Sheldon, *Chem. Ind.*, 1992, **23**, 903–906.

20 R. A. Sheldon, *Green Chem.*, 2007, **9**, 1273–1283.

21 F. Piccinno, R. Hischier, S. Seeger and C. Som, *ACS Sustain. Chem. Eng.*, 2015, **3**, 1047–1055.

22 D. C. Montgomery, *Design and Analysis of Experiments*, John Wiley & Sons Inc, Singapore, Seventh., 2009.

23 A. Paramarta and D. C. Webster, *React. Funct. Polym.*, 2016, **105**, 140–149.

24 H. Sasaki, *Prog. Org. Coatings*, 2007, **58**, 227–230.

25 L. H. Sperllng, J. A. Manson, S. Qureshl and A. M. Fernandez, *Ind. Eng. Chem. Prod. Res. Dev.*, 1981, 163–166.

26 M. Flores, X. Fernández-Francos, X. Ramis and A. Serra, *Thermochim. Acta*, 2012, **544**, 17–26.

27 T. Yang, C. Zhang, J. Zhang and J. Cheng, *Thermochim. Acta*, 2014, **577**, 11–16.

28 Z. Zhang, T. Yamashita and C. P. Wong, *Macromol. Chem. Phys.*, 2005, **206**, 869–877.

29 J. Lange, N. Altmann, C. T. Kelly and P. J. Halley, *Polymer (Guildf).*, 2000, **41**, 5949–5955.

30 Y. Li, J. Gao, G. Liu and R. Zhang, *Int. J. Polym. Mater.*, 2001, **49**, 441–455.

31 N. W. Manthey, F. Cardona and T. Aravinthan, *J. Appl. Polym. Sci.*, 2012, **125**, E511–E517.

32 L. Zhao and X. Hu, *Polymer (Guildf).*, 2010, **51**, 3814–3820.

33 G. Francucci, F. Cardona and N. W. Manthey, *J. Appl. Polym. Sci.*, 2013, **5**, 2030–2037.

34 J. L. Hong, C. K. Wang and R. H. Lin, *J. Appl. Polym. Sci.*, 1994, **53**, 105–112.

35 N. Supanchaiyamat, P. S. Shuttleworth, A. J. Hunt, J. H. Clark and A. S. Matharu, *Green Chem.*, 2012, **14**, 1759.

36 S. Montserrat and J. Malek, *Thermochim. Acta*, 1993, **228**, 47–60.

37 P. I. Karkanas, I. K. Partridge and D. Attwood, *Polym. Int.*, 1996, **41**, 183–191.

38 S. Montserrat, *J. Polym. Sci. Part B Polym. Phys.*, 1994, **32**, 509–522.

39 M. L. Costa and M. C. Rezende, *Polímeros Ciência e Tecnol.*, 1999, **12**, 37–44.

40 J. Ampudia, E. Larrauri, E. M. Gil, M. Rodríguez and L. M. Léon, *J. Appl. Polym. Sci.*, 1998, **71**, 1239–1245.

41 N. Boquillon and C. Fringant, *Polymer (Guildf).*, 2000, **41**, 8603–8613.

42 M. Li, Y. Wan, Z. Gao, G. Xiong, X. Wang, C. Wan and H. Luo, *Mater. Des.*, 2013, **51**, 257–261.

43 S. G. Tan, Z. Ahmad and W. S. Chow, *Ind. Crops Prod.*, 2013, **43**, 378–385.

44 Y. Hase, C. U. Davanzo, K. Kawai and O. Sala, *J. Mol. Struct.*, 1976, **30**, 37–44.

45 A. Streitwieser Jr and C. H. Heathcok, *Introduction to Organic Chemistry*, Macmillan Publishing, New York, United States of America, Third Edit., 1985.

46 C. S. M. F. Costa, A. C. Fonseca, A. C. Serra, J. F. J. Coelho, A. C. Fonseca, A. C. Serra and J. F. J. C. Dynamic, *Polym. Rev.*, 2016, **56**, 362–383.

47 J. Chen, A. J. Kinloch, S. Sprenger and A. C. Taylor, *Polym. (United Kingdom)*, 2013, **54**, 4276–4289.

48 R. P. Chartoff, J. D. Menczel and S. H. Dillman, in *Thermal Analysis Of Polymers: Fundamentals And Applications*, John Wiley & Sons Inc, 2009, pp. 387–490.

49 K. P. Menard, *Dynamic Mechanical Analysis*, CRC Press, Boca Raton, United States of America, Second., 2008.

50 J. R. Kim and S. Sharma, *Ind. Crops Prod.*, 2012, **36**, 485–499.

51 R. A. Pethrick, *Polymer Structure Characterization*, RSC Publishing, Cambridge, United Kingdom, Second., 2014.

52 A. Campanella, J. J. La Scala and R. P. Wool, *Polym. Eng. Sci.*, 2009, **49**, 2384–2392.

53 N. Karak, *Vegetable oil-based polymers.*, Woodhead Publishing, Cambridge, United Kingdom, 2012.

54 F. Jin and S. Park, *Polym. Int.*, 2008, **57**, 577–583.

55 A. Kadam, M. Pawar, O. Yemul, V. Thamke and K. Kodam, *Polymer (Guildf).*, 2015, **72**, 82–92.

56 S. G. Tan and W. S. Chow, *J. Am. Oil Chem. Soc.*, 2010, **88**, 915–923.

57 G. Das and N. Karak, *Prog. Org. Coatings*, 2009, **66**, 59–64.

58 P. Narute, G. R. Rao, S. Misra and A. Palanisamy, *Prog. Org. Coatings*, 2015, **88**, 316–324.

59 V. K. Chidara, S. Stadem, D. C. Webster and G. Du, *Catal. Commun.*, 2018, **111**, 31–35.

60 L. M. Breyer and C. E. Walker, *J. Food Sci.*, 1983, **48**, 955-.

61 M. M. Pierce and C. E. Walker, *Cereal Chem.*, 1987, 64, 222–225.

62 A. Z. Yu, J. M. Sahouani, R. A. Setien and D. C. Webster, *React. Funct. Polym.*, 2018, **128**, 29–39.

63 X. Pan, P. Sengupta and D. C. Webster, *Biomacromolecules*, 2011, **12**, 2416–2428.

64 X. Pan, P. Sengupta and D. C. Webster, *Green Chem.*, 2011, **13**, 965–975.

65 1959.

66 P. S. Deshpande, T. D. Deshpande, R. D. Kulkarni and P. P. Mahulikar, *Ind. Eng. Chem. Res.*, 2013, **52**, 15024–15033.

67 Y. Wang, S. Ou, P. Liu, F. Xue and S. Tang, *J. Mol. Catal. A Chem.*, 2006, **252**, 107–112.

68 K. Ren and B. P. Lamsal, *Food Chem.*, 2017, **214**, 556–563.

69 M. Ferrer, J. Soliveri, F. J. Plou, N. López-Cortés, D. Reyes-Duarte, M. Christensen, J. L. Copa-Patiño and A. Ballesteros, *Enzyme Microb. Technol.*, 2005, **36**, 391–398.

# Chapter 6

# Creating Sustainable Alternatives for Composites:

## Manufacturing WVO-based Composites Reinforced with Glass and Flax Fibres

## 6.1 Introduction

In the current study, we report the first production of composites laminates using WVO-derived matrices based on the refinements presented in the previous chapter. To create a library of composite formulations and identify the best opportunities in the area, both glass and flax fibres are examined at this stage of the study. This strategy permitted the investigation of reinforcing agents with different natures, targeting both renewable and traditional fibres.

In this regard, natural fibre reinforced composites (NFRC) have been receiving attention in industry and academia in the recent decades as environmentally-friendly and renewable alternatives for traditional materials produced with glass fibres (GFRC).[1] More specifically, vegetable fibres have been rediscovered as reinforcing agents due to advantageous properties such as reduced density, competitive price, biodegradability, and lower environmental burdens throughout the whole life cycle.[2–4] Consequently, vegetable fibres have successfully demonstrated their applicability in a number of industrial, ranging from the automotive sector (both in interior and exterior applications), construction, furniture, to design and packaging industry.[5–7]

Nevertheless, increasing environmental concerns, restrictive legislation and awareness about the toxicity of the products and methods have driven stakeholders to seek further sustainable alternatives to the composite industry.[8–12] After all, the utilisation of petroleum-derived resins for the production of composites laminates partially hinders the benign impact of natural fibre reinforced composites (NFRC) as green engineering materials.[13] In addition, the long-term viability of petrochemical platforms for composite manufacture is financially and ecologically unsustainable given these materials are finite and is prone to disruption in prices due to political and economic factors.[14] In this regard, literature has been slowly moving away from resins such as DGEBA for the production of laminates, and have advanced towards the production of thermoset matrices from environmentally-friendly resins as a strategy to manufacture sustainable composites.[15–17] That is exactly the gap that this thesis aims to tackle.

In this this scenario, vegetable oils have been considered a key platform for the polymer industry due to features such as price, availability, safety and chemical versatility.[18,19] Vegetable oil-based resins have successfully demonstrated their applicability for the preparation of biocomposites reinforced with a range of plant fibres such as hemp[20,21], kenaf, switchgrass,[22] oat hull,[23] rice husk ash[24], wheat straw and recycled paper.[25] These approaches manufactured composites marrying competitive mechanical properties and remarkable bio-based content. Most importantly, these materials delivered unique engineering properties in comparison to traditional resins such as such as biodegradability and improved impact performance, adding commercial value to the final components.[26,27] Moreover, the application

of the WVO-derived systems developed through this thesis appeared as an opportunity to drive the sustainability aspect even further.

In this chapter, flax (*Linum usitatissimum)* was explored as a reinforcement due to its commercial relevance and elevated mechanical properties as a consequence of its cellulose content and microstructural arrangement (Figure 6.1).[28] Flax is one of the most widely used natural fibres in industry, and its technical exploration as crude, spun, and woven textiles dates back to 5000 BC.[29] Long fibres have been commonly used for household textiles, short fibres explored to produce heavy yarns (used in tents, sails, and canvas, *etc*.) and lower grade fibres used in composite application. In this regard, a number of studies have recently demonstrated the use of flax fibres to reinforce systems with vegetable-oil based resins.[25,30] Grishchuk *et al.* have prepared composites combining flax fibres (nonwoven mats, twill weave, and quasi-unidirectional textile fabrics) and ELO-based matrix by compression moulding.[31] The authors reported that the mechanical properties could be controlled by the selection of the anhydride hardener.

Figure 6.1: Representation of the woven flax fibre mat utilised as reinforcement for the manufacture of biocomposites.

These matrices were compared to analogues produced from neat vegetable oil to investigate effects of the use-phase in the resulting networks and to DGEBA for benchmarking. The study also investigated the use of different molar ratios of hardener in the systems to find the best balance between the final properties of the thermoset and the renewable content. Chemical modification steps were implemented to NFRC to improve fibre/matrix adhesion given that this is one of the main challenges in the area. Also, the exploration of GFRC in this chapter permitted assessing the performance of the NFRC against

a commercial benchmark whilst also identifying the applicability of the WVO-based systems in this area.

## 6.2 Methodology

### 6.2.1 Materials

Bio-based epoxy resins were synthesised from purified waste vegetable oil (epoxidized purified vegetable oil – EPVO) and neat vegetable oil (epoxidized neat vegetable oil – ENVO) according to the methodologies developed in previous chapters.[32] Similarly, DGEBA used as internal benchmark was the same explored in previously (SuperSap® CLR, Entropy Resins, USA). Stearic acid, ethanol, and NaOH were supplied by VWR International. Flax fibres (Biotex Flax Fiber 2/2 Twill 200 GSM), glass fibres (Woven Glass 2/2 Twill 280 GSM) and consumables for vacuum bagging and wet lay-up were supplied by Easy Composites Ltd, UK.

### 6.2.2 Flax Fibre Modification

For the mercerization, flax fibres (40 × 40 $cm^2$ plies) were immersed in NaOH solution (4 wt%) and stirred for 1 h at room temperature, as previously optimised by Jacob *et al.*.[33] After this time, fibres were carefully washed with distilled water to remove the excess of NaOH and oven dried (ThermoScientific Heraterm, 95 °C for 6 h). Fibres obtained from this methodology were denominated NFF. The treatment with stearic acid followed the procedure described by Kalaprasad *et al.*, where flax fibres (40 × 40 $cm^2$ plies) were submerged in a 3 wt% stearic acid solution in ethanol and continuously stirred at 70 °C for 1 h.[34] After the treatment, fibres were oven dried (ThermoScientific Heraterm, 95 °C for 6 h). Fibres obtained through this methodology were denominated SFF.

### 6.2.3 Composite Manufacturing

After a brief study exploring different processing techniques, it was decided to use the wet lay-up process to manufacture the composites. In this methodology, glass and flax fibres were cut into 40×40 $cm^2$ squares from the roll of material, and oven dried (ThermoScientific Heraterm) at 95 °C for 4 h prior to the lamination. To obtain panels of suitable thickness for the mechanical tests, two sheets of flax fibres and four sheets of glass fibres were used in the composite manufacturing whilst keeping the same fibre volume fraction (30 vol%). Conversions between vol% and wt% were performed considering the following densities: $\rho_{Flax}$ = 1.5 g $cm^{-3}$, $\rho_{Glass}$ = 2.5 g $cm^{-3}$ and $\rho_{Matrix}$ = 1.1 g $cm^{-3}$.

The thermoset resin was formulated according to the procedure described in the section 5.2.4, using MHHPA as hardener and 2-MI as catalyst. Systems with EPVO, ENVO and DGEBA were investigated in this study. Part of the resulting blend was applied to a PTFE-covered steel plate tape with a brush, covering an area of approximately 40 ×40 $cm^2$. In sequence, one layer of reinforcing fibre was applied, and then resin was spread through the reinforcing layer with a roller. More resin was applied on the top of the fibre layer with a brush, and the process was repeated by intercalating equally divided layers of resin and reinforcing fibre until reaching the selected number of layers. Once the stacking was completed, the steel plate was placed in the programmable oven for the curing process. The thermoset resins were cured according to the following regime: 50 ° C to 140 °C at 1.5 °C $min^{-1}$; 10 h of isotherm at 140 °C; and from 140 °C to 50 °C at -1.5 °C $min^{-1}$. The resulting panels were post-cured in the same oven according to the following curing regime: from 50 °C to 160 °C at 1.5 °C $min^{-1}$, 2h isotherm at 160 °C; and 160 °C to 50 °C at -1.5 °C $min^{-1}$.

### 6.2.4 Characterisation of the Materials

Characterisation of the bio-based epoxy resin materials was performed by Infrared spectra (ATR-FTIR), $^1$H Nuclear Magnetic Resonance ($^1$H NMR), and thermogravimetric analysis (TGA) according to the methodologies described in Chapter 4. Dynamic Mechanical Analysis (DMA) was conducted in dual cantilever configuration, oscillating frequency of 1.0 Hz, displacement of 0.05 mm , from -100 to 120 °C and heating rate of 2 °C $min^{-1}$. Samples were cut with nominal dimensions of 1.5 x 5 x 24 $mm^3$. The glass transition temperature ($T_g$) was defined from the maximum of the peak of tanδ in curves of tanδ versus temperature.

For the tensile tests, composite panels were dimensioned according to ASTM D3039/D3039M. Tests were performed using an Instron Machine with 30 kN Static Load Cell, with extensometer (80 mm), at a test speed of 2 mm $min^{-1}$. A minimum of seven specimens was successfully tested for each formulation. Charpy impact test was performed according to ASTM D4812-1, with a pendulum adjusted for a flatwise impact of 7.5 J (Ray Ran Pendulum Impact Tester). A minimum of seven samples of nominal size 3 x 25 x 100 $mm^3$ (unnotched) were tested for each formulation. To obtain Scanning Electron Microscopy images (SEM, Hitachi TM3030Plus), untested impact test samples were cryo-fractured after immersion in liquid $N_2$ for 10 min and dimensioned according to sample holder size. Prior to the analysis, the surface of the samples was metallized for best results. Images were obtained using a secondary electron (SE) beam with an acceleration voltage of 15 kV.

The hygrothermal ageing test was performed according to the ASTM D570-99 standard. Three samples of each of the formulations were dimensioned to a nominal size of 2.5 x 25 x 75 $mm^3$ and conditioned in an oven (ThermoScientific Heraterm) at 50 °C for 24 h

prior to the test. Dried samples were measured with a digital callipers and submerged in a bath at 23 ± 1 °C. Weight variation was monitored every 48 h. Before weighing, the surface of each sample was dried with a tissue paper to remove the water excess. Weight changes were continuously recorded until they presented three consecutive measurements without significant variation. Density was measured by the Archimedes principle, Equation 6.1. In this expression, ρ is the density of the material, $M_{EtOH}$ is its mass in ethanol and $M_{Air}$ is its mass in the air as a medium. A Metter Toledo scale equipped with density kit was used to measure this property. Density was calculated in ethanol at 21.0 °C, and average values were calculated from three specimens. Ethanol was selected as a medium due to its low density in comparison with water, permitting specimens produced with flax fibres to submerge fully.

Equation 6.1 $$\rho = \frac{M_{EtOH}}{M_{Air} - M_{EtOH}}$$

## 6.3 Results

### 6.3.1 General Considerations

Biocomposites were prepared with purified waste vegetable oil (EPVO) and analogous resin produced from virgin vegetable oil (ENVO), allowing a direct investigation of impact of the oil use phase in the resulting properties. In terms of the reinforcing agents, flax fibres were explored as a strategy to maximize the renewable content of the composite. Also, similar composites were produced using glass fibres as reinforcement due to their commercial relevance of this agent and to benchmark this material against alternatives available in the composite sector. Table 6.1 summarizes the formulations investigated in the first stage of the study and the coding adopted for each of them.

Table 6.1: Summary of the composite formulations prepared in the study according to the origin of the epoxy resin, molar ratio of curing agent and reinforcing fibre.

| Formulation | Epoxy Resin | Molar Ratio (Anhydride: Epoxy) | Reinforcing Fibre |
|---|---|---|---|
| **10 Neat FF** | ENVO | 1.0:1.0 | Virgin Flax |
| **14 Neat FF** | ENVO | 1.4:1.0 | Virgin Flax |
| **10 Purif FF** | EPVO | 1.0:1.0 | Virgin Flax |
| **14 Purif FF** | EPVO | 1.4:1.0 | Virgin Flax |
| **DGEBA FF** | DGEBA | * | Virgin Flax |
| **10 Neat GF** | ENVO | 1.0:1.0 | Glass |
| **14 Neat GF** | ENVO | 1.4:1.0 | Glass |
| **10 Purif GF** | EPVO | 1.0:1.0 | Glass |
| **14 Purif GF** | EPVO | 1.4:1.0 | Glass |
| **DGEBA GF** | DGEBA | * | Glass |

*: Molar mass of the curing agent not reported by the manufacturer. Mass ratio between epoxy and curing agent is 100:47.

Initial investigations focused on finding the most suitable processing technique to produce the laminates. The first methodology explored was vacuum bagging, which exploits the use of negative pressure generated by a vacuum pump to improve the resin consolidation. This enhanced resin infusion can potentially lead to panels with less voids and bubbles. Also, since it creates a closed system, it decreases concerns about the emission of volatiles to users. The negative pressure also compresses the vacuum film against the fibres, resulting in a better surface finishing when compared to wet lay-up. Figure 6.2 presents a schematic representation of the performance of this methodology to produce composites.

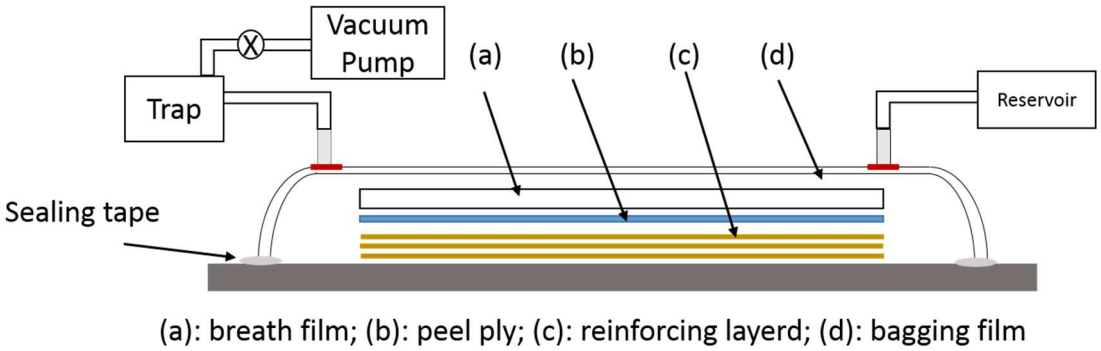


Figure 6.2: Schematic representation of the vacuum bagging technique.

Although vacuum bagging has been proven to be a highly effective methodology to produce composites with DGEBA resin, it was challenges to use the same methodology with when the bio-derived resins. For instance, the network formation promoted by anhydrides required high temperatures (> 140 °C), which was a problem since the peel ply film softened during the cure due to the temperature (even though the manufacturer indicated this temperature was within the application range). Consequently, the resin infused through the peel plies, which in turn contaminated the formulation and the cross-linked material, producing a low-quality laminate. Although the low viscosity observed for the bio-based resin was a desirable aspect to promote an efficient infusion, this feature proved to be another challenge since it migrated (and partially cure) into the breath film and tubes. This was a serious concern since the resin can potentially damage other parts connected to the system, such as the vacuum pump. Therefore, the vacuum bagging led to composites with dry fibres and with high void content. As a result, the vacuum bagging technique was abandoned at this point, and alternative methodologies were explored.

Since problems in the processing stage were linked with elements of the vacuum bagging, subsequent studies were conducted exploring the wet lay-up lamination. Although this technique has a limited capacity of resin impregnation and compromised surface finishing, the wet lay-up process is hugely economically advantageous and versatile, being one of the

most commonly used techniques in the industry. In this approach, the resin is applied manually through the plies of the reinforcing agent with a brush and a roll. Therefore, inherent features observed for systems investigated in this studied such as low viscosity and the use of non-toxic volatile compounds (*i.e.* does not contain styrene) enabled the exploitation of manual lamination from the practical and safety point of view. A simplified scheme of the operation of this methodology can be found in Figure 6.3.

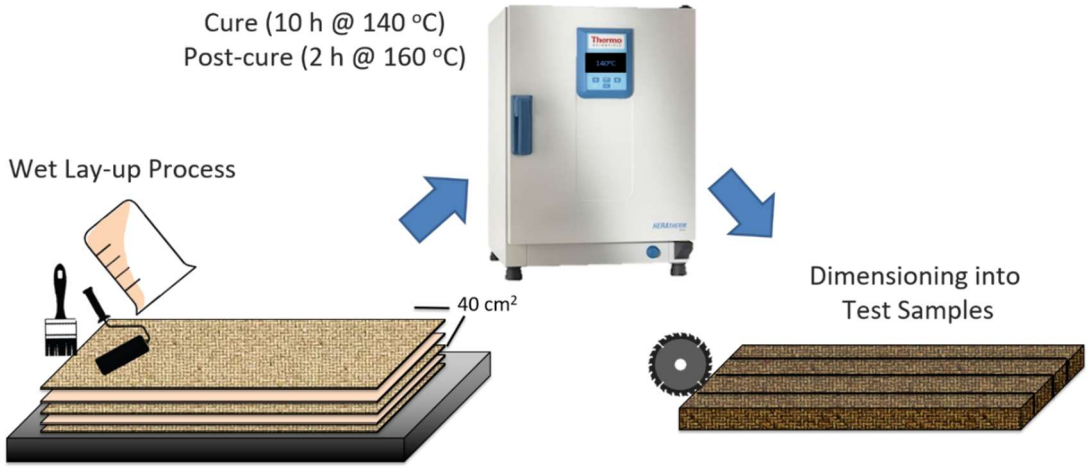


Figure 6.3: Scheme of composites manufacturing by wet lay-up process, curing and dimensioning of the panels.

Model composites were prepared using a matrix an equimolar molar ratio of MHHPA and ENVO reinforced with both flax and glass fibres at different volume ratios (20, 30 and 40 vol%). At this stage, small-scale panels (10 × 10 $cm^2$) were prepared to investigate the feasibility (and limitations) of the technique (*i.e.* wetting efficiency) and to maximise the fibre content. Despite the successful production of panels with 20 and 30 vol% of fibres, composites with volumetric fractions above 30% presented extensive presence of voids and poorly wetted fibres, particularly in flax fibre reinforced composites.

These voids can be seen as artefacts that ultimately weaken the material, consequently resulting in less reliable results.[35] Therefore, the following studies focused on the production of composites with a maximum reinforcement content of 30 vol% in both series (glass and flax), ensuring greater consistency. The following sections address the characterization of fibres and composites produced with EPVO and ENVO resins. Thermal, mechanical and physical properties were benchmarked against panels produced with commercial resin based on DGEBA and reinforced with both glass and flax fibres.

### 6.3.2 Fibre Characterisation

The compatibilization between the hydrophilic nature of vegetable fibres and the hydrophobicity of commonly applied polymeric matrices is a well-known challenge in the field of NRFC.[6] As presented in Chapter 3, literature offers a number of different methodologies that allow the modification of the surface of vegetal fibres both through chemical and physical processes.[36] Therefore, flax fibres was used in natural form and also after chemical treatments to produce composites with enhanced fibre/matrix interaction. Based on the literature review, the mercerization and the treatment with stearic acid were selected to modify flax fibres. In summary, the mercerization technique extracts lignin and hemicellulose from the fibres, increasing the relative content of cellulose while also causing fibrillation and increasing the fibre aspect ratio.[36,37] On the other hand, the treatment with stearic acid functionalises the surface by esterifying the cellulose units, reducing the concentration of hydroxyls in the surface and simultaneously attaching long aliphatic chains ($C_{17}$) to the fibre.[38] Both methods are discussed in more depth in Chapter 3.

Modified fibres had their chemical characteristics investigated by ATR-FTIR. Spectra of samples before the after the chemical treatment (Figure 6.4) revealed a decrease in signals at 1730 $cm^{-1}$ and 1450 $cm^{-1}$, evidencing partial removal of hemicellulose and lignin, respectively.[39] Interestingly, the region between 3300 and 3500 $cm^{-1}$ (ν O-H of cellulose) does not show any significant changes with respect to its shape. This observation indicated that there are no significant transformations in the inter- and intramolecular arrangement between the cellulose chains despite the decrease in the levels of hemicellulose and lignin. Such an effect has been previously observed and discussed by Barreto *et al.*.[40] In addition, the signal present at 1703 $cm^{-1}$ (ν C=O stearic acid) was exclusively observed in the SFF samples. Table 6.2 presents a detailed assignment of the main absorption peaks before and after the alkaline treatments.

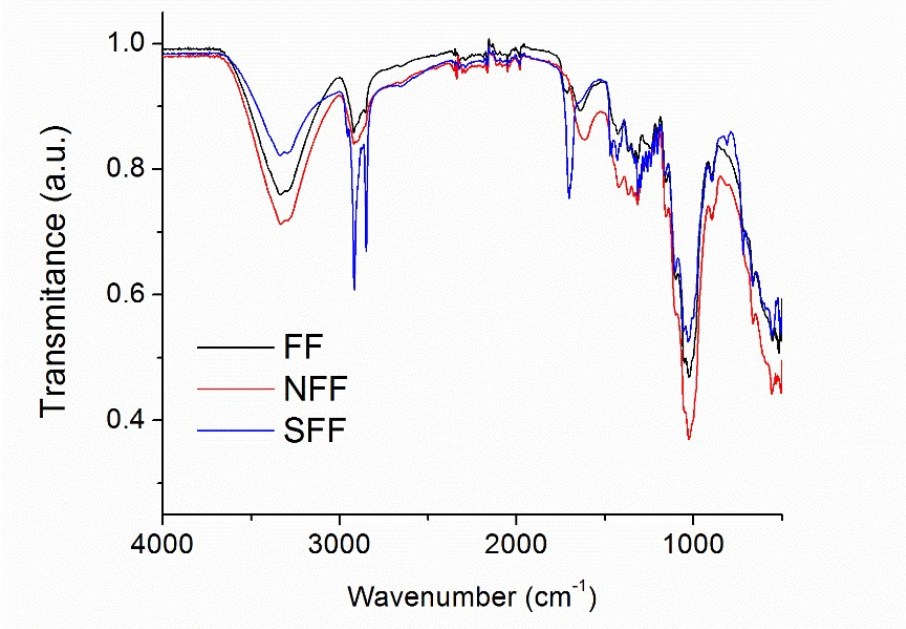


Figure 6.4: ATR-FTIR spectra of the flax fibre before (FF) and after the alkaline (NFF) and stearic acid (SFF) treatments, from 4000 to 500 $cm^{-1}$.

Table 6.2: Wavenumber and assignment of the main bands in the infrared spectrum of flax fibre (FF), alkaline treated flax fibres (NFF) and stearic acid treated fibres (SFF)

| **Wavenumber ($cm^{-1}$)** | **Assignment** |
|---|---|
| 3600 - 3100 | ν O-H |
| 3000 - 2800 | ν C-$H_n$ |
| 1740 – 1700 | ν C=O (Hemicellulose e cellulose) |
| 1703 | ν C=O (stearic acid) |
| 1650 – 1600 | ν C=C (Lignin units) |
| 1436 | σ CH |
| 1468 | O-CH |
| 1230 | ν C-O-C |
| 1207 | ν C-O |
| 1168, 1048 | ν C-O-C |
| 1011-1040 | ν C-O-C |

Changes in the fibres' surface and morphology were monitored through scanning electron microscopy (SEM) images. The topological and microstructural arrangements of the flax fibres were dramatically altered by both treatments (Figure 6.5). Surfaces became more irregular after the chemical modification, with increased roughness and the presence of grooves that can act as a point of physical interaction with the matrix.[41] Additionally, medium

and high magnification images revealed the effect of fibrillation characterized by the opening of the fibre bundles. This phenomenon is responsible for altering the aspect ratio of the fibres and contributed to increasing the surface area.

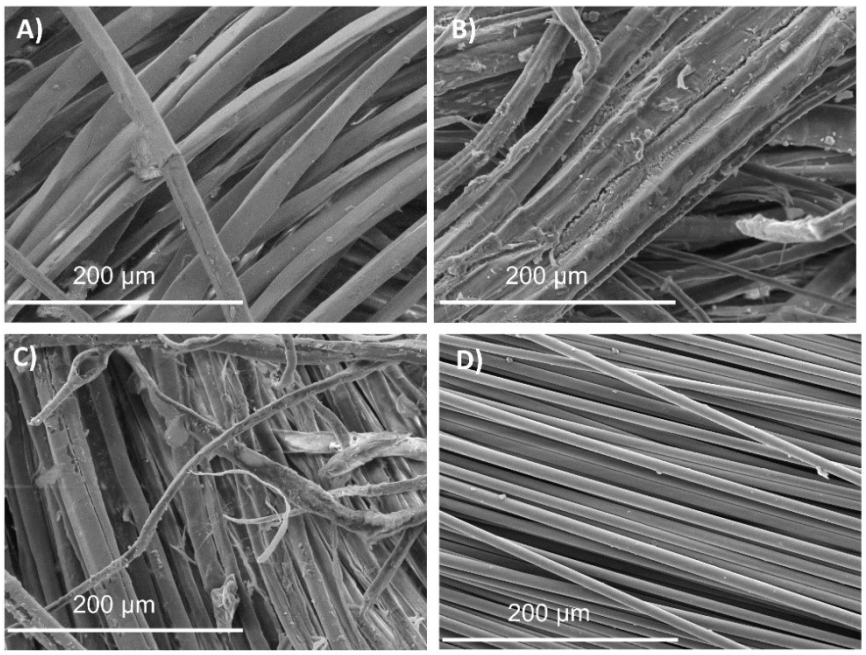


Figure 6.5: SEM images of A) flax fibres (FF), B) NaOH-treat flax fibres (NFF), C) stearic acid-treated fibres (SFF) and D) glass fibres (GF), magnification of 500x.

The topology of SFF fibres also indicated the accumulation of stearic acid so that fibres were also physically covered by a thin layer of the fatty acid in some locations. Based on these images, the thickness of the SFF layer was estimated at approximately 0.4 µm. For comparison, micrographs of glass fibres were also included in Figure 6.5. A comparison revealed differences between the natural and synthetic fibres: glass fibres presented a much more uniform distribution of diameters and surface finishing, while flax fibres have inherent variability as a natural product.

To ensure the curing temperature would not thermally degrade the natural fibres, TGA was performed to determine their thermal stability. Lignocellulosic fibres are known for thermally degrading through a series weight-loss events. The first stage commonly detected is the loss of moisture, occurring around 100 °C. The hydrophilicity observed in these fibres is a consequence of cellulose's polar nature, which absorbs the ambient humidity. Therefore, vegetable fibres generally present a natural water content between 5 and 10 wt%.[42] The following step is the cellulose decomposition, starting between 210 and 260 °C and taking place until up to 450 °C. Chemically speaking, this process can be interpreted as a sequence of dehydration reactions followed by endothermic depolymerization.[43]

Hemicellulose, the fibres' second most abundant component, thermally decomposes at a maximum temperature of 290 °C through a mechanism like the one observed for cellulose. Finally, lignin degradation takes place in an extensive range of temperatures, from 280 up to 520 °C. This slow and broad thermal degradation event is linked to lignin's heterogeneous chemical structure, which presents a wide range of phenolic moieties with different molecular weights. Also, products formed during the thermal degradation of both cellulose and hemicellulose usually are entirely charred and volatilized during TGA while lignin leaves non-volatile residues. These components accumulate as char and can be detected by the presence of mass at the end of the analysis (600 °C).

Figure 6.6 shows the thermogravimetric curves of flax fibres, from 25 to 600 °C, and the first derivative of weight-loss percentage with respect to temperature. The curve obtained for the virgin flax fibres illustrated the initial event associated with loss of moisture at approximately 100 °C, followed by the main weight loss event that present $T_{Onset}$ at 355 °C assigned to cellulose degradation. Since thermal degradation of cellulose and hemicellulose took place at similar temperatures, events have overlapped, and a single response was observed in this region. Furthermore, this thermal degradation step was accentuated in comparison to any of the other weight-loss events, as evidenced by the first derivative curve. This observation could be related to the high content of cellulose present in flax fibres when compared to other lignocellulosic fibres.[44] Also, the degradation of lignin was evidenced by the presence of an inflection point in the first derivative curve at approximately 400 °C. In TGA, changes in the rate in which a material degrades can illustrate alterations in the degradation mechanism.

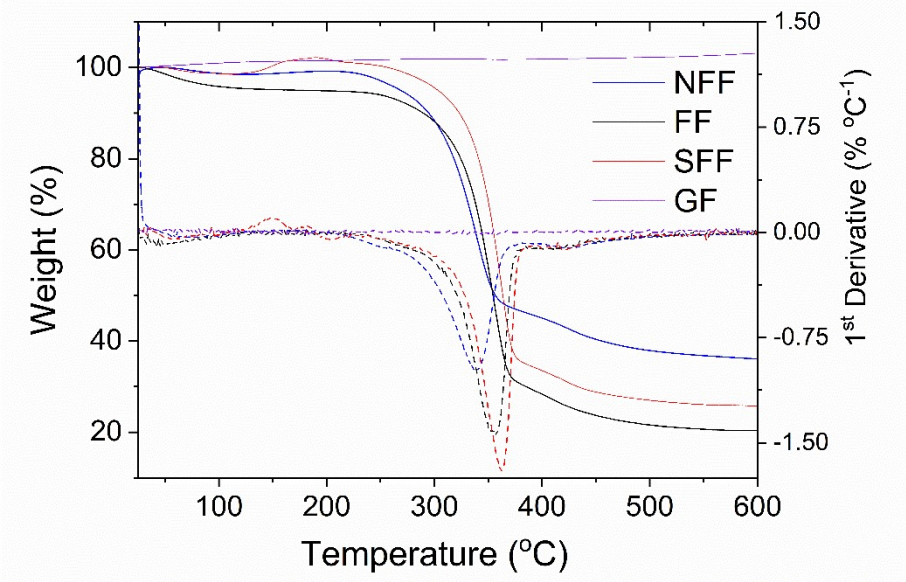


Figure 6.6: Thermograms (full line) and first mass loss derivative with respect to temperature (dashed line) of reinforcing fibres, from 25 °C to 600 °C, under $N_2$ atmosphere.

Figure 6.6 also demonstrated that NFF fibres were less thermally stable in comparison to virgin fibres ($T_{Onset}$ of 297.2 and 323.2 °C, respectively). As NFF fibres became proportionately richer in cellulose, the other components lose the ability to protect the polysaccharide chains from thermal degradation.[45] It should be noted, however, that other studies also have illustrated that the thermal stability of some fibres can also be increased by the alkaline treatment process due to the removal of less stable fractions.[46] This demonstrated the mercerization methodology could lead to different results depending on the combination of temperature and time that the fibres are exposed to the alkali medium.[47]

Conversely, SFF presented increased thermal stability ($T_{Onset}$ = 336.1 °C) in comparison to virgin flax due to the addition of stearic acid to the structure. Therefore, this fatty acid created a barrier effect that prevented the thermal degradation of the cellulosic units.[48] Values of $T_{Max}$ followed the same behaviour observed for $T_{Onset,}$ with 357.7 °C for the unmodified flax, 339.3 °C for NFF and 372.1°C for SFF, Table 6.3. The thermogravimetric curve obtained for glass fibres demonstrated the superior thermal stability of this material in comparison to all natural fibres, with no degradation being observed in this temperature range. The remarkable thermal resistance behaviour is a consequence of the stability of the $SiO_2$ and $Al_2O_3$ bonds formed during the spinning process of this material.[49] In conclusion, the thermogravimetric analysis have demonstrated that these fibres can be safely exposed to the cure conditions without any thermal damage since $T_{Onset}$ is above the processing temperature.

Table 6.3: Initial temperature of degradation ($T_{Onset}$) and maximum degradation ($T_{Max}$) temperatures of the chemically modified flax fibre (NFF) compared to virgin fibre (FF).

| **Formulation** | $T_{Onset}$ **(°C)** | $T_{Max}$ **(°C)** |
|---|---|---|
| FF | 323.2 | 357.7 |
| NFF | 297.2 | 339.3 |
| SFF | 336.1 | 372.1 |
| GF | Do not degrade | Do not degrade |

### 6.3.3 Mechanical Performance: Tensile and Impact Properties of Composites

#### a) Composites Reinforced with Glass Fibres

Test specimens sized according to ASTM D3039 had their mechanical properties characterized by tensile tests. In this type of mechanical test, the material suffers from a uniformly applied stress in a single direction, and the response to this perturbation is the spatial deformation. During the tensile test of composites, both the matrix and the reinforcing agent are subjected to the perturbation caused by the mechanical stress. However, composites are designed using fibres with high elastic modulus (ideally superior to that observed for the

polymer matrix) so that the mechanical stress can be transferred from the polymer matrix to the fibre. As a result, a material with better mechanical performance, resistance to flow and rupture is obtained.[50] Representative stress-strain curves obtained for each formulation are shown in Figure 6.7, illustrating the difference between the biocomposites (full coloured lines) and reference materials (dashed line).

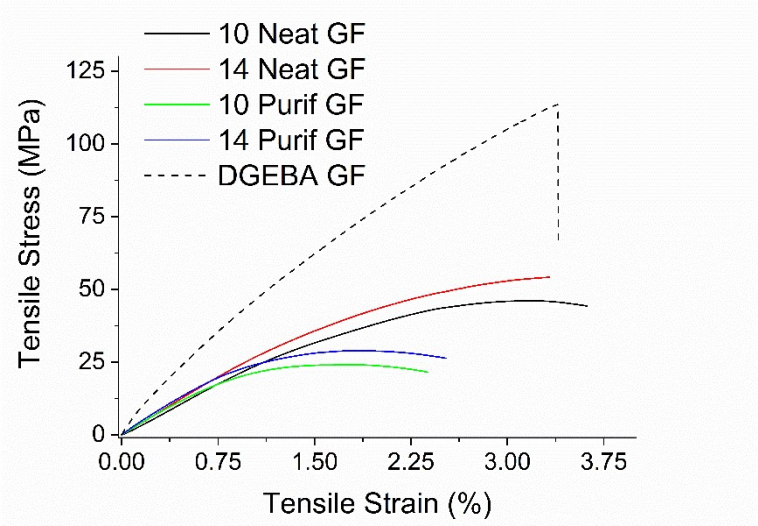


Figure 6.7: Representative stress-strain curves of the composites with glass fibres.

Table 6.4 presents average values observed for Young's tensile moduli and tensile strength of each composite formulation. GFRC materials prepared with WVO-based epoxy and anhydride-rich matrix (*14 Purif GF*) exhibited tensile modulus (7.6 ± 2.1 GPa), which was statistically equivalent to those observed for the reference formulation produced virgin oil (7.8 ± 1.1 GPa) and the commercial benchmark with DGEBA (8.3 ± 0.3 GPa). These results demonstrated the capacity of production of alternative materials with highly elastic character that emulated the benchmark material even though it comes from waste sources. The comparison of these materials with those produced with oil-rich networks (*10 Neat GF* and *10 Purif GF*) demonstrated the reduction in tensile moduli of 22% and 17% lower, respectively. The incorporation of less hardener molecules in the network could be associated with an overall reduced rigidity and less tightly connected cross-linked networks.

Table 6.4: Young's Modulus, tensile strength, density and specific properties of composites reinforced with glass flax fibres

| Formulation | Young's Modulus (GPa) | Tensile Strength (MPa) | Density (g $cm^{-3}$) | Specif. Modulus (GPa $g^{-1}$ $cm^3$) | Elongation at Break (%) |
|---|---|---|---|---|---|
| **10 Neat GF** | 6.3 ± 0.4 | 77 ± 10 | 1.37 ± 0.03 | 4.6 ± 0.3 | 4.3 ± 1.2 |
| **14 Neat GF** | 7.6 ± 2.0 | 91 ± 22 | 1.41 ± 0.02 | 5.5 ± 0.7 | 1.3 ± 0.4 |
| **10 Purif GF** | 6.0 ± 0.2 | 26 ± 5 | 1.33 ± 0.04 | 4.6 ± 0.2 | 6.6 ± 3.1 |
| **14 Purif GF** | 7.7 ± 1.1 | 46 ± 5 | 1.37 ± 0.04 | 5.7 ± 0.8 | 7.2 ± 1.0 |
| **DGEBA GF** | 8.3 ± 0.4 | 151 ± 14 | 1.51 ± 0.02 | 5.5 ± 0.3 | 2.1 ± 0.1 |

Moreover, the calculation of specific tensile moduli (modulus divided by density) revealed that anhydride-rich composites (*14 Neat* and *14 Purif* series) produced with glass fibres were capable of directly rivalling with DGEBA in this particular property, therefore being interesting sustainable alternatives. Nevertheless, it is important to highlight that the specific properties can be deceptive in terms of real-life application, and should be considered carefully to avoid scenarios where actual properties are below safe or specified thresholds.

Similar effects were observed in terms of tensile strength, which proved to be dependent on the oil origin and the amount of hardener in the formulation. In this regard, the superior strength of laminates produced with ENVO could be associated with the higher number of oxirane rings per unit of triglyceride unit due its unsaturated nature.[51] In terms of molar ratio, the use of an excess of MHHPA led to an increase of 77% in the tensile strength of materials produced with WVO. Therefore, adjustments in the formulation from the hardener point of view proved to be a key factor to control the properties of the resulting composites and mitigate the reductions caused by the less functionalised resin (EPVO).

Although these vegetable oil-derived networks demonstrated Young's moduli property comparable with the commercial benchmark, no bio-based formulation rival the DGEBA composites in terms of tensile strength (150 ± 13 MPa) due to differences in the molecular backbone. In fact, the use of triglyceride-based epoxies instead of DGEBA reduces the aromatic character of the network, which is responsible for providing high strength properties due to good intermolecular forces. Nevertheless, these results demonstrated that GFRC produced with WVO-based matrix can be valid alternatives when stiffness is a more critical parameter than tensile strength. Most importantly, the use of WVO based resin led to improvements in comparison with other systems in some areas. For example, the substitution

of DGEBA for WVO resulted in a reduction of 12% in density, therefore being an attractive alternative for applications where weight-reductions is a critical design parameter.

The impact resistance of composite laminates is an additional property that can be critical depending on the area of application. From the mechanical point of view, an impact test can be comprehended as a highly intense application of mechanical load in a very short time frame.[52] In comparison to other conventional mechanical tests (such as the tensile test), impact tests may involve mechanical stresses at intervals 100 to 1000 times shorter.[53] Therefore, phenomenological observations detected during an impact test represent a completely different polymer chains behaviour, which must react much more quickly during the transference of mechanical stress.

A "Charpy" impact test was investigated in this study, which has the principle of absorption of kinetic energy from the impact of a hammer-pendulum system with a known initial potential energy, Figure 6.8. Therefore, the energy required to promote mechanical failure is the sum of the energies involved in different processes (material deformation, fracture initiation, fracture propagation, *etc.*). In summary, the equipment compares the differences between the initial and final energy of the hammer due to the impact process, providing the impact strength of the material per unit of area.


Figure 6.8: Representation of the Charpy impact test.

As illustrated in Figure 6.9, significant improvements were observed in impact resistance due to the utilization of bio-based epoxy. Composites manufactured with WVO-based resins demonstrate higher impact strength than laminates produced with neat oil and DGEBA (up to 86% and 176%, respectively), Table 6.5. This feature is a consequence of the capacity of quick relaxation of networks based on long aliphatic chains, therefore facilitating

the phenomenon of the rapid energy dissipation through relaxation.[54] These results represent substantial improvements since DGEBA is known for its brittle nature with poor resistance to crack propagation.[55] The reduction in brittleness through the use of bio-based is also observed in higher values of elongation at break.

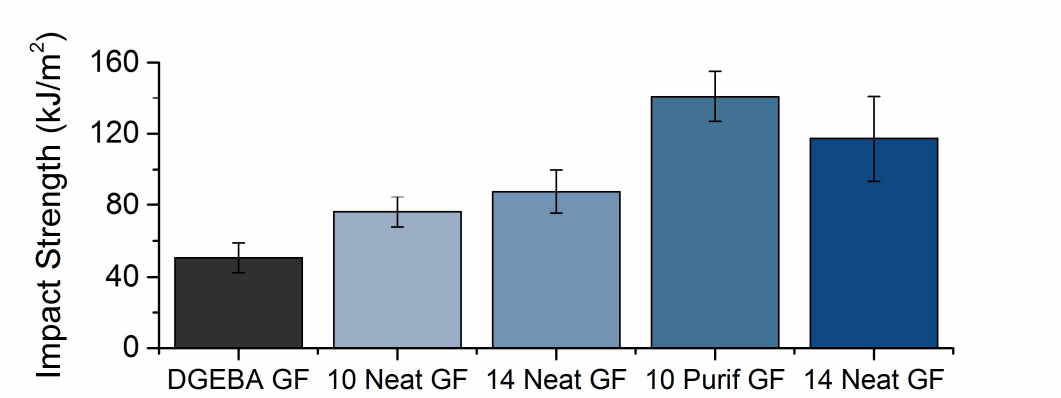


Figure 6.9: Impact strength of composite samples prepared with glass fibres in 7.5 J Charpy impact test.

Table 6.5: Impact strength of composites reinforced with glass fibres.

| Formulation | Impact Strength (kJ $m^{-2}$) |
|---|---|
| **10 Neat GF** | 76 ± 8 |
| **14 Neat GF** | 87 ± 12 |
| **10 Purif GF** | 141 ± 14 |
| **14 Purif GF** | 117 ± 23 |
| **DGEBA GF** | 51 ± 8 |

Additional control of over the impact performance was achieved by the use of different amounts of hardener: anhydride-rich networks presented lower impact strength associated with the creation of denser and more rigid networks with reduced capacity for fast relaxation. The use of larger quantities of hardener decreased in the impact resistance, which was associated with the creation of denser and more rigid networks with a reduced capacity of fast relaxation.[58]

Figure 6.10 presents radar plots, summarising the findings in GFRC formulations in terms of mechanical properties (tensile and impact), density and renewable content and comparing the best laminates prepared with WVO versus the laminates manufactured with virgin vegetable oil and DGEBA matrices. This comparison permitted a holistic assessment of the properties of these materials, highlighting improvements and trade-offs. The plot visually demonstrated that materials herein produced are promising candidates for

applications demanding stiffness, toughness and lightweight over strength. In terms of this property, a trade-off between impact strength and tensile strength was observed when bio-based epoxies from different origins (ENVO or EPVO) were explored. This can be taken as a critical design parameter when selecting the most adequate source of bio-based epoxy for composites production. Moreover, the bio-based content could be improved without sacrifices in Young's modulus.

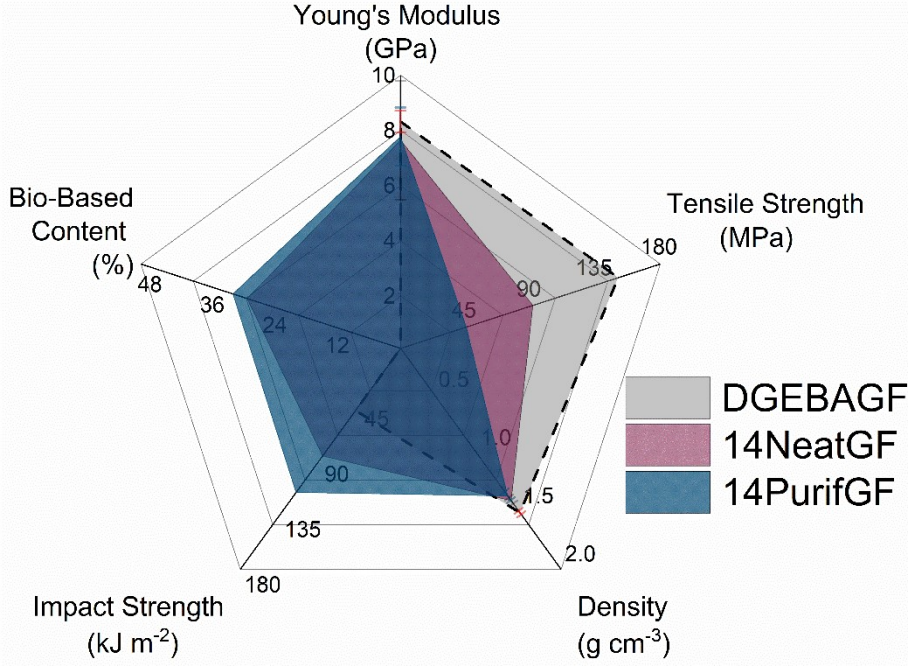


Figure 6.10: Radar plot of composites reinforced with glass fibres (top) and flax fibres (bottom) in terms of mechanical properties (tensile and impact), density and bio-based content.

### b) Composites Reinforced with Untreated and Chemically Modified Flax Fibres

The library of laminates was expanded by the production of composites reinforced with flax fibres as an approach to manufacture materials with improved environmental performance and distinct properties from GF equivalents. As illustrated in Figure 6.11, these biocomposites presented a very different mechanical behaviour when compared to the commercial benchmark. Materials combining EPVO and untreated natural fibres presented a maximum Young's Modulus 0.60 ± 0.05 GPa and tensile strength of 22.7 ± 0.9 MPa of tensile strength, Table 6.6. The utilisation of resins produced from neat oil produced laminates with very similar properties, while *DGEBAFF* resulted in laminates with much superior performance. These observations indicated that the fibre/matrix interaction in these systems was deficient, clearly illustrating the challenge of compatibilising natural fibres and triglyceride-based matrices. In this case, that mechanical stress is inefficiently transferred from the polymer

matrix to the reinforcing filler. Consequently, the material suffers from mechanical failure more promptly.

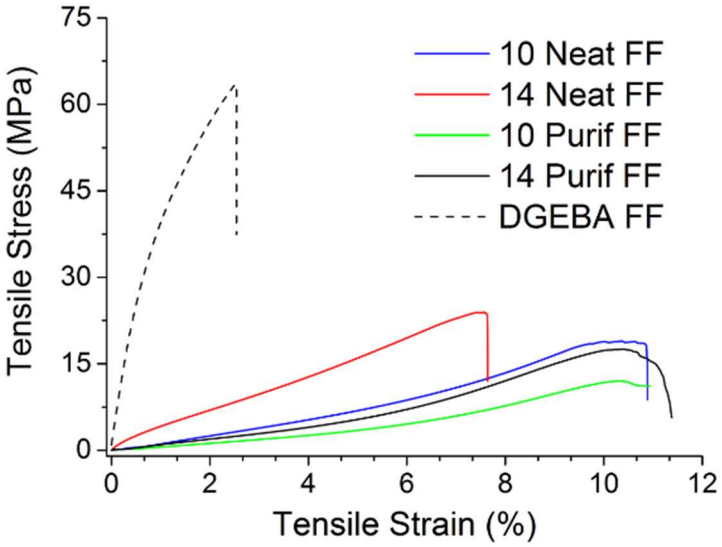


Figure 6.11: Representative stress-strain curves of the composites with untreated flax fibres.

Table 6.6: Young's Modulus, tensile strength, density and specific properties of composites reinforced with untreated flax fibres.

| Formulation | Young's Modulus (GPa) | Tensile Strength (MPa) | Density (g cm$^{-3}$) | Specif. Modulus (GPa g $^{-1}$ cm$^3$) | Elongation at Break (%) |
|---|---|---|---|---|---|
| **10 Neat FF** | 0.48 ± 0.03 | 20.3 ± 0.6 | 1.08 ± 0.01 | 0.44 ± 0.03 | 12.2 ± 1.7 |
| **14 Neat FF** | 0.65 ± 0.14 | 30.2 ± 1.8 | 1.08 ± 0.01 | 0.60 ± 0.13 | 6.3 ± 0.6 |
| **10 Purif FF** | 0.47 ± 0.03 | 14.2 ± 1.0 | 1.03 ± 0.01 | 0.46 ± 0.03 | 14.3 ± 2.9 |
| **14 Purif FF** | 0.60 ± 0.05 | 22.7 ± 0.9 | 1.11 ± 0.01 | 0.55 ± 0.05 | 7.0 ± 1.1 |
| **DGEBA FF** | 4.6 ± 0.2 | 43.2 ± 3.2 | 1.17 ± 0.01 | 3.9 ± 0.2 | 3.6 ± 0.5 |

Despite the modest specific tensile moduli, it is noteworthy that reductions of up to 27% were obtained in the density values by the replacement of glass by untreated flax fibres, with a minimum of 1.032 ± 0.012 g cm$^{-3}$. This represents an opportunity to explore these materials for non-structural applications where the design constrain is linked with weight savings, such as the automotive sector that seeks weight reductions to be aligned with emission targets.[56] Similarly to what observed for GFRC, values of tensile strength and tensile modulus fluctuated according to the relationship with anhydride content and the resin origin, presenting strategies to mitigate the loss in performance through adjustments in the formulation.

The impact properties of laminates produced with FF were also investigated, revealing the toughening effect introduced by WVO-based resins, Figure 6.12. Improvements of up to 135% and 274% were achieved for systems cured with EPVO compared to formulations manufactured with ENVO and DGEBA, respectively (Table 6.7). Due to the reduced brittleness, these WVO-based composites also presented increased elongation at break versus both neat oil and commercial counterparts. Interestingly, all composites produced with flax fibres presented lower impact property than glass fibre analogues. These results are similar to those previously reported by Ramamoorthy *et al.* in investigations with hybrid biocomposites combining jute and glass fibres.[59] Another interpretation of this phenomenon is that these composites presented reduced fibre/matrix interaction. Therefore, the weak interaction between these components led to the formation of microcracks in the interface, which could act as crack propagators and reduce the impact properties. This feature will be investigated in more depth later in this study.

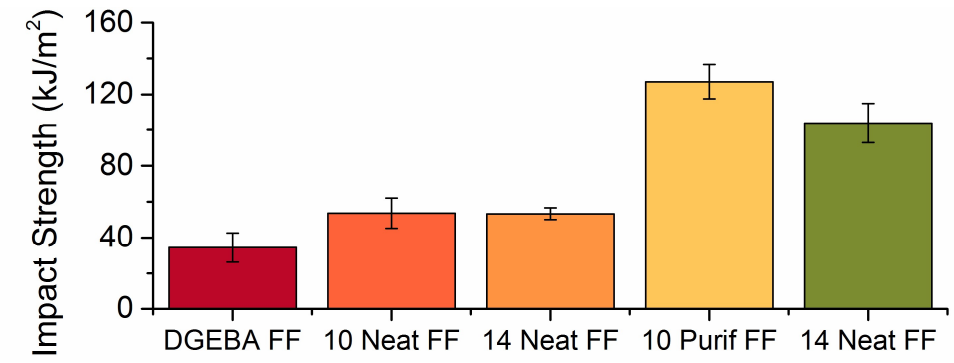


Figure 6.12: Impact strength of composite samples prepared with untreated flax fibres in 7.5 J Charpy impact test.

Table 6.7: Impact strength of composites reinforced with untreated flax fibres.

| Formulation | Impact Strength (kJ $m^{-2}$) |
|---|---|
| **10 Neat FF** | 54 ± 8 |
| **14 Neat FF** | 54 ± 4 |
| **10 Purif FF** | 127 ± 10 |
| **14 Purif FF** | 104 ± 11 |
| **DGEBA FF** | 34 ± 8 |

Given the limited results achieved for composites prepared with untreated FF, chemically-modified fibres were used to boost the mechanical performance of NFRC produced with bio-based matrices. In comparison with laminates produced with WVO and

untreated fibres (*14 Purif FF*), the alkaline treatment increased the tensile modulus by 36%, Table 6.8. Similar improvements are observed when these reinforcements are combined with ENVO-based with matrix, so that the Young's modulus of these laminates exceed the 1.0 GPa mark (59% higher). SFF fibres are also capable of producing laminates with moduli 35% and 15% higher for resins synthesised from neat oil and WVO, respectively. These results demonstrate the improved adhesion deriving from changes in chemical and physical properties of the fibres, with NFF fibres leading to more significant results.

Table 6.8: Young`s Modulus, tensile strength, density and specific properties of composites reinforced with NaOH-treated fibres.

| Formulation | Young`s Modulus (GPa) | Tensile Strength (MPa) | Density (g $cm^{-3}$) | Specific Modulus (GPa $g^{-1}$ $cm^3$) |
|---|---|---|---|---|
| **10 Neat NFF** | 0.54 ± 0.04 | 28.0 ± 2.9 | 1.08 ± 0.01 | 0.50 ± 0.04 |
| **14 Neat NFF** | 1.03 ± 0.07 | 34.6 ± 2.8 | 1.08 ± 0.01 | 0.95 ± 0.07 |
| **10 Purif NFF** | 0.47 ± 0.03 | 24.6 ± 3.5 | 1.03 ± 0.01 | 0.44 ± 0.03 |
| **14 Purif NFF** | 0.82 ± 0.15 | 25.3 ± 1.7 | 1.11 ± 0.01 | 0.7 ± 0.1 |
| **10 Neat SFF** | 0.45 ± 0.06 | 20.7 ± 1.7 | 1.17 ± 0.01 | 0.42 ± 0.06 |
| **14 Neat SFF** | 0.88 ± 0.22 | 30.7 ± 2.9 | 1.08 ± 0.01 | 0.8 ± 0.2 |
| **10 Purif SFF** | 0.40 ± 0.10 | 17.2 ± 2.4 | 1.083 ± 0.005 | 0.38 ± 0.09 |
| **14 Purif SFF** | 0.69 ± 0.12 | 21.8 ± 1.3 | 1.088 ± 0.010 | 0.7 ± 0.1 |

These results demonstrated improved mechanical stress transference caused by changes in chemical and physical properties of the fibres, which was achieved by the compatibilization effect. The tensile strength of these panels proved to be also positively affected by the treatment: an increase of 14% was observed for anhydride-rich laminates. Moreover, oil-rich formulations (*10 Neat NFF* and *10 Purif NFF)* presented improvements of 23 and 73%, respectively. The quantity of anhydride in the network proved to replicate the same behaviour previously observed for laminates presenting unmodified fibres. Comparing both treatments, NFF led to significant improvements in tensile properties in than SFF equivalents.

Moreover, panels produced with modified fibres presented enhanced impact properties because of improvements in the fibre/matrix interaction (Table 6.9). Therefore, the mechanical load could be more effectively transferred from the matrix to the fibre, enhancing the reinforcing effect. In comparison to composites prepared with virgin flax fibres, both methodologies presented improvements between 10 and 23% in terms of impact strength. This

higher impact performance of materials could be associated with the reduction of microcracks in the interface between the two components, therefore reducing the presence of crack propagation agents.

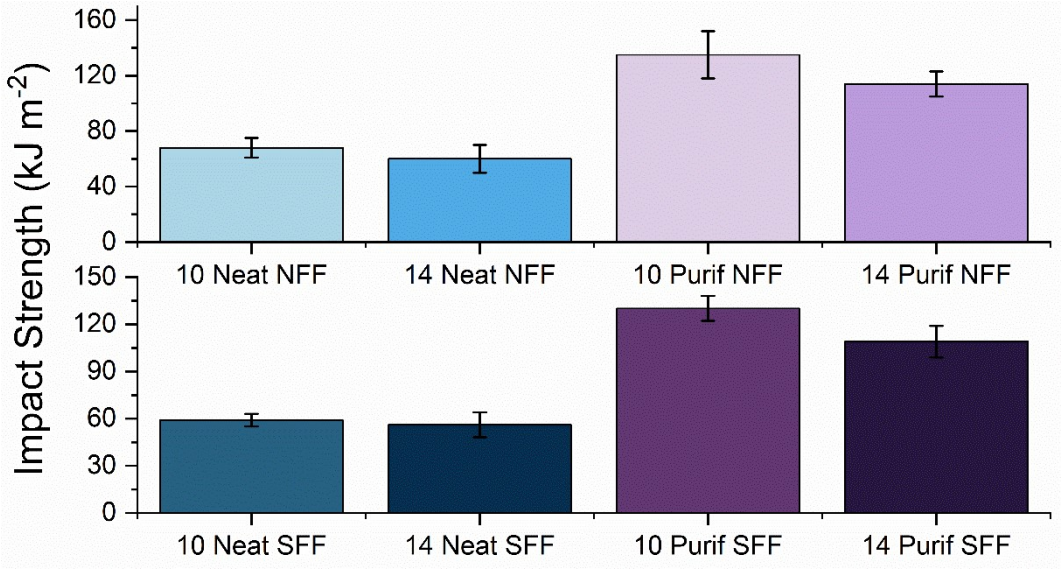


Figure 6.13: Impact strength of composite samples prepared with NFF (top) and SFF (bottom) fibres in 7.5 J Charpy impact test.

Table 6.9: Impact strength of laminates produced with bio-based epoxy and chemically modified flax fibres.

| Formulation | Impact Strength (kJ m$^{-2}$) |
|---|---|
| **10 Neat NFF** | 68 ± 7 |
| **14 Neat NFF** | 60 ± 10 |
| **10 Purif NFF** | 135 ± 17 |
| **14 Purif NFF** | 114 ± 9 |
| **10 Neat SFF** | 59 ± 4 |
| **14 Neat SFF** | 56 ± 8 |
| **10 Purif SFF** | 130 ± 8 |
| **14 Purif SFF** | 109 ± 10 |

Radar plots (Figure 6.14) summarise the performance of materials produced with untreated flax fibres and those obtained through the best chemical treatment (NaOH). Positive results are observed in all tensile parameters, and the treatment also boosted the impact performance while leaving density and bio-based content unchanged. This collection of improvements are direct consequences of the fibre/matrix interaction enhancement achieved by the treatments. Overall, these findings support the application of the chemical modification

to produce NFRC from WVO with better mechanical properties. Nevertheless, it is important to acknowledge the limitations of this approach in comparison with the commercial benchmark. Contrary to what observed for GFRC, NFRC produced from WVO are indicated for non-structural applications when untreated fibres are used, and intermediate applications after the fibre treatments.

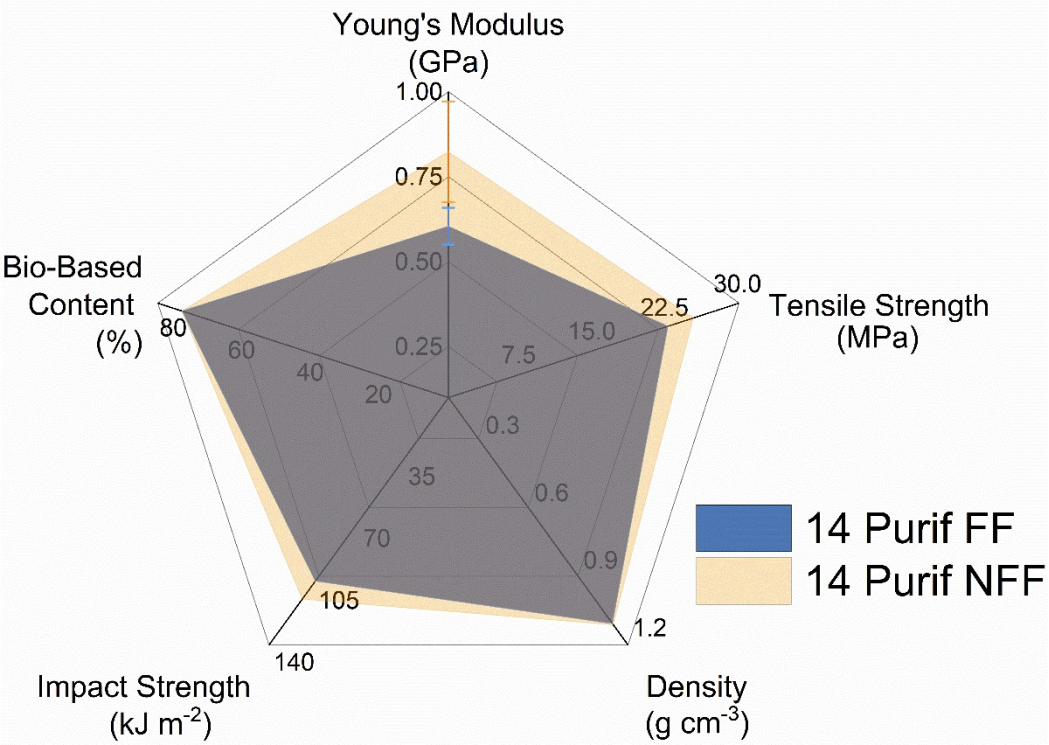


Figure 6.14: Radar plot of composites produced with WVO-based resin and reinforced with unmodified (FF) and NaOH-treated flax fibres (NFF) in terms of mechanical properties (tensile and impact), density and bio-based content.

### 6.3.4 Comprehending the Fibre/Matrix Interaction through Microscopy

SEM images were explored to investigate topological and morphological characteristics of the composites, associating them with the mechanical performance observed in mechanical tests. Panoramic SEM images were used to identify the bundles and the homogeneous surface of each of the fibres. High magnification images of GFRC (Figure 6.15A.3-E.3) demonstrated that fibres were not sufficiently adhered to the matrix in oil-rich formulations, therefore explaining the reduced of mechanical properties observed previously in comparison with other formulations. On the other hand, images of *14NeatGF* and *14PurifGF* formulations indicated that fibres were satisfactorily wetted by the polymer matrix, so that the mechanical stress was transferred from to the reinforcing agent more efficiently.

As exemplified by Figure 6.15E.3, the cryo-fracture process leads to fibre breakage rather than fibre pull-out, which indicates that the fibre/matrix interaction is sufficiently higher than the cohesive forces in the fibres. This indicated that the fibres presented increased affinity to less hydrophilic matrices (*i.e.* anhydride-rich networks).

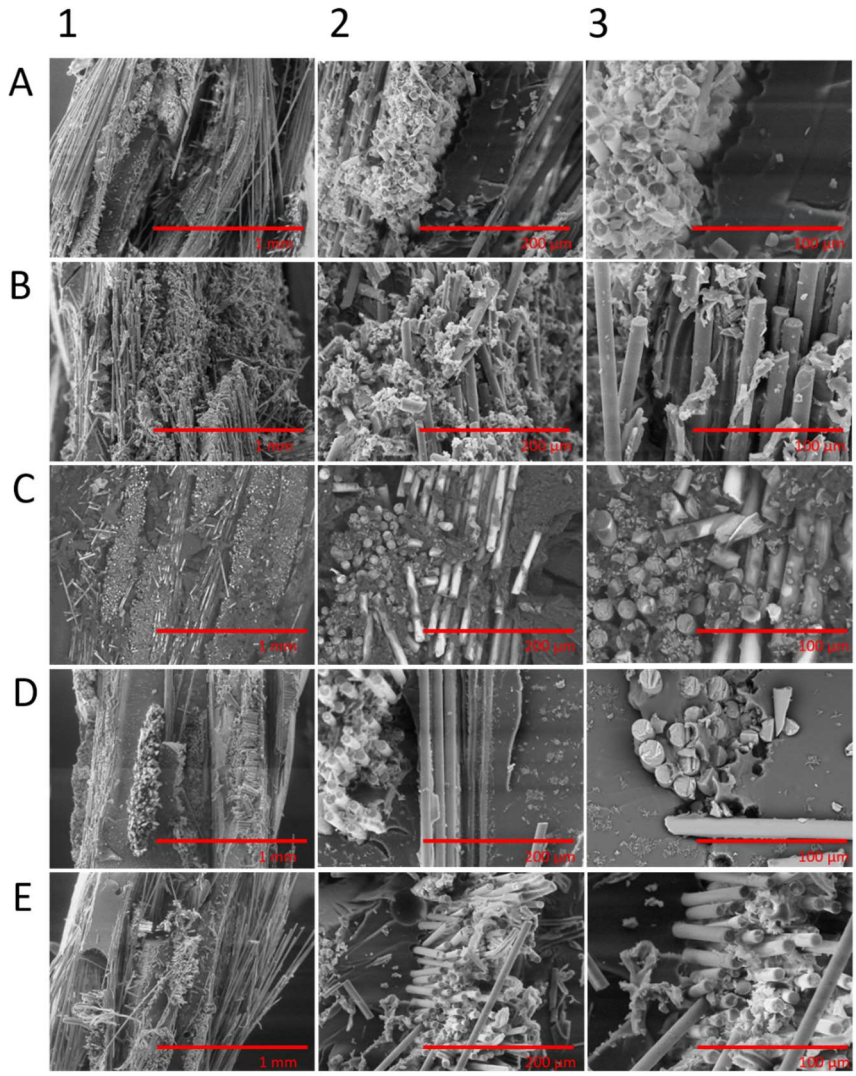


Figure 6.15: SEM images obtained in three magnifications (left: 100x, centre: 500x, right: 1000x) of samples A) 10NeatGF B) 14NeatGF C) 10PurifGF, D) 14PurifGF and E) DGEBAGF.

Figure 6.16A-E revealed details of the flax fibre reinforced composites, demonstrating extensive fibre pull-out effect, (for example, in A.1 and C.1). These figures showed the detachment of whole fibre bundles from the polymer matrix during the fracture process, visually representing interfacial problems encountered in these formulations. Therefore, adhesion between the reinforcing fibre and the polymer matrix was not strong enough to keep a cohesive interaction. As discussed in Chapter 3, this process is commonly observed in this

class of materials due to the differences in polarity of the reinforcing agent (hydrophilic) and the polymer matrix (hydrophobic). Also, microcracks were detected in the interface between the fibre and the matrix for composite prepared with unmodified flax, confirming previous predictions about the composite topology and further reducing the overall mechanical response of the composite.

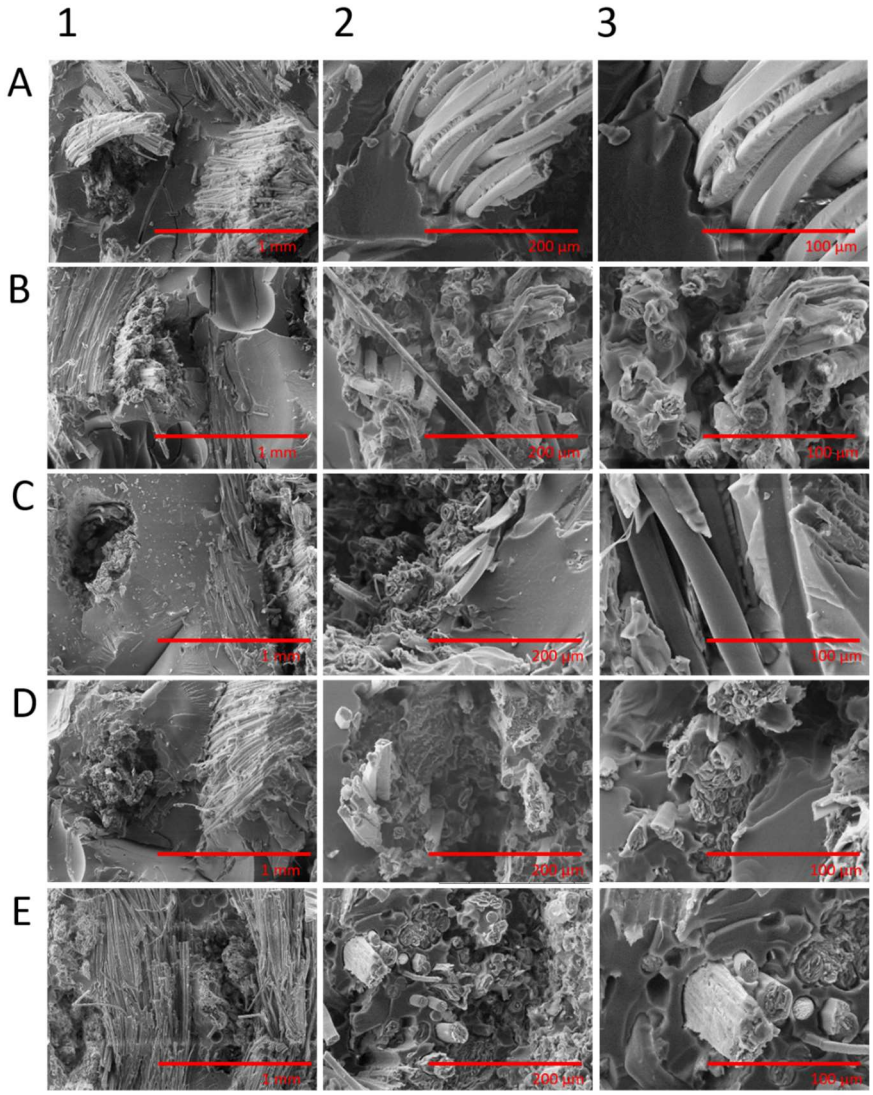


Figure 6.16: SEM images obtained in three magnifications (left: 100x, centre: 500x, right: 1000x) of samples A) 10NeatFF B) 14NeatFF C) 10PurifFF, D) 14PurifFF and E) DGEBAFF.

SEM micrographs of composites prepared with chemically modified fibres (Figure 6.17A-E) were used to investigate the relationship between the improved mechanical properties and the fibre matrix interaction. Lower magnification images (100x) demonstrated the reduction of pull-out and fibre breakage achieved by both treatments, evidencing stronger interfacial interaction between the components. In addition, micrographs obtained at higher

magnification (1000x) displayed that the matrix is efficiently wetting surfaces and grooves created by the chemical modifications step. Consequently, a reduced number of defects and microcracks were detected in the interface, positively impacting the mechanical performance of this formulations. These observations reiterated what was discussed in terms of improvements in mechanical properties promoted by the chemical treatments.

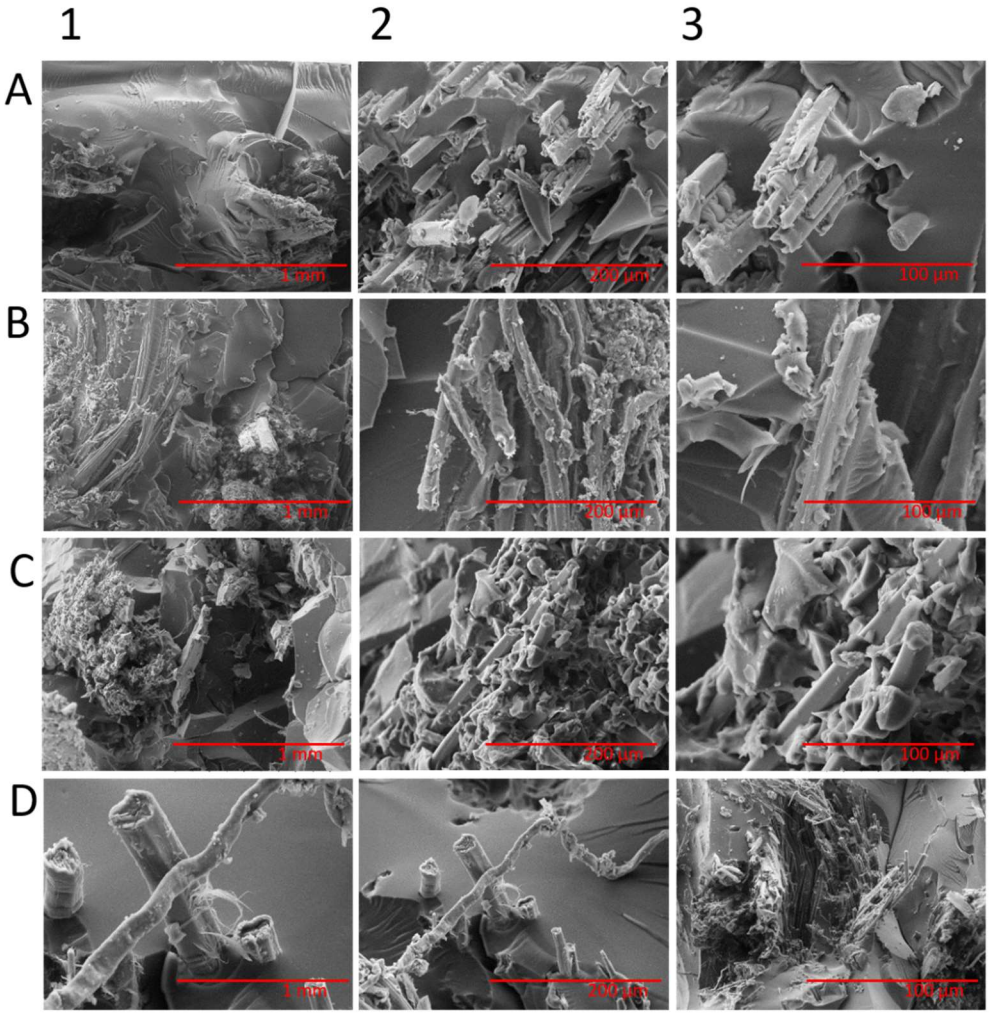


Figure 6.17: SEM images in three magnifications (left: 100x, centre: 500x, right: 1000x) of samples A) 10NeatNFF B) 14NeatNFF C) 10PurifNFF and D) 14PurifNFF.

### 6.3.5 Dynamic-mechanical Properties

Dynamic mechanical analysis (DMA) was performed to investigate the viscoelastic and mechanical responses of the polymer matrix present in the composite, comprehending how the addition of fibres regulate these properties. Figure 6.18 shows the curves of E' versus temperature for glass and flax fibre reinforced composites, comparing results obtained from bio-based matrices and reference materials produced with DGEBA resin. These curves demonstrated that formulations prepared with DGEBA had superior values of storage modulus

at the elastic plateau due to the superior molecular stiffness of the aromatic DGEBA backbone in comparison with the aliphatic EVOs, as observed in previous chapters. Also, curves showed that no formulation presented significant gains in E' during the heating process, demonstrating no residual curing under these conditions. Similarly, no phenomena were observed in the lower temperature range, thus demonstrating that the systems do not exhibit secondary transitions (*i.e.*, Tβ). Although the addition of fibres can potentially cause an increased in the E' values due to additional mobility constraints, no differences were observed when comparing values obtained for the composites (this chapter) and the matrices (Chapter 5).[61]

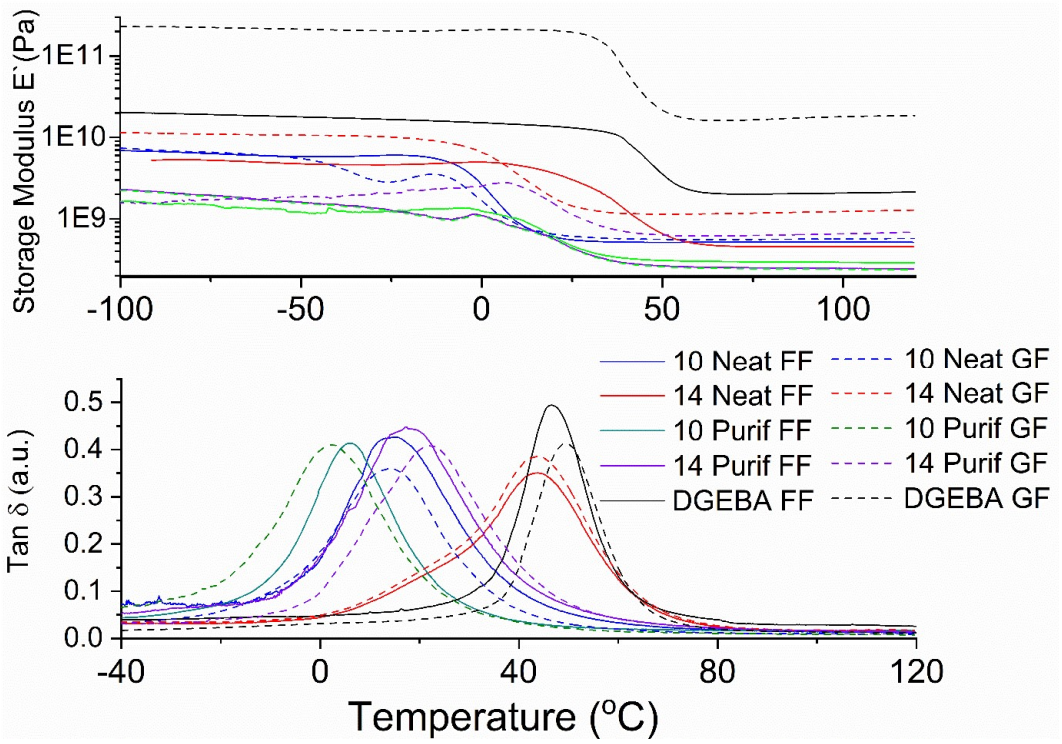


Figure 6.18: Storage modulus (top) and tan δ curves versus temperature of composites produced with flax (full lines) and glass fibres (dashed lines).

With respect to the effect of the origin of the oil, formulations prepared from virgin oil demonstrated higher initial storage modulus than WVO equivalents because of the formation of polymer matrices with denser crosslinks. In this regard, previous studies published by Kim and Sharma have shown that the use of EVOs derived from highly unsaturated oils results in composites with higher mechanical properties.[62] Consequently, it is evident that the frying was limiting the properties of the composites. Curves also demonstrated that other parameters in the formulations were also capable of affecting the dynamic mechanical properties of the resulting composites. For example, formulations with higher

amounts of anhydride in the network were responsible for increasing the E' response, which is aligned with what observed for non-reinforced materials (Chapter 5).

The growth of the elastic properties due to the presence of anhydrides was a consequence of the relatively higher molecular stiffness of these compounds compared to the units derived from the triglycerides, a concept that has been previously explored in this study Along these lines, the network becomes richer in the stiffer component, resulting in higher E' (superior elastic component). Both series of composites produced with flax and glass fibres presented very similar values of E'; however, *DGEBAGF* formulation has shown E' an order of magnitude greater than the equivalent produced with flax fibres.

Table 6.10: Storage modulus values at room temperature, $T_g$ and crosslink density of glass and flax reinforced composites.

| Formulation | E′(25 °C) (MPa) | $T_g$ (°C) |
|---|---|---|
| **10 Neat FF** | 556 | 14.6 |
| **14 Neat FF** | 2996 | 43.9 |
| **10 Purif FF** | 451 | 6.6 |
| **14 Purif FF** | 462 | 17.9 |
| **DGEBA FF** | 19610 | 46.7 |
| **10 Neat GF** | 626 | 13.3 |
| **14 Neat GF** | 1444 | 43.6 |
| **10 Purif GF** | 449 | 3.4 |
| **14 Purif GF** | 1156 | 22.2 |
| **DGEBA GF** | 13411 | 49.5 |

To further understand the changes in the mechanical properties of the composites caused by temperature variation and the relaxation phenomena, the glassy transition was investigated through the construction of tan δ curves versus temperature. As shown in Table 6.10, $T_g$ values followed the same pattern discussed for the E', where composites prepared with anhydride-rich polymer matrices and/or with virgin vegetable oil-derived resins presented superior properties as a combination of more rigidity and denser networks.

The presence of one single tan δ peak in the curves indicates the formation of a single polymeric phase. Nevertheless, the broadened shape of the peaks evidenced the formation of heterogeneous polymeric networks, similar to what observed for characterisation of the thermoset polymer.[63,64] Moreover, the addition of vegetable fibres is responsible for broadening the tan δ peaks since the reinforcement agent could inhibit the relaxation process, making the material response more heterogeneous.[61] Among the group of formulations

studied, only *14NeatFF* and *14NeatGF* presented glass transition temperatures above room temperature. This is an essential characteristic from the applicability point of view and permitted establishing a connection between $T_g$ and E' values at 25 °C, as observed in Table 6.10. The comparison of $T_g$ determined for the composites with those observed for the thermoset matrices (Chapter 5) reveals that, although the movement hindrance caused by the insertion of fibres did not cause any significant increase in the values of E', it was responsible for shifting the glass transition to much higher temperatures.[61,65]

Tan δ curves also allowed the evaluation of the damping capacity of these materials, characteristic which is related to the ability to dissipate vibrational energy. [66] This property is crucial in terms of real-life applications because composites are exposed to vibrational disturbances during the use-phase, particularly as components for automotive and aerospace sectors. Therefore, reducing the vibration in these parts decreases fatigue effects and consequently increases the service time of these components.[67] In addition, the ability of dispersing vibrational energy associated with the damping property can be closely associated with the capacity of application of a given material as an acoustic insulation.[68] This property is mainly explored in the automotive sector, which seeks materials capable of reducing internal noise caused by the motor, enhancing the user experience.[69]

The incorporation of fibres as a reinforcing agent affects the damping behaviour of the polymer matrix due to shear stress concentrations in the fibres. Chandra *et al.* discussed that fibres can act synergistically with the phenomenon of viscoelastic dissipation of energy promoted by the matrix, enhancing the damping characteristics.[70] This property is notably observed in vegetable fibres due to its inherent morphological characteristics.[71] Damping characteristics are manifested in DMA runs through the increase of the loss modulus and, consequently, higher tan δ values.

Conversely, the phenomenon of adhesion between the matrix and the reinforcing agent can negatively affect the damping properties of a composite material.[6] Materials presenting good interfacial interaction between the components have lower tan δ values since the matrix becomes partially immobilized by the fibres, consequently contributing less towards the damping capacity.[72,73] Therefore, the final shape of the tan δ corresponds to the net balance between these two antagonistic effects. Experimentally, tan δ curves demonstrated that composite formulations had smaller peak values in comparison to curves obtained for unreinforced polymers (Chapter 5). This finding revealed that the immobilisation effect suppressed the additional damping caused by the addition of fibres in all scenarios, therefore the resulting damping was in fact reduced in the composite laminates.

Composites using chemically-modified fibres were also investigated from the dynamic-mechanical point of view. As presented in Figure 6.19, these composites presented similar behaviours to those observed for materials produced with virgin fibres. For example,

curves of E' were again controlled by factors such as the oil origin and the amount of hardener used in the formulation. However, it was noteworthy that the values of $T_g$ for NFF and SFF-reinforced composites were superior to those obtained from virgin flax fibres (Table 6.11). This change illustrated the improvements in the fibre matrix interactions, introducing immobilization effects that reduced chain mobility and translated into higher $T_g$ values.[65] Interestingly, despite the increase in tensile properties, DMA revealed that E' was not significantly altered by the chemical treatment.[22]

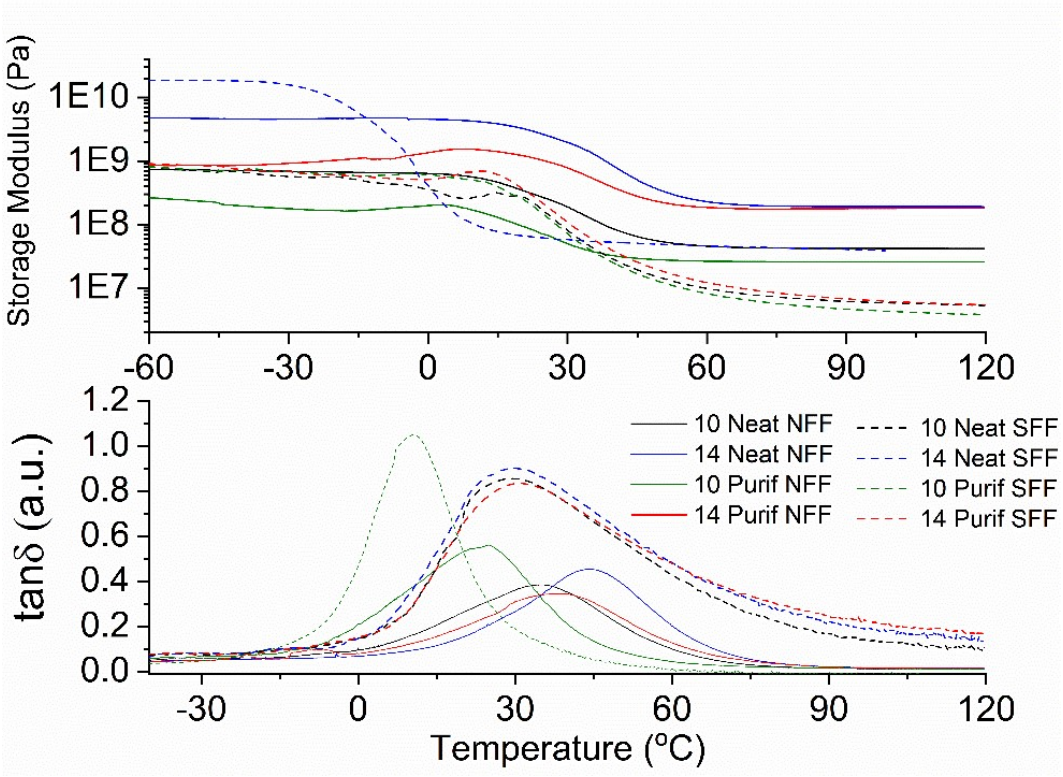


Figure 6.19: Storage modulus (above) and tan δ (below) curves versus temperature of composites produced with NaOH-modified flax fibres (NFF).

Table 6.11: Storage modulus values at room temperature, $T_g$ and crosslink density of glass and flax reinforced composites.

| Formulation | E' (25 °C) (MPa) | $T_g$ (°C) |
|---|---|---|
| **10 Neat NFF** | 246 | 34.8 |
| **14 Neat NFF** | 2529 | 44.1 |
| **10 Purif NFF** | 74 | 24.4 |
| **14 Purif NFF** | 1041 | 34.5 |
| **10 Neat SFF** | 133 | 28.8 |
| **14 Neat SFF** | 613 | 30.2 |
| **10 Purif SFF** | 131 | 10.9 |
| **14 Purif SFF** | 205 | 29.6 |

From the group of materials produced with modified fibres, NFF-reinforced composites demonstrated the best improvements in the $T_g$ values. This indicated mercerization promoted the best enhancement of the interfacial interaction between the two methods herein investigated. This finding also reflected the observations previously discussed from the mechanical characterisation of the panels. Additionally, small improvements in $\nu_e$ were detected after the fibre modification, contributing towards composites with better mechanical properties.

### 6.3.6 Thermal Stability of Composites

Figure 6.20 shows thermogravimetric curves of composites reinforced with both flax and glass fibres, as well the first derivatives of weight-loss percentage with respect to temperature. $T_{Onset}$ have demonstrated the similarities between the two series of composites with respect to this property (Table 6.12). Although the thermal stability of the matrix was regulated by the anhydride content in the formulation (higher contents are responsible for forming less thermally stable crosslinks, Chapter 5), the addition of vegetable fibres changed this behaviour. Since the polymeric network and natural fibres undergo thermal degradation processes in very similar temperature ranges, there was a competition between these two events that ultimately disguised the effect of the anhydride observed in the previous chapter. In contrast, the expected pattern was observed for GFRC since the reinforcing agent did not thermally degrade at the same temperature range of the matrix.

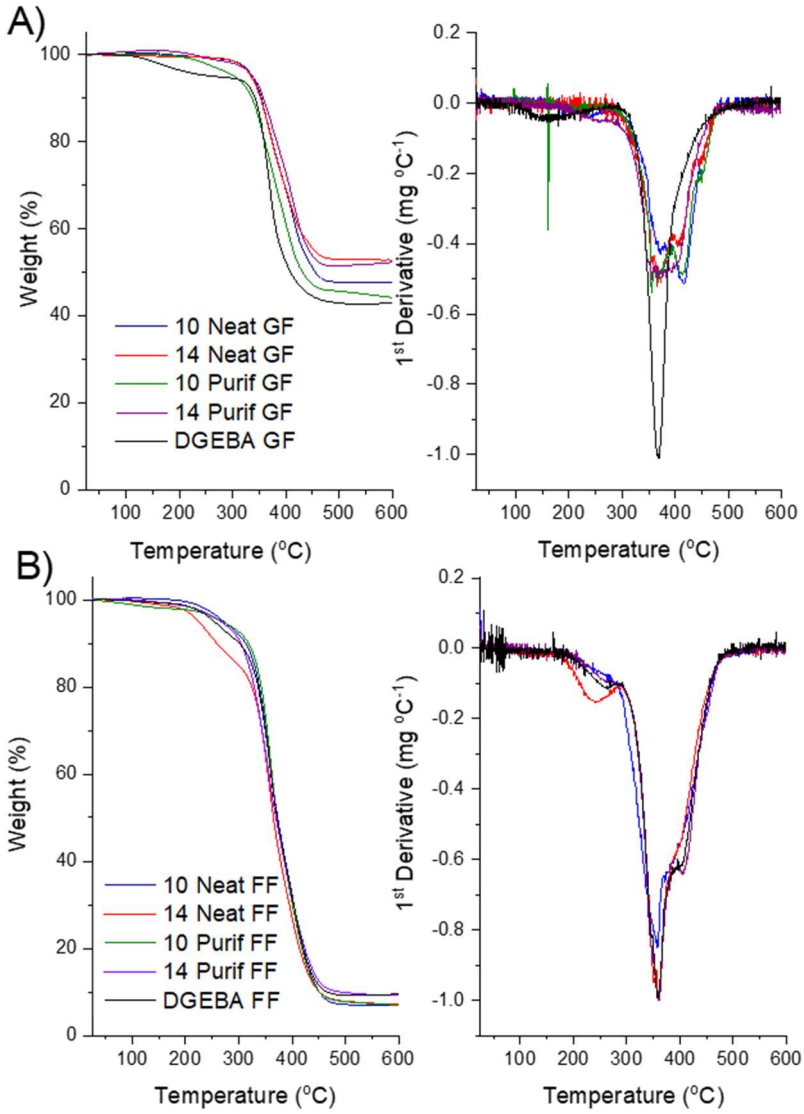


Figure 6.20: Thermograms and First derivative curves of the weight-loss percentage of the biocomposites reinforced with A) glass fibres and B) flax fibres, from 25 °C to 600 °C, under $N_2$ atmosphere.

Thermograms of the NFRC demonstrated that the weight-loss caused by moisture was negligible since no event is observed around 100 °C. In addition, all composites presented the formation of non-volatile residues at the end of the analysis, as detectable by the presence of approximately 10% residual mass after heating the sample at 600 °C. Thermograms presented in Chapter 5 demonstrated that degradation products formed by the bio-derived polymer were volatile, leaving no significant amounts of residues at 600 °C. Therefore, all residual mass can be attributed to the degradation products derived from the lignin in the fibres, which formed highly condensed products and led to the formation of the carbonized residues.[74] On the other hand, residues observed in the thermogravimetric curves of GFRC could be associated with

the presence of undegraded reinforcing agents. Therefore, thermal events observed in GFRC curves essentially followed the same behaviour observed for the polymer matrix, as discussed in the previous chapter.

Thermal degradation events also were followed with more details through the curves of the first derivative. By comparing the curves obtained from composites reinforced with flax and those obtained for the separated components (the fibre and the matrix), it was demonstrated that the peak of degradation rate at 355 °C was associated with the thermal degradation of the cellulose Table 6.12. The second degradation event evidenced by the peak at 400 °C was then associated with the simultaneous thermal degradation of the crosslinks and of the units derived from the modified triglycerides / curing agent. Furthermore, the peak associated with lignin degradation was not clearly evidenced in thermogravimetric curves because this event occurred in the same temperature range as the degradation of the polymer network. Interestingly, a unique event at 235 °C was observed in the *14 Neat FF* thermogram, which may be associated the presence of unincorporated hardener molecules.

First derivative curves obtained from GFRC evidenced the simultaneous degradation mechanisms observed during the destruction of the network, with the shape of the first derivative curves resembling those observed for unreinforced polymers. On the other hand, all bio-based formulations presented two thermal phenomena that ranged from 320 °C to 460 °C, indicating more clearly the degradation of the reinforcing fibre (first peak) and the polymeric network (second peak)

Table 6.12: Temperature of initial degradation ($T_{Onset}$) and temperature of maximum degradation rate ($T_{Max}$) of glass and (virgin and treated) flax fibre reinforced biocomposites.

| Formulation | $T_{Onset}$ (°C) | $T_{Max}$ (°C) |
|---|---|---|
| **10 Neat GF** | 337.6 | 414.9 |
| **14 Neat GF** | 330.6 | 416.3 |
| **10 Purif GF** | 336.8 | 413.7 |
| **14 Purif GF** | 330.8 | 407.3 |
| **DGEBA GF** | 348.5 | 369.0 |
| **10 Neat FF** | 339.3 | 359.0 |
| **14 Neat FF** | 336.8 | 360.3 |
| **10 Purif FF** | 331.1 | 361.0 |
| **14 Purif FF** | 333.7 | 360.3 |
| **DGEBA FF** | 347.0 | 370.3 |
| **10 Neat NFF** | 324.0 | 355.0 |
| **14 Neat NFF** | 326.2 | 354.1 |
| **10 Purif NFF** | 322.1 | 355.3 |
| **14 Purif NFF** | 320.0 | 353.3 |
| **10 Neat SFF** | 331.3 | 368.3 |
| **14 Neat SFF** | 323.0 | 353.7 |
| **10 Purif SFF** | 326.1 | 352.3 |
| **14 Purif SFF** | 325.4 | 351.0 |

In terms of the chemical modification process, composites prepared with NFF fibres presented a slight reduction in $T_{Onset}$ in comparison with virgin equivalents, reflecting the results observed for the isolated fibres, Figure 6.21A. However, the lower thermal stability was not as accentuated as what was observed in the comparison between FF and NFF, evidencing that the matrix could suppress the degradation due to its higher thermal stability, Table 6.12. Interestingly, SFF fibres did not caused any expressive enhancements of thermal stability as expected. Nevertheless, the more accentuated reduction in the amount of non-volatile residues after the analysis observed for SFF-reinforced composites demonstrated the stearic acid method was the most effective one in terms of delignification. The second degradation event observed in NFF and SFF-reinforced formulations, evidenced by the peak at 400 °C, was also associated with the simultaneous thermal degradation of the crosslinked units. However, in SFF-composites, this peak was broader and ill-defined due to the additional degradation of the stearic acid at the same temperature range, adding to the complexity of the thermal response. Most importantly, TGA results revealed that the substitution of resins from

neat oil for waste oil in the production of bio-based resins causes no sacrifices from the thermal stability standpoint.

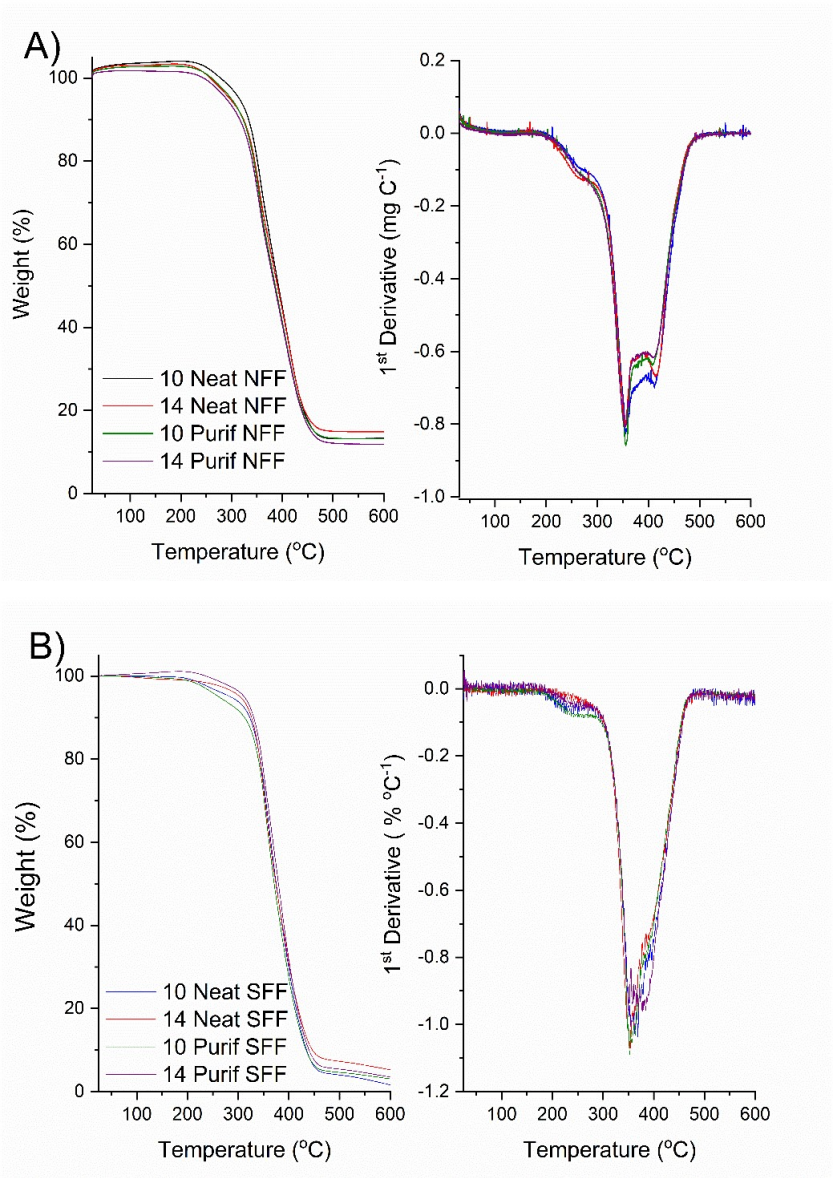


Figure 6.21: Thermograms and first derivative curves of the weight-loss percentage of the biocomposites reinforced with A) NaOH-treated flax fibres and B) Stearic acid-treated flax fibres, from 25 °C to 600 °C, under $N_2$ atmosphere.

### 6.3.7 Hygrothermal Ageing

As highlighted previously, vegetable fibres' high hydrophilic nature derives from presence of hydroxyl groups derived from cellulose and hemicellulose repeating units. Therefore, when used as reinforcing agents, these fibres increase the water uptake of the resulting composites in comparison with unreinforced materials or fibres such as glass or carbon. This can cause critical consequences since the water absorption leads to fibre swelling,

spatial deformity and formation of internal cracks in the polymer matrix, potentially compromising the fibre/matrix interaction and ultimately to the reduction of the mechanical properties of the material irreversibly.[75]

According to literature, the water adsorption/absorption in composites occur typically through three different mechanisms. In the first one, water molecules may diffuse through the polymer chains or the network; the second mechanism is described as the transport of water through capillaries in flaws, imperfections and gaps at the interface between the fibres and the matrix.[76] Finally, the third water sorption mechanism is similar to the second one; however, it occurs through microcracks inherently formed during the material processing step. The latter mechanism is mainly observed in thermoplastic composites manufactured by techniques such as injection moulding, which may leave superficial marks on the final part due to tooling damage/scratches.

Vegetable fibres contribute towards the water uptake through an additional mechanism that occurs by capillarity in the fibre itself due to its hydrophilicity. In this way, the vegetal fibre acts like a preferential pathway towards water penetration, acting like a like a straw transporting liquid to the interior of the composite.[77] Considering the importance of this phenomenon in vegetable fibre reinforced composites from the applicability point of view (particularly in external structural applications), a hygrothermal ageing test was explored to investigate the water uptake property. Weight gain curves were constructed as a function of the ageing time for all formulations prepared with glass and virgin flax, Figure 6.22. It is noteworthy that the weight fluctuation over time represents not only water absorption but in fact the overall result of different phenomena that occur during the test, such as the leaching of soluble matter and water desorption.[22] The driving force for the water absorption phenomenon, in this case, is chemical potential created by the concentration gradient of penetrating molecule, which continues to migrate until the chemical equilibrium is reached.[78]

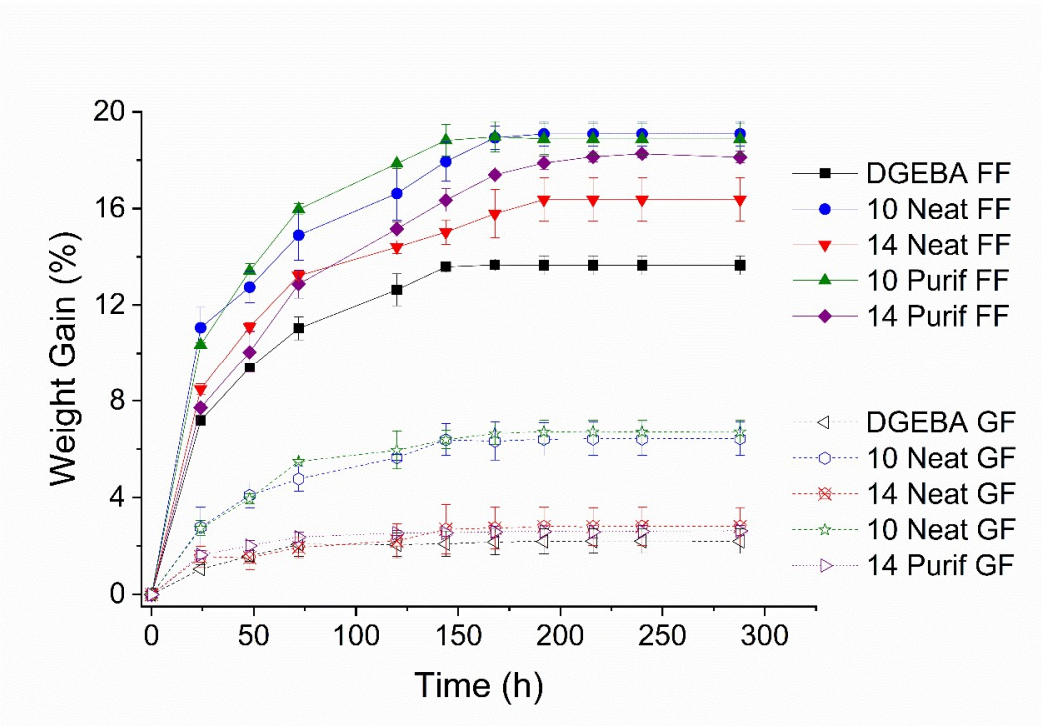


Figure 6.22: Weight gain curves as a function of the hygrothermal ageing time for composites reinforced with flax (full lines) and glass fibres (dotted line).

Experimental curves demonstrated differences in the water uptake behaviour caused by using either glass fibres or flax fibres as a reinforcing agent. Curves built with full lines, corresponding to the composites with flax fibre, absorbed up to almost 3 times more water than formulations with glass due to the hydrophilic character of the natural fibre. Similarly, the steady state, *i.e.* point where the mass gain variation is insignificant, was achieved in shorter times in glass fibre reinforced composites (about 150 h) than in those with flax fibre (190 h). Therefore, this observation indicated that the additional amount of penetrant is also responsible for altering the conditions under which the equilibrium state was established.

From the formulations point of view, it was established that composites with higher anhydride content resulted in reduced water uptake in comparison to oil-rich counterparts. As these systems present a higher density of crosslinking, it was possible to relate this effect to the hindrance of the chains mobility, therefore the diffusion of the penetrant was more difficult and consequently reduced.[78,79] Additionally, an alternative water uptake phenomenon associated with the dynamic-mechanical properties could be derived from these observations. The diffusional process was facilitated in matrices with $T_g$ lower than the test temperature (23 °C) because polymer chains presented greater ability to respond to the stress caused by the penetrant. Consequently, water molecules diffused with less resistance in formulations with low anhydride content, creating a more noticeable chemical gradient.

Surface treatments were also investigated from the hygrothermal ageing point of view. It was initially postulated that laminates manufactured with chemically modified fibre would present smaller water uptake since these methodologies altered the morphology of the fibre surface, cellulose content and fibre/matrix interaction. Indeed, weight gain curves (Figure 6.23) demonstrated a reduction from 4 to 5.1% in the absolute total of water uptake throughout the range of formulations when compared to materials produced with unmodified flax (Figure 6.22). This finding was associated with the elimination of microcracks in the fibre/matrix interface, eliminating a preferential penetration path and reducing the chemical gradient. Nonetheless, the steady state was achieved at similar times. Comparing the two methodologies, materials reinforced with fibres coated with stearic acid presented reduced the water uptake in comparison with NFF due to the attachment of apolar segments to the cellulosic chains, reducing its affinity to water. These results revealed an alternative benefit brought by the chemical modification of the flax fibres.

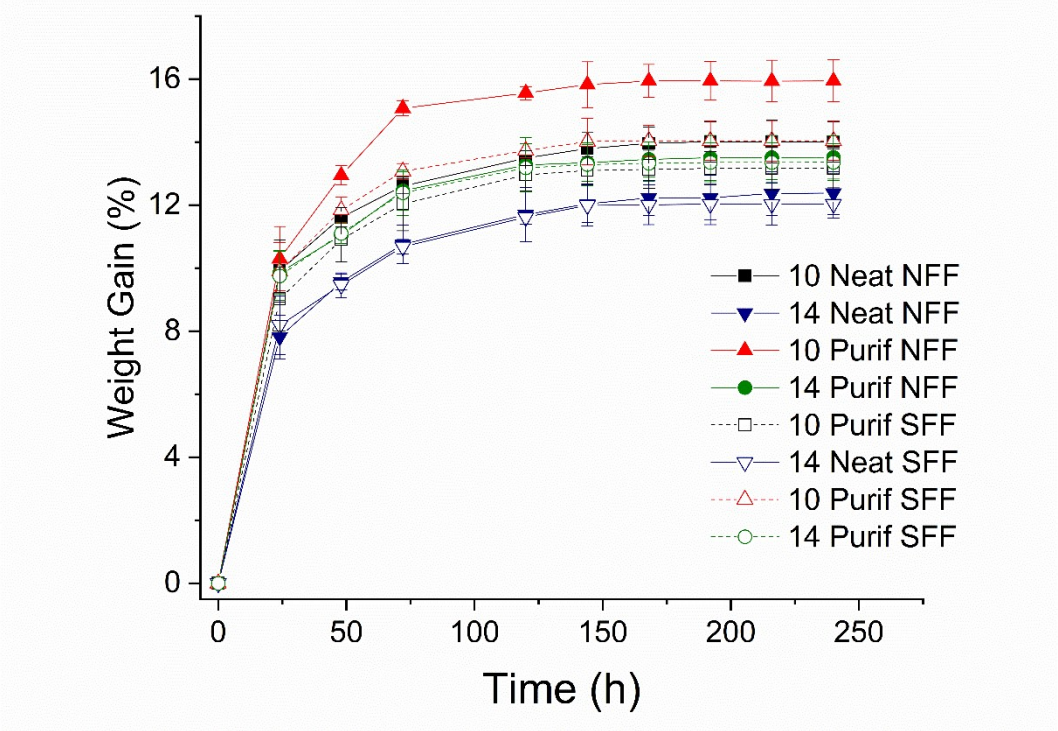


Figure 6.23: Weight gain curves as a function of the hygrothermal ageing time for composites reinforced with NFF (full lines) and SFF (dotted line) fibres.

Although literature discusses that different water sorption mechanisms can act independently, they take place simultaneously so that authors have modelled the whole phenomenon according to one single global diffusion process.[80] This coordinated penetration process can be mathematically described according to the Fick model of diffusion, Equation 6.2. In this expression, $M_t/M_{t0}$ represents the mass fluctuation due to sorption of water/loss of

soluble material along the hygrothermal ageing, *k* is a constant of proportionality, *t* is the immersion time of the material in the liquid medium and *n* is a parameter related to the type of diffusion.

Equation 6.2 $$M_t / M_{t0} = kt^n$$

Therefore, the overall diffusion process can be described according to the sum of the contributions of each of the mechanisms, which in turn are affected by the relative mobility of the penetrant in relation to the relaxation process observed in the polymer chains. In this regard, the Fickian model is able to describe and classify the diffusion phenomenon according to three different cases based on the relative penetration/relaxation behaviours: [76,81]

- Case I: Also described as Fickian diffusion case. In systems exhibiting this behaviour, the relative diffusion rate of the penetrant is much smaller than the mobility of the polymer chains. Chain relaxation and equilibrium are achieved very quickly. Mathematically, this process is identified constant n = 0.5.
- Case II: Opposite the previously described behaviour, this case describes processes of diffusion where the penetrating mobility is much greater than the relaxation of the polymer chains. Mathematically, Case II is characterized by constant n = 1.
- Case III: The diffusion described by this case occurs in an intermediate state between two previously presented cases. Consequently, the diffusion rate of the penetrating and the relaxation of the polymer chains take place in comparable time frames. This case is known as anomalous or non-Fickian diffusion, and is mathematically identified by constant n between 0.5 and 1.

Constants *n* were calculated from the experimental data through the linearization of Equation 6.2, which was transformed into Equation 6.3. In this expression, the parameter *n* can be calculated through the angular coefficient of $\log {M_t}/{M_{to}}$ versus $\log t$ plots.

Equation 6.3 $$log\, {M_t}/{M_{to}} = log\, K + n log t$$

Through the application of this mathematical method, values of the constant *n* were calculated from the mass gain curves for each composite formulations, Table 6.13 and 6.12. As observed, values of *n* were below the critical value 0.5 that defines the Fickian behaviour for all the formulations. Consequently, the fourth case of diffusional phenomena needs to be introduced to mathematically describe this kind of experimental observations: the so-called

Pseudo-Fickian sorption mechanism. This model is mathematically characterized by n < 0.5 and also commonly referred to in the literature as the two-stage diffusion.[82]

Table 6.13: Parameters n of the Fick model and mean diffusion coefficient for composites reinforced with flax and glass fibres.

| Formulation | Parameter n | $\overline{D}$ ($\times 10^3$ cm$^2$ min$^{-1}$) |
|---|---|---|
| **10NeatFF** | 0.35 | 5.56 |
| **14NeatFF** | 0.27 | 2.48 |
| **10PurifFF** | 0.33 | 9.35 |
| **14PurifFF** | 0.29 | 5.17 |
| **DGEBAFF** | 0.42 | 2.68 |
| **10NeatGF** | 0.35 | 0.07 |
| **14NeatGF** | 0.28 | 0.06 |
| **10PurifGF** | 0.44 | 0.81 |
| **14PurifGF** | 0.45 | 0.76 |
| **DGEBAGF** | 0.46 | 0.03 |

Table 6.14 Parameters n of the Fick model and mean diffusion coefficient for composites reinforced with chemically modified flax fibres (NFF and SFF).

| Formulation | Parameter n | $\overline{D}$ ($\times 10^3$ cm$^2$ min$^{-1}$) |
|---|---|---|
| **10NeatNFF** | 0.35 | 1.91 |
| **14NeatNFF** | 0.29 | 1.34 |
| **10PurifNFF** | 0.22 | 8.58 |
| **14PurifNFF** | 0.29 | 5.08 |
| **10NeatSFF** | 0.26 | 1.02 |
| **14NeatSFF** | 0.47 | 0.64 |
| **10PurifSFF** | 0.26 | 2.93 |
| **14PurifSFF** | 0.24 | 1.97 |

This particular diffusional phenomenon is not yet fully elucidated by literature; however, models discussed by Wind and Lenderink associate this observation to a process in which penetrant migrates at a non-constant rate over time. The presence of different diffusion rates within the same material is linked to the presence of defects in the structure, such as pores and voids, and of heterogeneous networks.[83,84] Alternatively, the Pseudo-Fickian diffusion can be described from the thermodynamic point of view. The phenomenon of penetration through the polymeric chains induces mechanical stress in the system and causes

localized swelling so that the polymer chains need to reorganize to accommodate this new state (*i.e.,* relaxation process). Therefore, Frisch discussed that the Pseudo-Fickian diffusion case represents a process where the chain relaxation is not fast enough to create a homogeneous gradient of penetrant concentration along the polymer in the long term. Consequently, zones with different concentrations of penetrating are formed, creating a scenario that diverges from the Fickian cases.[84] Based on this principle, Berens and Hopfenberg were able to elucidate more about the Pseudo-Fickian process through the elaboration of diffusion models based on the constants associated with the penetration rate and the rate of relaxation of the chains. This model demonstrated that, in the Pseudo-Fickian case, the global diffusion occurs in different stages: a fast step ruled by the Fickian regime, a transitional step where the relaxation and migration are similar, and finally a slow process controlled by the relaxation of the polymer chains.[84]

Even though the above-mentioned models could partially describe diffusional phenomenon more clearly, literature discusses that the analysis of Pseudo-Fickian cases is complex and far from being compeletly elucidated.[84] For instance, literature still fails to include additional factors that can also contribute to the diffusion of the penetrant, such as the presence of water-absorbing fibres. Therefore, these complex microscopic interactions in the diffusional phenomenon were approximate one case-free global phenomenon from the macroscopic point of view, which allows the calculation of the mean diffusion coefficient ($\overline{D}$). This measurement can be physically interpreted as the sum of the individual contributions of each of the mechanisms addressed, being obtained from Equation 6.4, which assumes that the diffusion process occurs with the square root of the time and is dependent on the width of the test body tested (given through b), as the general Fickian and Pseudo-Fickian consideration of transport by diffusion.

Equation 6.4

$$\frac{M_t}{M_\infty} = \frac{4}{b}\left(\frac{\overline{D}}{\pi}\right)^{0.5} t^{0.5}$$

The values of $\overline{D}$ for materials produced with glass and unmodified flax fibres (Table 6.13) demonstrated differences in the order of magnitude due to the incorporation of vegetable fibres into the composites. Since the flax fibres provided an additional preferential path of penetration absorption, $\overline{D}$ increases significantly in comparison with glass counterparts. Also, the effect caused by the cross-linking density, which decreases the chain mobility, could be quantitatively analysed through the decrease in the diffusion coefficients. Regarding the chemical modification methodologies (Table 6.14), all formulations presented reduced $\overline{D}$ in

comparison with analogous materials manufactured with unmodified fibre, reflecting the observations of improvements in the polymer/fibre interaction and reduction of micro cracks.

## 6.4 Summary

Chapter 6 presented the preparation of composite by wet lay-up using bio-based epoxy resin produced from WVO and reinforced with glass, flax and chemically modified flax fibres. The comparison between the mechanical properties of these materials with those produced with DGEBA revealed a dependency with the reinforcing fibre. Bio-based GRFC emulated the tensile properties to the commercial materials in terms of Young`s modulus, proving to be competitive alternatives. On the other hand, flax fibre reinforced composites presented smaller tensile properties due to incompatibility with the polymeric with the matrix, as detected by microscopy. In this regard, the chemical modification of the fibre surface with NaOH and stearic acid was able of increasing the tensile properties without sacrificing other parameters. Consequently, composites with intermediate tensile properties were produced by this approach, and improvements in the fibre/matrix interaction confirmed by SEM images and DMA (*i.e.* increase in the $T_g$). Chemical treatments have also reduced the water uptake, which is a known problem in the NFRC area. Adjustments in the formulation through the selection of a suitable hardener molar ratio demonstrated to mitigate the property losses caused by resins with reduced functionality, mimicking results from the previous chapter. Most importantly, the use of waste-based resins greatly improved impact properties in comparison with the brittle DGEBA matrix, demonstrating the usability of this class of resins in applications that demand toughness and stiffness over strength. Improvements in density were also reported. The replacement of DGEBA or resins from virgin oil sources for waste-based matrices caused no observable effect in the thermal stability, which proved to be mainly ruled by the natural fibre.

Results obtained in this Chapter demonstrated a mixture of opportunities and drawbacks associated with the mechanical behaviour of composites manufactured with WVO-derived matrices, particularly when thinking about the use of these laminates for structural applications. Therefore, these findings indicated that the application of these systems in high-performance composite formulations would require the exploration of different fibre and polymeric systems. In response to this scenario, investigations presented in the subsequent chapter explored the carbon fibres as reinforcing agents to promote improvement in the mechanical properties, while also taking advantage of the benefits brought by the WVO-based epoxy. To preserve the sustainability aspect of this thesis, Chapter 7 explored the use of recycled fibres.

## 6.5 References

1 O. Faruk, A. K. Bledzki, H.-P. Fink and M. Sain, *Prog. Polym. Sci.*, 2012, **37**, 1552–

1596.

2 K. L. Pickering, M. G. A. Efendy and T. M. Le, *Compos. - Part A Appl. Sci. Manuf.*, 2016, **83**, 98–112.

3 A. K. Bledzki and J. Gassan, *Prog. Polym. Sci.*, 1999, **24**, 221–274.

4 S. Mishra, A. K. Mohanty, L. T. Drzal, M. Misra and G. Hinrichsen, *Macromol. Mater. Eng.*, 2004, 955–974.

5 A. K. Mohanty, M. Misra and G. Hinrichsen, *Macromol. Mater. Eng.*, 2000, **276**–**277**, 1–24.

6 M. Ramesh, K. Palanikumar and K. H. Reddy, *Renew. Sustain. Energy Rev.*, 2017, **79**, 558–584.

7 M. P. M. Dicker, P. F. Duckworth, A. B. Baker, G. Francois, M. K. Hazzard and P. M. Weaver, *Compos. Part A Appl. Sci. Manuf.*, 2014, **56**, 280–289.

8 M. Y. Chen, M. Ike and M. Fujita, *Environ. Toxicol.*, 2002, **17**, 80–86.

9 T. R. Moore-Ambriz, D. G. Acuña-Hernández, B. Ramos-Robles, M. Sánchez-Gutiérrez, R. Santacruz-Márquez, A. Sierra-Santoyo, B. Piña-Guzmán, M. Shibayama and I. Hernández-Ochoa, *Toxicol. Appl. Pharmacol.*, 2015, **289**, 507–14.

10 H. Okada, T. Tokunaga, X. Liu, S. Takayanagi, A. Matsushima and Y. Shimohigashi, *Environ. Health Perspect.*, 2008, **116**, 32–38.

11 The European Comission, *Comission Regulation (EU) No 10/2011 of 14 January 2011 on plastic materials and articles intended to come into contact with food*, 2011.

12 S. G. Tan and W. S. Chow, *Polym. Plast. Technol. Eng.*, 2010, **49**, 1581–1590.

13 M. D. Samper, R. Petrucci, L. Sánchez-Nacher, R. Balart and J. M. Kenny, *Compos. Part B Eng.*, 2015, **71**, 203–209.

14 C. Zhang, T. F. Garrison, S. A. Madbouly and M. R. Kessler, *Prog. Polym. Sci.*, 2017, **71**, 91–143.

15 A. Maiorana, L. Ren, G. Lo Re, S. Spinella, C. Y. Ryu, P. Dubois and R. A. Gross, *Green Mater.*, 2015, **3**, 80–92.

16 F. Seniha Güner, Y. Yağcı and a. Tuncer Erciyes, *Prog. Polym. Sci.*, 2006, **31**, 633–670.

17 R. Auvergne, S. Caillol, G. David, B. Boutevin and J. Pascault, *Chem. Rev.*, 2014, **114**, 1082–1115.

18 U. Biermann, U. Bornscheuer, M. a R. Meier, J. O. Metzger and H. J. Schäfer, *Angew. Chem. Int. Ed. Engl.*, 2011, **50**, 3854–71.

19 Y. Xia and R. C. Larock, *Green Chem.*, 2010, **12**, 1893.

20 N. Boquillon, *J. Appl. Polym. Sci.*, 2006, **101**, 4037–4043.

21 W. Liu, T. Chen, T. Xie and R. Qiu, *Compos. Part A Appl. Sci. Manuf.*, 2016, **82**, 1–7.

22 D. P. Pfister and R. C. Larock, *J. Appl. Polym. Sci.*, 2013, **127**, 1921–1928.

23 R. L. Quirino, Y. Ma and R. C. Larock, *Green Chem.*, 2012, **14**, 1398–1404.

24 V. Ribeiro Da Silva, M. A. Mosiewicki, M. I. Yoshida, M. Coelho Da Silva, P. M. Stefani and N. E. Marcovich, *Polym. Test.*, 2013, **32**, 665–672.

25 R. P. Wool, in *Bio-Based Polymers and Composites*, eds. R. P. Wool and X. S. Sun, Elsevier Inc., 2005, pp. 114–148.

26 K. Adekunle, D. AKesson and M. Skrifvars, *J. Appl. Polym. Sci.*, 2010, **116**, 1759–1765.

27 M. Q. Zhang, M. Z. Rong and X. Lu, *Compos. Sci. Technol.*, 2005, **65**, 2514–2525.

28 L. Yan, N. Chouw and K. Jayaraman, *Compos. Part B Eng.*, 2014, **56**, 296–317.

29 D. B. Dittenber and H. V. S. Gangarao, *Compos. Part A Appl. Sci. Manuf.*, 2012, **43**, 1419–1429.

30 Z. Liu, S. Z. Erhan, D. E. Akin and F. E. Barton, *J. Agric. Food Chem.*, 2006, **54**, 2134–2137.

31 M. Fejős, J. Karger-Kocsis and S. Grishchuk, *J. Reinf. Plast. Compos.*, 2013, **32**, 1879–1886.

32 F. C. Fernandes, D. Lehane, K. Kirwan and S. R. Coles, *Eur. Polym. J.*, 2017, **89**, 449–460.

33 M. Jacob, S. Thomas and K. T. Varughese, *Compos. Sci. Technol.*, 2004, **64**, 955–965.

34 G. Kalaprasad, B. Francis, S. Thomas, C. R. Kumar, C. Pavithran, G. Groeninckx and S. Thomas, *Polym. Int.*, 2004, **1638**, 1624–1638.

35 L. G. Stringer, *Composites*, 1989, **20**, 441–452.

36 J. George, M. S. Sreekala and S. Thomas, *Polym. Eng. Sci.*, 2001, **41**, 1471–1485.

37 A. K. Mohanty, M. Misra and L. T. Drzal, *Compos. Interfaces*, 2001, **8**, 313–343.

38 M. M. Kabir, H. Wang, K. T. Lau and F. Cardona, *Compos. Part B*, 2012, **43**, 2883–2892.

39 M. Z. Rong, M. Q. Zhang, Y. Liu, G. C. Yang and H. M. Zeng, *Compos. Sci. Technol.*, 2001, **61**, 1437–1447.

40 A. C. H. Barreto, D. S. Rosa, P. B. A. Fechine and S. E. Mazzetto, *Compos. Part A Appl. Sci. Manuf.*, 2011, **42**, 492–500.

41 B. Wang, S. Panigrahi, L. Tabil and W. Crerar, *J. Reinf. Plast. Compos.*, 2007, **26**, 447–463.

42 E. Zini and M. Scandola, *Polym. Compos.*, 2011, **32**, 1905–1915.

43 S. N. Monteiro, V. Calado, R. J. S. Rodriguez and F. M. Margem, *Mater. Sci. Eng. A*, 2012, **557**, 17–28.

44 M. A. Fuqua, S. Huo and C. A. Ulven, *Polym. Rev.*, 2012, **52**, 259–320.

45 A. R. Martin, M. A. Martins, O. R. R. F. da Silva and L. H. C. Mattoso, *Thermochim.*

*Acta*, 2010, **506**, 14–19.

46 A. Oushabi, S. Sair, F. O. Hassani, Y. Abboud, O. Tanane and A. El Bouari, *South African J. Chem. Eng.*, 2017, **23**, 116–123.

47 N. Moigne and P. Navard, *Cellulose*, 2009, **17**, 31–45.

48 X. Li, L. G. Tabil and S. Panigrahi, *J. Polym. Environ.*, 2007, **15**, 25–33.

49 F. T. Wallenberger and P. A. Bingham, *Fiberglass and Glass Technology Energy-Friendly Compositions and Applications*, 2010.

50 S. V. Canevarolo, *Ciência dos Polímeros: Um Texto Básico para Tecnólogos e Engenheiros*, Artiliber, São Paulo, 1st edn., 2004.

51 F. C. Fernandes, K. Kirwan, P. R. Wilson and Coles, *Green Mater.*, 2018, **6**, 38–46.

52 M. Flanagan, in *Polymer Characterisation*, eds. B. M. Hunt and M. I. James, Blackie Academic and Professional, London, 1st edn., 1993, p. 287.

53 S. V. Canevarolo, *Técnicas de Caracterização de Polímeros*, Artiliber, São Paulo, 1st edn., 2004.

54 H. Miyagawa, M. Misra, L. T. Drzal and A. K. Mohanty, *Polym. Eng. Sci.*, 2005, **45**, 487–495.

55 G. Mashouf Roudsari, A. K. Mohanty and M. Misra, *ACS Sustain. Chem. Eng.*, 2017, **5**, 9528–9541.

56 G. Koronis, A. Silva and M. Fontul, *Compos. Part B Eng.*, 2013, **44**, 120–127.

57 G. Mashouf Roudsari, A. K. Mohanty and M. Misra, *ACS Sustain. Chem. Eng.*, 2017, acssuschemeng.7b01422.

58 A. J. Lesser, *Polymer (Guildf).*, 1997, **18**, 16–27.

59 S. K. Ramamoorthy, Q. Di, K. Adekunle and M. Skrifvars, *J. Reinf. Plast. Compos.*, 2012, **31**, 1191–1200.

60 S. S. Morye and R. P. Wool, *Polym. Compos.*, 2005, **26**, 407–416.

61 C. S. M. F. Costa, A. C. Fonseca, A. C. Serra, J. F. J. Coelho, A. C. Fonseca, A. C. Serra and J. F. J. C. Dynamic, *Polym. Rev.*, 2016, **56**, 362–383.

62 J. R. Kim and S. Sharma, *Ind. Crops Prod.*, 2012, **36**, 485–499.

63 A. Campanella, J. J. La Scala and R. P. Wool, *Polym. Eng. Sci.*, 2009, **49**, 2384–2392.

64 N. Karak, *Vegetable oil-based polymers.*, Woodhead Publishing, Cambridge, United Kingdom, 2012.

65 J. M. F. De Paiva and E. Frollini, *Macromol. Mater. Eng.*, 2006, **291**, 405–417.

66 L. A. Pothan, Z. Oommen and S. Thomas, *Compos. Sci. Technol.*, 2003, **63**, 283–293.

67 S. V. Hoa and P. Ouellette, *Polym. Compos.*, 1984, **5**, 334–338.

68 M. a. Mosiewicki and M. I. Aranguren, *Eur. Polym. J.*, 2013, **49**, 1243–1256.

69 S. Prabhakaran, V. Krishnaraj, M. Senthil Kumar and R. Zitoune, *Procedia Eng.*, 2014, **97**, 573–581.

70 R. Chandra, S. P. Singh and K. Gupta, *Compos. Struct.*, 1999, **46**, 41–51.

71 H. P. Lee, B. M. P. Ng, A. V. Rammohan and L. Q. N. Tran, *J. Nat. Fibers*, 2017, **14**, 71–77.

72 D. Shanmugam and M. Thiruchitrambalam, *Mater. Des.*, 2013, **50**, 533–542.

73 V. Fiore, G. Di Bella and A. Valenza, *Compos. Part B Eng.*, 2015, **68**, 14–21.

74 D. Watkins, M. Nuruddin, M. Hosur, A. Tcherbi-Narteh and S. Jeelani, *J. Mater. Res. Technol.*, 2015, **4**, 26–32.

75 W. Chunhong, L. Shengkai and Y. Zhanglong, *J. Reinf. Plast. Compos.*, 2016, **35**, 1062–1074.

76 A. Espert, F. Vilaplana and S. Karlsson, *Compos. Part A Appl. Sci. Manuf.*, 2004, **35**, 1267–1276.

77 Z. N. Azwa, B. F. Yousif, a. C. Manalo and W. Karunasena, *Mater. Des.*, 2013, **47**, 424–442.

78 A. Toscano, G. Pitarresi, M. Sca, M. Di Filippo, G. Spadaro and S. Alessi, *Polym. Degrad. Stab.*, 2016, **133**, 255–263.

79 A. A. C. Pereira and J. R. M. D'Almeida, *Polímeros*, 2016, **26**, 30–37.

80 S. Panthapulakkal and M. Sain, *J. Compos. Mater.*, 2007, **41**, 1871–1883.

81 G. K. Van Der Wel, *Prog. Org. Coatings*, 1999, **37**, 1–14.

82 D. Jou, J. Camacho and M. Grmela, *Macromolecules*, 1991, 3597–3602.

83 M. S. Hedenqvist, M. Krook and U. W. Gedde, *Polymer (Guildf).*, 2002, **43**, 3061–3068.

84 M. M. Wind and H. J. W. Lenderink, *Prog. Org. Coatings*, 1996, **28**, 239–250.

# Chapter 7

# WVO-Based Matrices Reinforced with Recycled Carbon Fibres:

## Investigation of the Resistance to Barely-Visible Impact Damage

Contents of this chapter have been published at:

F. C. Fernandes, K. Kirwan, P. R. Wilson, C. Froemder and S. R. Coles, *Proceedings of SAMPE Europe 2018,* 2018.

## 7.1 Introduction

One of the main lessons from the previous chapter was the necessity of exploring alternative fibre systems to push further the properties of WVO-derived resins and consequently enable its implementation in commercial systems. In this regard, composites produced with thermoset resins and high-performance reinforcements such as carbon fibres (CF) have been historically selected to replace traditional materials such as steel and aluminium in a number of applications due to characteristics such as lightweight, high strength and stiffness.[1] For example, aerospace and commercial aircraft industries have been incorporating an increasing number of structural parts in the fuselage manufactured with carbon fibre reinforced composites (CFRC) To illustrate this trend, latest commercial aircrafts such as the Boeing 787 Dreamliner uses up to 50 wt% of advanced composites in different components, Figure 7.1.[2] Recent market reports indicated that this trend will keep expanding in the following years and will be propelled by new manufacturing technologies being matured to cope with the volumes of production and safety requirements.[3–6] Therefore, the exploration of CFRC in this final experimental chapter appeared as an interesting opportunity to expand the library of composite formulations with commercially-relevant materials and investigate the potential applicability of WVO in high-end products.

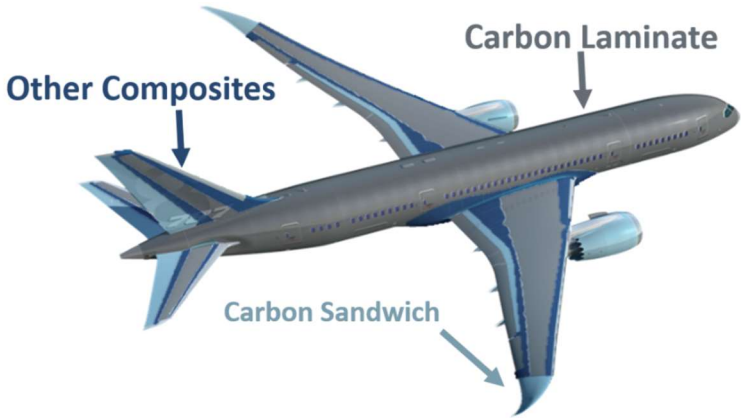


Figure 7.1: Representation of composite structural parts found in a Boeing 787 Dreamliner. Adapted from Boeing.com.[2]

As presented in previous chapters, the use of triglyceride-based epoxies led to improvements in impact behaviour by facilitating quick relaxation of the networking. In here, this particular behaviour was investigated as a way to tackle some of the current challenges in the epoxy/CFRC field. Despite many advantages offered by these systems, CFRC produced with epoxy matrices present challenges linked with the maintenance and detection of critical damage.[7,8] For example, as a consequence of the inherent brittleness of these systems, low-velocity impacts can lead to internal delamination whilst leaving a visually undamaged

surface. This phenomenon is known as barely visible impact damage (BVID) and is a serious issue from the integrity standpoint, Figure 7.2.[9] Although the low-energy impact is not drastic enough to cause fibre failure, it may lead to matrix cracking at inter-ply locations due to interlaminar sheer and tensions.[10] The action of further stresses during the component's use phase slowly increases this delamination point, progressively reducing stiffness and ultimately leading to catastrophic failure. The latter represents a scenario where the failure is sudden and total, and recovery of integrity is impossible.[11] In aircrafts, BVID can occur as consequence of the impact of small objects (*e.g.* as runaway debris during take-off/landing) at moderate speeds or moderately heavy objects at slow speeds (*e.g.* tools dropped on the component during assembly/maintenance).[10]

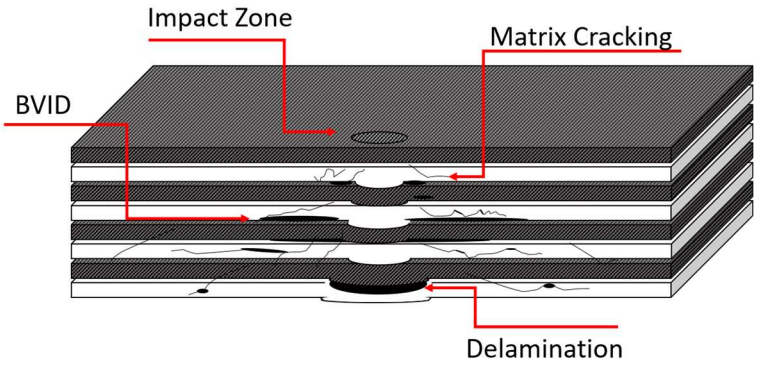


Figure 7.2: Representation of Barely-Visible Impact Damage (BVID) and consequences of this phenomenon in a composite laminate.

In this stage of the study, we propose the utilisation of bio-based epoxy blends from WVO in CF laminates to reduce the brittleness of these systems and consequently prevent delamination caused by BVID.[12] The strategy of preparing blends combining bio-based epoxy and DGEBA was decided as an effective approach to mitigate the inferior mechanical performance of VO-based while maintaining the environmental benefits and reducing delamination due to impact.[13] Furthermore, the use of WVO for this application adds a new layer of sustainability never experienced in CFRC laminates, bringing environmental, economic and social benefits to the composite manufacturing area.[14,15] The use of rCF and WVO-based resins permitted the combination of two waste streams into one single material for engineering purposes.

Additionally, the exploration of recycled carbon fibres (rCFs) in composite manufacturing appears as an attractive approach to simultaneously tackle the challenges associated with the manufacturing step and end-of-life of CFRC, producing more environmentally-friendly composites.[16,17] The reintegration of CF in the production loop reduces the environmental footprint of composite manufacture since the recycling process is

less energy-intensive than the production of the virgin materials.[18] Recyclates can be obtained in different grades by methodologies such as mechanical recycling, pyrolysis, oxidation and solvolysis.[16,19] Despite the reduction in tensile strength as a consequence of the recycling processes, rCFs are competitive materials since they can present values of stiffness similar to virgin feedstock.[20] Consequently, rCFs can make CF more accessible and ultimately enable novel applications for this material.[21,22]

In this chapter, blends were optimised according to their formulation/property relationships, and CFRC manufactured by vacuum-bagging technique for better consolidation and finishing. Composites were also produced using virgin feedstock (vCF) to investigate the effect caused only by the addition of the bio-based epoxy in the formulation and assessing the feasibility the incorporation of waste-derived EVO in high-end products. Finally, a study focused on the impact of composite laminates permitted the assessment of these formulations as alternatives to reduce BVID-related issues in CFRC.

## 7.2 Methodology

### 7.2.1 Materials

Bio-based epoxy resin was produced from WVO according to the methodologies presented in Chapter 5. Recycled carbon fibres (rCF) were supplied by ELG Carbon Fibres (Carbiso M100$^{TM}$, roll, 100 gsm) and virgin fibres were supplied by Sigmatex UK Limited (Sigmatex T700 SC, 299 gsm). Consumables used for the vacuum bagging were supplied by Easy Composites UK. Super Sap CLR® was used reference epoxy (DGEBA with 17 wt% of bio-based additives, Entropy Resins, United States) and Aradite® HY (methylhexahydrophthalic anhydride – MHHPA – SilMid Limited, UK) was used as hardener.

### 7.2.2 Thermosets and Composites Preparation

Thermosets were produced by combining the DGEBA resin with EPVO at varying quantities according to the ratios presented in Table 7.1. The quantity of the curing agent was adjusted according to variations in the epoxy equivalent caused by the addition of the bio-based resin. Based on the methodologies presented in Chapter 5, triethylamine (1 mol%) was added in all formulations as the initiator, and the system was mixed thoroughly for 2 min and degassed for 5 min. The resulting mixtures were poured in test sample-shaped silicon moulds (scaled version of ASTM D638) and cure in an oven (ThermoScientific Heraterm) according to the following cycle: from 50 °C to 150 °C in 1 h, 8 h at 150 °C and from 150 °C to 50 °C in 1 h.

Table 7.1: Thermoset samples, their bio-based content and ratio of the components in each formulation.

| Sample | Bio-Based Epoxy Content (wt%) | Ratios (EPVO:DGEBA:Aradur) |
|---|---|---|
| *0EPVO* | 0 | 0:100:98 |
| *10EPVO* | 10 | 10:90:85 |
| *20EPVO* | 20 | 20:80:75 |
| *30EPVO* | 30 | 30:70:67 |
| *40EPVO* | 40 | 40:60:61 |
| *50EPVO* | 50 | 50:50:55 |

For the composite preparation, CF mats (rCF and vCF) were cut into 40×40 $cm^2$ squares from the roll of material, and oven dried (ThermoScientific Heraterm) at 95 °C for 4 h. Four sheets of CF were used for tensile tested panels and twelve sheets for flexural tested panels to achieve a satisfactory thickness. After drying, plies were manually laminated and infused with the resin using a roll and a brush onto a PTFE-covered steel place (42×42 $cm^2$) to produce a panel with 30 wt% of fibre. vCF reinforced composites were produced a fibre content of 50 wt% since the previous content would force the excess amounts of resin to overflow and potentially damage the vacuum system. The laminated was covered with another steel plate and the panel was wrapped in breath fabric. A vacuum bag with a port located in the centre of the panel was assembled as schematically presented in Figure 7.3, with the combination of the weight of the steel plate and negative pressure simulating compression conditions. Finally, the system was cured in an oven (ThermoScientific Heraterm) according to the same cycle presented above.

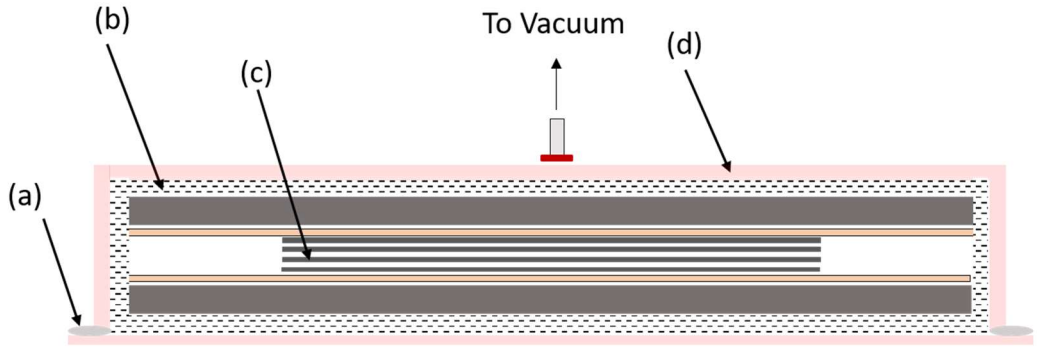


Figure 7.3: Experimental set-up for the production of carbon fibre reinforced composite panels.

Table 7.2: Summary of the composite formulations prepared with recycled (rCF) and virgin (vCR) carbon fibres.

| Sample | Bio-Based Epoxy Content (wt%) | Ratio (EPVO:DGEBA:Aradur) | Carbon Fibre Type | Fibre Content (wt%) |
|---|---|---|---|---|
| *DGEBA rCF* | 0 | 0:100:98 | Recycled | 30 |
| *Blend rCF* | 30 | 30:70:67 | Recycled | 30 |
| *DGEBA vCF* | 0 | 0:100:98 | Virgin | 50 |
| *Blend vCF* | 30 | 30:70:67 | Virgin | 50 |

### 7.2.3 Characterisations

Thermogravimetric Analysis (TGA), Dynamic Scanning Calorimetry (DSC) and Dynamic Mechanical Analysis (DMA) and the calculation of the crosslinking ($\nu_e$) were done according to the procedures described in Chapter 5. Resin viscosity measured were carried out using a Brookfield Viscometer DV2T, using a LV-3 spindle, speed of 150 rpm, temperature of 19.0 °C. For the tensile tests, composite panels were dimensioned according to ASTM D3039/D3039M and tested using an Instron 100 kN Static Load Cell equipped with video extensometer, test speed of 2 mm $min^{-1}$ . A minimum of seven successfully specimens were tested for each formulation. For flexural tests, panels were dimensioned following the ISO 14125 and tested using an Instron 30 kN Static Load Cell equipped with four-point bending rig, head displacement of 22 mm, the gauge length of 66 mm with a 40 mm extensometer and test speed of 2.3 mm $min^{-1}$ . Specimen produced from rCF composites were tested at different fibre alignment (parallel and perpendicular orientation) to understand the impact of this characteristic. Densities were calculated with a Mettler Toledo balance with density measurement accessory. Values were obtained in ethanol at 21.1 °C.

For ultrasound, impact specimen (100 x 150 $mm^2$) were analysed with an AmsTech Miniscanner. The scanned area was 12 x 25 $mm^2$, scan time of 4 s, wave speed of 3000 m $s^{-1}$ and resolution of 0.1 mm. For impact tests, panels were dimensioned according to the standard ASTM D7136/ D7136M into specimen of 100 x 150 $mm^2$, positioned in the 300 x 300 $mm^2$ fixture base with a cut out 75 x 125 $mm^2$ and fixed with four toggle clamps with rubber tips centred 6 mm from the edge of the cut-out. Damage was inflicted out-of-plane (perpendicular to the plane of the laminated plate) using a drop weight (1 kg) with a hemispherical striker tip from a 51 cm height (5 J impact). Compression tests were carried out using damage and undamaged test panels according to ASTM D7137/D8137M using an Airbus AITM1.0010 fixture and an Instron 100 kN Static Load Cell. Speckled specimens (black and white pattern)

were mounted in the compression rig, submitted to a 150 N pre-load to check alignment and tested at 1.25 mm $min^{-1}$ crosshead speed until failure. Three specimens were tested for each composite formulation. During the test, two Teledyne Dalsa cameras equipped with 75 mm lenses pointed at specimen at an angle of 25° (calibrated at a deviation of 0.028 pixels) were used to record images at 5 Hz for the digital image correlation (DIC) analysis. Deformantion surfaces were calculated using a GOM Aramis Professional 2018® software, with facets of 19 pixels.

## 7.3 Results and Discussions

### 7.3.1 Investigation of the Partially Bio-Based Blends

After demonstrating the successful production of polymers and composites entirely based on WVO-derived resins in previous chapters, systems herein investigated again explored the production of blends with DGEBA. Although this approach can initially seem as a step backwards in terms of sustainability, this strategy was adopted to ensure the manufacture of materials with mechanical performance compatible with those demanded by the composite market. Also, blends applied at this stage have incorporated the knowledge generated in previous chapters in terms of comprehending the epoxidized WVO reactivity versus different hardeners. Therefore, it was anticipated that these new blend formulations would provide better properties than those investigated in Chapter 4. Finally, TEA was selected over 2-MI as a catalyst to avoid the heating stage required to homogenise the mixture, which could be a challenge considering the volumes of resin used at this late stage. Therefore, this decision was taken to facilitate future process scale-up.

Preliminary studies concentrated on the investigation of new relationships between the bio-epoxy content and the properties of the resulting thermosets. This optimisation step would enable the production of matrices with suitable mechanical properties and maximum renewable content for the manufacture of composites. DSC was explored to comprehend the effect the EPVO content in the network, Figure 7.4. The integration of the main exothermic peak ($\Delta H_{Cure}$) revealed a reduction of the total heat of reaction when the increase in the bio-based content, Table 7.3. These results are similar to those observed by Samper *et al.*, who demonstrated the relationship between the epoxy equivalent and the exothermicity of the network formation.[23] Also, this behaviour was previously detected for thermosets produced with amines in Chapter 4.[24] In this regard, the comparison between the two systems (anhydride versus amine-cured polymers) revealed smaller values of $\Delta H_{Cure}$ for the networks cured with MHHPA, demonstrating the reduced exothermicity this phenomenon when it is led by anhydrides.[25]

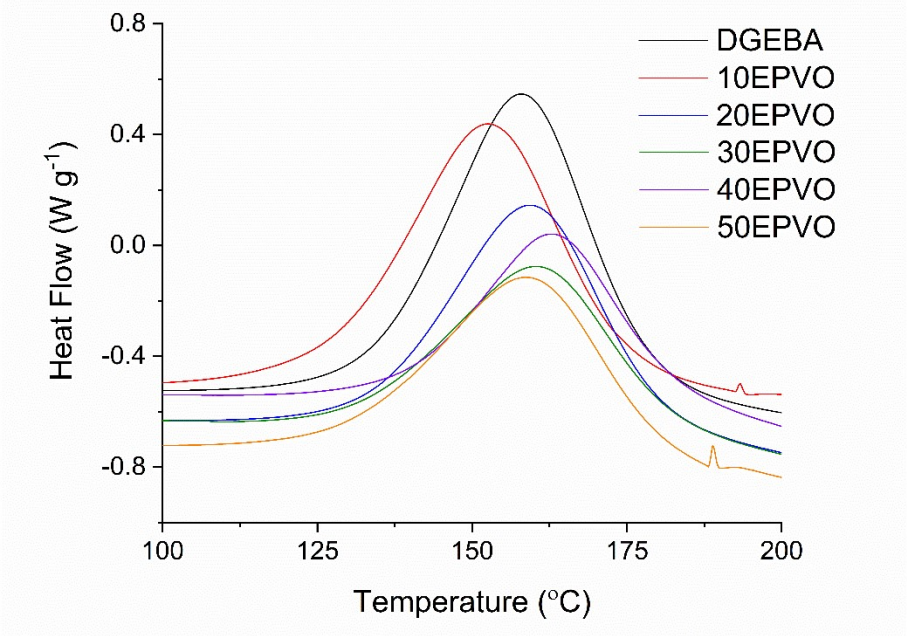


Figure 7.4: Peaks of cure of calorimetric curves obtained from dynamic DSC of blends with different bio-based content, heating rate of 10 °C $min^{-1}$.

Table 7.3: Enthalpy of cure and peak of the enthalpy of blends with different bio-based contents

| Sample | $\Delta H_{Cure}$ (J $g^{-1}$) | $\Delta H_{Cure}$ (kJ $mol^{-1}$) | $\Delta H_{Cure}$ Peak (°C) |
|---|---|---|---|
| DGEBA | 31.9 | 5.50 | 157.8 |
| 10EPVO | 30.4 | 5.42 | 152.7 |
| 20EPVO | 24.9 | 5.18 | 158.8 |
| 30EPVO | 21.2 | 4.57 | 158.7 |
| 40EPVO | 20.3 | 4.56 | 160.1 |
| 50EPVO | 18.7 | 4.41 | 160.6 |

Despite the reduction in $\Delta H_{Cure}$, peaks remained unchanged in terms of position, indicating that the bio-based epoxy does not alter the reaction mechanism, following the same cure regime observed for DGEBA formulations. Additionally, it is noteworthy that this strategy has demonstrated the incorporation of up to 50 wt% of EPVO without significant drawbacks in the network formation. Previously, networks with EPVO content above 30 wt% failed to yield rigid thermosets due to an excessive plasticization effect, meaning that the units derived from the triglyceride were not integrated into the crosslinks.

Blends were also investigated from the dynamic-mechanical point of view, and curves of E' versus temperature evidenced differences in the elastic behaviour of the network caused by the addition of EPVO, Figure 7.5. Similarly to what observed in Chapter 4, systems

presented reduced elastic behaviour when EPVO was gradually incorporated in the formulations due to the reduced molecular rigidity observed in the aliphatic backbones.[26] The lack of aromaticity resulted in weaker intermolecular, contributing towards a reduced elastic behaviour. Consequently, maximum E` was gradually reduced (from 10% to 40%) with the increments of bio-based epoxy in the DGEBA formulation. Interestingly, the formulation containing 10 wt% of waste-based epoxy presented an initial storage modulus 62% higher than the reference formulation containing only DGEBA. Moreover, curves demonstrated no significant increase of E` with temperature associated residual cure process.

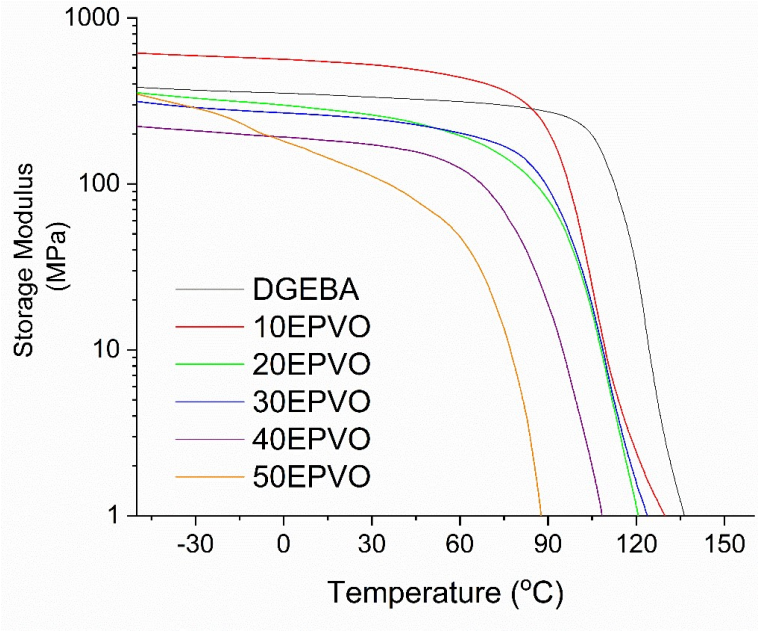


Figure 7.5: Storage modulus of thermoset polymers with different contents of bio-based epoxy.

These curves were also used to investigate the $T_g$ of the resulting networks, Table 7.4. An inversely proportional relationship between the $T_g$ and the bio-based content was observed in these systems, result which was aligned with previous studies in the literature.[27] This demonstrated that structural factors associated with the triglyceride unit, such as its aliphatic nature, are responsible for facilitating the coordinated mobility gain in the blends with. Despite the increased E', the formulation *10EPVO* followed the same pattern observed for the other partially bio-based blends.

Table 7.4: Glass transition temperature ($T_g$) of thermoset polymers with contents of bio-based epoxy.

| Sample | $T_g$ (°C) | $v_e \times 10^{-4}$ |
|---|---|---|
| DGEBA | 104.4 | 0.40 |
| 10EPVO | 86.8 | 0.36 |
| 20EPVO | 85.5 | 0.33 |
| 30EPVO | 83.4 | 0.31 |
| 40EPVO | 69.0 | 0.24 |
| 50EPVO | 61.2 | 0.20 |

Above all, these systems could produce networks with $T_g$ ranging from 86.8 to 61.2 °C, representing a significant improvement from polymers developed in Chapter 4. For example, the comparison between formulations with the same amount of EPVO (10 wt%) revealed an increase almost 40 °C (47.4 versus 86.8 °C) due to the incorporation of the developments from Chapter 5 in terms of formulation optimisation (*i.e.* the selection of appropriate hardener/catalyst). Moreover, values of $T_g$ observed for all bio-based formulations were compatible with previous reports in the literature due to the selection of the right combination of between hardener and curing conditions, demonstrating the applicability of these thermosets.[14,28,29]

As discussed in previous chapters, the reduced $T_g$ could also be associated with EPVO's limited capacity of forming networks. The investigation of the cross-linking density ($v_e$, Table 7.4) demonstrated that became gradually less tightly-connected due to the reduced capacity of network formation observed in EPVO versus DEGBA due to factors such as steric hindrance.[30] The variation of $T_g$ and $v_e$ with the bio-based content revealed not only the interconnection between these two properties but also provided support for the selection of the most suitable formulation in this study, Figure 7.6. In this regard, significant drops were observed from *30EPVO* to *40EPVO*, where the addition of 10 wt% of EPVO in the formulation reduced the $T_g$ by 14.4 °C. Since the maximization of $T_g$ was considered as an essential criterion towards producing oil-based polymers, the formulation *30EPVO* was elected as the one presenting the best balance of properties at this stage.

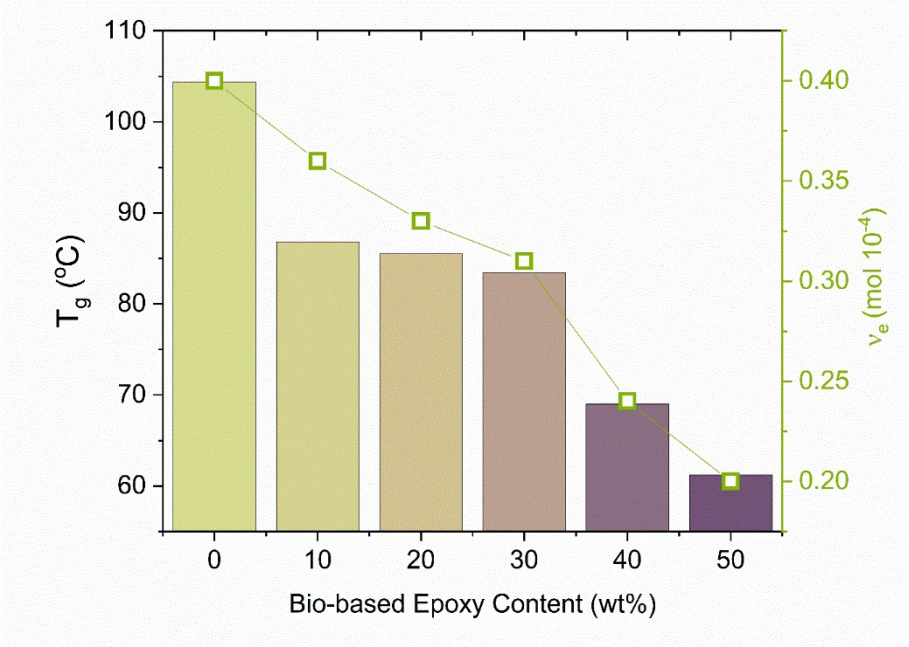


Figure 7.6: Glass transition temperature ($T_g$) and crosslinking density ($\nu_e$) as a function of the bio-based epoxy content in blended formulations cured with anhydride.

Despite the changes discussed above, weight-loss curves obtained by TGA (Figure 7.7) demonstrated that all blends presented similar thermal behaviour to that observed for the reference formulation. Curves of the first derivative of the weight-loss in respect to the temperature (bottom image) also demonstrated the remarkable similarity in terms of how the blend and the reference polymer thermally degraded.[31] Nevertheless, small distinctions can be detected from the analysis of the minor and major weight-loss events ($T_{Onset}$1 and 2, respectively). The first degradation step was associated with the presence of unreacted epoxy as this event coincided with what was observed for the isolated materials (Chapter 4). On the other hand, the following weight-loss event was attributed to the thermal degradation of the network itself. Despite the presence of different amounts of WVO-based resin, formulations *10EPVO* to *50EPVO* presented similar values of $T_{Onset}$ and $T_{Max}$ (Table 7.5). This observation evidenced that the quantity of bio-based resin does not alter the thermal degradation mechanism. Interestingly, blends produced in this chapter resulted in networks with thermal stability up to 63 °C higher than those produced previously with amines, demonstrating another advantage of the use of anhydrides.

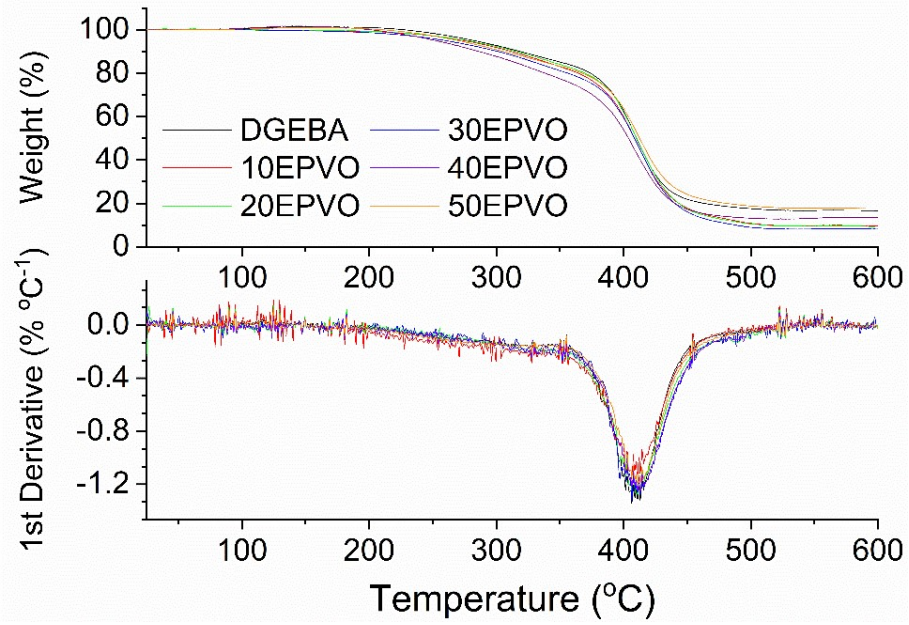


Figure 7.7: Weight-loss curves (top) and first derivative curves with respect with temperature (bottom) of formulations with varying contents of bio-based epoxy resin.

Table 7.5: Temperature of initial degradation and of maximum rate of degradation for formulations with varying contents of bio-based epoxy resin.

| Sample | $T_{Onset}$ 1 (°C) | $T_{Onset}$ 2 (°C) | $T_{Max}$ (°C) |
|---|---|---|---|
| DGEBA | 250.7 | 385.0 | 406.3 |
| 10EPVO | 264.8 | 387.5 | 409.7 |
| 20EPVO | 282.8 | 389.0 | 406.3 |
| 30EPVO | 280.3 | 390.9 | 411.0 |
| 40EPVO | 286.3 | 391.6 | 406.3 |
| 50EPVO | 285.8 | 391.6 | 413.0 |

### 7.3.2 Carbon Fibre Reinforced Composites

Based on the characterisations discussed above, the formulation with a 30wt% bio-based content was selected to produce the composite laminates with rCF and vCF. Laminates were prepared using a vacuum bag with two steel plates sandwiching the panel, providing extra compression and consequently enhancing the resin impregnation. Additionally, the use of two plates ensured the production of panels with smooth surface finishing in both sides. It is important to mention that Chapter 6 highlighted that the use of a vacuum bag could damage components of the vacuum line and of the panels themselves. However, these issues were minimised by using an excess of breath fabric around the plates to prevent resin leak and a more appropriated vacuum bag film. Figure 7.8 presents cuts of specimens resulting from

panels produced combining bio-based blend and A) rCF and B) vCF, demonstrating differences in their physical aspect.

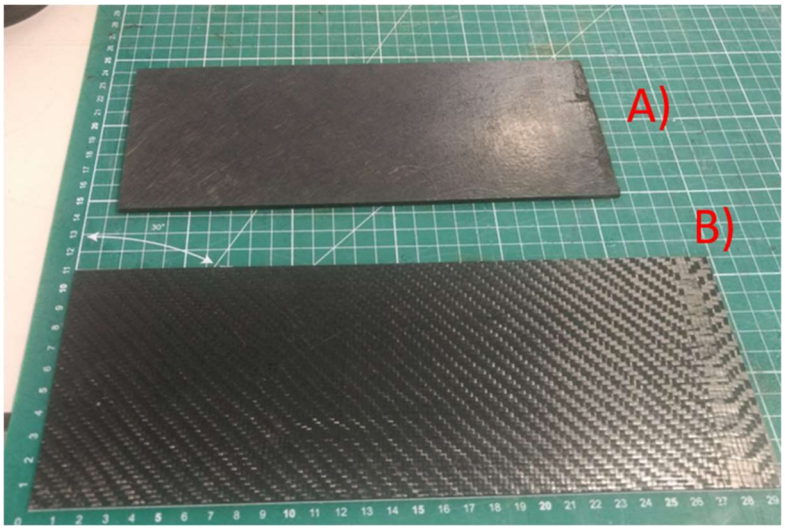


Figure 7.8: Composite panels produced with bio-based blend reinforced with A) recycled carbon fibres (rCF) and B) virgin carbon fibres (vCF)

**a) Tensile performance**

Panels were cut according to ASTM 3039 and tested with the presence of end-tabs prepared with epoxy and glass fibres. The addition of these tabs is recommended when tensile testing brittle materials (such as DGEBA/ CF) since the pressure induced by the grips can damage the sample surface, causing micro-cracks and consequently leading to premature failure outside the gauge length.[32] Figure 7.9 displays characteristic tensile stress/strain curves of panels produced with the blended resin versus benchmark manufactured with DGEBA (for both rCF and vCF). These curves illustrated the stiffness of these laminates (particularly with vCF), elevated stress at the break but brittle nature, with mechanical failures taking place at small displacements values. Also, representative stress versus strain curves suggested a dependence between the mechanical response and the addition of bio-based resins to the blends.

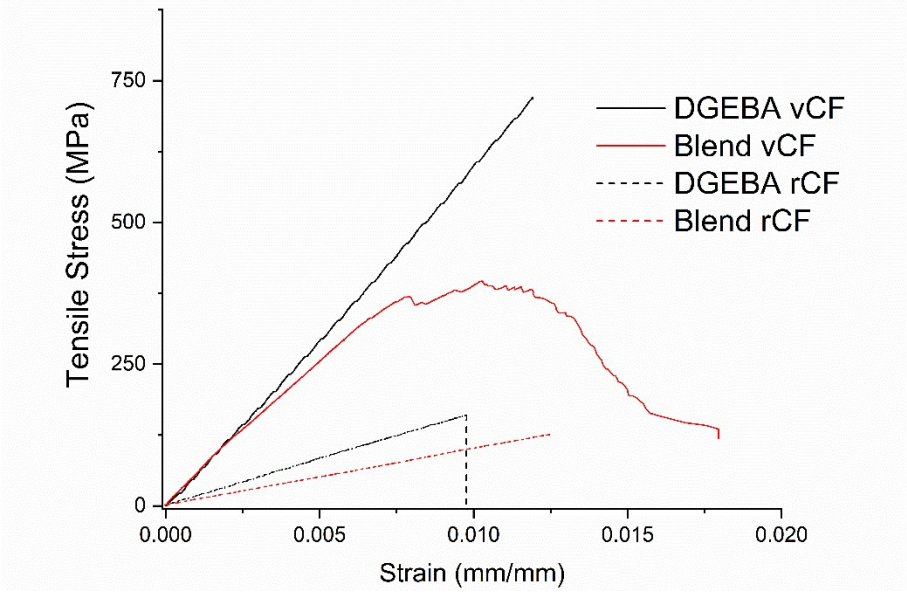


Figure 7.9: Representative stress/strain curves of composites prepared with commercial (black) and blended (red) resins, reinforced with virgin (full lines) and recycled (dashed lines) fibres.

Another interesting feature detected in some curves was the delamination process, exemplified by the *Blend vCF* curve. In these cases, the specimen continued to be deformed without complete compromise in physical integrity after the maximum stress point, so the mechanical energy was responsible for the continuation of delamination. Typically, this process is one of the most common failure modes on composite laminates, together with matrix cracking and fibre fracture, and takes place parallel to the surface.[33] Overall, this phenomenon inserted a yield point to the composite tensile response, which can be associated with a pseudo plasticity behaviour and could be used to detect an imminence catastrophic failure.[34] Also, the delamination could be interpreted as a consequence of intrinsically low interlaminar shear stress between the matrix and the laminates and was particularly observed for the combination between the bio-based blend and vCF.[35,36]

A more detailed comparison in terms of the performance of these materials is found in Table 7.6 and Figure 7.10. Partially bio-based composites presented tensile strength (400 ± 20 MPa) and Young`s modulus (40 ± 4 GPa) smaller than the benchmark, reflecting previous results obtained in Chapters 4 and 6. Nevertheless, these properties were the highest registered for any composite prepared with WVO so far in the study. Also, as demonstrated in Table 7.6, the elongation at break was increased when the bio-based epoxy was added to the DGEBA system. Although the same trend was detected in Chapter 4, that case could be associated with a plasticization effect due to the scale of the elongations obtained. Herein, the increased elongation at break demonstrated by composites produced with EPVO revealed that these materials could resist to a higher deformation before it catastrophically failed. This is an

interesting feature considering the typical challenge associated with the elevated brittleness of DGEBA composites reinforced with carbon fibres.[37,38]

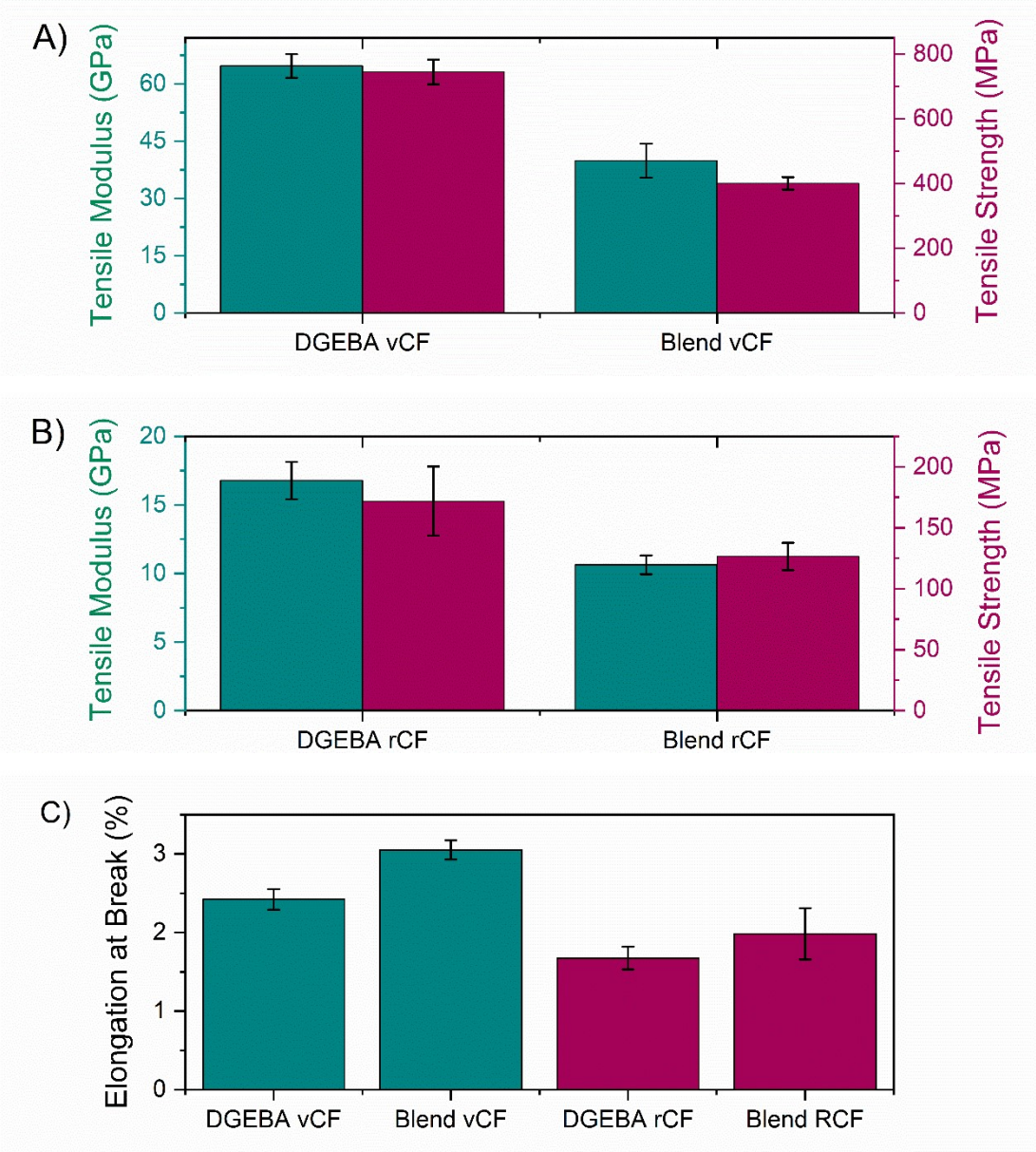


Figure 7.10: Young's modulus and tensile strength of composites reinforced with A) virgin (vCF) and B) recycled carbon fibres (rCF) and C) elongation at break for all formulations.

Table 7.6: Young's modulus, tensile strength and extension at break of composites reinforced with virgin (vCF) and recycled carbon fibres (rCF).

| **Formulation** | **Tensile Modulus (GPa)** | **Tensile Strength (MPa)** | **Elongation at Break (%)** | **Density (g cm$^{-3}$)** | **Specific Tensile Modulus (GPa g$^{-1}$ cm$^3$)** |
|---|---|---|---|---|---|
| DGEBA vCF | 65 ± 3 | 745 ± 38 | 2.4 ± 0.1 | 1.45 ± 0.02 | 44 ± 4 |
| Blend vCF | 40 ± 4 | 400 ± 20 | 3.1 ± 0.1 | 1.42 ± 0.04 | 28 ± 3 |
| DGEBA rCF | 17 ± 1 | 172 ± 28 | 1.7 ± .1 | 1.11 ± 0.08 | 15 ± 2 |
| Blend rCF | 11 ± 1 | 126 ± 10 | 2.0 ± 0.3 | 1.05 ± 0.07 | 11 ± 1 |

Composites prepared with rCF (Figure 7.10B) have demonstrated similar behaviour in terms of how properties varied with the EPVO content. *Blend rCF* presented an average of 11 ± 1 GPa of Young's Modulus and 126 ± 10 of tensile strength, reductions of 35% and 26% in comparison with the *DGEBA rCF*, respectively. These observations can be associated again with the intrinsic differences between DGEBA and EPVO resins at the molecular level. Therefore, changes were consistent regardless the fibre used to reinforce the composite. Also, materials produced with recycled feedstock presented relative larger standard deviations, demonstrating the intrinsic variability of the rCF due to the recycling process. Considering the specific properties (Table 7.6), composites prepared with EPVO could deliver similar properties to DGEBA equivalents when the properties gain is normalised by the weight gain.

More important than revealing the reductions caused by the addition of bio-based epoxy was the analysis of properties that were enhanced by this strategy. The addition EPVO reduced the density of the resulting panels in comparison with commercial resin, as observed for both kinds of reinforcing fibres (2 and 5% for vCF and rCF, respectively), Table 7.6. These result reiterated observations from the previous chapter that demonstrated that WVO-based networks were lighter than DGEBA counterparts, producing laminates with a minimum density of 1.05 ± 0.07 g cm$^{-3}$. This demonstrated the applicability of these materials in areas targeting weight-reduction. Furthermore, differences in the density value of panels produced with vCF and rCF derived from the higher fibre weight fraction achieved in materials produced with the virgin feedstock.

Also in terms of weight-reduction, one valid approach to incorporate rCF in a wider range of applications is to use them as partial substitutes for glass fibres through the preparation of hybrid composites or even the total replacement.[18,39] This strategy targets one of the main problems associated with glass fibres reinforced composites: weight gains due to

high density. Therefore, the adoption of rCF in applications dominated by glass fibres can improve the energy efficiency associated with the use-phase of these composites.

In this regard, the properties of biocomposites produced with rCF were compared with materials reinforced with glass obtained previously prepared in Chapter 6, Figure 7.11. The comparison indicated the advantages of employing rCF as a replacement for glass. For example, an increase of 32% was observed in terms of Young's Modulus, followed by a reduction in density of 30% and the addition of an element of renewable content as given by the bio-based content (BBC). On the other hand, the substitution of DGEBA for bio-based blend led to composites with tensile strength 16% smaller. It is important to keep in mind that these laminates were produced via different manufacturing techniques (wet lay-up for *DGEBA GF* and vacuum bagging for *Blend rCF*), therefore some of the changes can be associated with the processing stage. Nevertheless, these were promising results given the use of glass in applications that require stiffness.

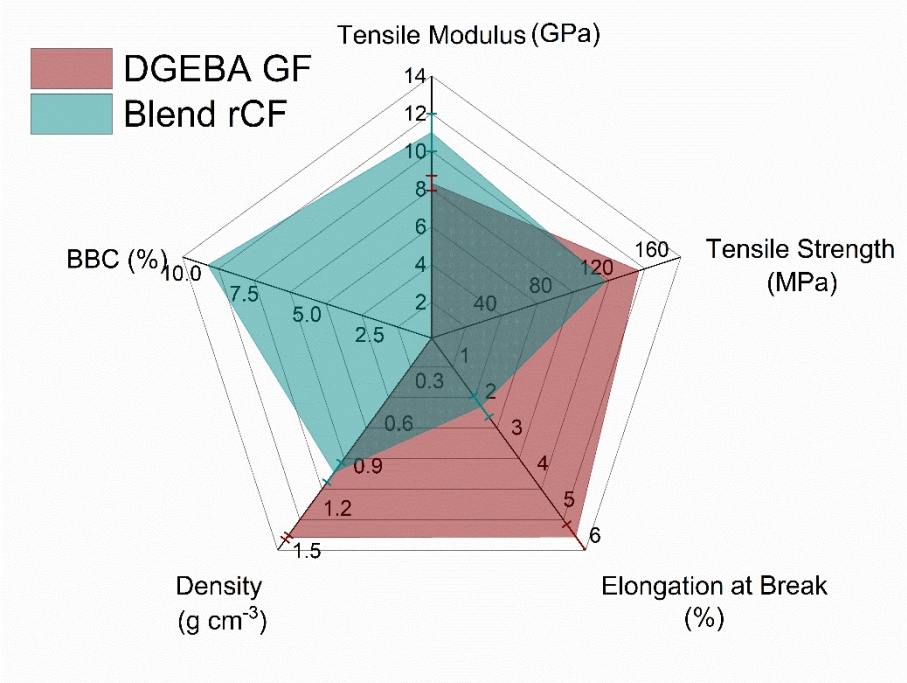


Figure 7.11: Radar plot comparing DGEBA composites reinforced with DGEBA and blends reinforced with recycled carbon fibres in terms of tensile properties density and bio-based content.

Overall, composite laminates manufactured with the bio-based blend and different grades of CF presented the same compromises in tensile performance observed in previous chapters. Nevertheless, this approach led to panels with reduced density and higher elongation at break in all cases, demonstrating usability in light-weight applications and when deformation is a critical parameter. Also, this strategy permitted the production of composites

using WVO with the highest properties so far. Interestingly, the tensile performance of bio-based laminates reinforced with rCF was more similar to the benchmark than in vCF counterparts, which indicated a preferred application in this area. Nonetheless, composites prepared with WVO and vCF achieved the highest tensile performance so far in this study, presenting promising characteristics in terms of real-life applications.

**b) Flexural Performance**

The flexural performance was analysed by through a 4-point bending test. This mechanical test was introduced in this stage due to its importance in laminate composites, providing a more comprehensive view of how shear forces affect the laminate whilst also exposing the specimen to tension and compression stresses.[40] In a 4-point bending test, the specimen volume under stress is more extensive than in a 3-point bending due to the presence of the two loading pins separated by an inner span, Figure 7.12. Therefore, the flexural stress is distributed over a whole section of the beam. Consequently, mechanical properties observed for 4-point bending tests are typically lower than the 3-point equivalent since a more substantial volume represents a larger probability of finding imperfections in the sample, such as cracks of flaws.[41] Therefore, 4-point bending tests are indicated for heterogeneous samples, such as composites or wood, since it represents with more fidelity the critical flexural properties of a given material.[42]

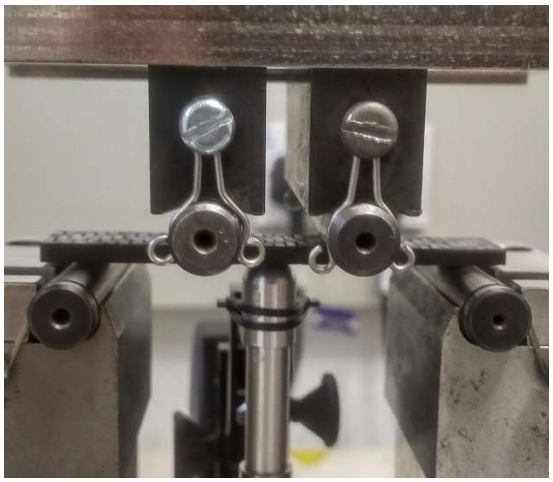

Figure 7.12: Illustration of the four-point bending flexural test.

The flexural performance of composites (Figure 7.13A and B) revealed a number of differences caused by resin formulation, fibre orientation and fibre type. For example, composites prepared with the vCF demonstrated a reduction in flexural modulus (16%) and maximum flexural strength (35%) when the bio-based epoxy was added to the system

reflecting results observed for tensile properties. Nevertheless, these partially bio-based formulations still presented remarkable flexural performance, peaking at (51 ± 6) GPa for flexural modulus and (480 ± 50) MPa of flexural strength.

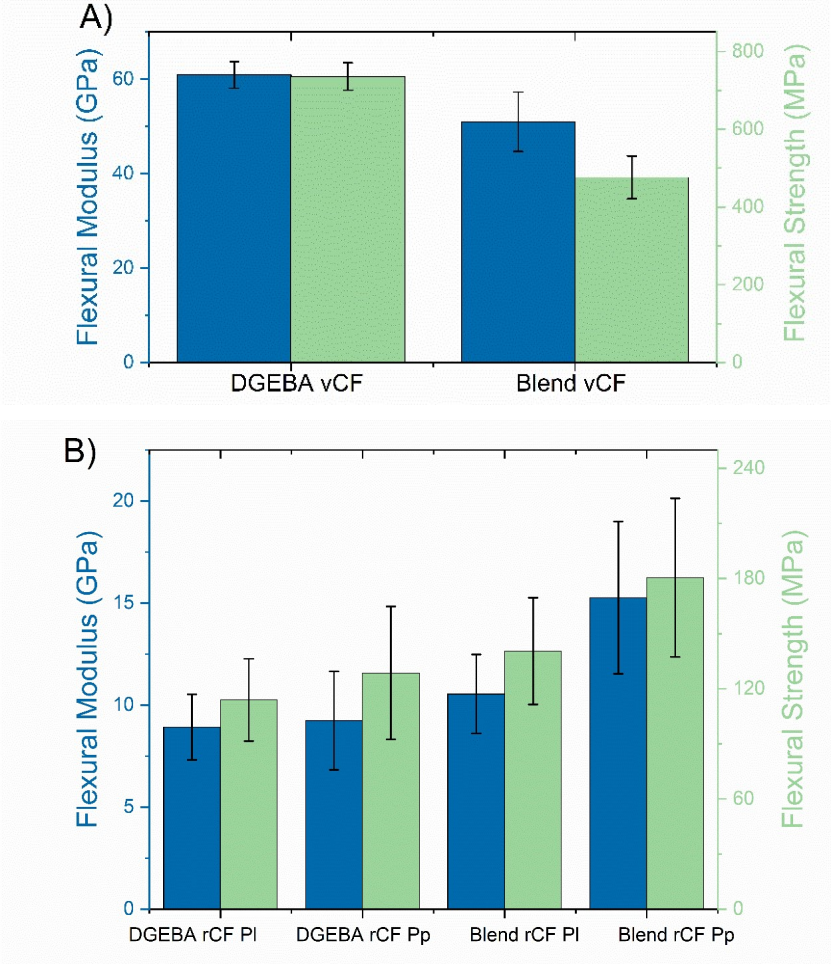


Figure 7.13: Flexural Modulus and flexural strength of composites reinforced with A) virgin and B) recycled carbon fibres. Pl represents panels with fibres parallel to the beam orientation, and Pp represents panels with fibres perpendicular to the beam orientation.

Regarding the rCF reinforced composites, flexural tests were conducted with specimens presenting different fibres orientations: parallel and perpendicular to the beam axis. This strategy permitted understanding some of the effects of the orientation in the final flexural performance. Specimen tested perpendicularly presented slightly higher values for both flexural modulus and strength, regardless of the resin system, Table 7.7. In this regard, improvements of 2% and 13% were observed for the flexural modulus and strength (respectively) in DGEBA-based systems, and of 45% and 28% (respectively) for bio-based blends. In fact, perpendicular fibres are capable of reducing the crack propagation phenomenon and increase fracture toughness, resulting in higher strength and modulus.[43]

Also, this observation demonstrated that although the fibre was used as a non-woven mat, fibres are not entirely randomly aligned, and a preferred orientation is presented in these materials.

Table 7.7: Flexural modulus, flexural strength and density of composites reinforced with virgin (vCF) and recycled carbon fibres (rCF).

| **Formulation** | **Flexural Modulus (GPa)** | **Flexural Strength (MPa)** | **Extension at Break (%)** |
|---|---|---|---|
| DGEBA vCF | 61 ± 3 | 735 ± 35 | 5.8 ± 1.1 |
| Blend vCF | 51 ± 6 | 476 ± 55 | 6.9 ± 1.4 |
| DGEBA rCF Pl | 9.0 ± 2.0 | 114 ± 22 | 8.6 ± 2.5 |
| DGEBA rCF Pp | 9.2 ± 2.4 | 129 ± 35 | 9.0 ± 2.1 |
| Blend rCF Pl | 10.5 ± 2.0 | 140 ± 29 | 5.7 ± 0.6 |
| Blend rCF Pp | 15.3 ± 4.0 | 180 ± 43 | 5.6 ± 0.8 |

Overall, the comparison between rCF and vCF revealed a noticeable difference in properties due to the inherently higher stiffness and strength of the fibres prior to the pyrolysis treatment. Interestingly, composites prepared with the bio-based blend presented improvements in both flexural modulus and strength over the benchmark formulations produced with DGEBA when reinforced with rCF. At first, this behaviour goes against what was observed for tensile samples produced with the same resin/fibre system. Therefore, changes could be attributed to differences in the panels produced for these two tests. In fact, for the flexural specimen, the resin viscosity played a more critical role in producing well-consolidated with small void content since they had double the thickness of the ones used for the tensile test (4.0 versus 2.0 mm, respectively). Also, this behaviour was particularly observed for composites prepared with rCF because of these fibres were more difficult to be manipulated due to its woolly nature. The calculation of the void content for each panel enabled the comparison between *DGEBA rCF* and *Blend rCF*, revealing a void contents of 12.3 and 7.8%, respectively. It is noteworthy that the manual lamination limited the impregnation level, leading to void contents above 5% regardless of the resin system.[44]

To investigate this issue in more details, the viscosity of the resins was measured with a rotational viscometer. This technique explores the relationship between a torque measurement of a motor rotating a spindle in a fluid and the viscosity of this fluid.[45] In order to adjust the torque measurements to the viscosity of the resins analysed at this point, the rotation speed of the spindle was adjusted to 150 rpm. The viscosity measured for DGEBA at these conditions

was 0.78 Pa.s, whereas the addition of 30 wt% of EPVO in the formulation reduced this value by 12% (0.69 Pa.s). Therefore, the lower viscosity facilitated the impregnation process, which resulted in composites with fewer voids and well-wetted fibres. This demonstrated the importance of additional parameters related to the final part manufactured when designing composite formulations.

**c) Microscopy**

SEM images (Figure 7.14 A-D) permitted the investigation of the interaction between the different CF and matrices. Micrographs obtained at 500 times magnification of laminates produced with rCF revealed that both DGEBA and blends (Figure 7.14A and B, respectively) were capable of wetting the reinforcing fibres effectively. Interestingly, Figure 7.14A demonstrated that the matrix presented a much clearer fracture due to its increased brittleness in comparison with the matrix that contains WVO-based epoxy (Figure 7.14B). Figures also revealed the presence of voids between the fibre bundles, indicating a reduced level of consolidation and limited performance. Furthermore, signs of fibre pull-out pointed to a sub-optimal fibre/matrix interaction.

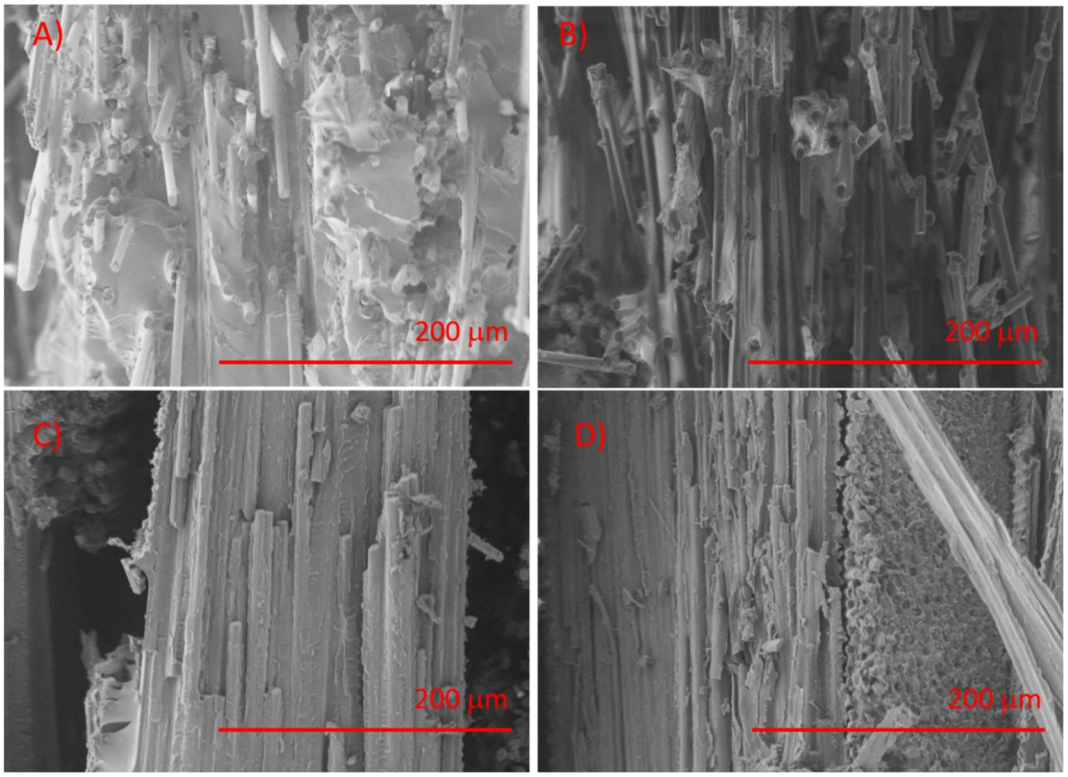


Figure 7.14 SEM images of composites reinforced with recycled carbon fibres (A: DGEBA matrix and B: bio-based blend) and virgin carbon fibre (C: DGEBA matrix and D: bio-based blend), at 500x magnification.

Due to intrinsically different fibre properties, both in terms of mechanical and surface chemistry, micrographs obtained for materials reinforced with vCF presented fibres excellently wetted by both petrochemical and partially renewable matrices´(Figure 7.14C and D). Also, it was evidenced the prevalence of fibre breakage over pull-out, demonstrating a strong interfacial bonding and the brittle characteristic of these reinforcing fibres. Moreover, Figure 7.14D demonstrated not only the differences in fibre orientation in the woven virgin fibre but also the presence of interfacial microcracks. As discussed in Chapter 6, these defects can facilitate crack propagation and ultimately lead to a reduction in properties. Therefore, it is essential to acknowledge the presence of defects in the samples as a consequence of the limited consolidation capacity achieved through the wet lay-up process.

**d) Non-destructive Tests: Ultrasound**

Structural characterisation of composites via non-destructive testing (NDT) allows the inspection of parts without compromising its physical integrity or cause any damage of reduction on its original properties. Within this group of techniques, ultrasonic methods have been extensively explored to analyse the presence of defects inside a composite structure such as micro-cracks and delamination.[46,47] A schematic representation of this technique is illustrated in Figure 7.15. Sound waves above the acoustic frequency (20 kHz) are emitted through the sample of interest, and parameters such as transit time and amplitude are registered as a function of the echo phenomenon. In turn, this is dependent on the speed of the sound in this given material and the distance travelled by the wave before being reflected.

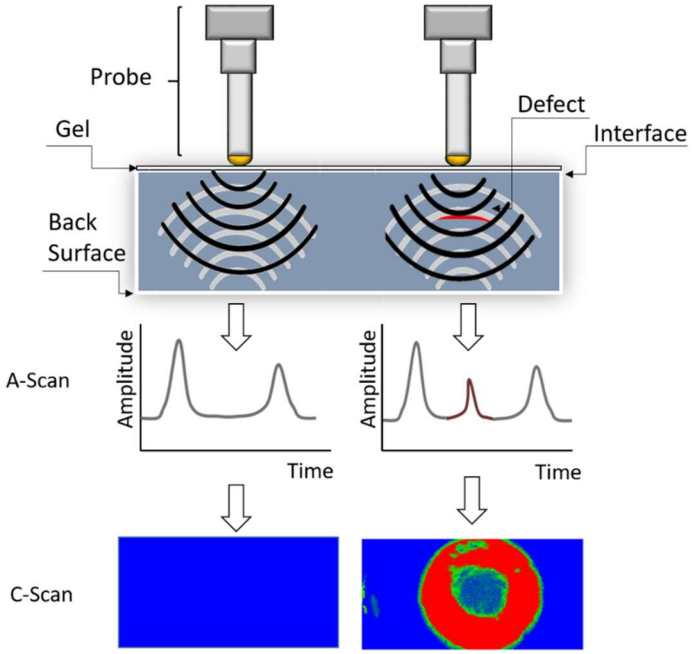


Figure 7.15 Schematic representation of non-destructive ultrasonic detection of defects in composites for perfect and imperfect samples.

The most basic display of this effect is observed in the form of an A-scan, which represents the variation of the wave amplitude over time of flight. In a perfectly homogeneous specimen, two signals will be detected by the transducer: one related to the material interface and one that represents these waves being reflected by the back wall. However, sub-superficial defects will present discontinuations in the specimen, consequently interfering with the wave propagation and causing a premature reflection that will be observed as an additional amplitude signal between the interface and the back wall (red signal in Figure 7.15). In composites, straight beam testing is preferred over angle beam testing due to its higher sensitivity to detect the transverse microcracks and delamination taking place in parallel to the surface, whilst the latter is indicated for the detection of perpendicular defects.[48]

Knowledge about the relationships found in the A-scan enables the construction of another representation known as C-scan. In this mode, the specimen is bi-dimensionally mapped to create a top or planar view of the defects to illustrate their shape and physical location in the specimen. The construction of this 2D representation depends on gating the signal amplitude related to the imperfection that is being analysed, similarly to adjusting the focus of a microscope in the desired depth.

To probe the applicability of this technique in this study, small samples (10 x 10 $cm^2$) were manufactured with defects intentionally introduced between plies of reinforcing. Small patches of PTFE film were used to simulate defects caused by the delamination process, creating a zone of discontinuity in the composite at a known location due to the presence of

the foreign object to test the equipment available for the measurement. As illustrated Figure 7.16A, the image obtained provided evidence of zones of discontinuation, although not very clearly. The same experimental procedure was repeated for *Blend vCF* specimens before and after the impact, Figure 7.16B and C, respectively. Scans obtained of the centre of panels before the impact revealed a relatively homogenous interior, with patterns representing the woven nature of the fibre. Figure 7.16B also reveal the presence of voids detected by orange zones in the C-Scan. On the other hand, the impacted sample demonstrated that the impact was responsible for creating areas of delamination and damage around the collision zone. Nevertheless, none of the images collected with the AmsTech Miniscanner presented enough resolution to permit a quantitative analysis of the impact damage.

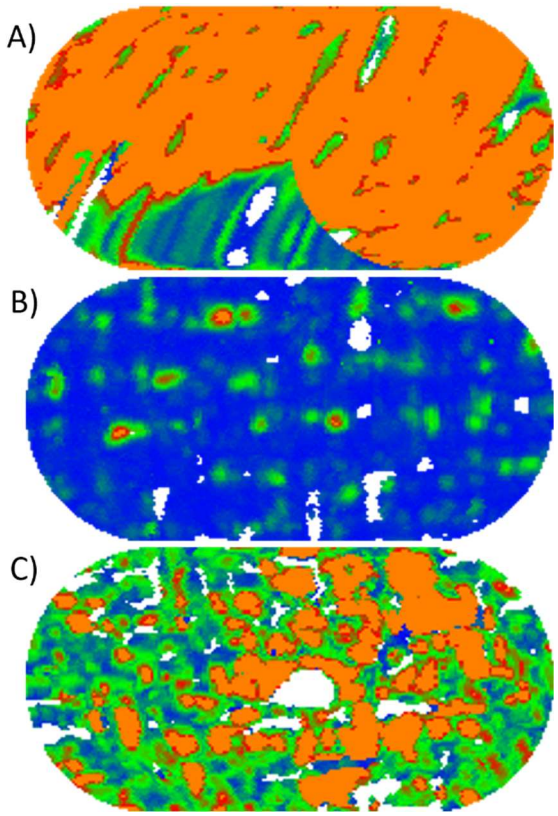


Figure 7.16: C-Scan obtained ultrasonic analysis of from vCF composite samples A) containing an introduced defect, B) before any impact and C) after a 5 J impact. Image corresponds to an area of 12 x 25 $mm^2$.

In this regard, it is essential to consider that the inherent heterogeneity of composites makes the ultrasonic testing more challenging than in other materials such as metals. For example, ultrasonic waves suffer from high signal attenuation and reflections in the boundaries between the ply and the matrix, reducing signal intensity in A-Scans and consequently the resolution of C-Scans.[49] Also, the equipment used for this study was designed for the analysis of metal welding joints, so that the system was not adjusted to

investigate defects in composite laminates, providing suboptimal readings. Experimentally, parameters such as the depth of the gates and the wave speed (around the 4000 m/s range) on were adjusted according to similar studies in the area without any significant improvements in the image quality.[48] Therefore, this test was not further explored in this study despite its importance in the area.

**e) Evaluation of barely-visible impact damage (BVID) via Compression after Impact (CAI) tests.**

Impact test was utilised to investigate the ability of the blend of reducing internal delamination promoted by a toughening effect. To simulate a scenario involving BVID, panels prepared according to ASTM D7136/ D7136M were impacted with a hemispherical drop weigh dart of 1 kg with 5 J of force using the rig presented in Figure 7.17A. As illustrated by Figure 7.17B, the damage caused by this impact could be classified as a dent/depression, and successfully represent a case in which in the composite panel can be internally damaged but with minimum visual feedback. Also, the back face presented deformation corresponded to the hemispherical impact, closely to what represented in Figure 7.2 Naked eye inspection revealed that formulations prepared with DGEBA and the bio-based blend presented the similar type of damage.

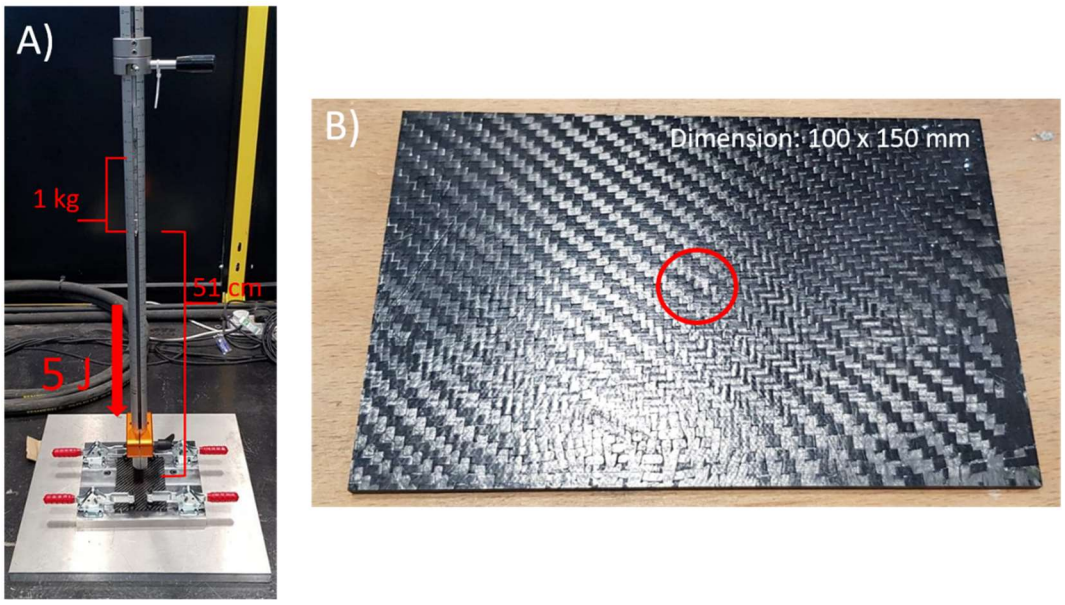


Figure 7.17: A) Representation of the impact test rig and B) DGEBA vCF sample after the impact, illustrating the dent created by the test.

Since the ultrasonic imaging proved to lead to inconclusive results, a destructive test was employed to investigate the behaviour of samples produced with the bio-based blend and

the commercial epoxy. In this regard, compression after impact (CAI) test was explored as a methodology to evaluate the internal delamination produced by the collision since it is possible to correlate the damage induced by the impact with the reduction in compression properties.[50] Figure 7.18 presents the setup utilised for the test, which also used a digital image correlation (DIC) equipment. The DIC technique consists in recording images of the specimen under mechanical stress whilst tracking the physical changes, enabling the application of correlation algorithms to create a deformation mapping.[51] In this context, DIC permitted analysing the differences in the failure behaviour in samples produced with DGEBA and the blend. Also, DIC could be explored as a way to measure the strain accurately during the test without having to use strain gauges on both sides of the panel.

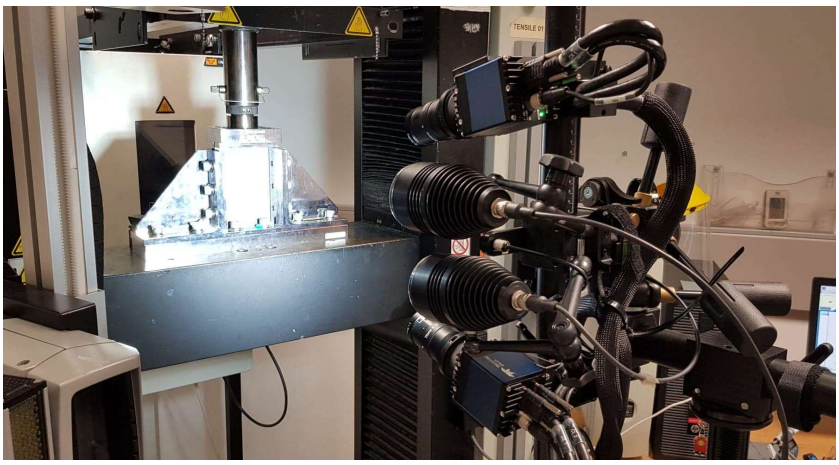

Figure 7.18: Experimental setup for the compression after impact tests followed by digital image correlation.

Figure 7.19A presents characteristic curves obtained from the compression test of the specimen before and after being impacted, demonstrating a premature failure due to the damage. In this regard, the loss in compressive strength could be associated with the presence of internal cracks and delamination, which also reduced the displacement at break.[13] Interestingly, the damage caused by the impact also proved to alter the location of failure. As also represented in Figure 7.19A, non-impacted samples failed closer to the upper grip, whereas some of the impacted samples had their failure located near the point of impact (*i.e.* in the centre of the panel). Therefore, delamination points formed during the impact acted as crack propagators, facilitating the failure at that location.

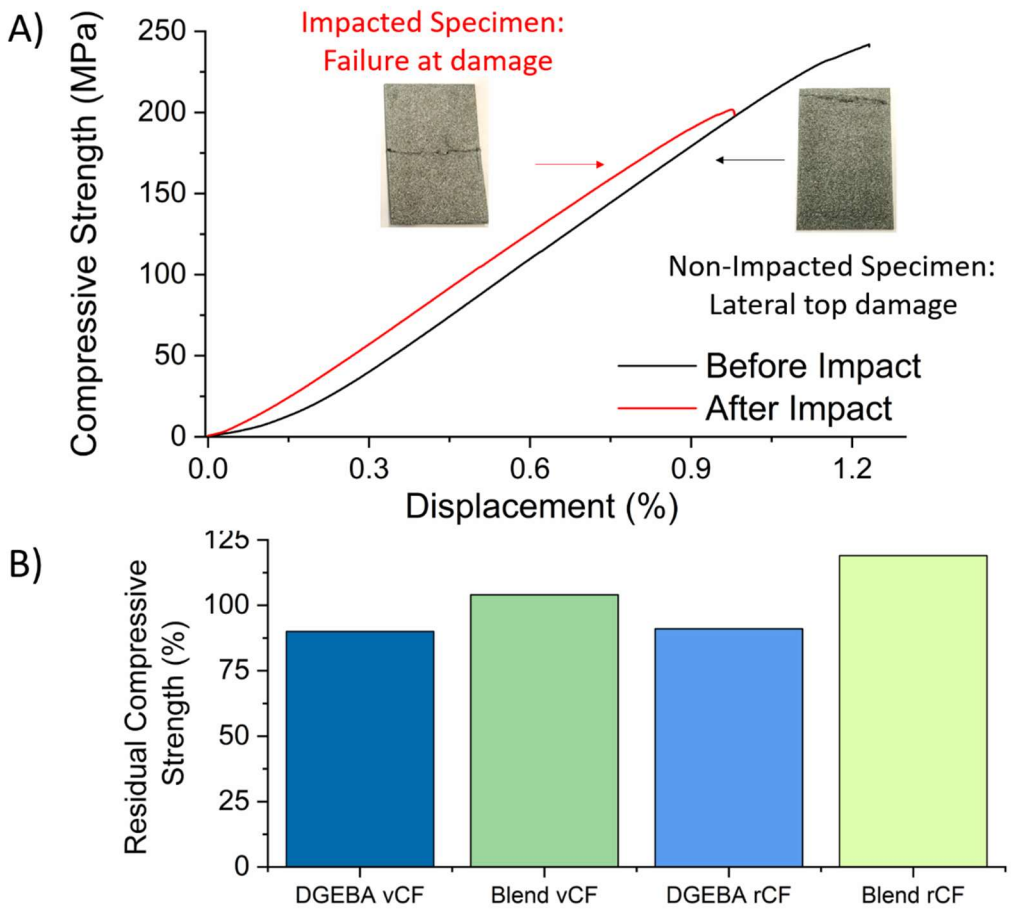


Figure 7.19: A) Representative curves from the compression tests illustrating the relationship between the damage and the impact and B) residual compressive strength for samples prepared with DGEBA and the bio-based blend.

In CAI tests, the residual compressive strength is typically taken as a criterion to analyse the development of the delamination damage.[52] In this regard, *DGEBA vCF* samples presented retention of 90% of the original compressive strength after the impact, while *Blend vCF* presented no significant losses, Figure 7.19B. This observation could indicate that the addition of bio-based epoxy prevented internal damage due to the impact by a toughening mechanism. In order words, the flexibility found in aliphatic chains were able to dissipate mechanical energy more effectively than in rigid DGEBA-based network, therefore presenting preventing delamination damage. Similar effects were observed for Charpy impact tests conducted in Chapter 6. Therefore, this result highlighted a very important contribution added by the presence of WVO-based epoxy in the formulation.

However, it is noteworthy mentioning that only one non-impacted specimen of *Blend vCF* was tested at this stage since two other specimens were undersized due to imprecision in the cutting stage and consequently did not fitting the test rig. Therefore, a more representative

study with a larger amount of specimen would permit a more precise comparison of samples before and after the impact. Nevertheless, this finding demonstrated that the addition of bio-based epoxies did not lead to any compromises in impact performance / crack-propagation, preliminary supporting its potential inclusion in epoxy formulations to boost the renewable content whilst also providing additional engineering value.

Table 7.8 present the complete set of data obtained from the compression tests. Interestingly, *Blend rCF* panels presented increased compression modulus and strength versus non-impacted samples, indicating heterogeneity in terms of consolidations throughout the panel. Similarly, these samples presented superior strength than *DGEBA rCF*, demonstrating a similar relationship previously observed for the flexural performance in terms of processability. Nevertheless, the damage introduced by the impact was capable of reducing the displacement before the break in all rCF-based panels, indicating that samples were less resistant to deformations due to crack propagation.

Table 7.8: Compression properties of commercial and bio-based formulations before and after impact test.

| **Sample** | **Compressive Modulus (GPa)** | **Compressive Strength (MPa)** | **Residual Compressive Strength (%)** | **Displacement (%)** |
|---|---|---|---|---|
| DGEBA vCF (non-impacted) | 175 ± 8 | 226 ± 15 | 90 | 1.11 ± 0.06 |
| DGEBA vCF (impacted) | 169 ± 17 | 204 ± 10 | | 1.1 ± 0.2 |
| Blend vCF (non-impacted) | 144 | 140 | 104 | 0.98 |
| Blend vCF (impacted) | 132 ± 2 | 148 ± 10 | | 1.14 ± 0.16 |
| DGEBA rCF (non-impacted) | 63 ± 6 | 56 ± 15 | 91 | 0.9 ± 0.1 |
| DGEBA rCF (impacted) | 78 ± 9 | 51 ± 9 | | 0.7 ± 0.1 |
| Blend rCF (non-impacted) | 57 ± 4 | 62 ± 2 | 119 | 1.3 ± 0.4 |
| Blend rCF (impacted) | 80 ± 1 | 74.1 ± 0.1 | | 0.6 ± 0.2 |

Furthermore, DIC images were used to comprehend the relationships between the impact damage, the crack propagation phenomenon and the overall failure mechanism of different samples. As presented in Figure 7.20A/C and 7.21A/C, the stress was homogenously distributed throughout the specimen, and the failure occurred either internally or in places in which a defect is deriving from the manufacturing step (*e.g.* Figure 7.21A) was present. However, this scenario changed when the impact-induced damage was present in the panels. In this case, DIC images (Figure 7.20B/D and Figure 7.21B/D) revealed a stress concentration around the dent formed by the impact, which consequently led to the formation of a centrally-located crack that led to the failure.[53] Also, DIC images evidenced more clearly the more brittle nature of the vCF composites in comparison with rCF counterparts. Therefore, it is suggested that rCF can be further explored as a strategy to reduce the creation of brittle fractures in lightweight composites.

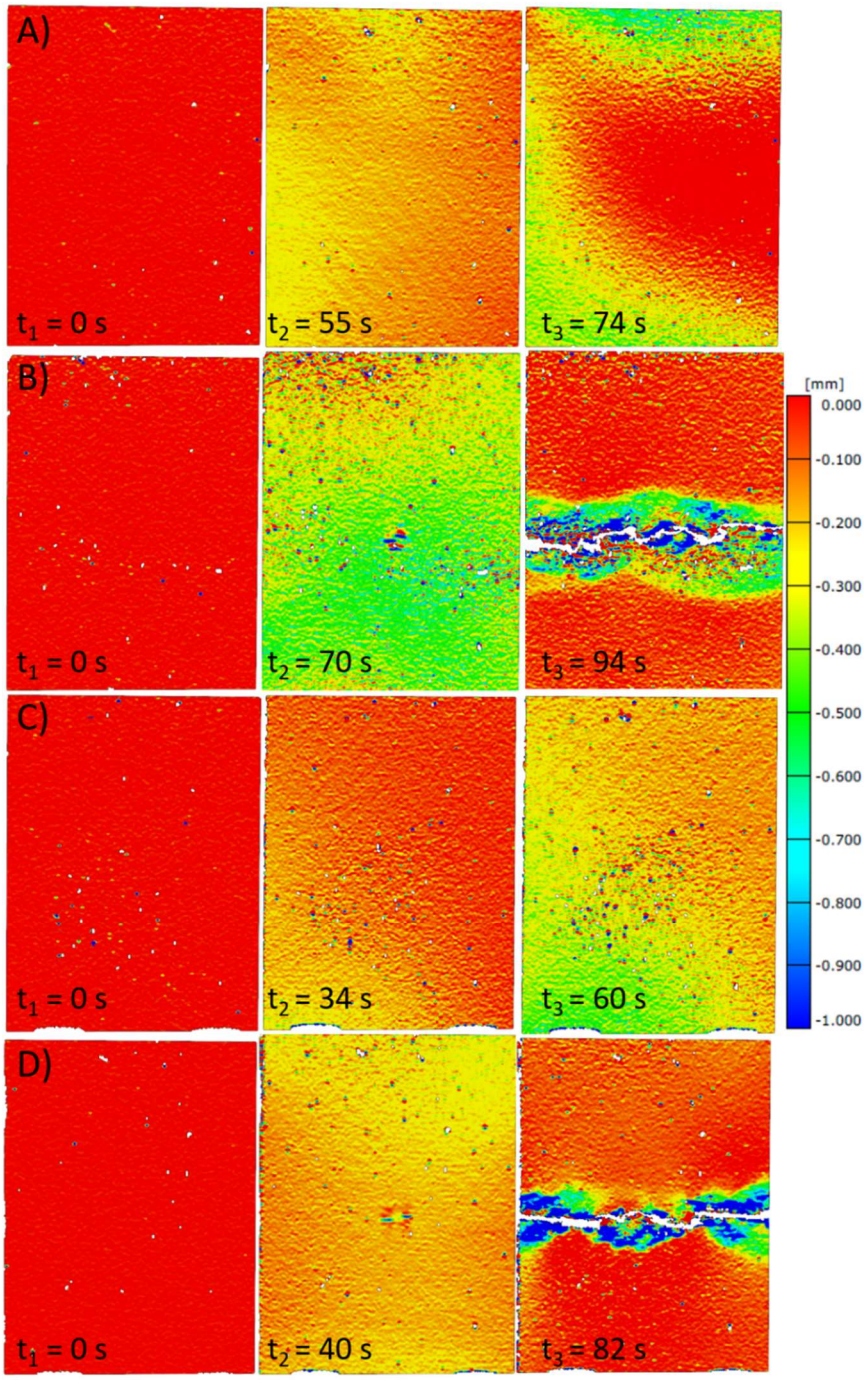


Figure 7.20: DIC images obtained from compression test of specimens from formulations: A) DGEBA vCF before impact, B) DGEBA vCF after impact, C) blend vCF before impact and D) blend vCF after impact.

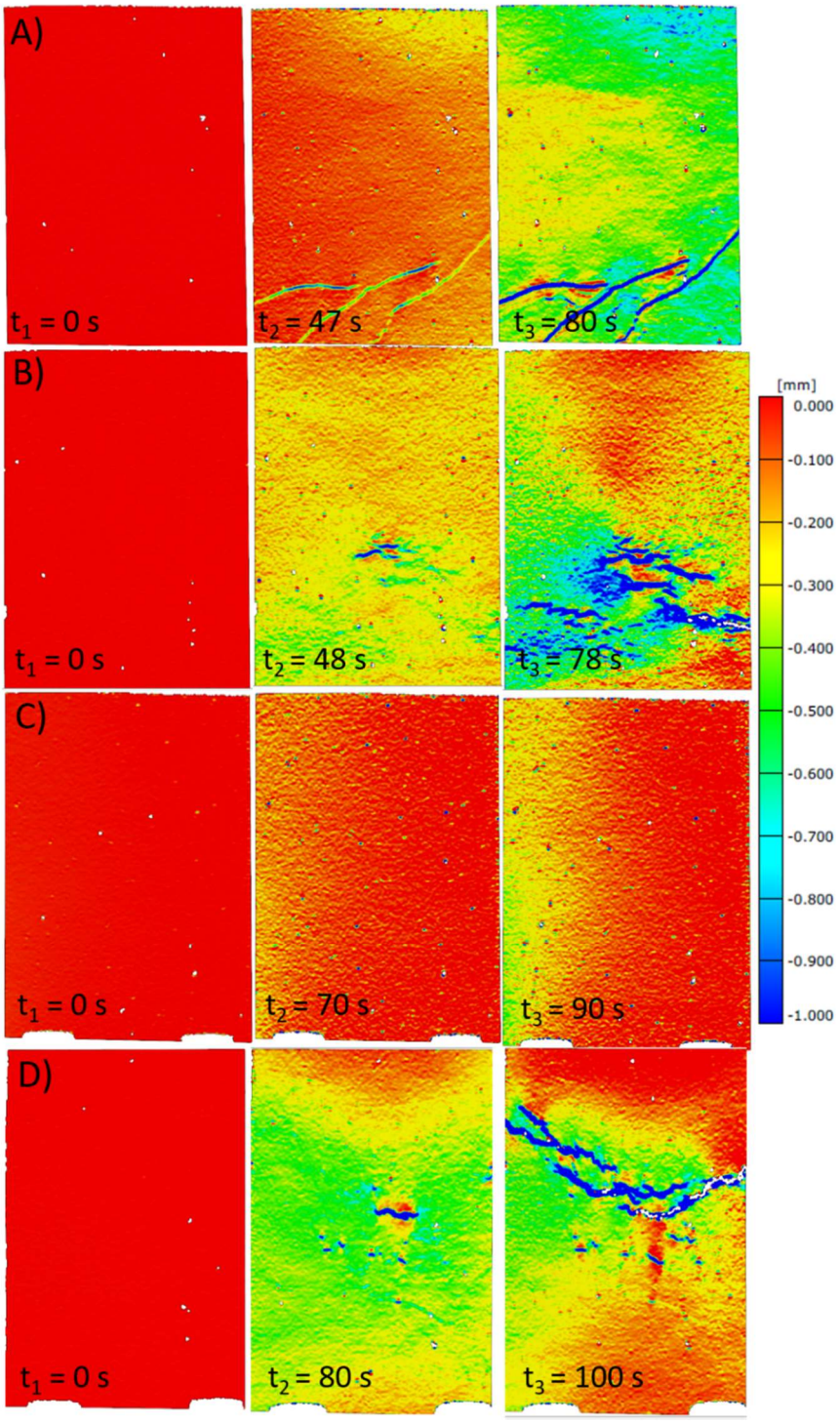


Figure 7.21: DIC images obtained from compression test of specimens from formulations: A) DGEBA rCF before impact, B) DGEBA rCF after impact, C) blend rCF before impact and D) blend rCF after impact.

Despite the effect observed in terms of conservation of compressive strength, the application of WVO-based epoxy in blends did not produce any evident effects in terms of how the stress relaxation occurred in impacted samples, as observed by DIC. In this regard, partially bio-based formulations presented a very similar behaviour to DGEBA counterparts,

indicating that their effect is not significant enough to alter the failure mechanism. Nonetheless, these results could be seen as positive since they also demonstrated that the addition of epoxies from waste sources did compromise this behaviour. Therefore, these results were still valid to preliminarily indicate that WVO-based epoxies are able to reduce BVID.

## 7.4 Summary

Epoxy blends combining bio-based epoxy resin synthesised from waste vegetable oils and DGEBA were used to produce thermoset formulation. Relationships between thermal and dynamic mechanical properties and the bio-based content were established by this study. Changes in properties were attributed to the presence of long aliphatic chains and a reduced degree of functionality of the bio-based epoxy in comparison with DGEBA. A formulation with 30 wt% of bio-based content was selected to manufacture composites with virgin and recycled carbon fibres due to best the balance between renewability and $T_g$. Composites manufactured with WVO-containing resin and recycled carbon fibres presented promising tensile (157 ± 24 MPa for tensile strength and 18 ± 8 GPa for Young`s modulus) and flexural (180 ± 43 for flexural strength and 15 ± 4 GPa for flexural modulus) properties, as well as improved processability and reduced density. This expanded the library of formulations in this thesis and represented the production of laminates with WVO with the highest mechanical properties in this thesis. Finally, this study demonstrated the first indications that these bio-based resins were capable of reducing the BVID phenomenon, as observed via the analysis of the residual compressive strength in compression after impact tests. Further studies focusing on the production of a larger subset of specimens would be required to investigate this characteristic in more details. Nevertheless, these results opened space for the development of sustainable alternatives for the composite industry based on the valorisation of waste streams, aggregating new properties whilst leading to environmentally-friendly materials.

## 7.5 References

1 P. D. Mangalgiri, *Bull. Mater. Sci.*, 1999, **22**, 657–664.

2 Boeing 787: Advanced Composite Use, https://www.boeing.com/commercial/787/by-design/#/advanced-composite-use.

3 E. Witten, T. Kraus and M. Kühnel, *Composites Market Report 2016*, 2016.

4 M. Belhaj, M. Deleglise, S. Comas-Cardona, H. Demouveau, C. Binetruy, C. Duval and P. Figueiredo, *Compos. Part B Eng.*, 2013, **50**, 107–111.

5 A. R. Aziz, M. A. Ali, X. Zeng, R. Umer, P. Schubel and W. J. Cantwell, *Compos. Sci. Technol.*, 2017, **152**, 57–67.

6 A. S. Lectez, K. El Azzouzi, C. Binetruy, S. Comas-Cardona, E. Verron and J. M. Lebrun, *J. Compos. Mater.*, , DOI:10.1177/0021998317752229.

7 R. Toivola, P. N. Lai, J. Yang, S. H. Jang, A. K. Y. Jen and B. D. Flinn, *Compos. Sci. Technol.*, 2017, **139**, 74–82.

8 Y. Yang, R. Boom, B. Irion, D. J. van Heerden, P. Kuiper and H. de Wit, *Chem. Eng. Process. Process Intensif.*, 2012, **51**, 53–68.

9 U. Polimeno and M. Meo, *Compos. Struct.*, 2009, **91**, 398–402.

10 X. C. Sun and S. R. Hallett, *Int. J. Impact Eng.*, 2017, **109**, 178–195.

11 P. W. R. Beaumony, in *The Structural Integrity of Carbon Fiber Composites*, Springer, Switzerland, 2017, pp. 497–503.

12 A. Campanella, M. Zhan, P. Watt, A. T. Grous, C. Shen and R. P. Wool, *Compos. Part A Appl. Sci. Manuf.*, 2015, **72**, 192–199.

13 S. G. Tan and W. S. Chow, *Polym. Plast. Technol. Eng.*, 2010, **49**, 1581–1590.

14 F. C. Fernandes, D. Lehane, K. Kirwan and S. R. Coles, *Eur. Polym. J.*, 2017, **89**, 449–460.

15 A. H. Suzuki, B. G. Botelho, L. S. Oliveira and A. S. Franca, *Eur. Polym. J.*, 2018, **99**, 142–149.

16 S. Pimenta and S. T. Pinho, *Waste Manag.*, 2011, **31**, 378–392.

17 G. Marsh, *Reinf. Plast.*, 2008, **52**, 36–39.

18 R. A. Witik, R. Teuscher, V. Michaud, C. Ludwig and J. A. E. Månson, *Compos. Part A Appl. Sci. Manuf.*, 2013, **49**, 89–99.

19 G. Oliveux, L. O. Dandy and G. A. Leeke, *Prog. Mater. Sci.*, 2015, **72**, 61–99.

20 S. J. Pickering, Z. Liu, T. A. Turner and K. H. Wong, *IOP Conf. Ser. Mater. Sci. Eng.*, , DOI:10.1088/1757-899X/139/1/012005.

21 M. L. Longana, N. Ong, H. N. Yu and K. D. Potter, *Compos. Struct.*, 2016, **153**, 271–277.

22 J. Meredith, S. Cozien-Cazuc, E. Collings, S. Carter, S. Alsop, J. Lever, S. R. Coles, B. M. Wood and K. Kirwan, *Compos. Sci. Technol.*, 2012, **72**, 688–695.

23 M. D. Samper, V. Fombuena, T. Boronat, D. García-Sanoguera and R. Balart, *J. Am. Oil Chem. Soc.*, 2012, **89**, 1521–1528.

24 E. Choe and D. B. Min, *J. Food Sci.*, 2007, **72**, R77-86.

25 B. Ellis, *Chemistry and Technology of Epoxy Resins*, Springer-Science+Business Media, B.V, 1st Editio., 1993.

26 F. C. Fernandes, P. Wilson, K. Kirwan and S. R. Coles, .

27 F. D. Gunstone, *The Chemistry of Oils and Fats: Source, Composition, Properties and Uses*, Blackwell Publishing, CRC Press, 2004.

28 A. E. Gerbase, C. L. Petzhold and A. P. O. Costa, *J. Am. Oil Chem. Soc.*, 2002, **79**,

797–802.

29 H. Miyagawa, M. Misra, L. T. Drzal and A. K. Mohanty, *Polym. Eng. Sci.*, 2005, **45**, 487–495.

30 J. Ampudia, E. Larrauri, E. M. Gil, M. Rodríguez and L. M. Léon, *J. Appl. Polym. Sci.*, 1998, **71**, 1239–1245.

31 F. C. Fernandes, K. Kirwan, P. R. Wilson and Coles, *Green Mater.*, 2018, **6**, 38–46.

32 I. De Baere, W. Van Paepegem and J. Degrieck, *Polym. Compos.*, 2009, **30**, 381–390.

33 R. Ambu, F. Aymerich, F. Ginesu and P. Priolo, *Compos. Sci. Technol.*, 2006, **66**, 199–205.

34 J. R. Tarpani, M. T. Milan, D. Spinelli and W. W. Bose, *Mater. Res.*, 2006, **9**, 121–130.

35 M. Jalalvand, G. Czél, J. D. Fuller, M. R. Wisnom, L. P. Canal, C. D. González and J. LLorca, *Compos. Sci. Technol.*, 2016, **134**, 115–124.

36 M. Akay, G. R. Spratt and B. Meenan, *Compos. Sci. Technol.*, 2003, **63**, 1053–1059.

37 M. Fan, J. Liu, X. Li, J. Cheng and J. Zhang, *Thermochim. Acta*, 2013, **554**, 39–47.

38 M. Kuwata and P. J. Hogg, *Compos. Part A Appl. Sci. Manuf.*, 2011, **42**, 1560–1570.

39 S. R. Naqvi, H. M. Prabhakara, E. A. Bramer, W. Dierkes, R. Akkerman and G. Brem, *Resour. Conserv. Recycl.*, 2018, **136**, 118–129.

40 M. C. S. Moreno, A. R. Gutiérrez and J. L. M. Vicente, *IOP Conf. Ser. Mater. Sci. Eng.*, , DOI:10.1088/1757-899X/139/1/012047.

41 F. Mujika, *Polym. Test.*, 2006, **25**, 214–220.

42 L. Brancheriau, H. Bailleres and D. Guitard, *Wood Sci. Technol.*, 2002, **36**, 367–383.

43 J. P. Lucas, *Eng. Fract. Mech.*, 1992, **42**, 543–561.

44 L. G. Stringer, *Composites*, 1989, **20**, 441–452.

45 Q. Zhang, Y. heng Xu and Z. guang Wen, *Constr. Build. Mater.*, 2017, **153**, 774–782.

46 S. C. Ng, N. Ismail, A. Ali, B. Sahari, J. M. Yusof and B. W. Chu, *IOP Conf. Ser. Mater. Sci. Eng.*, , DOI:10.1088/1757-899X/17/1/012045.

47 R. Teti and N. Alberti, *CIRP Ann. - Manuf. Technol.*, 1990, **39**, 527–530.

48 A. Benammar, R. Drai and A. Guessoum, *Ultrasonics*, 2008, **48**, 731–738.

49 T. Barry, M. Kesharaju, C. Nagarajah and S. Palanisamy, *J. Compos. Mater.*, 2015, **50**, 861–871.

50 M. U. Saeed, Z. Chen, Z. Chen and B. Li, *Compos. Part B, Eng.*, 2014, **56**, 815–820.

51 M. Bornert, F. Brémand, P. Doumalin, J. C. Dupré, M. Fazzini, M. Grédiac, F. Hild, S. Mistou, J. Molimard, J. J. Orteu, L. Robert, Y. Surrel, P. Vacher and B. Wattrisse, *Exp. Mech.*, 2009, **49**, 353–370.

52 M. Siegfried, C. Tola, M. Claes, S. V. Lomov, I. Verpoest and L. Gorbatikh, *Compos. Struct.*, 2014, **111**, 488–496.

53 H. Yan, C. Oskay, A. Krishnan and L. R. Xu, *Compos. Sci. Technol.*, 2010, **70**, 2128–2136.

# Chapter 8

# Conclusions and Perspectives

## 8.1 Conclusions

Investigations presented in this doctoral thesis have explored the use of WVO as a novel and more sustainable source of triglycerides for polymers and composites industry. Based on the concept of waste valorisation, these studies produced new materials obtained through the development of purification methodologies, synthetic routes to insert polymerisable groups in the triglyceride backbone and exploration of these resins in thermoset and composites formulations. The following points summarise the main contributions of this thesis, establishing a connection between the findings of each chapter and the research objectives. Later, this chapter also introduces recommendations for further studies based on the impact of the current studies.

*I. Review of the state-of-the-art for the transformation of vegetable oils into reactive resins, with a focus on epoxy resins;*

A literature review conducted in Chapter 2 revealed a wide range of synthetic techniques to transform triglycerides into added-value chemicals. Among them, epoxidation has been widely preferred to insert polymerisable groups in these triglycerides, unlocking the chemical potential of these molecules in polymer and composite science. More specifically, the transformation based on the use of peracids have demonstrated versatility and scalability despite the drawbacks associated with side reactions. Novel applications based on enzymatic and metallic catalysis are pushing the boundaries to achieve maximum conversion and selectivity, but still far from commercialization. Also, the development of other synthetic methodologies such as metathesis has created space of new and more advanced applications in polymer science.

A key learning in this review was the challenge associated with the exploration of WVO as a chemical platform as a consequence of the frying process. In this step, the oil undergoes a number of transformations that alter its physical and chemical properties, including the degradation of the double bonds that are essential for the creation of reactive resins in further stages. Literature also revealed that parameters such as the origin of the oil used for frying and the frying conditions control the extent of this degradation process. Most importantly, it was possible to understand the nature of the impurities and by-products found in WVO, opening space for the development of purification methodologies targeting these components.

*II. Review of the state-of-the-art in the manufacture of green composites;*

The review has demonstrated the main trends in the composite market and within the area of green composites using vegetable oil-based resins and natural fibres. Features such as

the cellulose content and the microfibrillar angle were critical in terms of identifying vegetable fibres suitable to be used as reinforcement. Studies have also revealed that the use of vegetable fibres can lead to reductions in the use of primary energy during production and improvements in the amount of energy recovery at the end of the life cycle, significantly reducing the carbon footprints of the composite life.

An analysis of the methodologies used for the production of thermoset composites with natural fibres revealed the prevalence of wet lay-up as processing technique due to its simplicity and low cost. Also, these works have introduced the main challenges associated with the production of this class of material and the limited fibre/matrix interfacial interaction, which hinders the mechanical performance of these resulting composite. This review has also investigated the main strategies to overcome this barrier through chemical or physical modification of vegetable fibres. These methodologies exploit the reactivity of cellulose, the main component of the fibres, to insert functionalities that are more similar to the chemical nature of the matrix or to improve surface area and mechanical interlocking with the polymeric network.

*III. Development of a robust methodology for the obtainment of pure and reactive epoxy resins from WVO;*

The study has developed a purification procedure based on multiple liquid extractions capable of significantly reducing the level of polar impurities in the WVO based, as confirmed by $^{1}$H NMR. This methodology was the foundation for all subsequent studies that have used a purified version of the WVO as the main platform. The simplicity and low-cost characteristics of this method were aligned with the desire for scalability that has driven the research. Also, the robustness of this approach was confirmed by establishing that the purifications step did not compromise any chemical properties of the feedstock.

After an extensive study of the reaction parameters, the epoxidation step based on mCPBA was elected as the preferred in this stage due to the combination of high selectivity and conversation. The reactivity of bio-based epoxies produced from virgin, waste and purified oil was tested through the production of blends with commercial epoxy (DGEBA) and amine hardeners. This study represented the first production of networks from waste vegetable oil in literature. At this stage, it was confirmed that the purification step would lead to resins with similar reactivity to those obtained from virgin when added to blends.

However, thermoset polymers presented limited mechanical performance due the inherently reduced molecular stiffness of epoxies from triglycerides and to a plasticisation effect cause by unreacted molecules. The best balance of properties was observed when 10 wt% of bio-based epoxy was added (1.0 ± 0.1 GPa of Young's Modulus and 28 ± 4 MPa of tensile strength). Further explorations permitted the first demonstration of the application of

waste-based resins in composites area by reinforcing the matrix with recycled milled carbon fibre, enabling the production of materials combining two waste streams and recovering properties that were initially lost. Composites presented promising gains in tensile performance (3.2 ± 0.2 GPa of Young's modulus and 53 ± 7 MPa of tensile strength) when 30wt% of reinforcement was added.

Even though this stage of the study was accomplished with bio-based resins produced with mCPBA, later investigations returned to the use of peracetic acid due to atom economy and scalability issues. When mCPBA was substituted by $H_2O_2$/acetic acid, a significant amount of organic waste generation was avoided with minimum compromise in the overall selectivity and conversion. This feature was particularly important when the reaction had to be scaled up to cope with the demand for bio-based epoxy in later chapters regarding the volume of waste, cost of the oxidising agent versus the added value of this resin and the feasibility as a real platform.

Therefore, this study recommends the peracid technique as the most appropriate to produce epoxy resins from WVO. Also, the investigations demonstrated it was possible to use epoxidized vegetable oil in polymer and composite applications as hypothesized, providing the first couple of answers related to the researcher questions. Most importantly, this first experimental section evidenced that the reactivity of the bio-based epoxies was different and demanded further adjustments, which was the theme of later chapters.

*IV. Explore the use of WVO-derived resins for the production of thermoset polymers and optimised formulation parameters based the resin reactivity;*

Results obtained in Chapter 4 demonstrated the need for designing a formulation that appropriately explored the reactivity of the WVO-based epoxy. A critical decision was made when anhydrides were selected to create networks entirely based on bio-based epoxies, which led to satisfactory network formation and significantly reduced the amount of unreacted hardener entrapped in the cross-linked material. No commercial epoxy was used in these formulations in an attempt to maximise the renewable content and consequently reducing environmental footprint associated with these polymers. However, a drawback associated with this strategy was the sluggish nature of the reaction between anhydrides and oxirane rings, requiring longer reaction times and moderate temperature (approx. 150 °C).

Four formulation parameters (oil origin, anhydride type, hardener molar ratio and catalyst) were explored to build an optimised formulation matching the epoxidized WVO's reactivity. A design of experiments (DOE) approach was used to classify these parameters according to their contribution towards maximising the glass transition temperature. This strategy revealed that the amount of hardener (high load > low load) was the most critical parameter, followed by choice of catalyst (2-MI > TEA) and finally the origin of the

triglycerides (virgin oil > waste oil). Even though this study exposed the adverse effect of using WVO to produce polymers in terms of performance, results revealed that adjustments in other parameters were instrumental. Therefore, the use of high anhydride load and 2-MI as a catalyst could mitigate the performance losses and lead to rigid networks with $T_g$ maximum of above room temperature. An interesting discovery was the ability to establish a relationship between the chemical resistance and the cross-linking density. Overall, these studies produced optimised formulations that were applied throughout the next chapters that focused on the production of composites. Also, these results offered guidelines for future researchers aiming at maximising the physical properties of networks based on this type of triglycerides.

*V. Build a library of composites using different reinforcing fibres, identifying the best opportunities in terms of mechanical properties.*

A library of materials combining the optimised formulations and different reinforcing fibres was built, exploring the best opportunities in the area of composites. In Chapter 6, laminates were prepared with matrices entirely derived from bio-based epoxy and reinforced with glass and flax fibres. Although vacuum bagging was initially explored to produce the laminates, wet lay-up technique was selected to avoid issues with the low viscosity of the resin.

Investigation of the tensile properties of material reinforced with glass fibres demonstrated laminates with performance similar to DGEBA analogues in terms of Young's Modulus (7.7 ± 1.1 GPa). On the other hand, materials produced with flax revealed the challenges in compatibilising the apolar nature of the matrix and the polar characteristic of the natural fibre. As a result, poor interfacial interaction and reduced tensile properties (0.60 ± 0.05 GPa of Young's Modulus) were obtained for these materials. Nonetheless, the exploration of chemically modified flax fibres significantly improved the properties of these composites both in terms of tensile modulus and strength. More importantly, the study found that impact properties could be significantly improved (up to 175 %) by the addition of WVO-based resin as consequence of the increased capacity of these polymeric networks relax when under sudden mechanical stress when compared to DGEBA. The fibre treatment further improved this property by reducing the number of interfacial defects between fibres and matrix, which could act as crack propagators. Additional improvements caused by the chemical treatments were the reduction of the water uptake observed in a hygrothermal ageing test. Overall, these materials demonstrated the first application of waste-based resins for the production of laminates, which proved to be promising replacements for petrochemical epoxies in applications that demand stiffness and impact performance over high ultimate strength.

The ability to produce composites with improved impact response was further explored to expand the library of composites through the production of laminates reinforced with virgin and recycled carbon fibres. Although the production of networks entirely from bio-based epoxy was previously demonstrated in this thesis, composites manufactured in Chapter 7 once again utilised blend of WVO-based epoxy and DGEBA to produce laminates with a better balance in properties (and closer to industrial application). This required another optimisation run, which established the best formulation as the one incorporating 30 wt% of bio-based epoxy. However, materials with up to 50 wt% of WVO-based epoxy were produced, representing opportunities for the exploration of materials with increased waste-derived content. The exploration of a manufacturing technique combining the elements of vacuum bagging and compression proved to result in well-consolidated composites with low void content. These laminates presented the highest properties registered in this thesis, and an essential relationship between the resin viscosity and the processability was established. Finally, WVO-based resin proved to lead to higher residual compressive strength in CAI tests, revealing a potential opportunity to explore these bio-based resins in terms of overcoming one of the main limitations observed in CFRC.

Finally, based on the library of composites prepared herein produced, WVO-based epoxy resins presented limited ability to entirely substitute DGEBA due to the structural characteristics found in the triglycerides. Nevertheless, hybrid materials blending bio-based and petrochemical resins presented a favourable compromise in terms of mechanical and physical performance, combining the better of these two different systems. Therefore, this thesis recommends the utilisation of WVO-based resins as a partial substitute to DGEBA when intended for structural application at high TRL, so that the added properties (*e.g.* improved impact performance and reduced density) can be explored without significant sacrifices. Moreover, other composite formulations such as those produced in Chapter 5 can be used in non-structural parts. Most importantly, the main contribution was the demonstration of this waste-based chemical platform, enabling it to be further translated into other applications and mimic the versatility of other epoxy platforms.

## 8.2 Future Perspectives and Recommendations

This thesis has demonstrated the utilisation of WVO as an interesting and more sustainable source of triglycerides for the oleochemical industry. The following recommendations aim at expanding the scope of the current work to confirm the feasibility of these materials as a novel platform and potentially bring them closer to commercial exploitation.

*A) Preparation of polymers and composites with acrylated resins from WVO.*

Literature reviews presented in Chapters 2 and 3 have illustrated a wide interest in bio-based acrylated resins in polymer and composite sciences. These compounds can be produced directly from the epoxidized WVO via a ring-opening reaction with acrylic acid. Despite the extra synthetic step, these resins present advantages over epoxy systems due to increased reactivity and possibility to react with styrene, creating strong and tightly connected networks. The strategy of obtaining such molecules from WVO would widen the scope of this chemical platform, enabling the preparation of new resins systems and novel materials. Since the reactivity of these systems will be very different from the epoxy equivalents, the preparation of acrylated resins from WVO would require optimisation of steps associated with the synthesis and the network formation, as presented in Chapters 4 and 5.

*B) Investigate the scalability to a pilot scale production – from a methodological to a supply chain standpoint and identifying opportunities*

In the current study, the production volume of epoxidized WVO was limited to batches of a maximum of 500 mL due to constraints in the kit available to use. Although this amount was sufficient to demonstrate the applicability of this feedstock in polymer and composite sciences, these volumes are far from being enough to attend industrial levels of application. Therefore, a study assessing the scalability of technologies developed in this thesis is necessary to bring the WVO closer to be an industrial oleochemical platform. This challenge should be tackled not only from the technological side in terms of how to scale up the reaction itself, but also regarding the requirements to enable the production of this material in large scale, the robustness of this approach and the business opportunities behind it. When scaling up this technology, one should consider the following points as points of interest of potential bottlenecks:

• Convert the synthetic methodology from reaction flask to multi-litre reactors to make it more industrially attractive while considering the following challenges: mass transportation, temperature homogeneity, handling of larger volumes of hydrogen peroxide, recovery of the exchange resin catalyst and separation of the desired product

• Investigate the resilience of the waste cooking oil supply chain (the UK and worldwide) in accommodating this new technology by understanding opportunities regarding the waste management options for this material in the context of the circular economy

• Generate a business model exploring the opportunities found in the market.

*C) Understand the environmental benefits (and impacts) of implementing waste cooking oil as a chemical platform*

The work developed in this thesis must be supported by a framework that assesses and quantify the impacts of the adoption of WVO-based epoxies. This is the only way to rigorously demonstrate the environmental benefits associated with the technologies developed in this study and justify further investigations in the development of genuinely sustainable materials with this platform. In this regard, one can explore a life cycle assessment (LCA) to quantify these impacts based on the inputs and outputs already presented by the thesis and papers based on it. Furthermore, the elaboration of upscaling studies (Recommendation A) would provide a more realistic scenario regarding the potential of commercialisation of WVO-based epoxy resins and its application in composite industries.

*D) Further exploration of fracture toughness properties.*

Investigations presented in Chapter 7 have explored the incorporation of WVO-based resins in carbon fibre reinforced composites in order to reduce the barely-visible impact damage behaviour. Preliminary results have demonstrated the capacity of the highly flexible triglyceride-derived chains to modify the impact properties and impede crack propagation. Therefore, these systems can be further investigated to comprehend characteristics such as the interlaminar fracture toughness, which can be translated as the ability of a material to resist to fractures due to delamination or crack propagation through the laminated plies. This characteristic is critical from an application point of view since these crack can lead to catastrophic failure. DGEBA/ carbon fibre composites are particularly affected by this phenomenon due to their inherent brittleness. The evaluation of the interlaminar shear and fracture toughness (Modes I and II) of composites presenting WVO-based epoxy would provide more details about how the chemically modified triglycerides can improve the behaviour of composites reinforced with recycled and virgin carbon fibres.

Above everything, the main recommendation of this work is in fact an invitation for researchers to have a more pragmatic look towards resources that are currently considered as waste, developing strategies to valorise these materials and enable a more circular approach. Ultimately, the waste valorisation approach prevents the incorporation of new raw materials in the production chain while reducing waste simultaneously, bringing substantial benefits from a sustainability point of view.

# Appendix A – Supplementary Information for Chapter 4

## A.1 Chemical modification of activated carbon

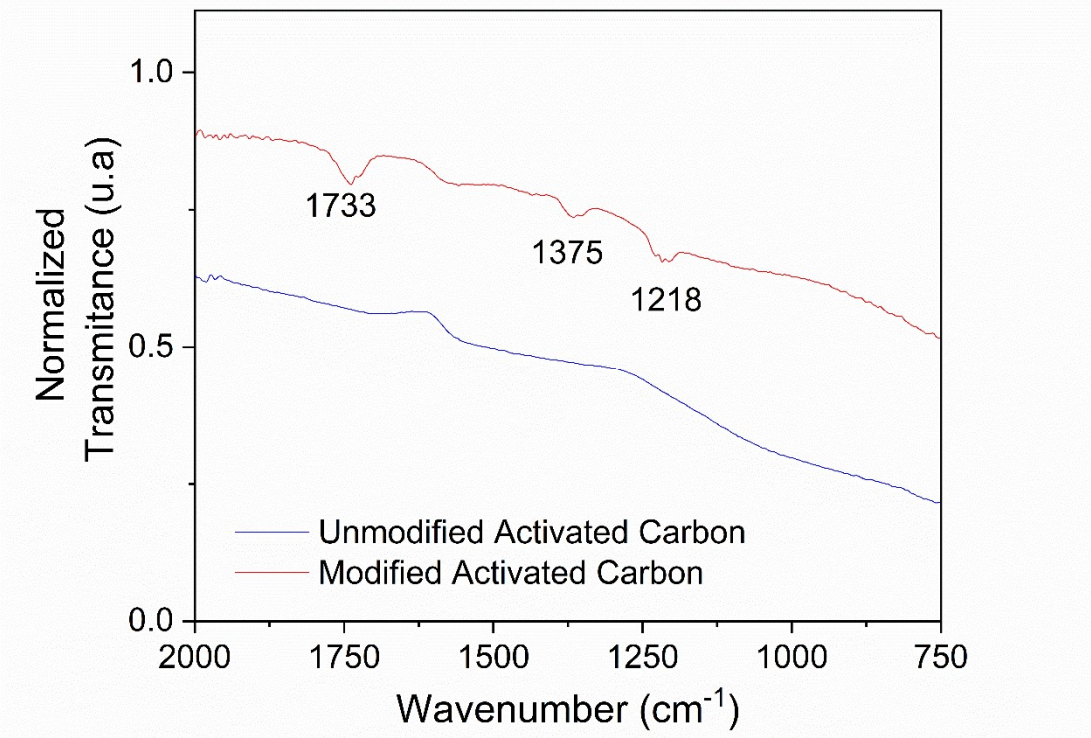


Figure A1: ATR-FTIR spectra of the chemically-modified activated carbon.

## A.2 Interpretation of Purification Methodologies

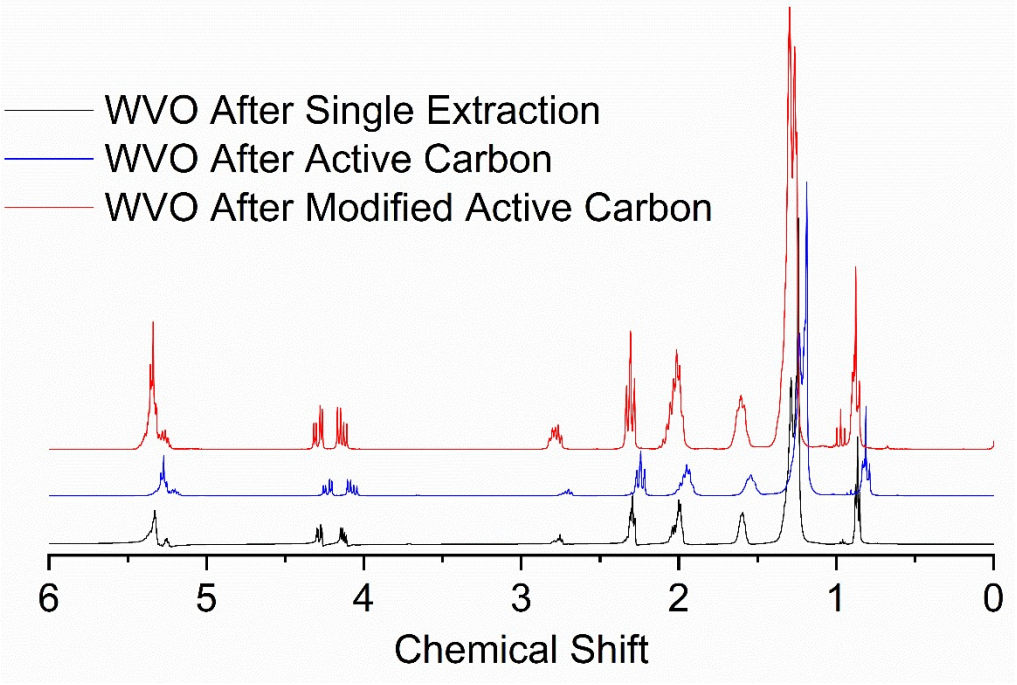


Figure A2: $^{1}H$ NMR spectra of waste vegetable oil samples after purification methodologies

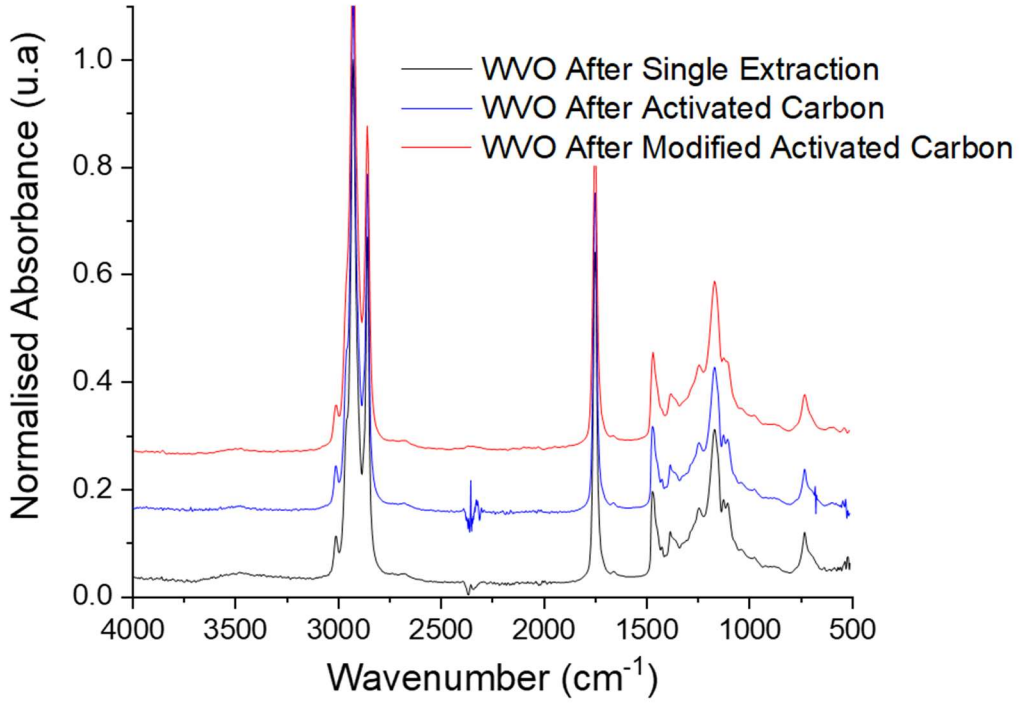


Figure A3: ATR-FTIR spectra of waste vegetable oil samples after purification methodologies.

Characterisation of NVO

$^{1}$H NMR (300 MHz, $CDCl_3$): $\delta_H$ (ppm) = 5.39 – 5.26 (2H, m, C*H*=C*H*), 5.25–5.20 (1H, m, C*H*O), 4.29 (2H, dd, $^{2}J_{HH}$ = 11.9 Hz, $^{3}J_{HH}$ = 4.3 Hz, C*H*HO), 4.11 (2H, dd, $^{2}J_{HH}$ = 12.0 Hz, $^{3}J_{HH}$ = 6.0 Hz, CH*H*O), 2.77 (2H, dt, $^{2}J_{HH}$ = 11.4 Hz, $^{3}J_{HH}$ 5.9 Hz , $CH_2$C*H*=), 2.29 (6H, t, $^{3}J_{HH}$ = 7.5 Hz, OCC*H*$_2$CH$_2$), 2.15 – 1.94 (2H, m, C*H*$_2$CH=CH), 1.70–1.52 (6H, m, OCOCH$_2$C*H*$_2$), 1.40–1.21 (56H, m, C*H*$_2$CH$_2$), 0.98 (9H, t, $^{3}J_{HH}$ = 7.1 Hz C*H*$_3$ linolenic acids), 0.88 (9H, t, $^{3}J_{HH}$ = 7.0 Hz C*H*$_3$ oleic and linoleic acids). FTIR: $\nu_{max}$ (cm$^{-1}$) 3009 (C–H *cis* double bond), 2947 ($CH_3$), 2926 and 2854 (C–H), 1745 (C=O), 1099 (C–O), 722 ($CH_2$).

Characterisation of WVO

$^{1}$H NMR (300 MHz, $CDCl_3$): $\delta_H$ (ppm) = 5.40 – 5.26 (2H, m, C*H*=C*H*), 5.26–5.20 (1H, m, C*H*O), 4.29 (2H, dd, $^{2}J_{HH}$ = 11.9 Hz, $^{3}J_{HH}$ = 4.3 Hz, C*H*HO), 4.10 (2H, dd, $^{2}J_{HH}$ = 11.9 Hz, $^{3}J_{HH}$ = 5.9 Hz, CH*H*O), 2.77 (2H, dt, $^{2}J_{HH}$ = 11.4 Hz, $^{3}J_{HH}$ 5.9 Hz , $CH_2$C*H*=), 2.30 (6H, t, $^{3}J_{HH}$ = 7.5 Hz, OCC*H*$_2$CH$_2$), 2.14 – 1.94 (2H, m, C*H*$_2$CH=CH), 1.70–1.52 (6H, m, OCOCH$_2$C*H*$_2$), 1.42–1.21 (56H, m, C*H*$_2$CH$_2$), 0.87 (9H, t, $^{3}J_{HH}$ = 6.7 Hz C*H*$_3$). FTIR: $\nu_{max}$ (cm$^{-1}$) 3009 (C–H

*cis* double bond), 2947 ($CH_3$), 2926 and 2854 (C–H), 1745 (C=O), 1116 (C-O intra-triglyceride due to frying) 1099 (C–O), 722 ($CH_2$).

Characterisation after Single Extraction Purification

$^1$H NMR (300 MHz, $CDCl_3$): $\delta_H$ (ppm) = 5.40 – 5.26 (2H, m, C*H*=C*H*), 5.26–5.20 (1H, m, C*H*O), 4.29 (2H, dd, $^2J_{HH}$ = 11.9 Hz, $^3J_{HH}$ = 4.3 Hz, C*H*HO), 4.10 (2H, dd, $^2J_{HH}$ = 11.9 Hz, $^3J_{HH}$ = 5.9 Hz, CH*H*O), 2.77 (2H, dt, $^2J_{HH}$ = 11.4 Hz, $^3J_{HH}$ 5.9 Hz , $CH_2CH$=), 2.30 (6H, t, $^3J_{HH}$ = 7.5 Hz, OCC$H_2CH_2$), 2.14 – 1.94 (2H, m, C$H_2$CH=CH), 1.70–1.52 (6H, m, $OCOCH_2CH_2$), 1.42–1.22 (56H, m, C$H_2CH_2$), 0.83 (9H, t, $^3J_{HH}$ = 7.4 Hz C$H_3$). FTIR: $\nu_{max}$ (cm$^{-1}$) 3009 (C–H *cis* double bond), 2947 ($CH_3$), 2926 and 2854 (C–H), 1745 (C=O), 1099 (C–O), 722 ($CH_2$).

Characterisation after Multiple Extraction Purification

$^1$H NMR (300 MHz, $CDCl_3$): $\delta_H$ (ppm) = 5.40 – 5.26 (2H, m, C*H*=C*H*), 5.26–5.20 (1H, m, C*H*O), 4.29 (2H, dd, $^2J_{HH}$ = 11.9 Hz, $^3J_{HH}$ = 4.4 Hz, C*H*HO), 4.10 (2H, dd, $^2J_{HH}$ = 11.9 Hz, $^3J_{HH}$ = 5.9 Hz, CH*H*O), 2.77 (2H, dt, $^2J_{HH}$ = 11.4 Hz, $^3J_{HH}$ = 5.9 Hz , C$H_2$CH=), 2.30 (6H, t, $^3J_{HH}$ = 7.5 Hz, OCC$H_2CH_2$), 2.14 – 1.94 (2H, m, C$H_2$CH=CH), 1.70–1.52 (6H, m, $OCOCH_2CH_2$), 1.42–1.22 (56H, m, C$H_2CH_2$), 0.83 (9H, m, C$H_3$). FTIR: $\nu_{max}$ (cm$^{-1}$) 3009 (C–H *cis* double bond), 2947 ($CH_3$), 2926 and 2854 (C–H), 1745 (C=O), 1099 (C–O), 723 ($CH_2$).

Characterisation after Modified Activated Carbon Purification

$^1$H NMR (300 MHz, $CDCl_3$): $\delta_H$ (ppm) = 5.40 – 5.25 (2H, m, C*H*=C*H*), 5.26–5.19 (1H, m, C*H*O), 4.29 (2H, dd, $^2J_{HH}$ = 11.9 Hz, $^3J_{HH}$ = 4.4 Hz, C*H*HO), 4.10 (2H, dd, $^3J_{HH}$ = 11.9 Hz, $^3J_{HH}$ = 5.9 Hz, CH*H*O), 2.77 (2H, dt, $^2J_{HH}$ = 11.4 Hz, $^3J_{HH}$ = 5.9 Hz, C$H_2$CH=), 2.30 (6H, t, $^3J_{HH}$= 7.5 Hz, OCC$H_2CH_2$), 2.14 – 1.94 (2H, m, C$H_2$CH=CH), 1.70–1.52 (6H, m, $OCOCH_2CH_2$), 1.42–1.22 (56H, m, C$H_2CH_2$), 0.83 (9H, m, C$H_3$). FTIR: $\nu_{max}$ (cm$^{-1}$) 3009 (C–H *cis* double bond), 2947 ($CH_3$), 2926 and 2854 (C–H), 1745 (C=O), 1099 (C–O), 724 ($CH_2$). FTIR modified activated carbon: $\nu_{max}$ (cm$^{-1}$) 2928 (C-H) 1733 ($NO_2$), 1373 (NOH),

Characterisation after Activated Carbon Purification

$^1$H NMR (300 MHz, $CDCl_3$): $\delta_H$ (ppm) = 5.40 – 5.26 (2H, m, C*H*=C*H*), 5.26–5.20 (1H, m, C*H*O), 4.29 (2H, dd, $^2J_{HH}$ = 11.9 Hz, $^3J_{HH}$ = 4.4 Hz, CH*H*O), 4.10 (2H, dd, $^2J_{HH}$ = 11.9 Hz, $^3J_{HH}$ = 5.9 Hz, C$H_2$O), 2.77 (2H, dt, $^2J_{HH}$ = 11.4 Hz, $^3J_{HH}$ = 5.9 Hz, C$H_2$CH=), 2.30 (6H, t, $^3J_{HH}$ = 7.5 Hz, OCC$H_2CH_2$), 2.14 – 1.94 (2H, m, C$H_2$CH=CH), 1.70–1.52 (6H, m,

$OCOCH_2CH_2$), 1.42–1.22 (56H, m, $CH_2CH_2$), 0.83 (9H, m, $CH_3$). FTIR: $\nu_{max}$ ($cm^{-1}$) 3009 (C–H *cis* double bond), 2947 ($CH_3$), 2926 and 2854 (C–H), 1745 (C=O), 1099 (C–O), 724 ($CH_2$).

### A.3 Interpretation of Epoxidation Methodologies

Epoxidation of WVO - Method A

$^1$H NMR (300 MHz, $CDCl_3$): $\delta_H$ (ppm) = 5.40 – 5.26 (2H, m, C*H*=C*H*), 5.26–5.20 (1H, m, C*H*O), 4.29 (2H, dd, $^2J_{HH}$ = 11.9 Hz, $^3J_{HH}$ = 4.3 Hz, C*H*HO), 4.10 (2H, dd, $^2J_{HH}$ = 11.9 Hz, $^3J_{HH}$ = 5.9 Hz, CH*H*O), 2.77 (2H, dt, $^2J_{HH}$ = 11.4 Hz, $^3J_{HH}$ 5.9 Hz , $CH_2CH$=), 2.30 (6H, t, $^3J_{HH}$ = 7.5 Hz, $OCCH_2CH_2$), 2.14 – 1.94 (2H, m, $CH_2CH$=CH), 1.70–1.52 (6H, m, $OCOCH_2CH_2$), 1.42–1.22 (56H, m, $CH_2CH_2$), 0.83 (9H, m, $CH_3$). FTIR: $\nu_{max}$ ($cm^{-1}$) 3009 (C–H *cis* double bond), 2947 ($CH_3$), 2926 and 2854 (C–H), 1745 (C=O), 1099 (C–O), 722 ($CH_2$).

Epoxidation of WVO - Method B

$^1$H NMR (400 MHz, $CDCl_3$): $\delta_H$ (ppm) = 5.40 – 5.26 (2H, m, C*H*=C*H*), 5.26–5.20 (1H, m, C*H*O), 4.29 (2H, d, $^2J_{HH}$ = 11.5 Hz, $^3J_{HH}$ = $CH_2O$), 4.10 (2H, dd, $^2J_{HH}$ = 11.5 Hz, $^3J_{HH}$ = 5.5 Hz, $CH_2O$), 2.90 – 3.20 (2H, m, C*H*OC*H* epoxy), 2.30 (6H, t, $^3J_{HH}$ = 10.6 Hz, $OCCH_2CH_2$), 1.80 – 1.70 (2H, m, $CH_2$ adjacent to epoxy ring), 1.70–1.52 (6H, m, $OCOCH_2CH_2$), 1.42–1.22 (56H, m, $CH_2CH_2$), 0.83 (9H, t, $^3J_{HH}$ = 6.7 Hz, $CH_3$). FTIR: $\nu_{max}$ ($cm^{-1}$) 3006 (C–H *cis* double bond), 2926 and 2854 (C–H), 1745 (C=O), 1099 (C–O), 844 (C-O-C epoxy ring), 724 ($CH_2$).

Epoxidation of WVO - Method C

$^1$H NMR (400 MHz, $CDCl_3$): $\delta_H$ (ppm) = 5.40 – 5.26 (2H, m, C*H*=C*H*), 5.26–5.20 (1H, m, C*H*O), 4.29 (2H, dd, $^2J_{HH}$ = 11.7 Hz, $^3J_{HH}$ = 3.0 Hz, $CH_2O$), 4.10 (2H, dd, $^2J_{HH}$ = 11.9 Hz, $^3J_{HH}$ = 5.9 Hz, $CH_2O$), 2.90 – 3.20 (2H, m, C*H*OC*H* epoxy), 2.30 (6H, t, $^3J_{HH}$ = 7.2 Hz, $OCCH_2CH_2$), 1.80 – 1.70 (2H, m, $CH_2$ adjacent to epoxy ring), 1.70 – 1.52 (6H, m, $OCOCH_2CH_2$), 1.42–1.22 (56H, m, $CH_2CH_2$), 0.83 (9H, t, $^3J_{HH}$ = 6.8 Hz, $CH_3$). FTIR: $\nu_{max}$ ($cm^{-1}$) 3006 (C–H *cis* double bond), 2926 and 2854 (C–H), 1745 (C=O), 1099 (C–O), 844 (C-O-C epoxy ring), 722 ($CH_2$).

Epoxidation of NVO - Method B

$^1$H NMR (400 MHz, $CDCl_3$): $\delta_H$ (ppm) = 5.40 – 5.26 (2H, m, C*H*=C*H*), 5.26–5.20 (1H, m, C*H*O), 4.29 (2H, d, $^2J_{HH}$ = 11.5 Hz, $^3J_{HH}$ = $CH_2O$), 4.10 (2H, dd, $^2J_{HH}$ = 11.5 Hz, $^3J_{HH}$ = 5.5

Hz, C$H_2$O), 2.90 – 3.20 (2H, m, C*H*OC*H* epoxy), 2.30 (6H, t, $^3J_{HH}$ = 10.6 Hz, OCC$H_2$CH$_2$), 2.10 (2H, m, C$H_2$ between epoxy ring and unsaturation), 1.80 – 1.70 (2H, m, C$H_2$ between epoxy rings), 1.70–1.52 (6H, m, OCOCH$_2$C$H_2$), 1.47 (2H, m, adjacent to epoxy ring), 1.42–1.22 (56H, m, C$H_2$CH$_2$), 0.83 (9H, t, $^3J_{HH}$ = 6.7 Hz, C$H_3$). FTIR: $\nu_{max}$ (cm$^{-1}$) 3006 (C–H *cis* double bond), 2926 and 2854 (C–H), 1745 (C=O), 1099 (C–O), 844 (C-O-C epoxy ring), 724 (CH$_2$).

# Appendix B Supplementary Information for Chapter 5

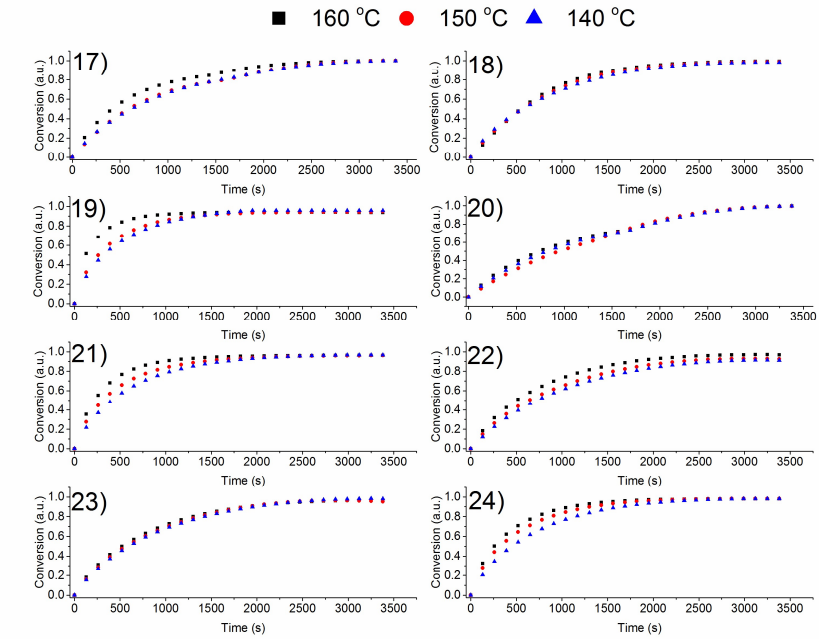


Figure B.1: Curves of conversion of formulations 17-24.

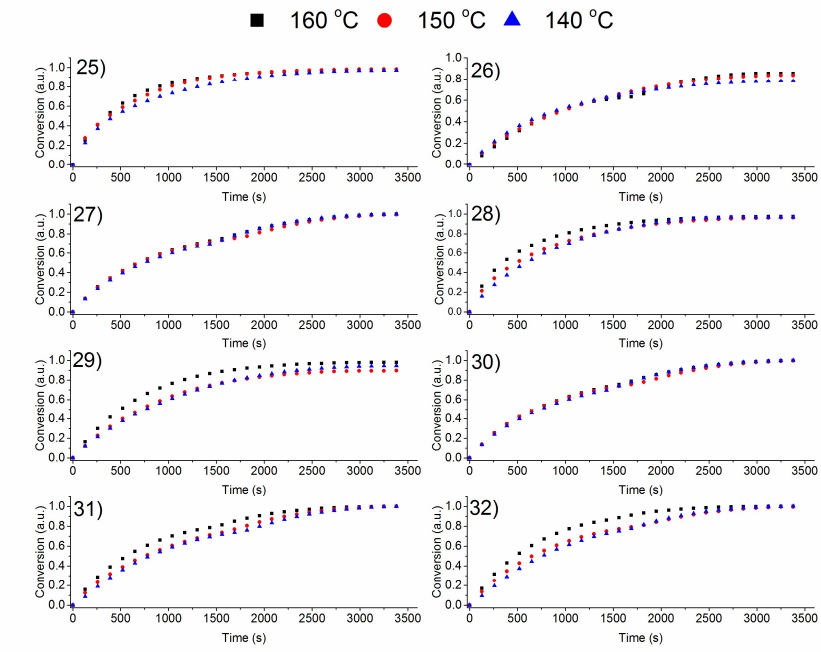


Figure B.2: Curves of conversion of formulations 25-32.

Table B.1: Parameters of the n$^{th}$ order kinetic model from the conversion curves of 17-24.

| **Entry** | **$T_{cura}$ (C)** | **K** $(1/mol\,L^{-'}\,s)$ | **n** | **$E_a$** **(kJ mol$^{-1}$)** | **A** $(1/mol\,L^{-'}\,s)$ |
|---|---|---|---|---|---|
| **17** | 160 | 0.241 | 1.35 | 86.6 | 7.65 |
| | 150 | 0.158 | 1.21 | | |
| | 140 | 0.126 | 1.14 | | |
| **18** | 160 | 0.335 | 1.14 | 47.8 | 10.36 |
| | 150 | 0.197 | 1.01 | | |
| | 140 | 0.145 | 0.90 | | |
| **19** | 160 | 0.215 | 1.60 | 84.5 | 6.69 |
| | 150 | 0.200 | 1.44 | | |
| | 140 | 0.193 | 1.22 | | |
| **20** | 160 | 0.138 | 1.39 | 68.4 | 4.54 |
| | 150 | 0.092 | 0.93 | | |
| | 140 | 0.083 | 0.86 | | |
| **21** | 160 | 0.326 | 1.57 | 57.0 | 26.69 |
| | 150 | 0.239 | 1.45 | | |
| | 140 | 0.173 | 1.22 | | |
| **22** | 160 | 0.167 | 1.04 | 48.9 | 2.10 |
| | 150 | 0.128 | 1.03 | | |
| | 140 | 0.128 | 1.04 | | |
| **23** | 160 | 0.161 | 1.06 | 62.1 | 1.03 |
| | 150 | 0.152 | 0.86 | | |
| | 140 | 0.145 | 0.85 | | |
| **24** | 160 | 0.461 | 1.26 | 57.2 | 9.41 |
| | 150 | 0.378 | 1.13 | | |
| | 140 | 0.311 | 1.00 | | |

Table B.2: Parameters of the nth order kinetic model from the conversion curves of 25-32

| Entry | $T_{cura}$ (C) | K $(1/mol\ L^{-'}\ s)$ | n | $E_a$ (kJ mol$^{-1}$) | A $(1/mol\ L^{-'}\ s)$ |
|---|---|---|---|---|---|
| **25** | 160 | 0.334 | 1.32 | 127.5 | 25.52 |
| | 150 | 0.221 | 1.08 | | |
| | 140 | 0.130 | 0.95 | | |
| **26** | 160 | 0.133 | 1.75 | 112.4 | 1.52 |
| | 150 | 0.099 | 1.24 | | |
| | 140 | 0.093 | 1.14 | | |
| **27** | 160 | 0.150 | 1.43 | 84.9 | 11.41 |
| | 150 | 0.094 | 1.30 | | |
| | 140 | 0.079 | 1.31 | | |
| **28** | 160 | 0.200 | 1.08 | 68.4 | 3.81 |
| | 150 | 0.157 | 0.84 | | |
| | 140 | 0.131 | 0.80 | | |
| **29** | 160 | 0.210 | 1.34 | 84.9 | 13.31 |
| | 150 | 0.170 | 1.08 | | |
| | 140 | 0.117 | 0.93 | | |
| **30** | 160 | 0.241 | 1.35 | 79.4 | 5.67 |
| | 150 | 0.159 | 1.21 | | |
| | 140 | 0.150 | 1.12 | | |
| **31** | 160 | 0.174 | 1.16 | 64.9 | 3.28 |
| | 150 | 0.129 | 1.22 | | |
| | 140 | 0.114 | 1.27 | | |
| **32** | 160 | 0.14 | 1.28 | 105.3 | 4.12 |
| | 150 | 0.10 | 1.04 | | |
| | 140 | 0.09 | 0.94 | | |

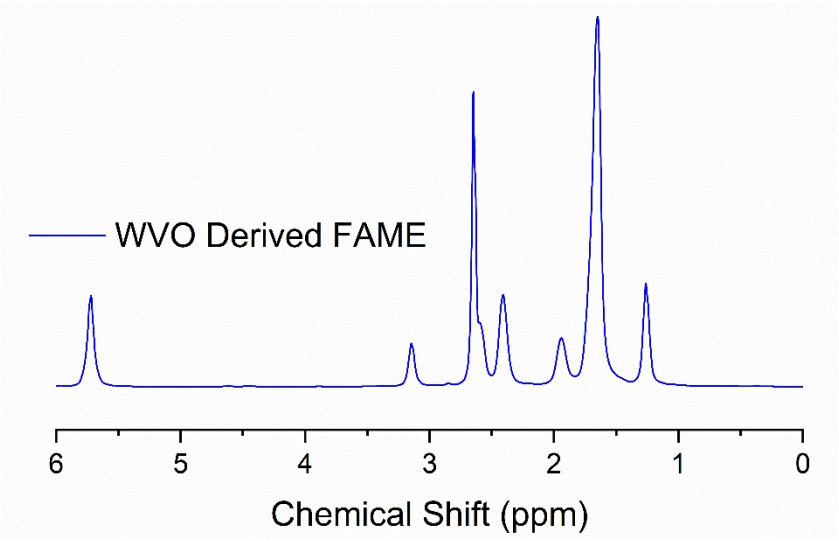


Figure B3: $^{1}$H NMR spectra of FAME sample obtained from transesterification